Università degli Studi di Cagliari

DOTTORATO DI RICERCA

Scienze della Terra

CICLO XXIV

Hydrozincite bioprecipitation: a promising tool for bioremediation of waters contaminated by harmful metals. Hydrochemical factors and morphological features of the biomineralization process

Settori scientifici disciplinari di afferenza

GEO /06

Presentata da:	Dott.ssa Daniela Medas
Coordinatore Dottorato	Prof.ssa Rosa Cidu
Tutor	Prof.ssa Rosa Cidu Dott. Giovanni De Giudici

ESAME FINALE ANNO ACCADEMICO 2010 – 2011

Dissertazione: 09 Marzo 2012

RIASSUNTO

BIOPRECIPITAZIONE DI IDROZINCITE: UNO STRUMENTO PROMETTENTE PER LA BIOREMEDIATION DI ACQUE CONTAMINATE DA METALLI NOCIVI. FATTORI IDROCHIMICI E CARATTERI MORFOLOGICI DEL PROCESSO DI BIOMINERALIZZAZIONE.

Il presente lavoro si inserisce all'interno del progetto Europeo UMBRELLA (Using MicroBes for the REgulation of heavy metaL mobiLity at ecosystem and landscape scAle: an integrative approach for soil remediation by geobiological process) al quale il Dipartimento di Scienze della Terra di Cagliari partecipa in collaborazione con l'Università di Jena (Germania). Il fine complessivo del progetto è rivolto all'uso di microrganismi in associazione con appropriate specie vegetali per sviluppare dei provvedimenti costo-efficienti e sostenibili per il trattamento e il risanamento dei suoli (soil remediation) in siti contaminati da metalli pesanti.

La bioremediation comprende quelle strategie che, attraverso l'uso di microrganismi, funghi, piante o i loro enzimi, consentono di riportare l'ambiente naturale, alterato dalla contaminazione, al suo stato originale. Nel caso dei processi di biomineralizzazione si fa riferimento alla capacità naturale di alcune associazioni biologiche (aerobiche o anaerobiche) di vivere in ambienti inquinati da metalli pesanti e/o sostanze tossiche e di trasformarle in specie mineralogiche scarsamente reattive che comportano la coprecipitazione e/o l'adsorbimento di altre specie chimiche presenti in soluzione. Il presente lavoro si pone come fine lo studio dei processi di biomineralizzazione in aree minerarie con particolare riguardo per la bioprecipitazione di idrozincite, $Zn_5(CO_3)_2(OH)_6$. L'area di studio è localizzata lungo il Rio Naracauli (Sardegna, Italia), dove avviene il processo di biomineralizzazione. Tale processo potrebbe esser usato per attenuare la contaminazione da metalli nocivi

nelle acque di miniera. La conoscenza delle condizioni chimiche e ambientali necessarie per la bioprecipitazione dell'idrozincite è fondamentale per sviluppare delle tecnologie di bioremediation in siti contaminati. A tal riguardo, in questa ricerca è stata dedicata particolare attenzione ai fattori che possono influenzare tale processo, come le condizioni ambientali che favoriscono la precipitazione dell'idrozincite, i caratteri idrochimici che ne influenzano la formazione e la valutazione del controllo batterico sulla morfologia e distribuzione del biominerale.

Il distretto minerario di Ingurtosu è ubicato nella Sardegna sud-occidentale ed è incluso in una delle otto aree appartenenti al Parco Geominerario Storico e Ambientale della Sardegna istituito il 16 Ottobre del 2006. Esso ha come fine la salvaguardia e valorizzazione delle aree minerarie dismesse sia da un punto di vista tecnico-scientifico che storico-culturale e ambientale. La cessazione delle attività minerarie avvenuta nel 1968 ha condotto a un significante degrado ambientale dovuto, particolarmente, ad una contaminazione da metalli nocivi di acque e suoli. Le acque degli affluenti mostrano le più basse concentrazioni in contaminanti. I contenuti più alti in metalli nocivi e tossici sono stati osservati nelle acque che drenano gli scarti di lavorazione mineraria. La concentrazione più alta in Zn nelle acque del bacino del Rio Naracauli raggiunge diverse centinaia di mg per litro, mentre le concentrazioni di Cd e Pb sono nell'ordine delle migliaia di μg per litro, nonostante i valori di pH siano prossimi alla neutralità o lievemente alcalini (6.2-8.4). La concentrazione dello Zn nelle acque è correlata positivamente con le concentrazioni di Pb, Cd, Ni e Co. La correlazione più forte si osserva tra lo Zn ed il Cd, con un rapporto circa costante Zn/Cd (≈100) tra i campioni; questa osservazione indicherebbe una sorgente dominante di Zn e Cd dall'alterazione di sfalerite con composizione relativamente uniforme presente negli scarti di lavorazione mineraria. I contenuti in metalli nelle acque variano in funzione delle condizioni di flusso. Le concentrazioni più alte sono state osservate sotto condizioni di alto flusso (Ottobre - Aprile), probabilmente a causa di una più intensa interazione delle acque di pioggia

con le discariche minerarie e al trasporto di questi metalli in associazione con particelle molto fini, inferiori a 0.4 µm.

Le concentrazioni di Zn, Pb, Cd, Cu e Ni nelle acque del Rio Naracauli, il fiume principale dell'area in studio, sono controllate dalla bioprecipitazione stagionale di idrozincite, $Zn_5(CO_3)_2(OH)_6$. La precipitazione dell'idrozincite è dovuta all'attività fotosintetica di una comunità microbica costituita da un cianobatterio della specie *Scytonema* e da un'alga della specie *Chlorella* (Podda et al. 2000). In accordo con le osservazioni *in situ*, correlate con i calcoli di speciazione e di equilibrio, le condizioni ottimali per la formazione dell'idrozincite si registrano nella tarda primavera di anni piovosi, quando il regime idrico nel fiume raggiunge delle condizioni stazionarie e i valori degli Indici di Saturazione rispetto all'idrozincite e i valori di pH raggiungono i valori più alti, in accordo con una più alta stabilità dell'idrozincite in contatto con acque leggermente alcaline. Contemporaneamente, si è osservato che il rapporto molare Zn^{2+}/CO_3^{2-} raggiunge valori prossimi a 1 nelle stazioni di massima bioprecipitazione, suggerendo che questo valore potrebbe corrispondere alle condizioni più favorevoli per attivare la bioprecipitazione della bio-idrozincite. Al contrario, gli intensi eventi piovosi che si registrano in tarda primavera sembrano inibire il processo di biomineralizzazione, probabilmente a causa della diminuzione degli Indici di Saturazione dovuta ad un effetto di diluizione da parte delle acque piovane.

Lo studio morfologico dell'idrozincite ha mostrato che la sua morfologia varia e dipende dalle condizioni ambientali di precipitazione. Sono stati osservati cambiamenti fra campioni raccolti in tarda primavera e campioni raccolti in estate, e tra campioni precipitati sotto diverse condizioni di flusso. Le idrozinciti campionate in estate sono caratterizzate da globuli con un diametro maggiore rispetto a quelle campionate in primavera. Queste differenze possono essere attribuite ad una variazione nella produzione delle guaine esterne dei cianobatteri in risposta a condizioni di stress. Un ulteriore controllo esercitato dal cianobatterio è stato individuato dall'analisi morfologica di idrozinciti precipitate in diverse condizioni di flusso. Si è osservato che le idrozinciti formate in condizioni di basso flusso sono

caratterizzate da tubuli aventi diametro costante per tutta la loro lunghezza e allineate secondo la direzione di scorrimento dell'acqua. Al contrario, le idrozinciti precipitate in condizioni di alto flusso sono caratterizzate da un diametro variabile che diminuisce verso l'estremità concorde con il verso del flusso. Dette morfologie sono state interpretate prendendo in considerazione l'effetto dell'idrodinamica sulla struttura del biofilm e, conseguentemente, sulla forma del biominerale.

Si è osservato inoltre che Zn, Ni, Co e Mn mostrano dei cicli giornalieri nelle acque del Rio Naracauli, con le concentrazioni più alte misurate durante le ore notturne. La variazione più importante è stata osservata per lo Zn, la cui concentrazione varia di circa il 35% tra il giorno e la notte (Zn_{min} = 3 mg/l; Zn_{max} = 4.7 mg/l). Correlando le variazioni dei contenuti in Zn con quelle misurate per la temperatura, il pH e la conducibilità, si è visto che temperatura e pH sembrano essere i parametri che maggiormente controllano l'andamento dello Zn in soluzione. La temperatura dell'acqua varia in funzione della temperatura dell'aria e della radiazione solare incidente (temperatura massima registrata fra le 13:00 e le 17:00). I cicli osservati per il pH sono attribuibili all'attività fotosintetica (prevalente durante il giorno) e alla respirazione (prevalente durante la notte) che comportano, rispettivamente, un aumento ed una diminuzione del pH. I cicli della temperatura e del pH potrebbero avere come conseguenza una precipitazione/dissoluzione ciclica di idrossidi di ferro, carbonati e altri minerali contenenti Zn. Prendendo in considerazione la variazione dei contenuti in Zn e dei parametri chimici che regolano la precipitazione dell'idrozincite (pH, SI, molZn^{2+}/molCO_3^{2-}) nell'arco di 45 ore, si è visto che le concentrazioni più basse dello Zn coincidono con valori di pH e SI elevati, e valori del rapporto molare Zn^{2+}/CO_3^{2-} vicini ad 1. Queste condizioni risultano essere quelle ottimali per una buona precipitazione di idrozincite che, perciò, risulta essere più intensa durante le ore diurne comportando una diminuzione in Zn e altri metalli presenti in soluzione. Inoltre, anche se le acque del fiume non danno luogo ad un effettivo ciclo di precipitazione/dissoluzione, esso potrebbe avvenire sulla superficie dei biofilms e delle cellule, dove la chimica dell'acqua dipende dal micro-ambiente legato all'attività microbica.

Le variazioni giornaliere in temperatura e pH potrebbero anche influenzare le reazioni di adsorbimento/desorbimento e, di conseguenza, i contenuti in metalli nelle acque. L'adsorbimento di cationi su collodi e/o sulle superfici batteriche e sui biofilms è, infatti, un processo endotermico, più intenso durante il giorno quando si registrano le temperature più alte. Contemporaneamente, durante il giorno, quando i valori di pH sono maggiori rispetto alla notte, l'adsorbimento dei metalli risulta favorito. Le reazioni di adsorbimento/desorbimento sono, perciò, una possibile spiegazione per i cicli giornalieri osservati e sono supportate dalla forte relazione tra le variazioni di pH, temperatura e concentrazioni dei metalli.

I cicli giornalieri dei metalli dovrebbero esser presi in considerazione per valutare le condizioni ambientali, i rischi potenziali e il potenziale risanamento dei siti contaminati.

I risultati ottenuti in questo lavoro forniscono conoscenze approfondite sul processo di bioprecipitazione, ovvero informazioni essenziali per sviluppare metodologie di bioremediation in acque influenzate dall'attività mineraria, passata o presente. La bioprecipitazione di idrozincite potrebbe esser usata per il risanamento di acque contaminate da metalli nocivi e aventi dei pH neutri o leggermente alcalini. L'inoculazione dei microrganismi, insieme all'alterazione e al controllo dei parametri idrochimici, potrebbe rappresentare un approccio promettente per l'uso di tecniche di bioremediation *in situ* consentendo di ottenere le condizioni necessarie per la precipitazione dell'idrozincite.

ABSTRACT

The Ingurtosu Pb-Zn deposit (Sardinia, Italy) was exploited for about a century until 1968. Huge amounts of tailings were abandoned, resulting in long-term harmful metal dispersion processes in both soils and waters. The maximum Zn concentration in waters from the Naracauli stream catchment area attains several hundreds of mg per litre, whereas Cd and Pb concentrations are in the order of thousands of µg per litre, despite the near neutral to slightly alkaline pH values (6.2-8.4). Zn concentration in waters is positively correlated with Pb, Cd, Ni and Co concentrations. The strongest correlation was observed between Zn and Cd, with a constant Zn/Cd ratio (close to 100) among samples that could suggest the weathering of a relatively uniform composition of sphalerite from tailings and mine wastes. Waters from tributaries show the lowest concentrations of contaminants. The highest contents in harmful and toxic elements were observed in waters that drain flotation tailings and mine wastes. Metals concentrations change under different seasonal conditions. The highest concentrations were observed under high-flow condition (October-April), probably due to the high runoff through the tailings and to aqueous transport of these metals in association with very fine particles, i.e. <0.4 µm.

Zn, Pb, Cd, Cu and Ni concentrations in waters of the Naracauli stream, the main stream of the area, are abated by the seasonal bioprecipitation of hydrozincite, $Zn_5(CO_3)_2(OH)_6$. Hydrozincite precipitation is promoted by a microbial community made up of a filamentous cyanobacterium (*Scytonema sp.*) and a microalga (*Chlorella sp.*). Hydrozincite could be used in a controlled process to attenuate metal pollution in mining waters. Information on environmental conditions that promote the biomineralization process is fundamental for the development of remediation strategies. This work aims to investigate the variables controlling the biomineralization process, and the hydrochemical factors that affect hydrozincite precipitation. According to field observations, correlated with speciation and equilibrium calculations, the optimum condition for hydrozincite precipitation occurs in late spring of rainy years, when the hydraulic regime in the stream reaches

stationary conditions, and SI values with respect to hydrozincite and pH reach the highest values, in agreement with the higher stability of the hydrozincite solid phase in contact with slightly alkaline waters. Concomitantly, Zn^{2+}/CO_3^{2-} molar ratio reaches values close to 1, indicating that kinetic processes have a role on the hydrozincite biomineralization process. Conversely, heavy rain events occurring in late spring appear to inhibit biomineralization, likely due to the decrease in the SI values resulting from the dilution effect of rain water.

Results from morphological analysis show that hydrozincite morphology varies, and depends on the environmental conditions. Changes were observed between samples collected in late spring and samples collected in summer, and among samples precipitated under different water flow conditions. Hydrozincite samples collected in summer are characterized by globules with a larger diameter than those collected in spring, this variation can be ascribed to a difference in the production of external mucilage sheaths by cyanobacteria colonies in response to stress conditions. Considering influence of water flow, it was observed that hydrozincite sheaths precipitated under low flow condition have more or less a constant diameter, whereas under high flow conditions sheaths become thinner at the final ends. This particular morphology is due to the influence of hydrodynamics on the structure of the biofilm and, consequently, on biomineral shape.

Diel cycles in dissolved Zn, Co, Ni and Mn were found to occur in a selected station along the Naracauli stream. The highest change in concentration was observed for Zn: the difference between the minimum (3 mg/l) and maximum (4.7 mg/l) Zn concentrations is 1.7 mg/l (about 35%). The minimum values occurred at h 17:00 and maxima between h 02:00 and h 05:00. The timing of diel cycles in Co and Ni is very similar to that for Zn, but the ranges of Co and Ni concentrations are much smaller than Zn. Increased nocturnal concentrations could result from a combination of geochemical and biological processes. Considering the relations among temperature, pH and Zn contents, temperature and pH would seem to be the parameters that control variations in Zn concentration. Water temperature shows a well defined diurnal cycle. Maximum water temperature was observed between the h 13:00 and h

17:00. Water temperature varies due to change in air temperature and incident solar radiation. The pH values vary between 7.7 and 8.1; the highest values were observed during the sunny hours and the lowest during the night or early morning. The diel pH cycle derives from photosynthesis (predominant during the day) and respiration (predominant during the night). Obtained results may be explained by adsorption-desorption reactions (onto colloids, carbonates, bacterial surfaces and biofilms) and/or different rates of mineral precipitation between the morning and the night time. Diurnal metal cycles should be taken into account to evaluate environmental conditions, potential risks and cleanup of contaminated sites.

This thesis is dedicated to my son, Francesco,

whose bright smile gives me the joy of living every day as if it were my last!

ACKNOWLEDGMENT

It is a pleasure to thank those people who made this thesis possible. First and foremost, I would like to express my deep and sincere gratitude to my supervisors, Prof.ssa Rosa Cidu and Dr. Giovanni De Giudici, whose encouragement, guidance and support, from the initial to the final level, enabled me to develop an understanding of the subject. I have appreciated all their contributions of time and ideas that have made my PhD experience productive and stimulating.

I express my deeply gratitude to Prof. Piero Lattanzi, Dr. Richard B. Wanty, and Dr. Briant Kimball, for their help and suggestions during my academic career.

I wish to express my sincere thanks to Dr. Francesca Podda. The joy and enthusiasm she has for research has been contagious for me, even during tough times in my PhD course. In addition, I want to thanks her because she is a colleague but also a true friend.

I would like to thank Prof. Gian Luigi Pillola for his courtesy in allowing me to use his lab instruments; Dr. Angelo Ibba for his help and suggestions about the samples metallization; Giorgio Contis for analyses by Ionic Chromatography; Dr. Sergio Piras for optical microscopy images, and Maria F. Lorenzoni for assisting me in the research of several books and papers.

During these years, I enjoyed the good company of Dr. Carla Ardau, Dr. Claudia Dadea, Dr. Stefania Da Pelo, and Dr. Riccardo Biddau who largely contributed to my scientific and personal growth.

I want to thank my family. First of all, I owe my loving thanks to my little baby, Francesco, a powerful source of energy, and to my husband, Cristian, for his patience and encouragement. My loving thanks to my brother, Roberto, to my sister in law, Luana, and to my parents, Anna e Diego, for their support and encouragement.

I wish to thank my friends, especially, Maurizio and Pamela, for providing a stimulating and fun environment in which to learn and grow. Moreover, I thank Elena, Maria Paola, Fabio, Matteo, Valeria, Claudio, Fabrizio, Cristina, Sara, Elisabetta, Dario, Filippo and Guglielmo.

Lastly, I offer my regards and blessings to all of those who supported me in any respect during the completion of the project.

PREFACE

This PhD work was carried out in the framework of the UMBRELLA project (Using MicroBes for the REgulation of heavy metaL mobiLity at ecosystem and landscape scAle: an integrative approach for soil remediation by geobiological processes, grant number 226870. Coordinator Erika Kothe, Friedrich-Schiller-Universität Jena, Germany; local coordinator Giovanni De Giudici, Earth Sciences Department, University of Cagliari, Sardinia-Italy). The overall goal of UMBRELLA is to use microorganisms to develop cost-efficient and sustainable measures for soil remediation at heavy metal contaminated sites throughout Europe. In this context, the aim of this work was to investigate the biomineralization processes, with special regard to bio-hydrozincite formation closely related to the bioremediation processes. Environmental conditions and hydrochemical characteristics that favour the hydrozincite precipitation were investigated because they are fundamental for developing successful remediation strategies at contaminated sites. At the same time, the role of bacteria on mineral morphology and distribution was also investigated.

This thesis reports the work carried out at the Earth Sciences Department, Cagliari University (Italy) under the supervision of Prof. Rosa Cidu and Dr. Giovanni De Giudici.

This dissertation is divided into four sections: a) the first section is dedicated to an overview on biominerals and biofilms occurrence. Moreover, this part presents a literature review about Naracauli hydrozincite; b) the second section is dedicated to the study area - geological setting and hydrogeological data, ore deposits and mining history; c) in the third section materials and analytical methods are shown; d) the fourth section is focused on the results and discussion concerning the hydrogeochemistry of the Naracauli stream catchment area and the biomineralization process.

TABLE OF CONTENTS

CHAPTER 1 INTRODUCTION

1.1 GENERALITIES

Biomineralization refers to the processes by which organisms form minerals. Since their appearance on the Earth's surface, cyanobacteria play key roles in the biosphere, particularly in the areas of element biogeochemical cycling, mineral transformations and evolution, bioweathering, and soil and sediment formation (Van Cappellen 2003; Hazen et al., 2008 and 2010; Gadd, 2010). A large number of biogenic minerals is known (Skinner, 2005), among them calcium carbonate minerals are the most abundant and widespread (Lowenstam et al., 1989; Gadd, 2010). Discovery of biogenic minerals and of organisms which form them is in continuous evolution, so that the true extent of biomineralization in the biosphere is still far from being completely known.

Phoenix et al. (2008) underline the benefits of the biomineralization. Biominerals perform a variety of roles in organisms, the most important being support, defence and feeding (Livingston et al., 2006). The biomineralization processes create heterogeneous accumulations, composites made up of organic and inorganic compounds, with inhomogeneous distributions that reflect the environment in which they form (Skinner, 2007; Cuif et al., 2011; Medaković et al., 2012). The environmental effect is very often filtered out by the physiological processes of the organism, which either completely or partially affect the solution characteristics of the microenvironment in which the crystals grow (Lowenstam et al., 1989).

Mineral precipitation mediated by microorganisms can be useful to decontaminate polluted soils and waters (Lloyd et al., 2001; Gad, 2004; Lloyd et al., 2005; Cutting et al., 2010). In fact, bioremediation is the application of biological systems to the clean-up of organic and inorganic pollution, with bacteria and fungi being the most important organisms for reclamation, immobilization or detoxification of metallic pollutants (White et al., 1995; Lloyd et al., 2005; Civilini et al., 2006; Gadd, 2010). The knowledge of chemical and environmental conditions necessary for biominerals

precipitation and their impact on biomineralization process is therefore fundamental for developing successful remediation strategies at contaminated sites.

1.2 WHAT IS A BIOMINERAL?

Biomineralization can be generally defined as the production of biominerals namely, inorganic or organic crystals by living organisms (Medina et al., 2011). The control exerted by organisms over biomineral formation distinguishes these processes from abiotic mineralization (Weiner et al., 2003). The resulting biominerals have unique morphologies, hierarchical structures and specific functions, and often exhibit remarkable properties. Microorganisms are capable of mediating the formation of a large number of minerals through two different processes, first reported by Lowenstam (1981) as biologically induced mineralization (BIM) and organic matrix-mediated formation of minerals. The latter is referred to as biologically controlled mineralization (BCM) (Mann, 1983). BIM (Fig. 1) refers to mineralization occurring in an open environment, and not in a specific space delineated for this purpose. The biological system has little control over the type and habit of minerals deposited that are very similar to those of their abiotic counterparts. In the BIM, the metabolic processes employed by the organism within its particular redox environment mediate pH, pCO_2 and the compositions of secretion products favouring particular mineral types in an indirect way (Weiner et al., 2003). In BCM (Fig. 2), there is a direct correlation between the living organism and mineral formation that occurs almost exclusively at specific sites (Lowenstam et al., 1989; Weiner et al., 2003). The organism has a great degree of crystal chemical control over the nucleation and growth of mineral particles. BCM processes can be described as occurring extra-, inter- or intracellularly. These distinctions refer to the locations of the mineralization site with reference to the cells responsible for mineralization (Lowenstam et al., 1989; Bazylinski et al., 2003; Weiner et al., 2003).

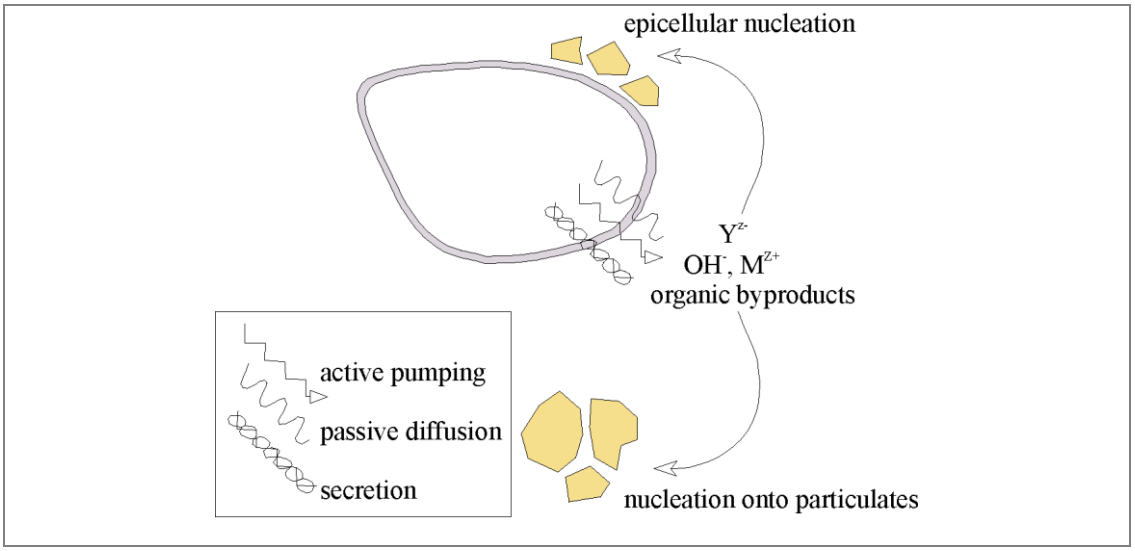

Figure 1. Illustration of biologically induced mineralization. Minerals form as a result of bacterial metabolic activities that affect pH, pCO_2, and secretion products. The cell is a causative agent only, without control over mineral type or habit (by Weiner et al., 2003, modified).

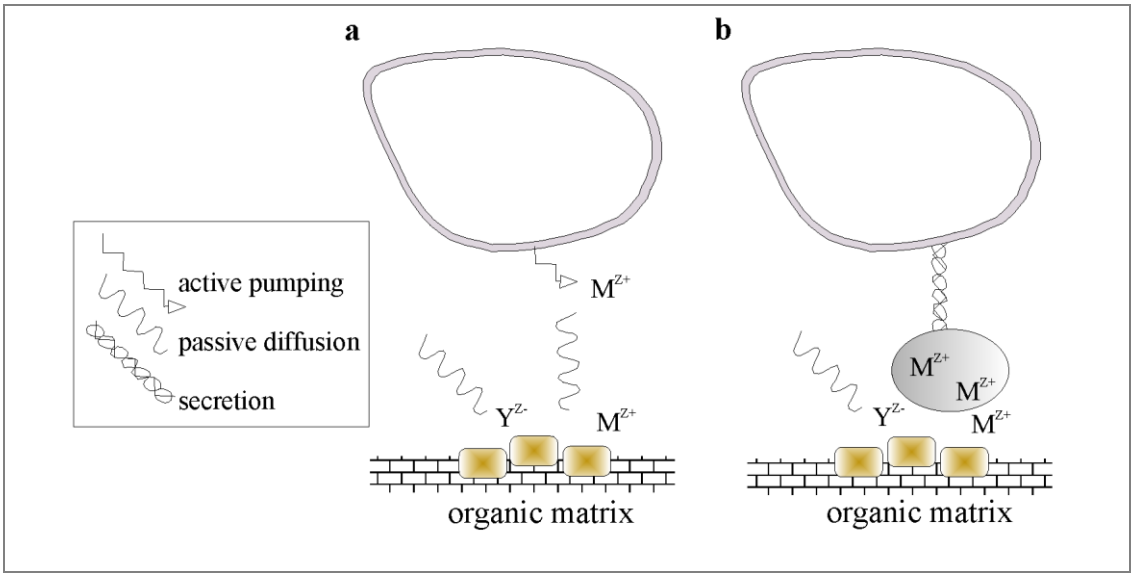

Figure 2. Illustrations of biologically controlled extracellular mineralization showing that this process is distinguished by nucleation outside of the cell. a.) Cations are pumped across the cell membrane and move by passive diffusion through extracellular fluids to the site of mineralization. b.) Cations are concentrated intracellularly as aqueous ions into a vesicle that is subsequently secreted. Compartment breakdown at site of mineralization releases cations for biomineral formation (by Weiner et al., 2003, modified).

Dupraz et al. (2009) introduced a new term, biologically influenced mineralization, to refer to passive mineralization of organic matter, such as cell surfaces or extracellular polymeric substances (EPS), whose properties influence crystal morphology and composition. In this case, the presence of living organisms is not required.

Biomineralization processes mediated by bacteria can be divided into two stages (González-Muñoz et al., 2010). The first is represented by active modifications of the physical-chemistry in the interior or surroundings of the bacteria (i.e. pH, Eh, ion concentrations, pCO_2). These physical-chemical variations lead to a state of supersaturation, which is a prerequisite for mineral precipitation. The second stage includes the nucleation of a mineral phase that can occur either homogeneously or heterogeneously (Mullin 1992; Yoreo et al., 2003; Meldrum et al., 2008). In homogeneous nucleation, the nucleus forms spontaneously from the solution itself when a critical supersaturation is reached. Heterogeneous nucleation is less energetically demanding, in fact the activation energy can be reduced by the presence of foreign surfaces or dispersed components, on which heterogeneous nucleation occurs. Bacteria can induce heterogeneous nucleation of minerals by providing not only a surface that lowers the energy barriers for mineral precipitation, but also a stereochemical arrangement of the mineral components (Jiménez-Lopez et al., 2007). Heterogeneous nucleation may occur on bacterial exopolymeric substances (EPS) (Dupraz et al., 2005; Braissant et al., 2007). Many studies show that cyanobacterial EPS is able to bind metal ions to various functional groups that are present in sugars and amino acids constituting the EPS (Dong et al., 2000; Mohamed, 2001; Bhaskar et al., 2006; Panwichian et al., 2011). For example, the negatively charged surface of the cyanobacterial EPS-containing sheath promotes nucleation and precipitation of calcium carbonate (Pentecost, 1985; Thompson et al., 1990; Riding, 2000; Dittrich et al., 2010). This process is explained by the so-called theory of organic-matrix mediated biomineralization (Mann, 2001). This theory states that organic molecules can (self)assemble into a template so that there can be electrostatic, geometric, or stereochemical affinity/matching between the template and the inorganic precipitate

(biomineral). Organic macromolecules are normally acidic polyanionic polymers (e.g. proteins, glycoproteins, proteoglycans) which include carboxylic or phosphatic functional groups. These charged groups play a key role in the heterogeneous nucleation of a new solid phase, as demonstrated by in vitro studies of calcium carbonate precipitation in the presence of amino acids (Jiménez-Lopez et al., 2003).

1.3 BIOFILMS

A biofilm is a thin coating comprised of living material (Karatan et al., 2009). It occurs in nearly every moist environment where sufficient nutrient flow is available and surface attachment can be achieved (Singh et al., 2006; Simões et al., 2010). Biofilms can form on environmental abiotic surfaces, such as minerals and stones, or air-water interfaces, and on biotic surfaces, such as plants, roots, leaves and other microbes. Biofilms can be distinguished into monolayer and multilayer biofilms. In the first case, single cells form attachments to the surface, and the bacterium is attached only to the surface. In the second case, the bacterium is attached both to the surface and to neighbouring bacteria. Biofilm matrix is mainly composed of microbial cells, waters (perhaps up to 97%; Zhang et al., 1998), secreted polymers (EPS), together with excreted cellular products and even particulate material and detritus from the immediate surrounding environment (Sutherland, 2001b). The cement of a biofilm is the EPS (Sutherland, 2001a; Flemming et al., 2010). Biofilms can be formed by a single bacterial specie, although they can also consist of many species of bacteria, fungi, algae and protozoa that are attached to abiotic or biotic surfaces through EPS (Singh et al., 2006).

Figure 3 shows the development of a biofilm (Singh et al., 2006). Initially, cells attach by physico-chemical interactions or extracellular matrix protein secretion to form a cell monolayer, this stage is followed by biofilm maturation and, finally, detachment of cells. Biofilm matrices are characterized not only by cell types, but also by their architecture, by the type of extracellular products that are concentrated

in the biofilm matrix, and by the environmental conditions and surfaces that favour their formation. Various environmental factors regulate bacterial biofilm formation such as variations in pH, availability of nutrients and oxygen and concentration of bacterial metabolites. One bacterium may build several different types of biofilms under different environmental conditions.

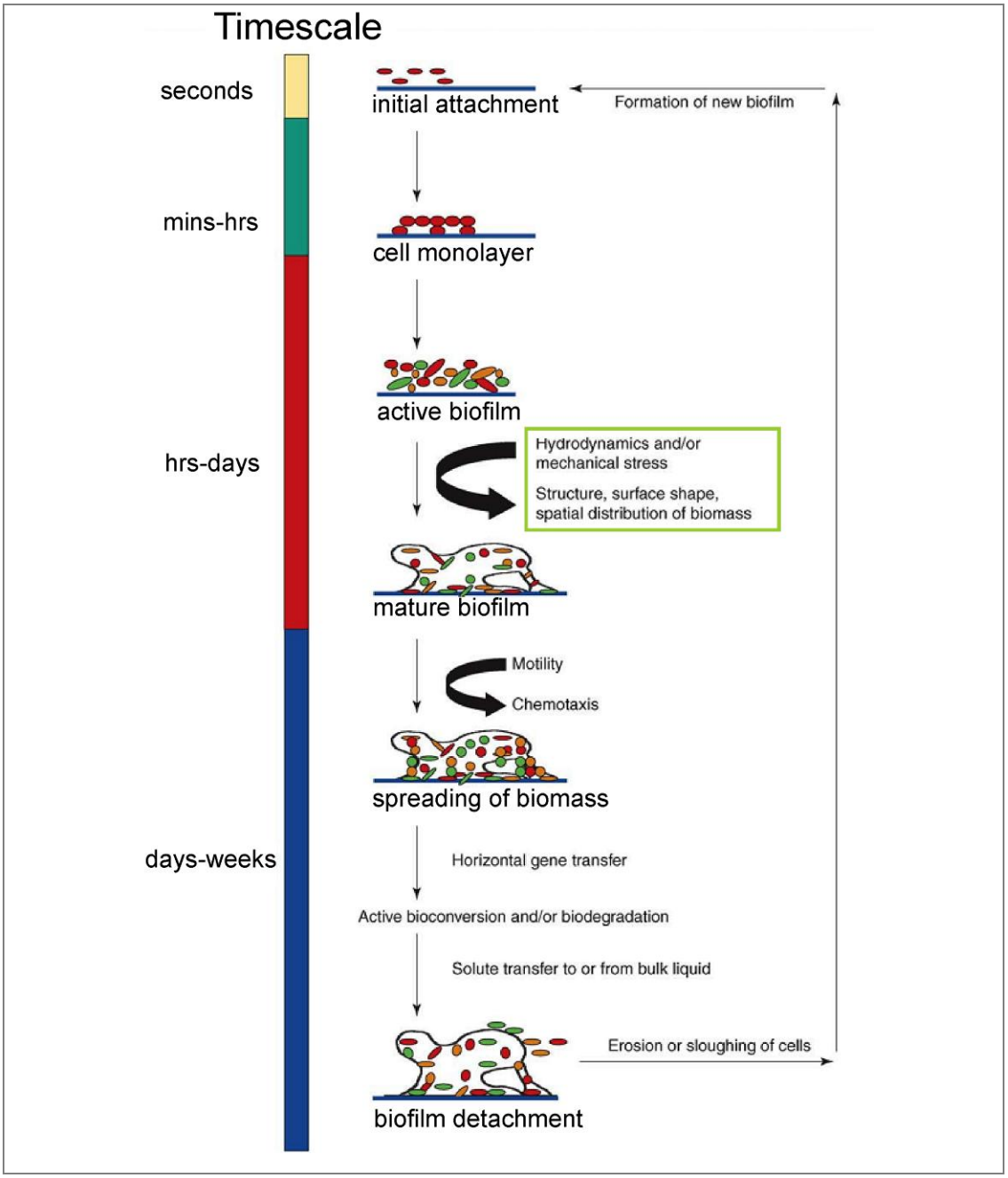

Figure 3. Scheme showing the development of a biofilm. Cells initially attach by physico-chemical interactions or extracellular matrix secretion to form a cell monolayer. Cells proliferate in the monolayer and other microbes attach to form an active biofilm, the development and distortion of which is influenced by environmental factors such as hydrodynamic and mechanical stress. As cells die, active bioconversion and/or biodegradation leads to solute transfer to or from the bulk liquid, which results in eventual biofilm detachment. The approximate time period for which each of the phases persist is shown on the left (by Singh et al., 2006, modified).

1.4 THE ROLE OF BIOMINERALIZATION AND BIOFILMS IN CONTAMINATED WATERS

Metal pollutants are of particularly critical environmental concern as they can accumulate throughout the food web and induce severe health problems (Boyd, 2010). The removal of toxic metals from polluted waters has been practised for several decades, using treatment technologies such as oxidation-reduction (James, 2001; Liang et al., 2004), filtration (Zivanovic et al., 2007), electrochemical treatment (Patermaraxis et al., 1990; Armstrong et al., 1997; Tröster et al., 2002), or permeable treatment walls (Vidic et al., 1996; Simon et al., 2000). These methods have some drawbacks (i.e. high reagent requirement and unpredictable metal removal; strong and contaminating reagents used for desorption). Microbes play an active role in biogeochemical processes leading to altered metal distributions and speciation, with a variety of physicochemical and biological mechanisms effecting transformations between soluble and insoluble phases (Gadd, 2004). In this regard, bioremediation, that offers the possibility to destroy or render harmless various contaminants using natural biological activity (Vidali, 2001), has received increasing attention in recent times (U.S. Geological Survey, 1997; Iwamoto et al., 2001; Johnson, 2005; Handley-Sidhu et al., 2011). Bioremediation is very safe because it relies on microbes that naturally occur in soil and/or water and dangerous chemicals are not used in bioremediation (U.S. Environmental Protection Agency, 2001). As such, bioremediation uses relatively low-cost, low-technology techniques, which generally have a high public acceptance and can often be carried out on site. The biological processes for treating toxic effluents are better than chemical and physical methods in terms of their efficiency and economy and the potential of biofilms for bioremediation processes has recently been realized (Tsezos et al., 2004; Singh et al., 2006). Cells in a biofilm have a better chance of adaptation and survival (especially during periods of stress), respect to planktonic microorganisms (Decho et al., 2000), because they are protected within the matrix.

Harmful metals bioremediation can be achieved by their immobilization, concentration and partitioning to an environmental compartment (Singh et al., 2006; Gadd, 2010). Microbial mineral formations have potential for the treatment of environmental pollution, playing an important role in the regulation of contaminants in ecosystems. Moreover, bio-mineral precipitation has the advantage of producing chemically stable forms of metals. Microbial precipitation of metals as sulphide (White et al., 1998 and 2000; Labrenz et al., 2000), hydroxide (Banfield et al., 2000), phosphate (Macaskie et al., 2000) and carbonate (Diels et al., 1999) minerals have potential and documented applications in bioremediation.

Biomineralization occurs naturally in very diverse environments. In order for microbes to precipitate harmful chemicals, the right temperature, nutrients, and amount of oxygen (right physico-chemical characteristics in general) must be present in the soils and waters. These conditions allow the microbes to grow and multiply (U.S. Environmental Protection Agency, 2001). Consequently, biomineralization may be stimulated in situ by injecting nutrients and oxygen, offering a potential remediation mechanism using indigenous microorganisms (Vidali, 2001; Renshaw et al., 2010). Therefore, knowledge of the biomineralization process is essential for the development of efficient methods for contaminated soil and water remediation.

1.5 Overview on Naracauli hydrozincite

Hydrozincite [$Zn_5(CO_3)_2(OH)_6$] occurs as a biomineral along the upper part of the Naracauli stream in the abandoned mine area of Ingurtosu (Sardinia, Italy). Bioprecipitation is observed in late spring and early summer, in association with a photosynthetic microbial community made up of a filamentous cyanobacterium, classified as *Scytonema sp.* strain ING-1, and a microalga *Chlorella sp.* strain SA-1 (Podda et al., 2000). *In vitro* experiments (De Giudici et al., 2007) indicated that the microbial community exerts a control on the morphology of hydrozincite particles;

indeed, natural and *in vitro*-formed hydrozincite minerals showed different morphological and crystallinity features.

Hydrozincite has a monoclinic structure (Fig. 4; Ghose, 1964), where an octahedral layer is linked to two tetrahedral layers in a T-O-T structure. Carbonate molecules are perpendicular to the tetrahedral layers. These layers lay on the (100) faces.

De Giudici et al. (2009) investigated the structure of the Naracauli biomineral, and found that hydrozincite biomineral is made up of nanocrystals, each a few nm in their longest dimension, aggregated with an imperfect orientation (Meldrun et al., 2007). The nanocrystal aggregation results in the formation of mesocrystals, i.e. platelets flattened onto the (100) crystal surface. These platelets are about 0.1 μm thick. In turn, they aggregate to form globules and sheaths all around the filamentous bacteria (Podda et al., 2000; De Giudici et al., 2009). XRD analysis indicated a progressive decrease in the size of particles in the biomineral compared to reference samples (typically obtained from supergene Zn deposits). Aging effects were never detected (i.e., XRPD patterns of the studied samples remained essentially unchanged after several years since collection). Recent studies include a systematic comparison of XRPD (from both conventional and synchrotron sources) of Naracauli hydrozincite with synthetic material and "typical" hydrozincite from Zn oxide deposits (De Giudici et al. 2009; Lattanzi et al. 2010a, b, c). The results showed that high precision synchrotron-based XRPD patterns of the Naracauli hydrozincites cannot be fitted to known structures of this mineral, which were obtained from "typical" hydrozincites. The largest difference is recorded for the a_o cell parameter ("typical" hydrozincite: 13.59 ± 0.03 Å; Naracauli hydrozincite 13.832± 0.006 Å), and suggests a difference in the stacking sequence of ZnO_6 octahedral sheets present in the hydrozincite structure. This could be associated to the distortion of carbonate group based on NMR evidences (De Giudici et al., 2009) and to some other crystallographic perturbation, namely, line defects and grain boundaries, and small amount of impurities in the Naracauli hydrozincite.

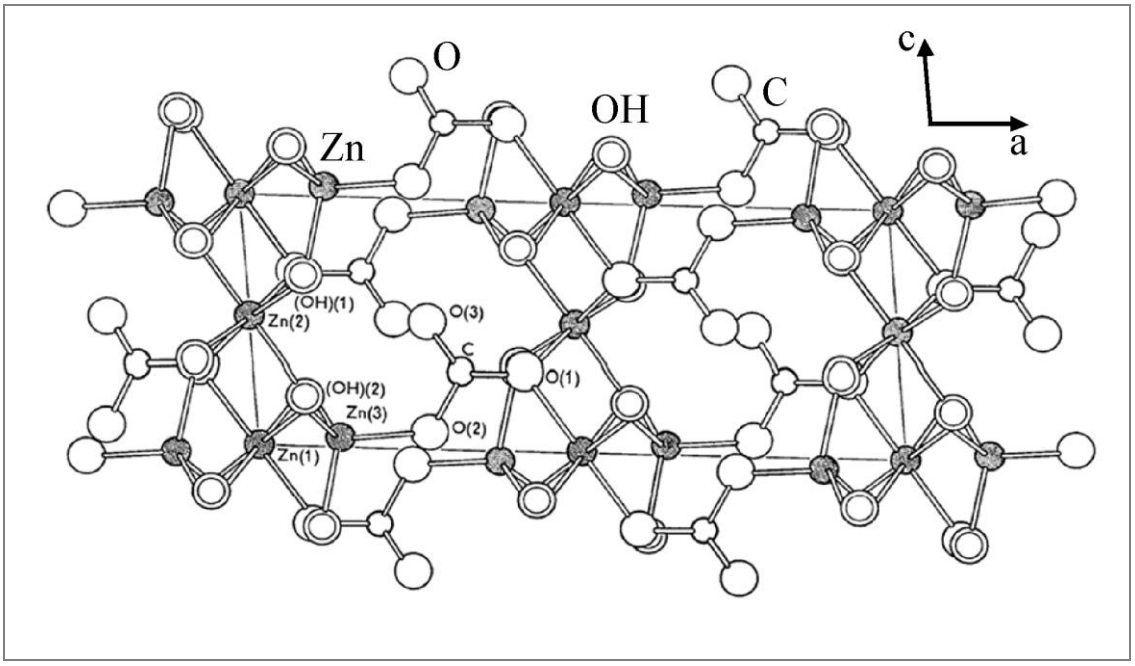

Figure 4. Projection of the structure of hydrozincite, $Zn_5(CO_3)_2(OH)_6$ along [010]. The atoms of Zn can occupy octahedral and tetrahedral position. The atoms of O are at the vertices of the polyhedra either stand-alone or bound with a hydrogen atom into an OH bond. CO_3 groups bind the sheets that are parallel to (100) (by Ghose 1964, modified).

Podda et al. (2000) and Zuddas et al. (2005) showed that bioprecipitation of hydrozincite produces significant decreases in the dissolved concentrations of Zn, Pb, Cd, Cu and Ni from mine waters. The binding nature of Cd and Pb to hydrozincite was investigated by X-ray absorption spectroscopy (XAS). For Cd, the results of extended X-ray absorption fine structure (EXAFS) analysis, backed by anomalous X-ray diffraction, suggest a disordered mode of occurrence, presumably as an amorphous surface precipitate (Lattanzi et al., 2010b). For Pb a more complex model is suggested (Lattanzi et al., 2010a): this metal is supposed to occur partly as an amorphous surface carbonate, partly either as a substituting ion in the tetrahedral Zn site of the hydrozincite structure or as an inner-sphere surface complex. Hydrozincite can thus be regarded as an effective trap for Pb, while any sequestration of Cd is only surficial.

1.6 OBJECTIVES OF THIS STUDY

The knowledge of chemical and environmental conditions necessary for hydrozincite precipitation is fundamental for developing bioremediation strategies at contaminated sites. Seasonal effects on microbial mineralization have been reported (Thompson et al., 1997; Dittrich et al., 2004). However, data on morphological changes in biomineralization along the seasonal precipitation are not well developed (Stolz, 2000).

The main purpose of this study was to investigate the biomineralization process taking into account environmental conditions that favour biomineral precipitation and hydrochemical changes affecting the hydrozincite precipitation. At the same time, this work was focused on assessing the control exerted by bacteria on mineral morphology and distribution.

The results acquired in this study will be presented as follows. First, the main hydrochemical characteristics of the waters from the Naracauli stream catchment will be reported.

Second, the biomineralization process will be discussed. This part is divided in:

1) mineralogical and chemical characterization of the samples;

2) investigation of bacterial control and environmental influences on hydrozincite morphology;

3) variations in water geochemistry induced by hydrozincite precipitation and optimum condition for the biomineralization process;

Third, results on the diel cycle in dissolved metals concentrations in a selected station along the Naracauli stream will be presented.

CHAPTER 2 STUDY AREA

2.1 GEOLOGICAL SETTING AND HYDROLOGICAL DATA

Figure 5 shows the schematic geological setting of the Arburese district (Carmignani et al., 1996, modified). The main unit is represented by an allochthonous low-grade metamorphic complex made up of sedimentary and volcano-sedimentary successions, dating to Cambrian-Ordovician time (Carmignani et al., 1996). This complex (Arburese tectonic unit) is part of the external nappe zone of the Variscan chain in south-western Sardinia, and was thrusted over the autochthonous successions of the Iglesiente complex during the Variscan orogeny. At the end of the orogeny (ca. 300 Ma), the Arburese igneous complex was emplaced. It is characterized by a roughly concentric structure, with dominant granodiorite in the border zone, and leucogranite in the core (Secchi et al., 1991). The igneous complex is characterized by radial fractures filled by acid and basic magmatic dykes, and by quartz and metalliferous hydrothermal veins. The mineralized vein system of Montevecchio-Ingurtosu occurs in the northern side of the Arburese igneous complex; minor deposits occur in the southern edge. Post-Paleozoic formations include a Cenozoic sedimentary complex made up of sandy, conglomeratic, marly and carbonate facies (Carmignani et al., 1996), and the volcanic complex of Monte Arcuentu. The latter is made up of basaltic flows overlapped by breccias and pillow lavas (Assorgia et al., 1984), dating to Upper Oligocene-Lower Miocene. Aeolian dunes along the coast (Piscinas dunal complex) and fluvial deposits in the internal area constitute the Quaternary covers.

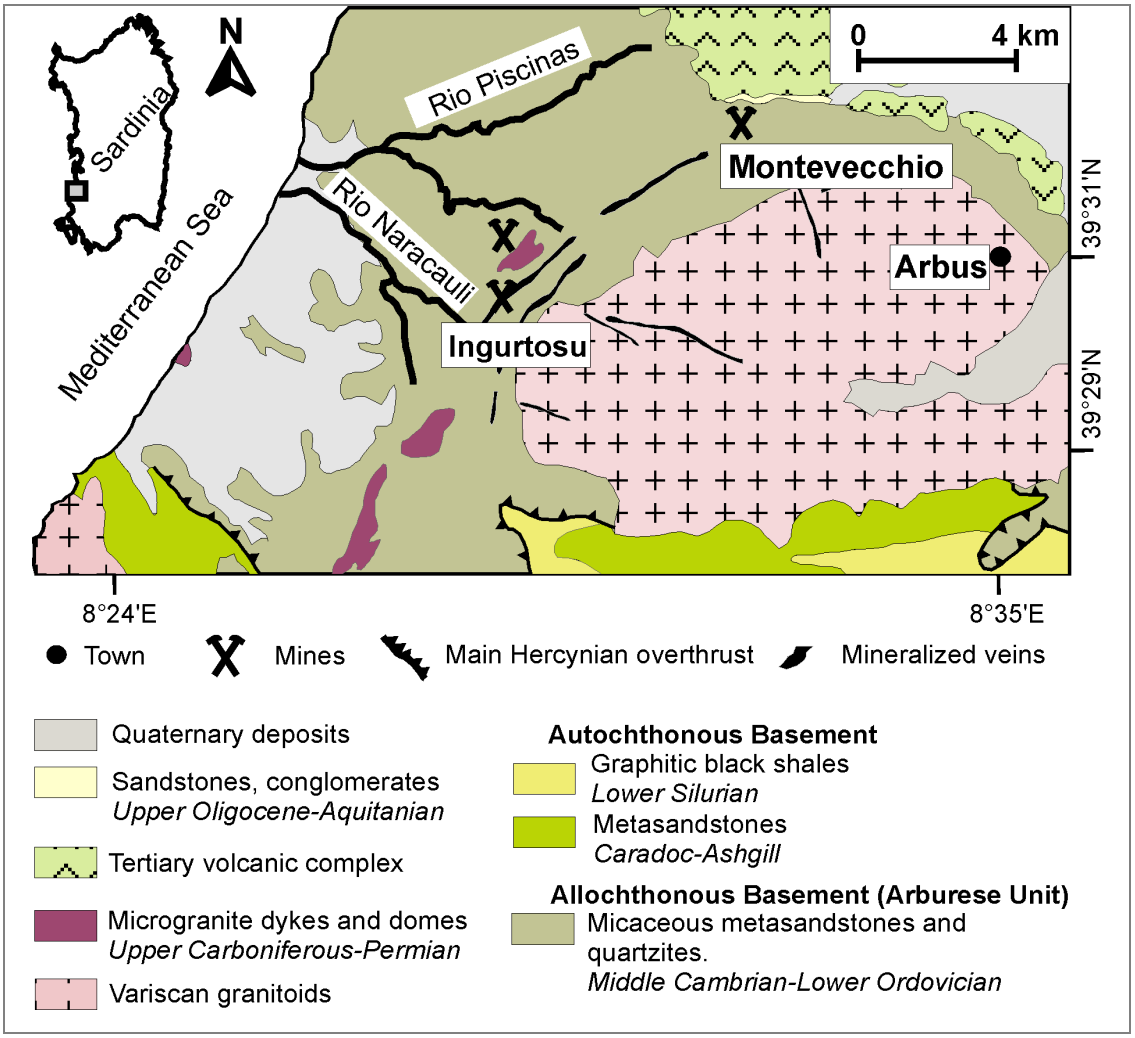

Figure 5. Schematic geological map of the Arburese district (by Carmignani et al., 1996, modified).

Based on records collected in 1979 - 2009 (Regione Autonoma della Sardegna, see the web page http://www.regione.sardegna.it/j/v/25?s=131338&v=2&c=5650&t=1), total annual rainfall was derived using Thiessen polygons. Rainfall (Fig. 6) ranges from 483 mm (1994 - 1995 hydrological year) to 1,040 mm (2008 - 2009 hydrological year) with a mean of 723 mm. Figure 7 shows that maximum rainfall occurs in autumn, especially in November. During spring the highest rainfall is in April, then it decreases reaching a minimum in summer (July). The mean annual

temperature is 17°C (Regione Autonoma della Sardegna, see the web page http://www.regione.sardegna.it/j/v/25?s=131338&v=2&c=5650&t=1).

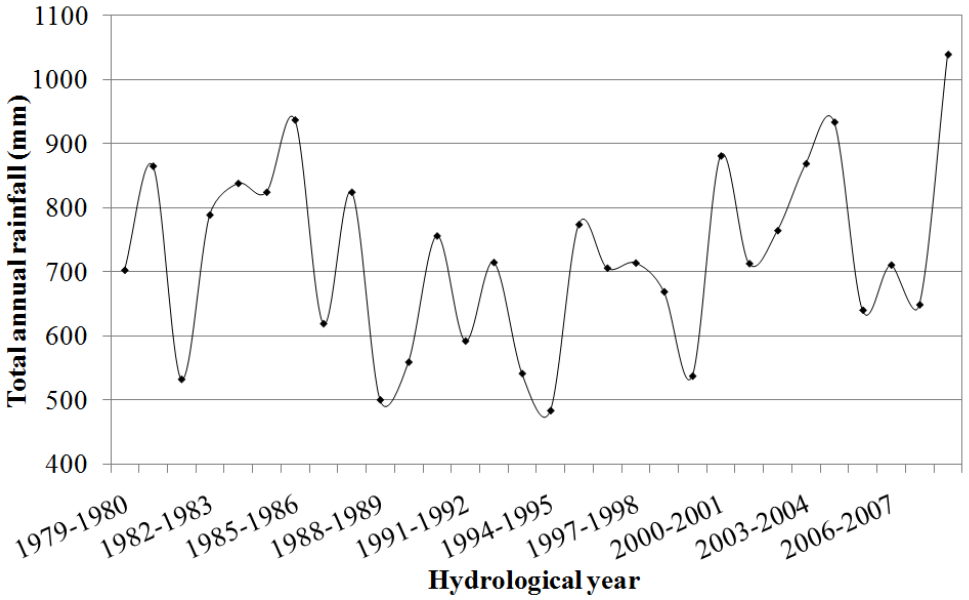

Figure 6. Variation in total annual rainfall from 1979 to 2009 in the Naracauli stream catchment area. Total annual rainfall was derived using Thiessen polygons and data from RAS and Pala et al., 1996.

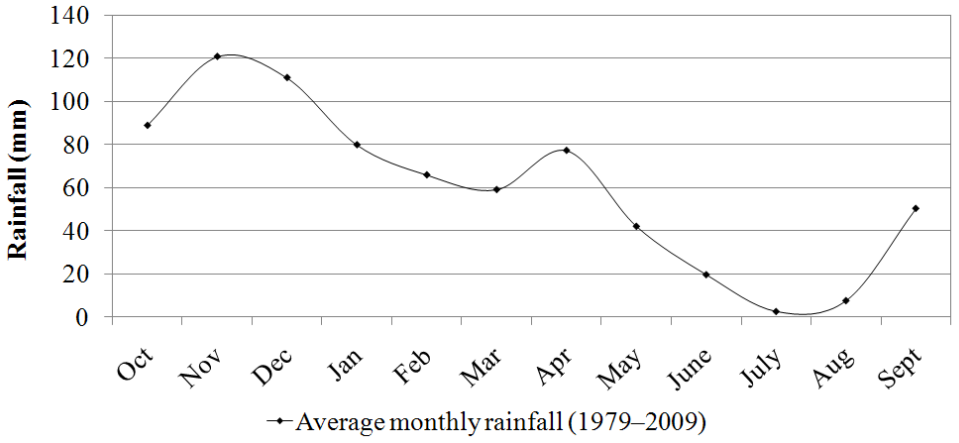

Figure 7. Average monthly rainfall distribution in the Naracauli stream catchment area. Average monthly rainfall was derived using Thiessen polygons and data from RAS and Pala et al., 1996.

The Naracauli stream drains the watershed and flows from Punta Tintillonis at 552 m a.s.l. down to the west and into the Mediterranean Sea (see Figs. 8 and 11). Its channel, which is 8.2 km long, flows across a landscape characterized by moderate relief and hilly morphology. Its pattern is structurally controlled. It receives drainage from four tributaries: Rio Pitzinurri, Rio Sa Roa, Rio Bau, and Rio Sciopadroxiu. Furthermore, Naracauli stream receives drainages from soil seepages and adits. The flow regime is typically torrential, with large flow variations between the wet (>100 l/s) and dry (<10 l/s) seasons.

2.2 ORE DEPOSITS

Ore deposits located in the Montevecchio-Ingurtosu district are attributable to the fourth metallogenic period related to Varisican Orogeny metamorphism and magmatism. These events had strong effects both as a promoter of the remoulding of pre-existing ore/mineral concentrations (by tectonic effects and/or by post-magmatic fluid circulation) and as a source of new ore and industrial minerals. Deposits formed during this period are classified as hydrothermal base-metal and industrial-mineral veins, some of which were among the most important mining reserves of Sardinia (Marcello et al., 2004). The vein system extends in a NNE-SSW direction for at least 12 km. The vein bodies were mostly emplaced within the thermo-metamorphic aureole of the Variscan intrusion, but partly cut the intrusion itself (so-called radial veins). The main veins at Ingurtosu were the Brassey vein and the Ingurtosu vein. The Brassey vein was the most important both for its length (more than 2 km) and for the mineralization grade.

The main ore minerals were galena and sphalerite; chalcopyrite and pyrite were present in small amounts. Gangue minerals were quartz and Fe-bearing carbonates (ankerite and siderite; Cavinato et al., 1948). Other accessory minerals were greenockite, arsenopyrite, Ni- and Co-sulfides, sulfosalts, goethite, hematite, and cuprite (Stara et al., 1996). Calcite and dolomite were locally found in the gangue.

Secondary minerals include smithsonite, cerussite, azurite, malachite, barite, anglesite, pyromorphite, and mimetite.

At Montevecchio-Ingurtosu, total tonnage was estimated at about 50-60 M tons of crude ore, grading 10-11 % combined Pb+Zn, 500-1,000 g Ag per ton of Pb, and 1,000 g of Cd per ton of Zn (Marcello et al., 2004). Metal production from the Montevecchio ores between 1848 and 1973 was 1.6 x 10^6 tons of Pb, 1.1 x 10^6 tons of Zn, and about 1 x 10^3 tons of Ag. By-products were Bi, Cd, Cu, Sb, and Ge (Salvadori et al., 1973).

2.3 MINING HISTORY

Because of the abundance of several metal minerals and rocks used in industry, Sardinia has for centuries been a prominent mining area in Europe. Specifically, the Iglesiente and Arburese districts were a world class resource of Pb and Zn.

In 1853, the Ligurians Marco and Luigi Calvo obtained permission for prospecting in Gennamari and Ingurtosu, and formed the *Società Mineralogica di Gennamari* (Mineralogical Society of Gennamari). Once they obtained the mining concession of Gennamari, they handed it over two years later, to the *Sociétè Civile des Mines d'Ingurtosu et Gennamari* (16 January 1855), a French capital society. In 1859 the French society obtained the mining concession for Ingurtosu, too (Concas et al., 1994), and started extraction of ore minerals from the Ingurtosu and Sant'Anna veins. The extracted mineral was both handpicked by the miners, to separate gangue material from the ore, and treated at Ingurtosu and Casargiu plants (Progemisa, 2001). In these years, Pb-sulphide production from the Ingurtosu ores reached 220 tons per month. In 1869, the development of horizontal tunnels reached a total length of 5,500 m; the maximum depth was about 160 m from the surface (Sella, 1999). In 1870 a new system of mine dewatering, that made use of mechanical pumps, was installed, a light railway was built to carry the concentrated ore from the processing plants to the loading wharf of Piscinas, where it would have been brought to the port

of Carloforte (Mezzolani et al., 1993; Stara et al., 1996). At the end of the 1800, a rich vein near the Casargiu yard (the Brassey vein) was discovered. A treatment plant (Brassey; Fig. 8) began operation in 1900 (Concas et al., 1994). Between 1903 and 1905, a cableway was built to transport the ore from the yards of Gennamari to the Brassey plant, with a remarkable saving on the production costs. In 1906, in the Brassey plant, magnetic grading machines Primosig were tried and found to be successful. Thanks to these machines it was possible to simplify the working of blendes rich in iron oxides (Mezzolani et al., 1993). Because of the increased production after the First World War, the Pireddu plant (Fig. 9) was established in the 1920s. In this period, building of the Ledoux Gallery was started. This was needed to transport mineral from Pinnadeddu and Gennamari mines to the Pireddu plant (Progemisa, 2001). In the early 1940s came the first signs of exhaustion of the veins on which the mine worked. The years following the Second World War saw several attempts to ration the production. At the end of the 1950s production steadily declined, and in 1968 the mine was definitively closed, and the last hundred miners that remained lost their jobs (Mezzolani et al., 1993; see the web page http://www.minesofsardinia.com).

Figure 8. Ruins of the Brassey treatment plant at Ingurtosu. The Brassey treatment plant was inaugurated by Thomas Alnutt Brassey on October 17 of 1900.

Figure 9. Ruins of the Pireddu treatment plant at Ingurtosu established in the 1920s.

During mining activities, the mining-related waste materials and flotation tailings were deposited near the flotation plants or along the valleys (Fig. 10); their distribution is shown in Figure 11. The total volume of mining residues in this area was estimated about 75 x 10^4 m^3 (Loi 1992). To avoid wind erosion and transport, flotation muds were covered with thin layers of gravel. Until 1968, runoff and creek waters were diverted by a system of galleries and channels. Tailing dams were built by simply using gravel and old train cars. Since the galleries and channel system were abandoned, the dams and the tailings have been deeply eroded by the action of water, resulting in a large, downstream dispersion of contaminated materials.

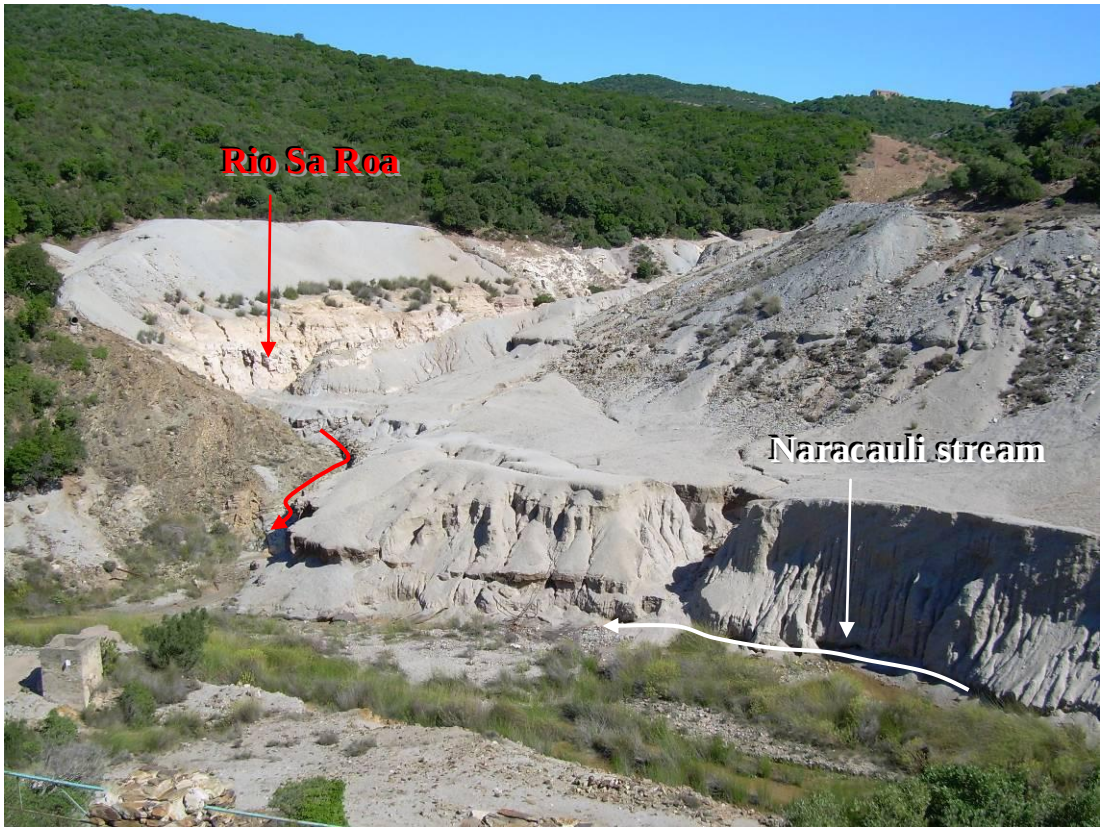

Figure 10. Mining-related waste materials and flotation tailings banked along the valleys of the Naracauli stream (white arrow) and the Rio Sa Roa (red arrow). The curved arrows indicate the flow direction of the two streams.

CHAPTER 3 MATERIALS AND ANALYTICAL METHODS

3.1 WATER SAMPLES

For the purpose of this study, water samples in the Naracauli stream catchment were collected from 2009 to 2011, under different seasonal conditions. Water characters showed distinct seasonal variations (described below), but no major change from year to year. Following these observations, data collected in 2009 have been selected to describe seasonal variations in water geochemistry because they represent the most complete data in terms of seasonal variations.

Locations of water sampling stations are shown in Figure 11. Water samples A, B and C drain mine tailings and wastes. At stations A and B (Figs. 12a and b), water flows first through an artificial channel, then into the Naracauli stream. Station C is located at the base of the tailings on the left side of the Naracauli stream. Water flow at station C is perennial, unlike stations A and B, which are dry in summer. Sample E is the water flowing out of the Ledoux Gallery. Samples D, F, G and H were collected from the tributaries Rio Pitzinurri, Rio Sa Roa, Rio Bau and Rio Sciopadroxiu. Samples from NS-100 to NS-5300 were collected along the Naracauli stream (NS). Numbers after the label NS indicate distance (m) measured along the Naracauli stream from a zero point established at station A. In Figure 11, a magnification from station NS-100 to NS-590 is shown, this is the part of the Naracauli stream where hydrozincite precipitates. Photos in Figures 12 and 13 show the sites where hydrozincite occurs.

For the investigation of short-term chemical variations in the Naracauli stream, at station NS-420 water sampling was performed over a 45-h period: from h 20:00 to h 17:00 two days later (June 13 - 15, 2011; 14 samples). The station NS-420 was chosen because it is the site characterized by the highest amount of hydrozincite precipitation in the Naracauli stream.

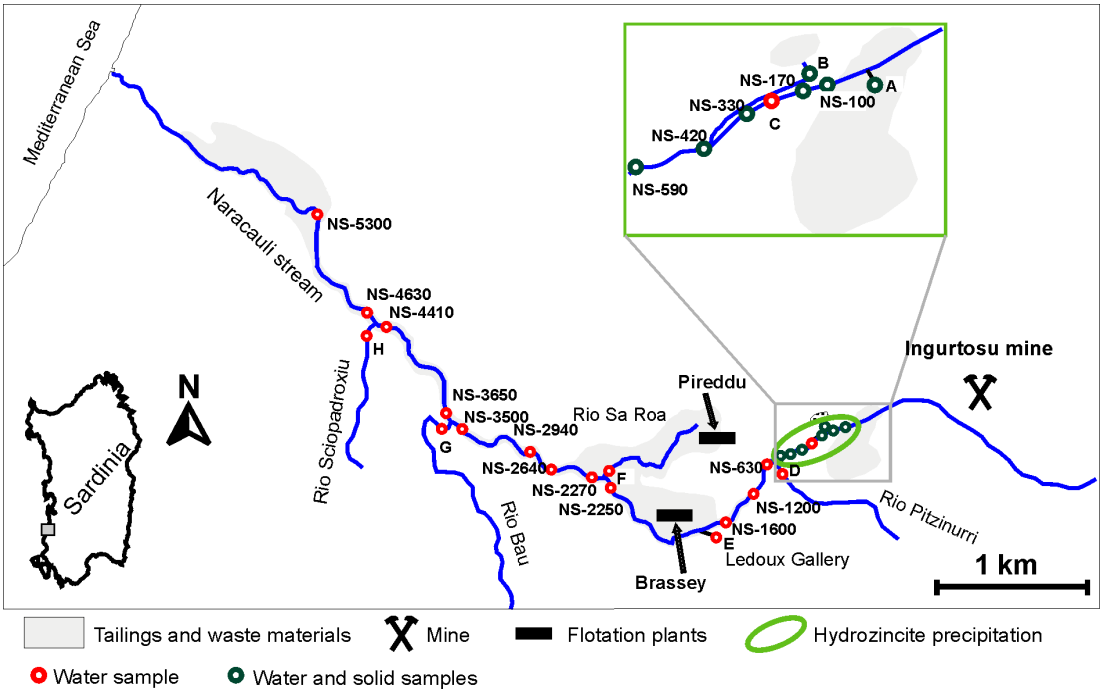

Figure 11. Map showing the location of water and solid samples, the distribution of mining-related residues and the stations where hydrozincite bioprecipitation occurs.

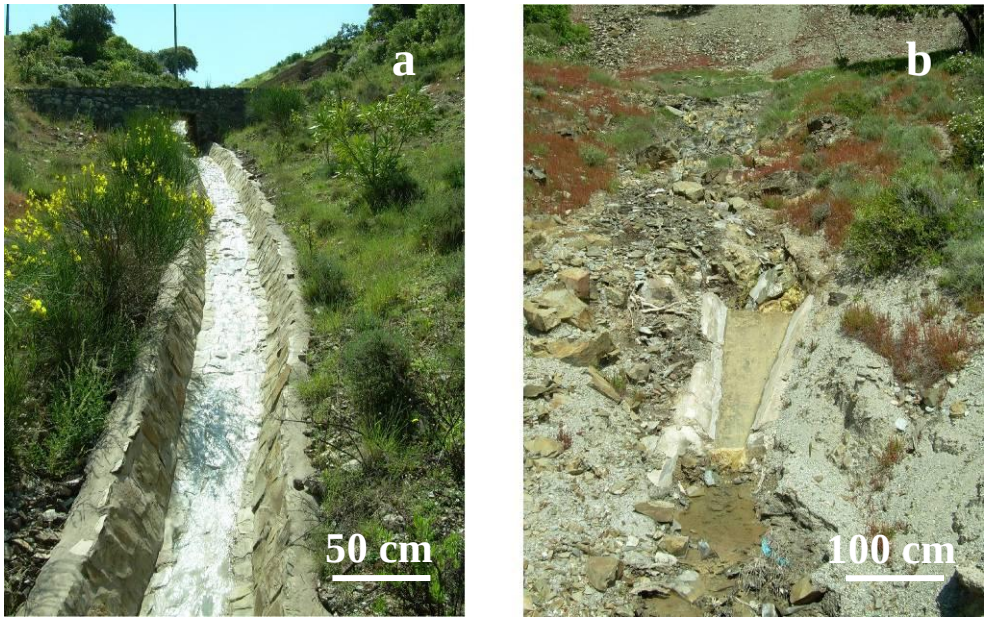

Figure 12. Water stations A (a) and B (b). Water at these stations drains mine tailings and wastes and flows first through an artificial channel, then into the Naracauli stream. Hydrozincite collected at these stations occurs either as white material in suspension (station A) or white-ochre crusts covering the channel or the stones (stations A and B).

Figure 13. Water stations NS-100 (a), NS-170 (b), NS-330 (c), NS-420 (d), NS-590 (e). At these stations, hydrozincite consists of crusts with variable thickness and colour (white, ochre, green) depending on the amount of organic matter and iron-oxides. In Figure 13d (station NS-420) a polycarbonate sheet is circled. Polycarbonate sheets were nailed on the riverbed to facilitate hydrozincite collection.

Temperature, pH, redox potential (Eh), electrical conductivity (EC) and dissolved oxygen were measured in the field. The Eh was measured with a platinum electrode, and values were corrected against the Zoßell's solution (Nordstrom, 1977). Alkalinity was measured both in the field and in the laboratory using the titration method with hydrochloric acid (indicator: methyl orange) and the Gran function plot method, respectively. Dissolved oxygen was measured with the dissolved oxygen meter AL20Oxi with air calibration. Water samples were filtered using a 0.4 μm Nuclepore filtering system, and collected in acid pre-cleaned polyethylene bottles; for cation analyses, a portion was acidified to 1% HNO_3, and analyzed by inductively coupled plasma optical emission spectrometry (ICP-OES) and/or by inductively coupled plasma mass spectrometry (ICP-MS). Non-acidified portions were analysed for anions by ion chromatography. As detailed below, many waters are very rich in Zn. To ascertain whether part of this high Zn content can be ascribed to sub-micrometer nanoparticles, water sample aliquots were filtered in the field using both 0.4 and 0.01 μm pore size filters. The difference between the two filtered aliquots, evaluated at selected sites, was always less than the analytical error (10% maximum). Therefore, only results from 0.4 μm filtered aliquots are considered in this work.

The detection limit (DL) for chemical elements was calculated at 10 times the standard deviation of the blank solutions. The DL may vary depending on instrument performance, and values obtained at each analytical sequence are reported. Field blank solutions were prepared at each campaign, and analysed to check contamination during sampling. To evaluate the accuracy and precision of trace elements, the SRM 1643e and ES-L-1 standard reference solutions were used. Moreover, rhodium was used as internal standard for ICP-MS analysis to correct for instrumental drift. The ionic balance was always less than ± 10%.

Speciation and equilibrium calculations were performed using the PHREEQC computer program (LLNL database); the saturation index (SI) with respect to hydrozincite is calculated as $SI = \log (IAP/K_s)$, where IAP is the Ionic Activity Product and K_s the solubility equilibrium constant at the specific water temperature

(Parkhurst et al., 1999). The solubility equilibrium constant of hydrozincite used to calculate SI is $10^{30.41}$ (Schindler et al., 1969) corresponding to the reaction:

$$Zn_5(CO_3)_2(OH)_6 + 8H^+ \leftrightarrow 5Zn^{2+} + 2\ HCO_3^- + 6\ H_2O$$

3.2 SOLID SAMPLES

From 2009 until 2011, about 30 hydrozincite samples were collected at several sites in the Naracauli stream, under different seasonal conditions. Hydrozincite collected at station A occurs either as white material in suspension or white crusts covering the channel. In station B, hydrozincite precipitates as white-ochre crusts on stones. Figure 14 shows some samples collected from station NS-100 to NS-590, where hydrozincite consists of crusts with variable thickness and colour (white, ochre, green) depending on the amount of iron-oxides and organic matter. Hydrozincite precipitates either on inorganic substrates like stones or on organic substrates such as roots, leaves and twigs. At some sampling sites, polycarbonate sheets (Figs. 13d and 14g) were nailed on the riverbed to facilitate hydrozincite collection. During the rainy season this material is largely washed away by the running waters.

The samples were lightly ground in an agate mortar and ~200 mg of the powder of each sample was packed into the sample holder for the X-ray diffraction (XRD) analysis. XRD analysis was performed using conventional θ-2θ equipment (Panalytical) with Cu Kα wavelength radiation (λ = 1.54060 Å), operating at 40 kV and 40 mA, using the X'Celerator detector.

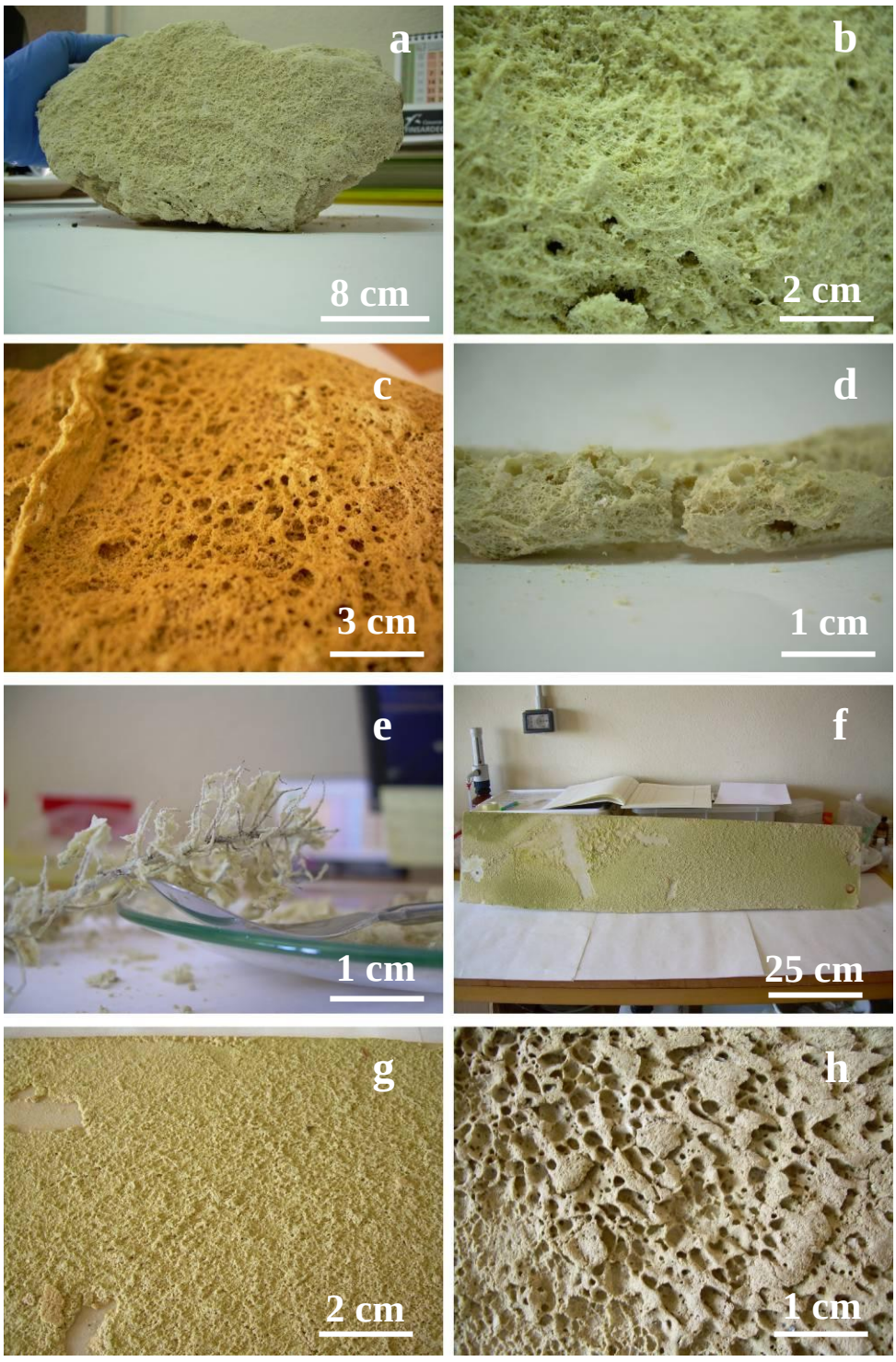

Figure 14. Photos of some solid samples collected from station NS-100 to NS-590. a, b and c) show hydrozincite precipitated on stones. d and e) show hydrozincite precipitated on twigs and roots, respectively. f, g and h) show hydrozincite precipitated on polycarbonate sheets nailed on the riverbed to collect the biomineral.

Elemental characterization of hydrozincite was performed with 0.5 g of each selected sample. A high-purity mixture of 5 ml of 1:1 HNO_3 and 3 ml of Milli Q water was added to the solid samples in a Teflon beaker. The mixtures were then heated in a hot-water bath (~24 hours, 70°C) then 4 ml of concentrated HNO_3 and 4 ml of H_2O_2 (30% by volume) were added. The final solutions were filtered (0.4 μm) and made up to 50 ml final volume using Milli Q water. Elements were determined by ICP-OES and ICP-MS.

Microscopic surface features were investigated using a scanning electron microscope (SEM QUANTA 200, FEI). The samples were coated with gold, using a SEM Coating Unit PS3 (Agar Aids for Electron Microscopy). Specifically, the morphological analysis on hydrozincite samples was performed from SEM photos using the ImageJ software (see http://rsb.info.nih.gov/ij/download.html).

CHAPTER 4 RESULTS AND DISCUSSION

4.1 WATER GEOCHEMISTRY

The analytical results of the water samples from the Naracauli stream catchment are reported in Appendix A. Samples are subdivided into four groups:

- Naracauli stream
- Tributaries
- Tailings drainages
- Mine gallery

Table 1 shows the range of values of pH, redox potential (Eh), electrical conductivity (EC), total dissolved solids (TDS) and saturation index (SI) with respect to calcite in water samples collected in the Naracauli stream catchment. Stream waters from Naracauli and tributaries, and waters from Ledoux Gallery have pH values (6.3 - 8.4) near neutral to slightly alkaline, suggesting a buffering effect of carbonate minerals. Indeed, most waters are at equilibrium or slightly supersaturated with respect to calcite ($SI_{calcite}$ in the range of 0.0 to 1.0). Drainages from tailings have different characteristics: waters at stations A and B show the lowest pH values (6.2 - 7.0), and are undersaturated with respect to calcite ($SI_{calcite}$ in the range of -2 to -1.7). Waters at station C have pH values between 7.0 and 7.6 and are at equilibrium with respect to calcite ($SI_{calcite}$ in the range of 0 to 0.5). Redox potential values (mainly between 0.40 and 0.52 V) indicate oxidizing conditions. TDS varies significantly in the Naracauli stream catchment (0.3 - 2.8 g/l). The drainages from the tailings (stations A and B) have the highest values (1.2 - 2.8 g/l TDS); waters from tributaries (0.3 - 1.1 g/l TDS) and Ledoux Gallery (0.4 - 0.5 g/l TDS) show the lowest values. Accordingly, the highest values of TDS in the Naracauli stream are observed upstream of the confluence with the Rio Pitzinurri (see Fig. 11), while TDS values decrease downstream due to dilution by less saline tributaries.

Table 1. Range of values of pH, redox potential (Eh), electrical conductivity (EC), total dissolved solids (TDS) and saturation index (SI) with respect to calcite in water samples collected in the Naracauli stream catchment area.

Type	pH	Eh	EC	TDS	$SI_{calcite}$
		[V]	[mS/cm]	[g/l]	
Naracauli stream	6.9 - 8.4	0.39 - 0.62	0.72 - 2.19	0.4 - 1.6	0.0 - 1.0
Tributaries	7.0 - 8.3	0.40 - 0.54	0.50 - 1.60	0.3 - 1.1	0.0 - 1.0
Tailings drainages	6.2 - 7.6	0.44 - 0.53	1.43 - 3.28	1.1 - 2.8	-2.0 - 0.5
Ledoux Gallery	6.3 - 8.1	0.44 - 0.46	0.69 - 0.86	0.4 - 0.5	0.1 - 0.6

All waters show NO_2^-, NH_4^+, and PO_4^{-3} below the detection limit of 0.1 mg/l. Nitrate concentrations in the Naracauli stream waters are always lower than the drinking water limit of 50 mg/l established by Italian regulations (D. Lgs 3 Aprile 2006, n. 152).

Water composition is shown in the Piper diagram of Figure 15. This diagram was modified to take into account Zn as major component in many samples. The Naracauli stream waters have a dominant Ca-Mg-sulphate composition, reflecting the composition of tributaries, the interaction with tailings banked close to this stream, and inputs from stations A, B, and C (see Fig. 11). Tributaries have variable composition. Water in Rio Bau has Ca-Mg-sulphate composition. Waters in Rio Pitzinurri and Rio Sciopadroxiu show Na-Ca-chloride and Ca-Na-chloride composition, respectively. Rio Sa Roa, that flows through mine tailings, has a Na-Mg-chloride(sulphate) composition. Waters at Ledoux Gallery have a Ca-Mg-bicarbonate character. Waters flowing out of tailings show variable composition. Stations A and B are characterized by waters showing a predominant Zn-sulphate composition. Waters at station C have a Ca-Mg-sulphate character and lower Zn concentrations, due to a different mineral composition in the waste dump, and because of the possible precipitation of hydrozincite, the saturation limit of which is always exceeded in the water samples at station C ($SI_{hydrozincite}$ in the range of 1 to 4).

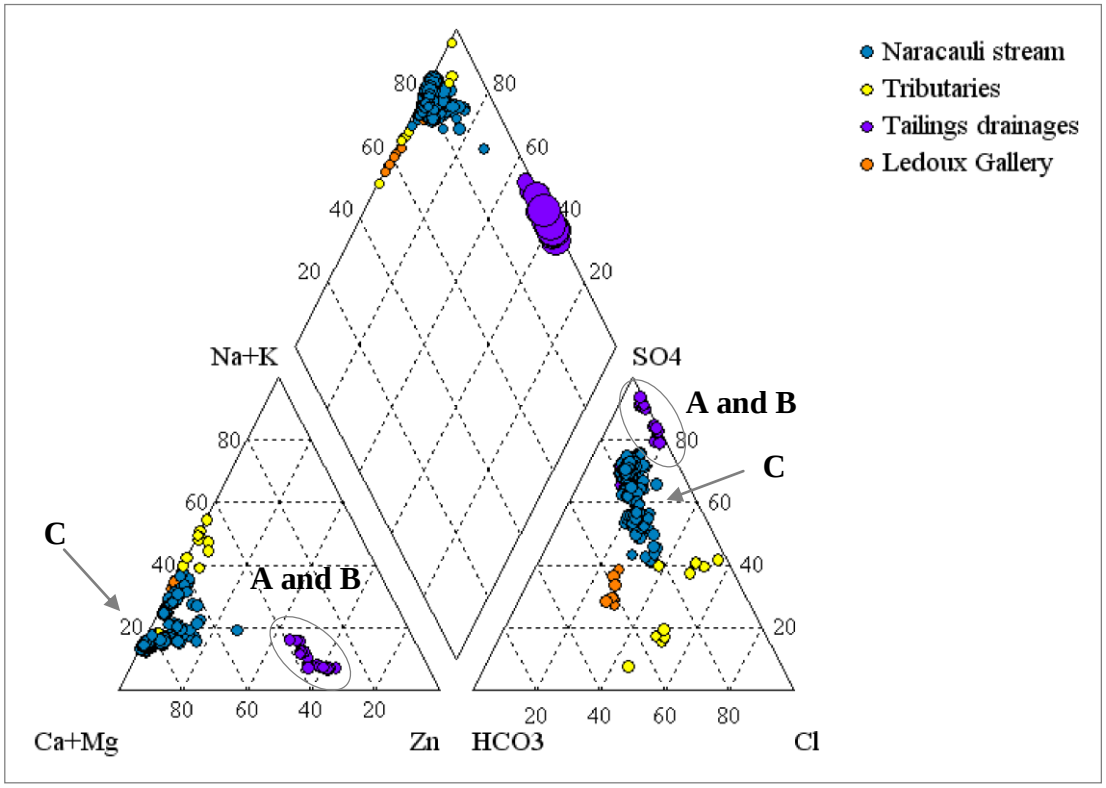

Figure 15. Piper diagram showing the main chemical composition of waters in the Naracauli stream catchment area. Zn is included among the main cations because it is a major component in many samples. The smallest circle correspond to 0.3 g/l TDS and the largest to 2.8 g/l TDS.

Correlation coefficients between various parameters of waters from the Naracauli stream, tributaries and tailings drainages (Nair et al., 2005) are shown in Tables 2a and b. Waters from tailings drainages were considered separately (stations A-B and station C) because of their different composition. Ca^{2+} and SO_4^{2-} values show a strong correlation with the TDS in all water types, Pearson correlation coefficient (ρ) in the range of 0.87 - 0.98 and 0.96 - 1, respectively. TDS is strongly correlated also with Mg^{2+} (ρ: 0.92 - 0.99) in waters from Naracauli stream, tributaries and station C, and with K^{+} (ρ: 0.86 - 0.93) and Zn (ρ: 0.88 - 0.98) in waters from stations A and B, and tributaries. In most waters, SO_4^{2-} shows a strong correlation with Ca^{2+} (ρ: 0.89 - 0.97) and Mg^{2+} (ρ: 0.84 - 0.96), and with Zn (ρ: 0.97) in waters from station A and B.

Table 2a. Results of correlation analysis between pH, TDS, Temperature, Ca, Mg, Na, K, Zn, Cl, SO_4 and HCO_3 in the waters from the Naracauli stream and tributaries. Correlation analysis was performed measuring the Pearson correlation coefficient (ρ). N indicates the number of samples. Significant correlation is shown in bold.

Naracauli stream
N = 152

	pH	**TDS**	**T**	**Ca^{2+}**	**Mg^{2+}**	**Na^{+}**	**K^{+}**	**Zn**	**Cl^{-}**	**SO_4^{2-}**	**HCO_3^{-}**
pH	1.00										
TDS	0.20	1.00									
T	0.33	0.35	1.00								
Ca^{2+}	0.30	**0.98**	0.36	1.00							
Mg^{2+}	0.30	**0.97**	0.38	**0.98**	1.00						
Na^{+}	0.48	0.35	0.44	0.40	0.44	1.00					
K^{+}	-0.07	0.62	0.17	0.57	0.52	-0.02	1.00				
Zn^{2+}	-0.75	0.01	-0.28	-0.12	-0.14	-0.53	0.34	1.00			
Cl^{-}	0.19	0.28	0.32	0.26	0.35	0.56	-0.10	-0.33	1.00		
SO_4^{2-}	0.18	**1.00**	0.34	**0.97**	**0.96**	0.31	0.63	0.04	0.23	1.00	
HCO_3^{-}	0.34	**0.82**	0.37	**0.83**	**0.88**	0.45	0.37	-0.29	0.45	0.77	1.00

Tributaries
N = 11

	pH	**TDS**	**T**	**Ca^{2+}**	**Mg^{2+}**	**Na^{+}**	**K^{+}**	**Zn**	**Cl^{-}**	**SO_4^{2-}**	**HCO_3^{-}**
pH	1.00										
TDS	-0.70	1.00									
T	-0.49	0.68	1.00								
Ca^{2+}	-0.47	**0.87**	0.72	1.00							
Mg^{2+}	-0.68	**0.99**	0.64	**0.83**	1.00						
Na^{+}	-0.72	0.57	0.17	0.09	0.59	1.00					
K^{+}	-0.64	**0.93**	0.74	**0.85**	**0.92**	0.44	1.00				
Zn^{2+}	-0.63	**0.88**	0.60	0.61	**0.86**	0.72	0.74	1.00			
Cl^{-}	-0.62	0.57	0.21	0.11	0.59	**0.97**	0.41	0.75	1.00		
SO_4^{2-}	-0.61	**0.96**	0.66	**0.93**	**0.96**	0.38	**0.92**	0.77	0.36	1.00	
HCO_3^{-}	0.01	0.26	0.55	0.63	0.17	-0.47	0.37	0.08	-0.42	0.33	1.00

Table 2b. Results of correlation analysis between pH, TDS, Temperature, Ca, Mg, Na, K, Zn, Cl, SO_4 and HCO_3 in the waters from the tailings drainages. Correlation analysis was performed measuring the Pearson correlation coefficient (ρ). N indicates the number of samples. Significant correlation is shown in bold.

Tailings drainages (stations A and B)
N = 18

	pH	**TDS**	**T**	**Ca^{2+}**	**Mg^{2+}**	**Na^{+}**	**K^{+}**	**Zn**	**Cl^{-}**	**SO_4^{2-}**	**HCO_3^{-}**
pH	1.00										
TDS	-0.08	1.00									
T	-0.56	-0.14	1.00								
Ca^{2+}	-0.06	**0.93**	-0.24	1.00							
Mg^{2+}	-0.26	-0.11	0.54	-0.32	1.00						
Na^{+}	-0.54	-0.44	0.65	-0.50	0.78	1.00					
K^{+}	0.03	**0.86**	-0.16	**0.82**	-0.07	-0.47	1.00				
Zn^{2+}	**0.81**	**0.98**	-0.22	**0.93**	-0.25	-0.53	**0.81**	1.00			
Cl^{-}	-0.53	-0.44	0.64	-0.54	0.73	**0.95**	-0.53	-0.51	1.00		
SO_4^{2-}	-0.02	**0.99**	-0.18	**0.93**	-0.15	-0.50	**0.88**	**0.97**	-0.51	1.00	
HCO_3^{-}	0.47	0.01	-0.37	-0.02	-0.48	-0.68	0.13	0.08	-0.71	0.08	1.00

Tailings drainage (station C)
N = 19

	pH	**TDS**	**T**	**Ca^{2+}**	**Mg^{2+}**	**Na^{+}**	**K^{+}**	**Zn**	**Cl^{-}**	**SO_4^{2-}**	**HCO_3^{-}**
pH	1.00										
TDS	0.36	1.00									
T	0.15	0.18	1.00								
Ca^{2+}	0.29	**0.95**	0.16	1.00							
Mg^{2+}	0.22	**0.92**	0.03	**0.96**	1.00						
Na^{+}	-0.24	0.38	0.22	0.50	0.51	1.00					
K^{+}	0.12	-0.51	0.15	-0.39	-0.44	-0.09	1.00				
Zn^{2+}	-0.08	-0.23	0.07	-0.36	-0.34	-0.49	-0.06	1.00			
Cl^{-}	0.07	0.39	-0.07	0.25	0.34	0.00	-0.54	0.03	1.00		
SO_4^{2-}	0.40	**0.98**	0.19	**0.89**	**0.84**	0.27	-0.55	-0.14	0.38	1.00	
HCO_3^{-}	0.28	0.74	0.05	0.79	0.76	0.47	-0.11	-0.62	0.24	0.65	1.00

Table 3 reports the minimum, maximum, mean (X), and standard deviation (σ) values of metals in waters of the Naracauli stream catchment. Many waters have high metal contents, Zn being the most abundant. In the Naracauli stream waters, Zn concentrations range from 1.6 to 120 mg/l, the highest values are observed from station NS-100 to station NS-330. Cd (30 - 1,200 µg/l) is the second most abundant metal, with 230 µg/l on average. Also, Pb and Ni have significant concentrations in the range of 3 - 280 and 12 - 150 µg/l, respectively.

Waters draining tailings show the highest concentration of metals, especially Zn and Cd in waters from stations A and B, probably reflecting a higher metal mobility at lower pH (Fig. 16). Generally, the tributaries have the lowest content of Zn, Cd, Pb, Ni and Cu, listed in decreasing order of abundance.

Table 3. Main harmful metal contents in the Naracauli catchment waters: minimum, maximum, mean (X) and standard deviation (σ). N indicates the number of samples.

Rio Naracauli (N = 152)				**Tributaries** (N = 11)			
	Min	Max	X ± σ		Min	Max	X ± σ
Zn (mg/l)	1.6	120	20 ± 18	Zn (mg/l)	0.3	26	10 ± 10
Cd (µg/l)	30	1,200	230 ± 180	Cd (µg/l)	2.3	305	100 ± 110
Pb (µg/l)	3	280	30 ± 30	Pb (µg/l)	2.1	90	20 ± 25
Ni (µg/l)	12	150	70 ± 40	Ni (µg/l)	0.6	40	10 ± 12
Cu (µg/l)	1.1	22	4 ± 3	Cu (µg/l)	0.9	6	4 ± 2
Station A (N = 9)				**Station B** (N = 9)			
	Min	Max	X ± σ		Min	Max	X ± σ
Zn (mg/l)	600	760	670 ± 51	Zn (mg/l)	280	540	400 ± 114
Cd (µg/l)	5,300	7,170	6,000 ± 585	Cd (µg/l)	2,300	5,065	4000 ± 1,117
Pb (µg/l)	490	1,010	700 ± 199	Pb (µg/l)	35	154	80 ± 41
Ni (µg/l)	273	360	320 ± 34	Ni (µg/l)	66	128	100 ± 21
Cu (µg/l)	12	112	60 ± 37	Cu (µg/l)	4.2	10	6 ± 1.9
Station C (N = 19)				**Ledoux Gallery** (N = 8)			
	Min	Max	X ± σ		Min	Max	X ± σ
Zn (mg/l)	12	22	16 ± 2.8	Zn (mg/l)	0.66	11	3 ± 3.5
Cd (µg/l)	48	188	140 ± 33	Cd (µg/l)	4.2	87	20 ± 28
Pb (µg/l)	38	243	160 ± 59	Pb (µg/l)	0.7	42	10 ± 16
Ni (µg/l)	70	120	80 ± 11	Ni (µg/l)	11	67	30 ± 19
Cu (µg/l)	3.2	9.3	6 ± 1.5	Cu (µg/l)	1.4	4	2 ± 1.2

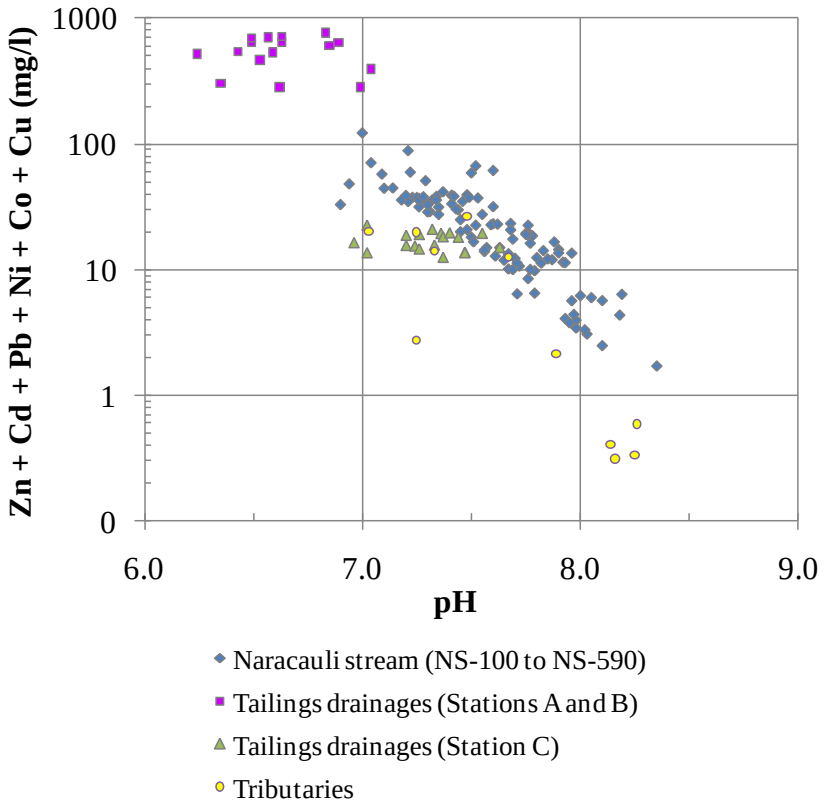

Figure 16. Diagram showing the sum of dissolved base-metal concentrations in the waters from station NS-100 to NS-590 (Naracauli stream), tailings drainages (stations A, B and C) and tributaries as a function of pH.

Figures 17 - 20 show binary plots for metals (Zn, Pb, Cd and Ni, respectively) and sulphate. In the part of the Naracauli stream where bioprecipitation occurs (from station NS-100 to NS-590) Zn, Pb and Cd have a negative correlation with SO_4. The waters draining mine tailings show two different trends: waters collected at stations A and B are characterized by a positive correlation between SO_4 and Zn, Pb, Cd and Ni; in waters at station C no correlation is observed.

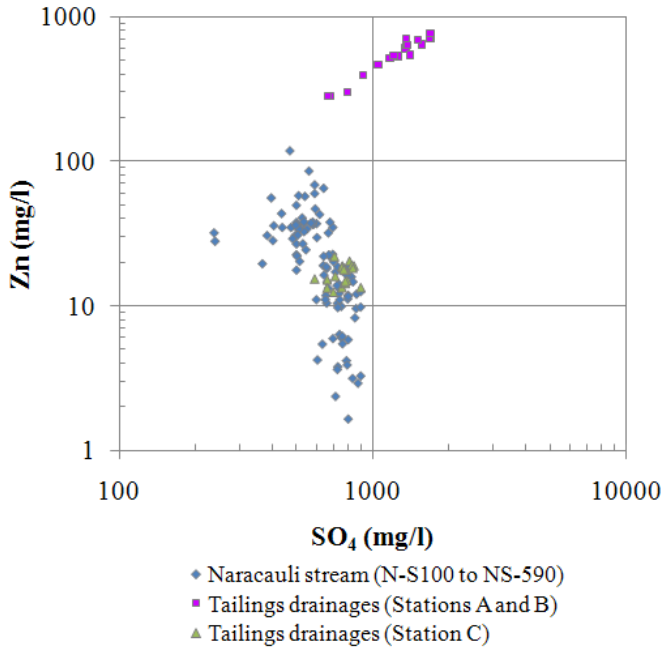

Figure 17. Plot showing Zn versus sulphate concentrations in the waters from station NS-100 to NS-590 (Naracauli stream) and tailings drainages (stations A, B and C).

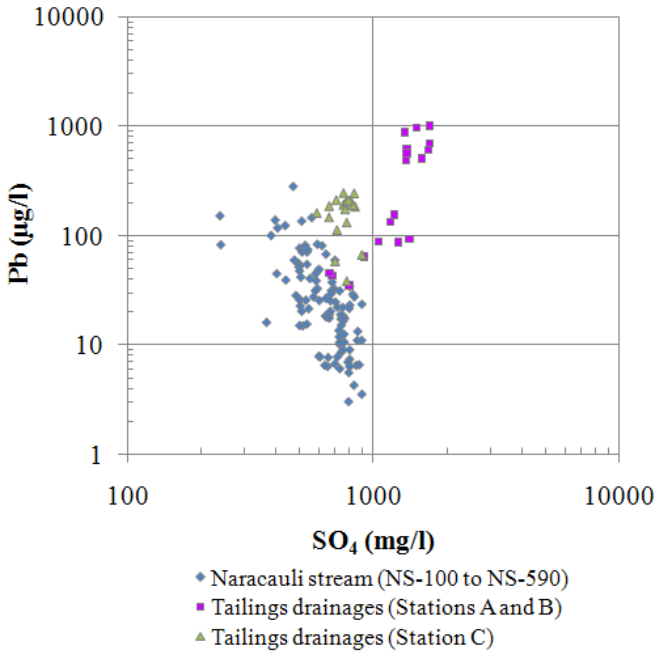

Figure 18. Plot showing Pb versus sulphate concentrations in the waters from station NS-100 to NS-590 (Naracauli stream) and tailings drainages (stations A, B and C).

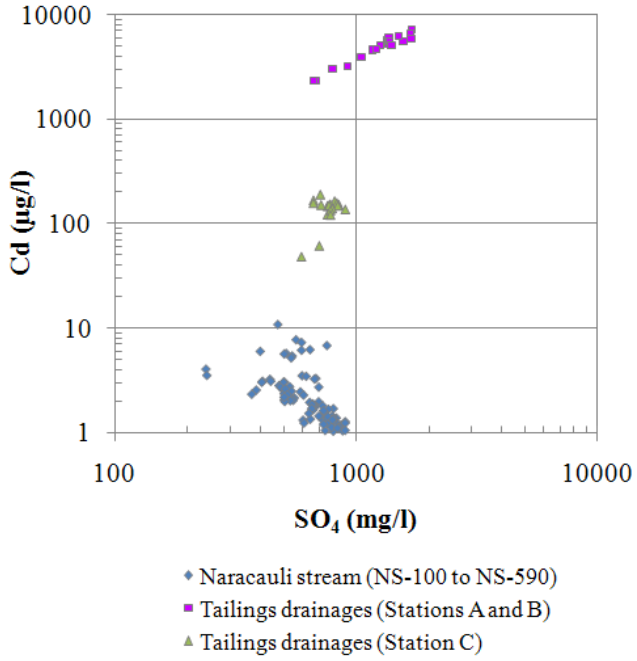

Figure 19. Plot showing Cd versus sulphate concentrations in the waters from station NS-100 to NS-590 (Naracauli stream) and tailings drainages (stations A, B and C).

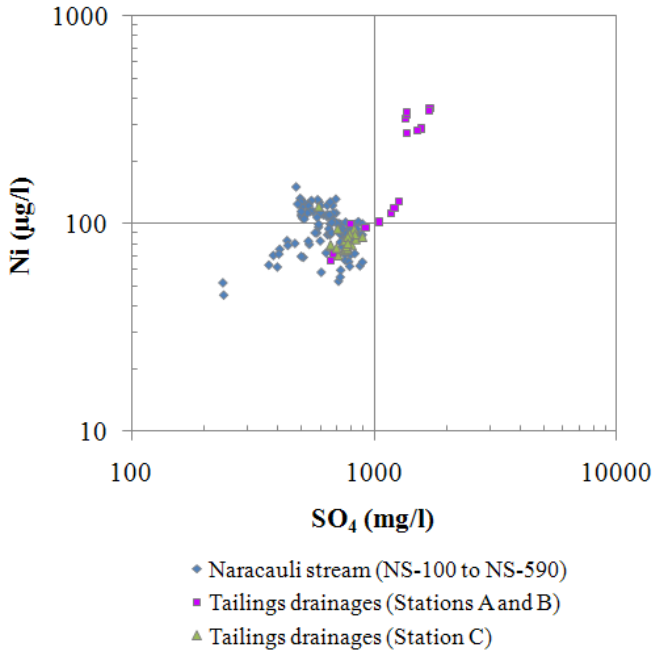

Figure 20. Plot showing Ni versus sulphate concentrations in the waters from station NS-100 to NS-590 (Naracauli stream) and tailings drainages (stations A, B and C).

Binary plots Zn/Pb, Zn/Cd, Zn/Ni and Zn/Co are shown in Figures 21 - 24, respectively. Both Naracauli stream waters (from station NS-100 to NS-590) and stations A and B (tailings drainages) show a positive correlation between Zn and the other metals. In waters at station C (tailings drainages) no correlations are observed except between Zn/Cd (Fig. 22). All water types included in Figure 22 show a strong logarithmic correlation between Zn and Cd concentrations. The nearly constant Zn/Cd ratio (close to 100) among samples could suggest the weathering of a relatively uniform composition of sphalerite from tailings and mine wastes.

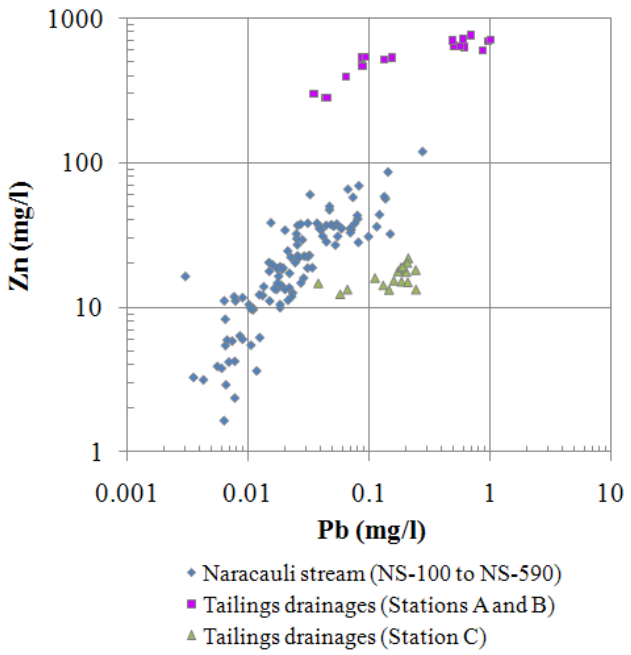

Figure 21. Plot showing Zn versus Pb concentrations in the waters from station NS-100 to NS-590 (Naracauli stream) and tailings drainages (stations A, B and C).

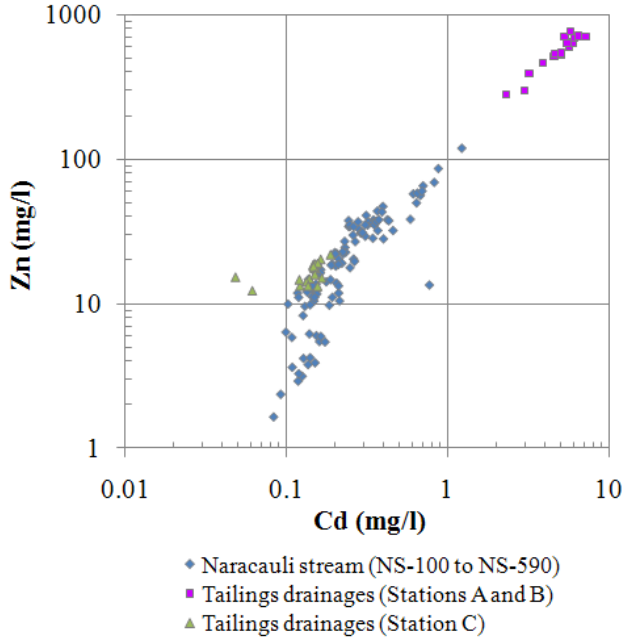

Figure 22. Plot showing Zn versus Cd concentrations in the waters from station NS-100 to NS-590 (Naracauli stream) and tailings drainages (stations A, B and C).

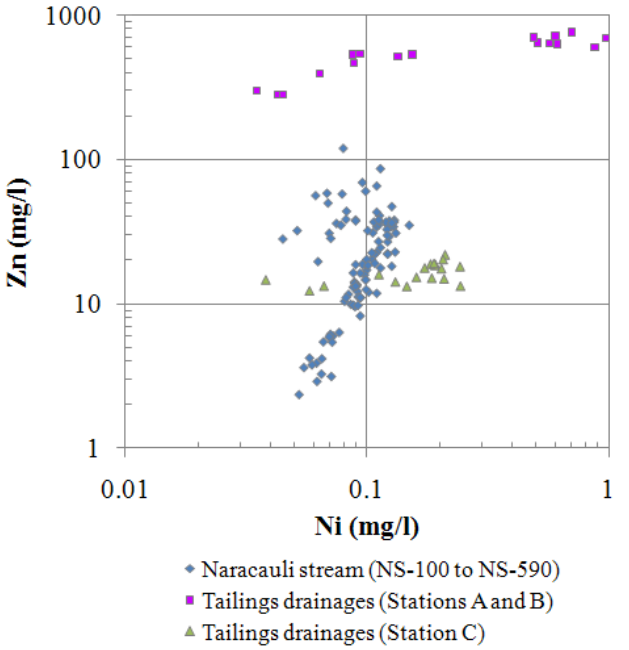

Figure 23. Plot showing Zn versus Ni concentrations in the waters from station NS-100 to NS-590 (Naracauli stream) and tailings drainages (stations A, B and C).

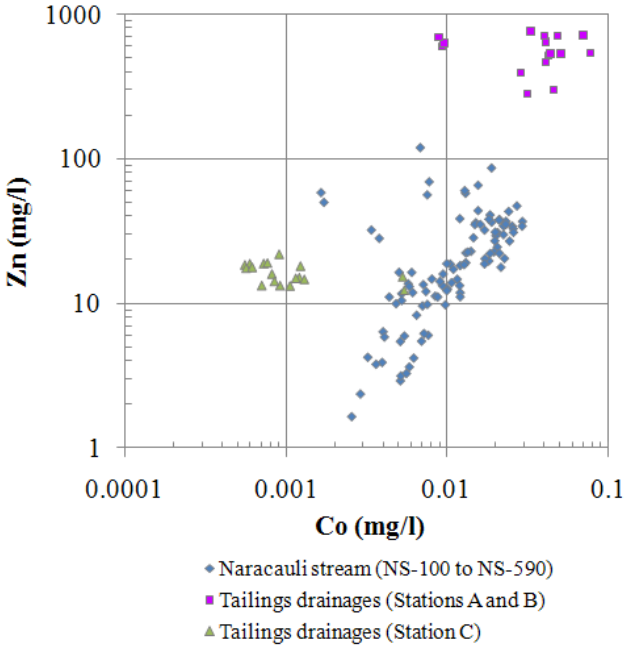

Figure 24. Plot showing Zn versus Co concentrations in the waters from station NS-100 to NS-590 (Naracauli stream) and tailings drainages (stations A, B and C).

Results of chemical speciation modelling of dissolved Zn, Cd, Pb, and Cu indicate that Zn^{2+} (70 - 85 %), $ZnSO_4^0$ (10 - 25 %), Cd^{2+} (50 - 55 %), $CdCl^+$ (40 - 45 %), $PbCO_3^0$ (70 - 90 %), Pb^{2+} (5 - 25 %), $CuCO_3^0$ (80 - 90 %) and $CuOH^+$ (5 - 10 %) are the dominant species in Naracauli stream waters. Pb^{2+} (80 - 85 %) and Cu^{2+} (50 - 60 %) species are more abundant than $PbCO_3^0$ (5 - 10 %) and $CuCO_3^0$ (10 - 20 %), respectively in waters at stations A and B, likely reflecting the low availability of carbonate ions due to their lower pH values.

Figures 25 - 28 show variations in Zn, Mn, Cd, Co, Ni, and Pb concentrations measured in non-filtered (nF) and filtered (F0.4) aliquots of some selected samples. Total (nF) and dissolved concentration (F0.4) of Zn, Mn, Cd, Co and Ni are similar with variations lower than the analytical error (<10%). Pb shows lower concentrations in filtered than non-filtered samples, probably, due to the tendency of Pb to associate with suspended particles.

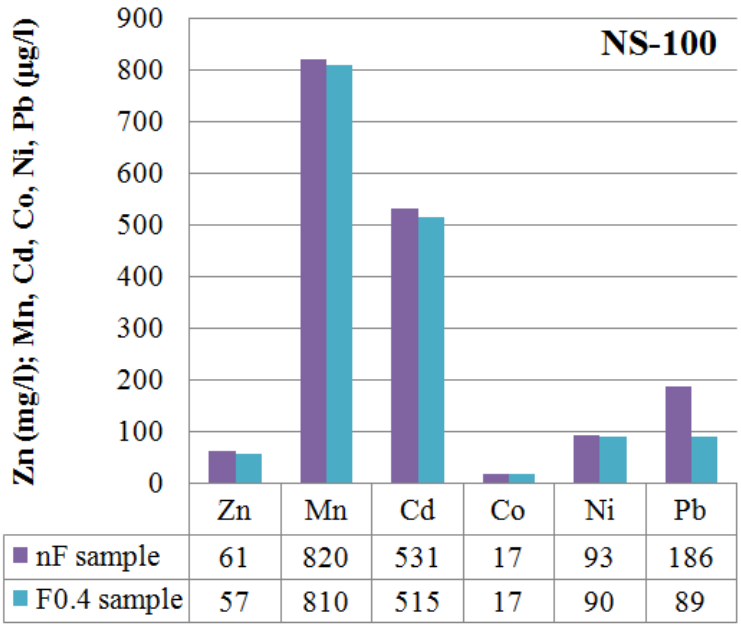

	Zn	Mn	Cd	Co	Ni	Pb
nF sample	61	820	531	17	93	186
F0.4 sample	57	810	515	17	90	89

Figure 25. Histogram showing Zn, Mn, Cd, Co, Ni and Pb concentration for non-filtered (nF) and filtered (F0.4) waters sampled at station NS-100 on May 19, 2010.

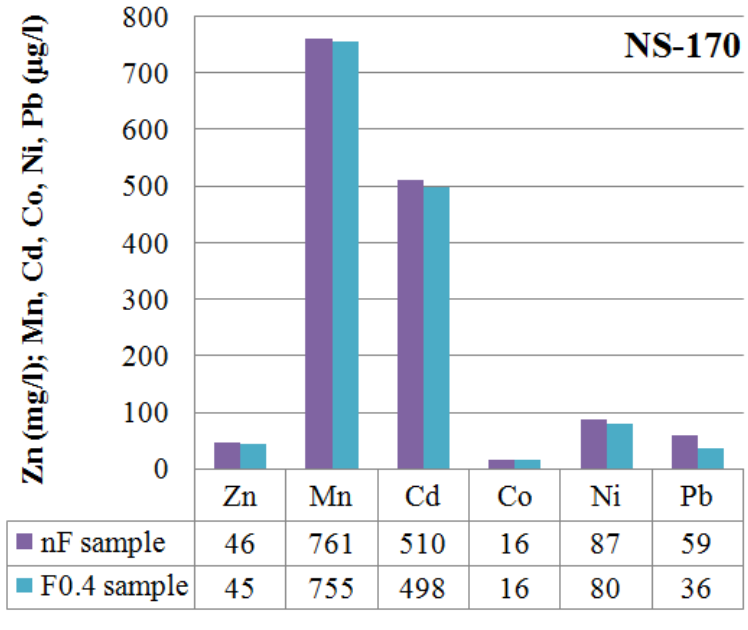

	Zn	Mn	Cd	Co	Ni	Pb
nF sample	46	761	510	16	87	59
F0.4 sample	45	755	498	16	80	36

Figure 26. Histogram showing Zn, Mn, Cd, Co, Ni and Pb concentration for non-filtered (nF) and filtered (F0.4) waters sampled at station NS-170 on May 19, 2010.

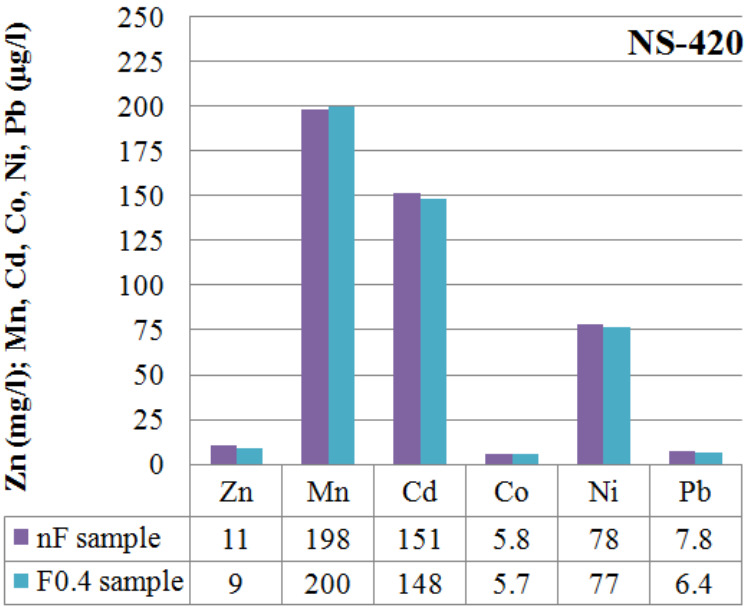

Figure 27. Histogram showing Zn, Mn, Cd, Co, Ni and Pb concentration for non-filtered (nF) and filtered (F0.4) waters sampled at station NS-420 on May 19, 2010.

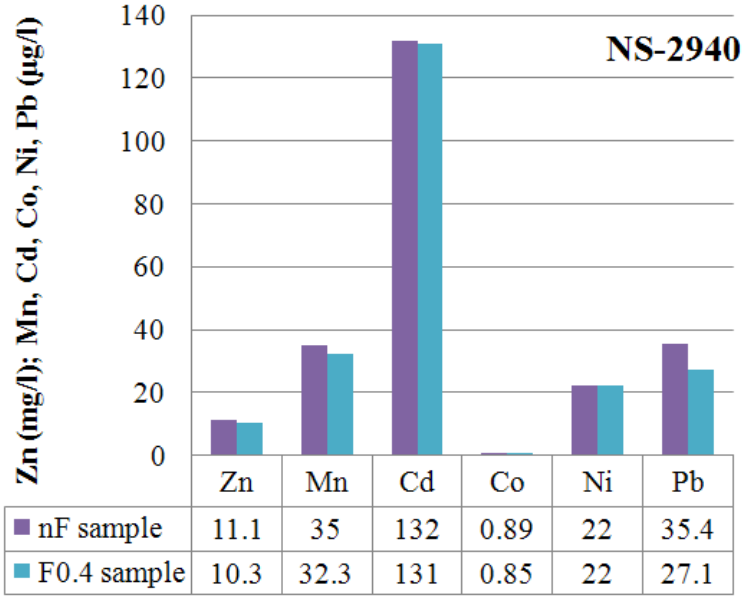

Figure 28. Histogram showing Zn, Mn, Cd, Co, Ni and Pb concentration for non-filtered (nF) and filtered (F0.4) waters sampled at station NS-2940 on May 18, 2010.

Taking into consideration the stations where bioprecipitation occurs (from station NS-100 to NS-590), concentrations of major and trace elements determined in the water filtered through 0.4 µm pore-size filters change under different seasonal conditions. Specifically, Ca, Mg, B, Sr (Fig. 29) and Li show higher concentrations in water samples collected under low-flow conditions (May-September), probably due to evaporation processes and/or a higher contribution of groundwater to the streams during low rain periods. On the contrary, concentrations of Zn, Cd, Pb and Ni (Fig. 30) are higher under high-flow condition (October-April), probably due to the high runoff through the tailings. Similar seasonal variations have been observed in previous studies of Sardinian rivers sampled under different flow conditions. Increasing concentrations of Zn, Cd, Pb and Ni in winter under high flow conditions were attributed to aqueous transport of these metals in association with very fine particles, i.e. <0.4 µm (Cidu et al., 2007; Cidu et al., 2009).

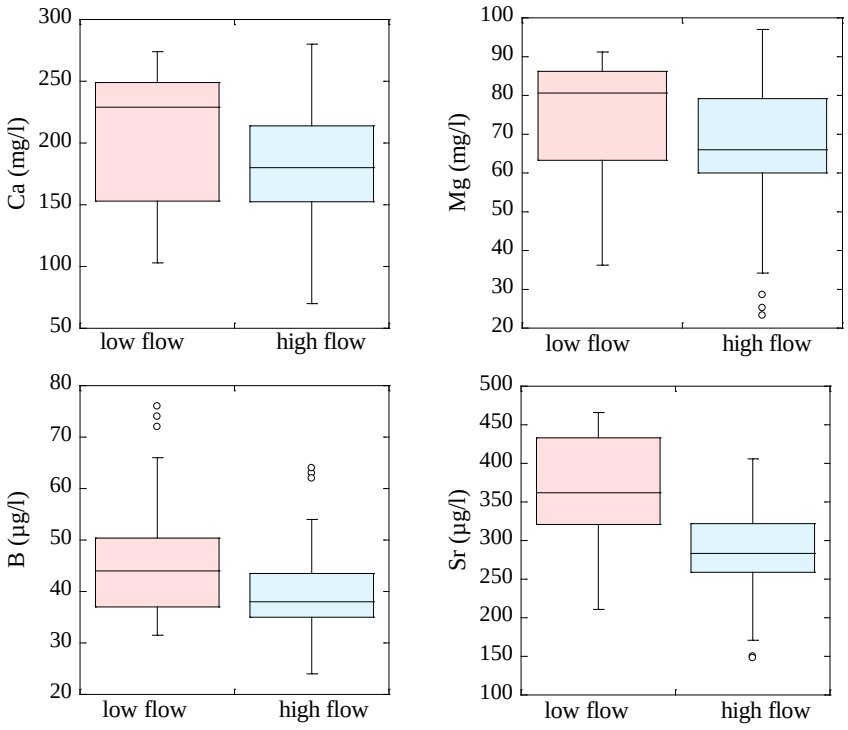

Figure 29. Box plots showing Ca, Mg, B and Sr concentrations for filtered waters sampled under low-flow (May-September) and high-flow (October-April) conditions from station NS-100 to NS-590 (Naracauli stream). Each box includes the 25th and 75th percentiles with the median displayed as a line. The outliers are displayed as individual points.

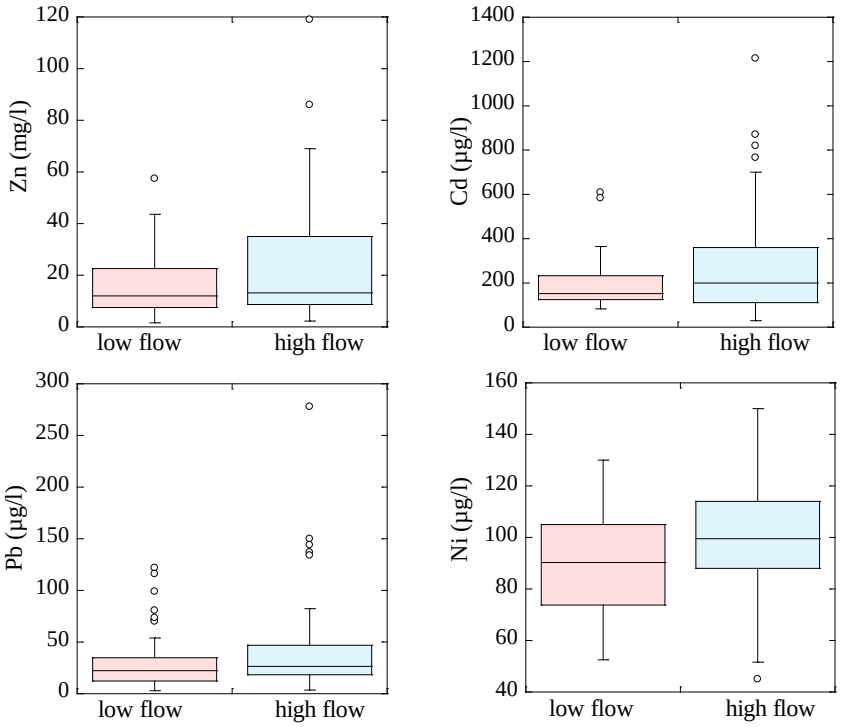

Figure 30. Box plots showing Zn, Cd, Pb and Ni concentrations for filtered waters sampled under low-flow (May-September) and high-flow (October-April) conditions from station NS-100 to NS-590 (Naracauli stream). Each box includes the 25th and 75th percentiles with the median displayed as a line. The outliers are displayed as individual points.

Figures 31 and 32 show the influence of rainfall on pH and selected metals concentrations at stations NS-100 and NS-420. The amount of rain reported in these figures corresponds to the average value calculated on five days before each sampling trip. In general, after heavy rain pH values tend to decrease, while Zn, Cd and Pb concentrations increase reaching higher concentrations than the mean values. This behaviour can be due to the effects of runoff flowing into the stream: high runoff carries high Zn, Cd, and Pb contents which are leached from the mining wastes, and the acidic contribution of rain water, together with a major oxidation of sulphides, causes the decrease in pH.

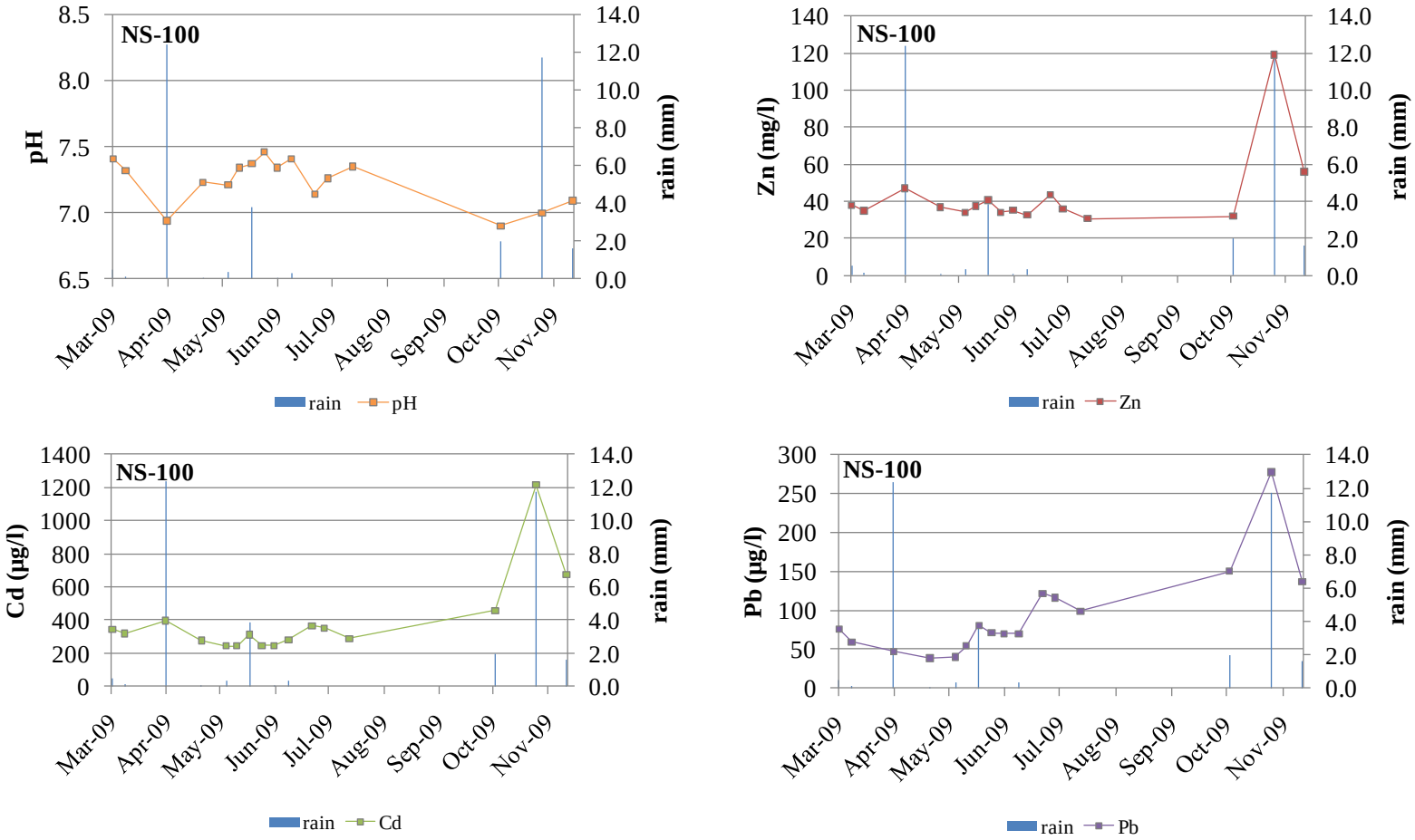

Figure 31. Plots showing the influence of rainfall on pH, Zn, Cd and Pb concentrations at station NS-100 (Naracauli stream). The reported amount of rain corresponds to the average value calculated on five days before surveys.

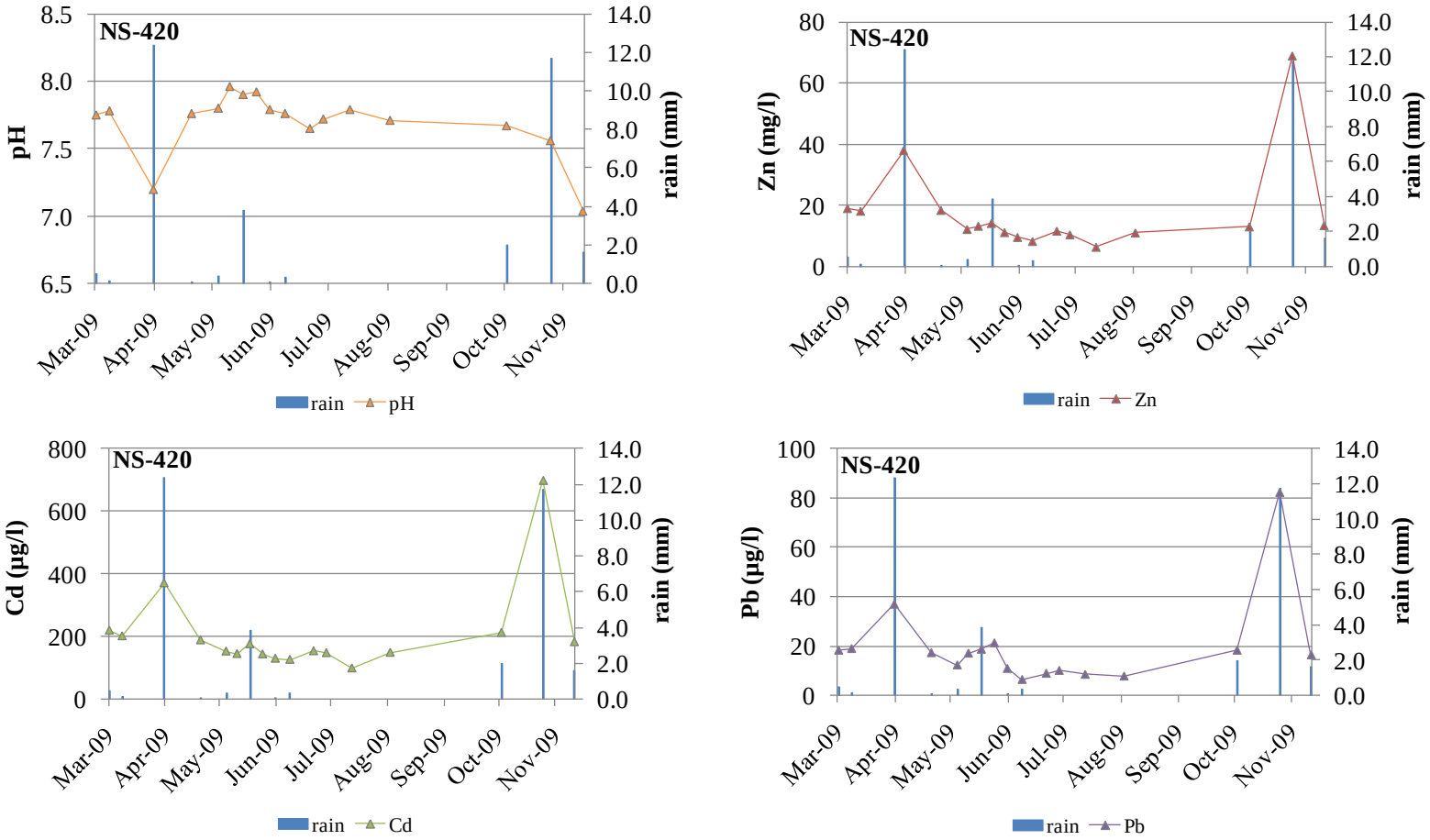

Figure 32. Plots showing the influence of rainfall on pH, Zn, Cd and Pb concentrations at station NS-420 (Naracauli stream). The reported amount of rain corresponds to the average value calculated on five days before surveys.

Concentrations of Y and of the rare earth elements (REE, La to Lu) in the Naracauli stream catchment waters are listed in Appendix B. Th is always less than detection limit (0.06 µg/l). Along the Naracauli stream, REE show a wide range in concentrations (∑REE 2 ng/l - 9 µg/l) and tend to decrease from upstream to downstream; the most abundant elements are Y, La, Ce and Nd. At stations A and B, ∑REE varies between 11 and 100 µg/l. In most water samples, the highest contents of REE were measured in those collected under high flow conditions.

Figures 33 - 36 show that total content of REE usually increases as Zn, Mn, Pb, or SiO_2 concentrations increase. The best correlation is observed between Zn/REE and Pb/REE, suggesting a possible association of the REE with Zn- and Pb-rich colloids or very fine particles.

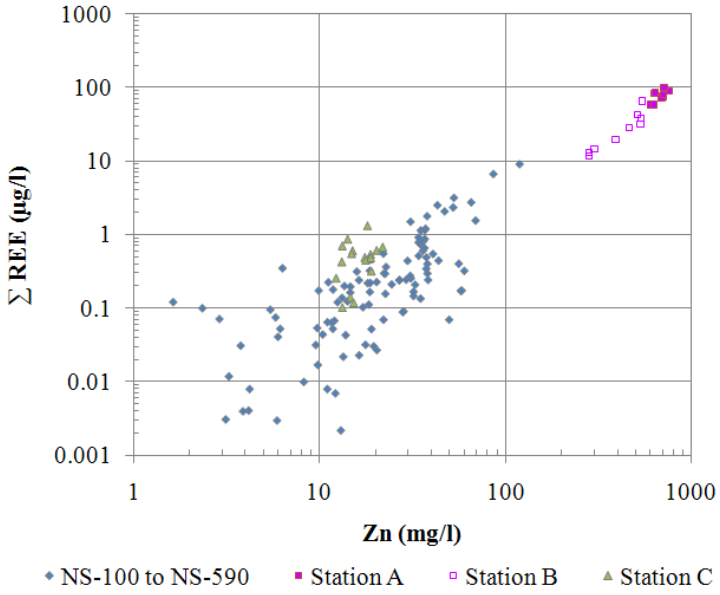

Figure 33. Plot showing ∑REE (La to Lu) versus Zn concentrations in filtered water samples collected from station NS-100 to NS-590 (Naracauli stream) and tailings drainages (stations A, B and C).

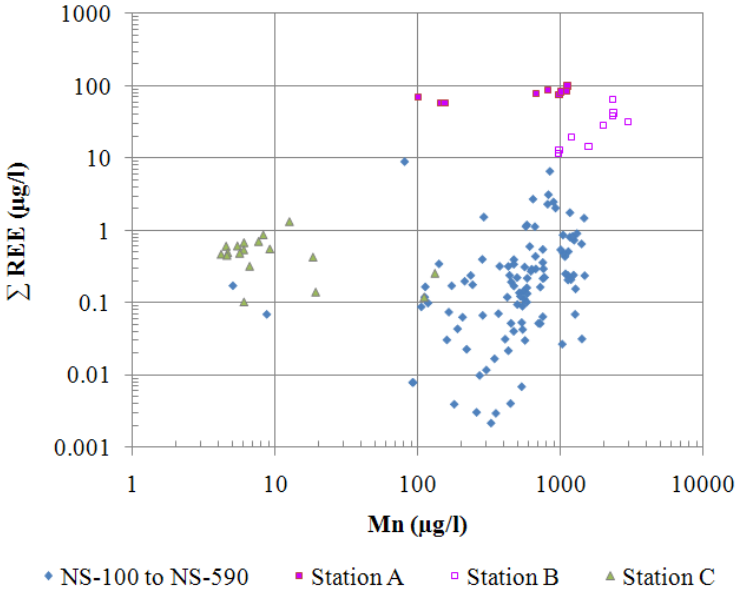

Figure 34. Plot showing ∑REE (La to Lu) versus Mn concentrations in filtered water samples collected from station NS-100 to NS-590 (Naracauli stream) and tailings drainages (stations A, B and C).

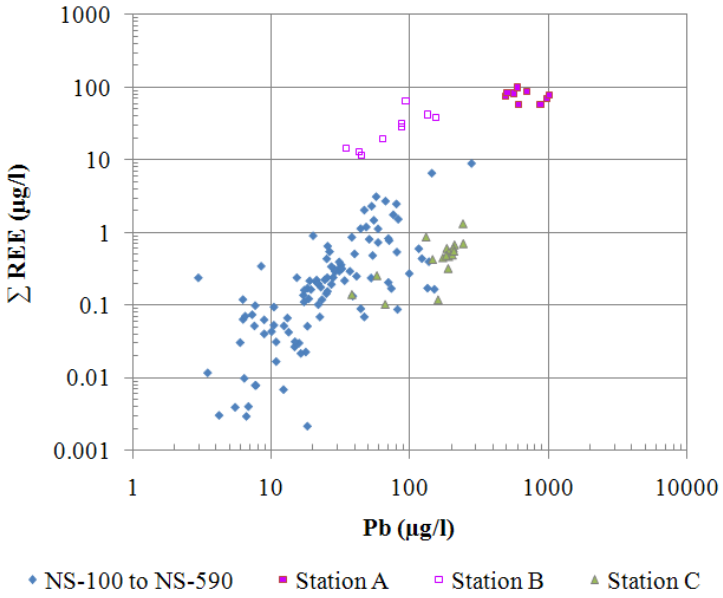

Figure 35. Plot showing ∑REE (La to Lu) versus Pb concentrations in filtered water samples collected from station NS-100 to NS-590 (Naracauli stream) and tailings drainages (stations A, B and C).

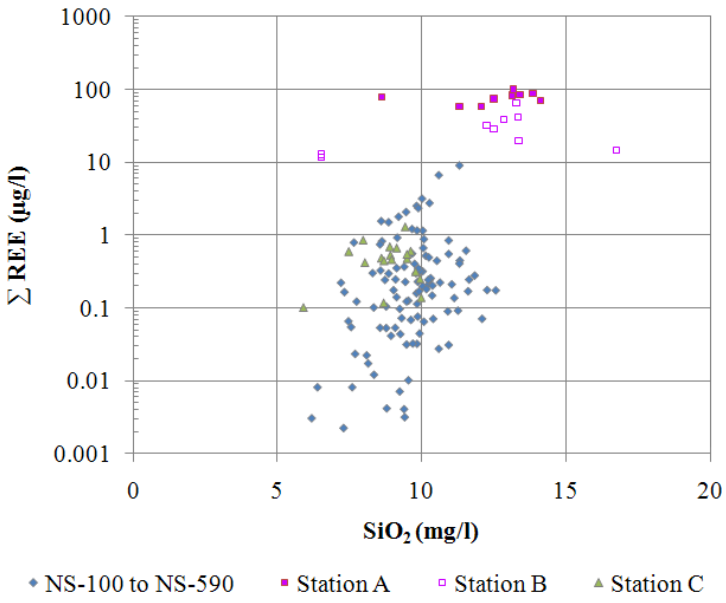

Figure 36. Plot showing ∑REE (La to Lu) versus SiO_2 concentrations in filtered water samples collected from station NS-100 to NS-590 (Naracauli stream) and tailings drainages (stations A, B and C).

The distribution of REE species in solution is often related to the pH and concentration of major anions in the waters. The $REE(CO_3)^+$ and $REE(CO_3)_2^-$ complexes are the prevalent species in the Naracauli stream waters. At stations A and B, characterized by lower pH values and higher sulphate contents, also the $REE(SO_4)^+$ species (up to 70 %) and the free-ion REE^{3+} (up to 60 %) occur. Although dissolved organic matter was not measured, it is important to remember the potential role of dissolved organic matter in controlling the REE species distribution. Tang et al. (2003) demonstrated that humic substances are important ligands for REE in natural waters. The role that humic substances play in complexing REE especially depends on pH and the concentrations of dissolved organic matter. In general, at low pH, organic complexes of REE will be important only in organic-rich waters (i.e., black waters). Otherwise, free ions and sulphate complexes dominate REE speciation. In circumneutral-pH waters, REE predominantly occur in solution as organic

complexes when dissolved organic carbon is higher than 0.7 mg/l. On the other hand, in alkaline water REE are mainly complexed by carbonate ions.

Figures 37 - 40 show the concentration of each REE at stations NS-100, NS-170, A and B normalized to the corresponding concentration in the Post-Archean average Australian Shale (PAAS; McLennan, 1989). The REE patterns in water at stations NS-100 and NS-170 are characterized by a negative Ce anomaly and a positive Eu anomaly. Considering the oxidizing conditions of the waters, the negative Ce anomaly might result from the preferential retention of Ce in solid phases, due to the poor solubility of Ce^{4+} species (Sholkovitz, 1992). More recent studies (Pourret et al., 2008) have demonstrated that in the presence of carbonate, in alkaline waters, Ce is readily oxidized to Ce^{4+}, which is easily removed from solution by preferential adsorption on humic acid. The positive Eu anomaly is probably due to dissolution of Eu-enriched minerals, such as Ca-feldspar, calcite (Lee et al., 2003) and sulphide (Leybourne et al., 2000). Moreover, REE patterns show an enrichment in the middle REE (MREE) with respect to the light REE (LREE) and heavy REE (HREE). This enrichment has been explained by various processes such as weathering of specific minerals (Nordstrom et al., 1995; Sholkovitz, 1995; Bundy et al., 1996), aqueous transport in association with the colloidal pool (Hoyle et al., 1984; Elderfield et al., 1990; Cidu et al., 2007), and solid-liquid exchange reactions, including adsorption/desorption and/or ion exchange between the water and MREE enriched surface coatings, suspended particles, or secondary minerals (Gosselin et al., 1992; Sholkovitz, 1995). The negative Ce anomaly is observed also in the REE pattern of water at station A, and it is less pronounced in water at station B. At these stations the positive Eu anomaly is not observed. Waters at stations A and B show an enrichment in LREE and MREE and a progressive depletion of HREE. These patterns do not change, significantly, under different seasonal conditions. They only are subject to a vertical shift along the y axis, due to a variation in concentration depending on water flow conditions.

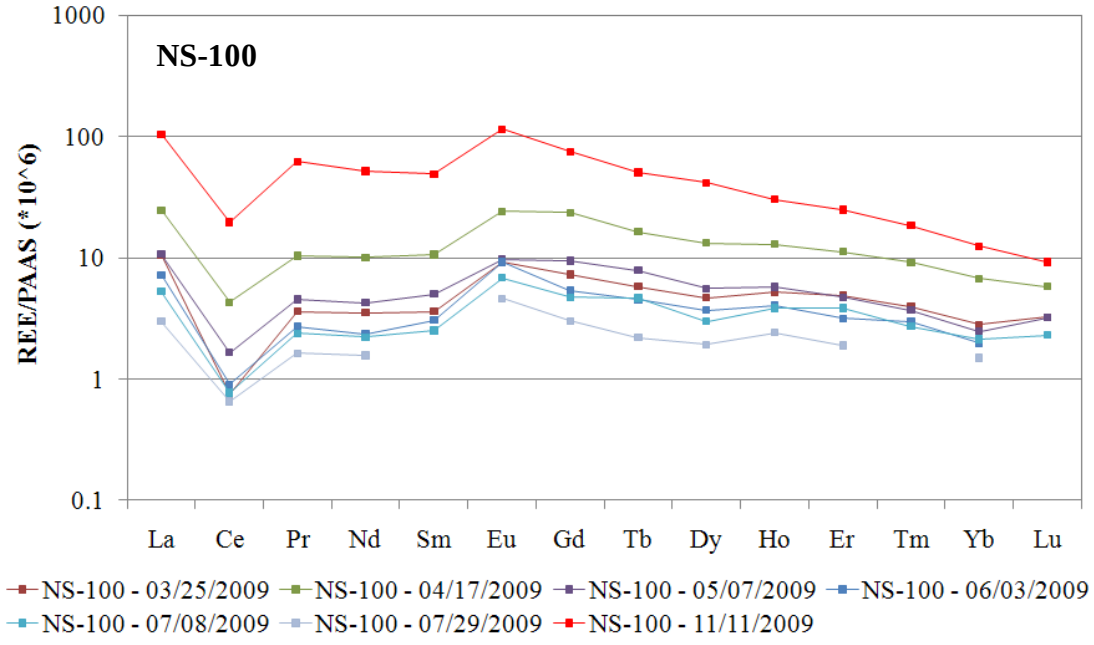

Figure 37. Patterns of REE in filtered water samples collected at station NS-100 (Naracauli stream). Concentrations normalized to the Post-Archean average Australian Shale (PAAS).

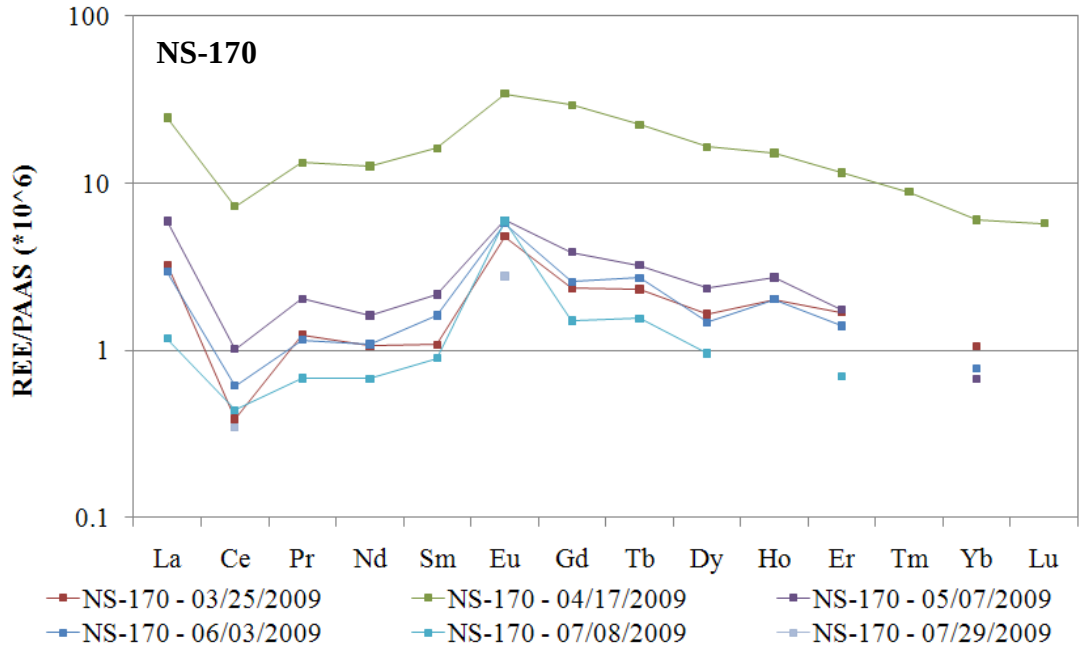

Figure 38. Patterns of REE in filtered water samples collected at station NS-170 (Naracauli stream). Concentrations normalized to the Post-Archean average Australian Shale (PAAS).

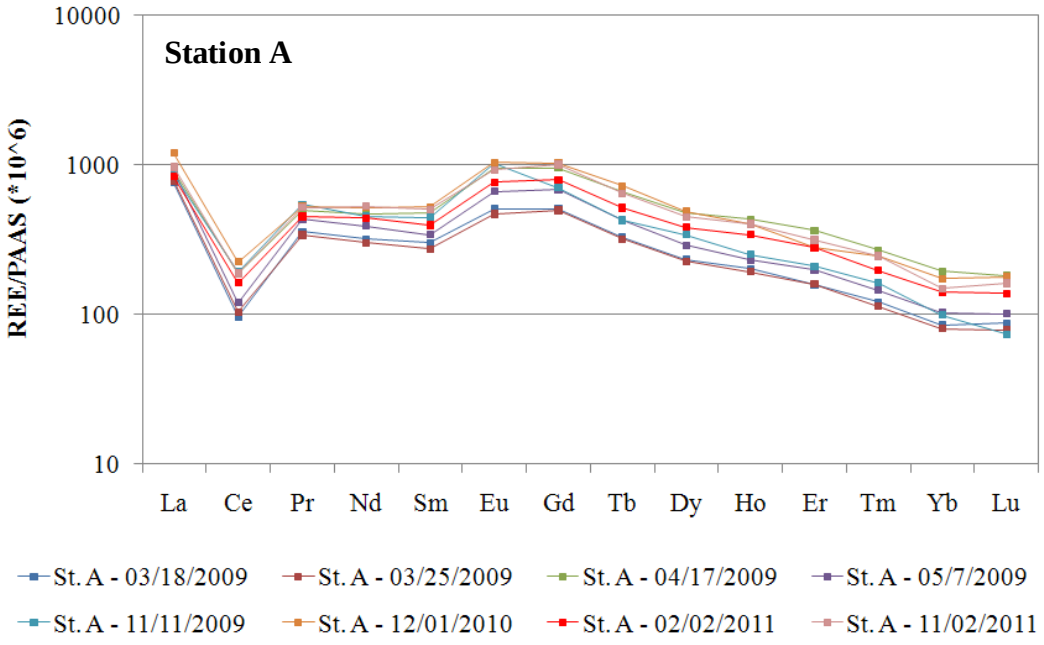

Figure 39. Patterns of REE in filtered water samples collected at station A (tailings drainage). Concentrations normalized to the Post-Archean average Australian Shale (PAAS).

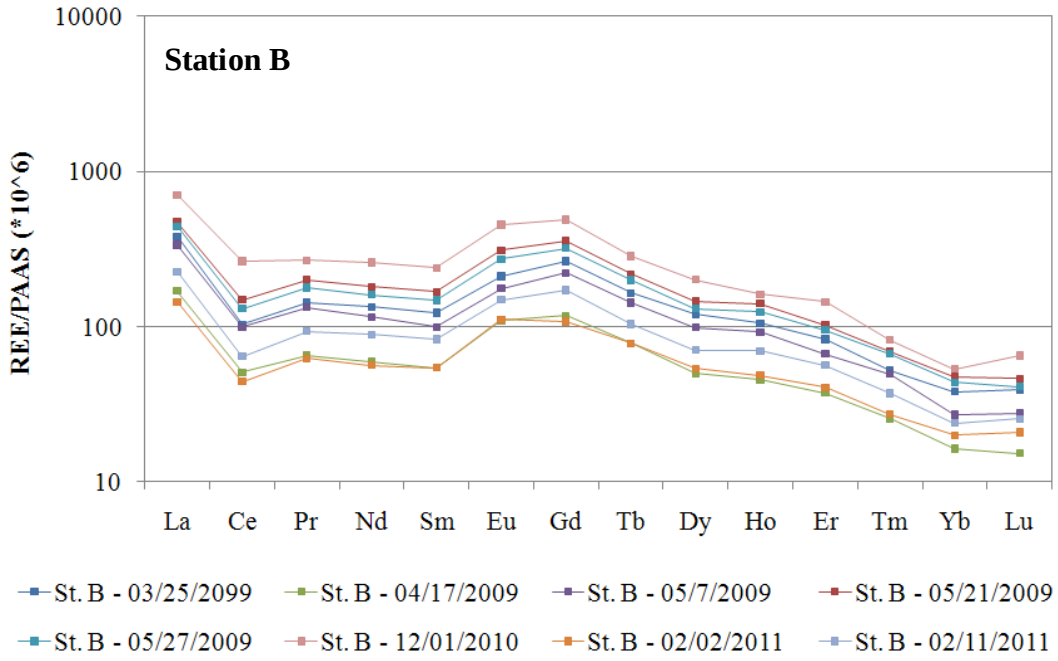

Figure 40. Patterns of REE in filtered water samples collected at station B (tailings drainage). Concentrations normalized to the Post-Archean average Australian Shale (PAAS).

4.2 BIOMINERALIZATION

4.2.1 X RAY DIFFRACTION STUDY AND CHEMICAL ANALYSIS

Figures 41 - 44 show some examples of collected XRD patterns. Other XRD patterns are reported in Appendix C. The XRD patterns confirm the dominant presence of hydrozincite in the Naracauli samples and quartz as an accessory mineral. Patterns in the biomineral samples from the Naracauli stream (N32, N34, N36 and N37A) show a peak broadening that suggests a lower crystallinity of these materials compared to the reference sample (sample Geo obtained from supergene Zn deposits, Malfidano Mine, Sardinia-Italy). This observation is in agreement with data previously shown by De Giudici et al. (2009).

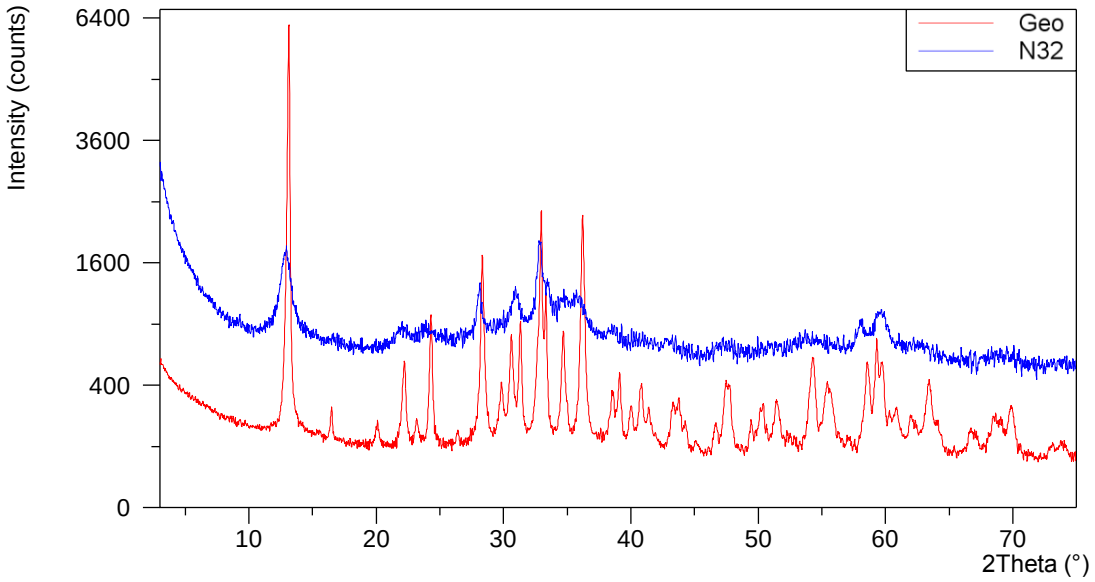

Figure 41. X-ray diffraction patterns of hydrozincite sample (N32) collected at station NS-170 and reference sample (Geo) obtained from supergene Zn deposits, Malfidano Mine, Sardinia-Italy. Pattern of sample N32 is vertically shifted for the sake of clarity.

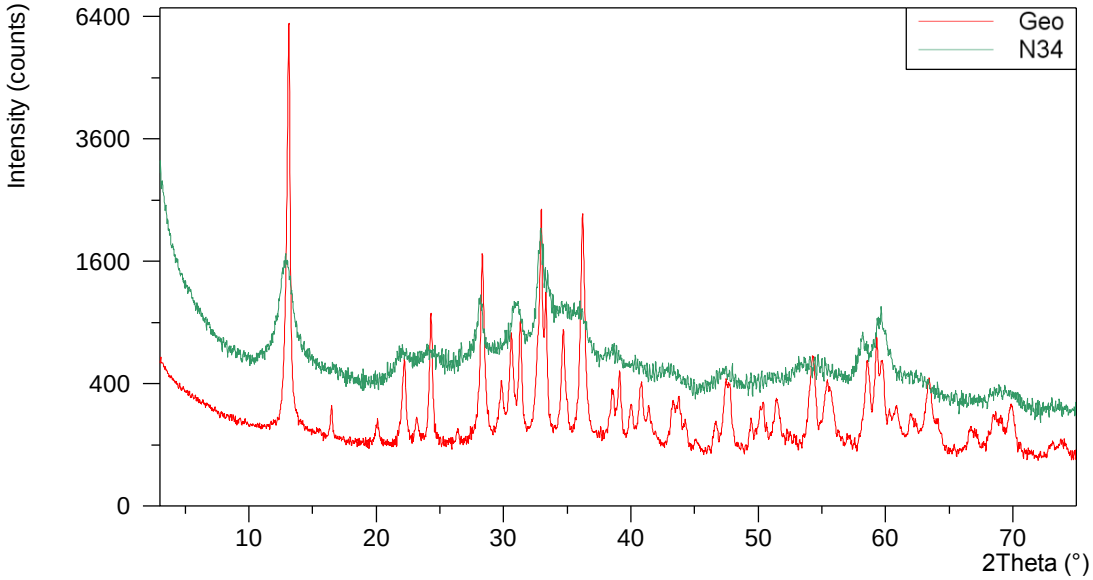

Figure 42. X-ray diffraction patterns of hydrozincite sample (N34) collected at station NS-590 and reference sample (Geo) obtained from supergene Zn deposits, Malfidano Mine, Sardinia-Italy. Pattern of sample N34 is vertically shifted for the sake of clarity.

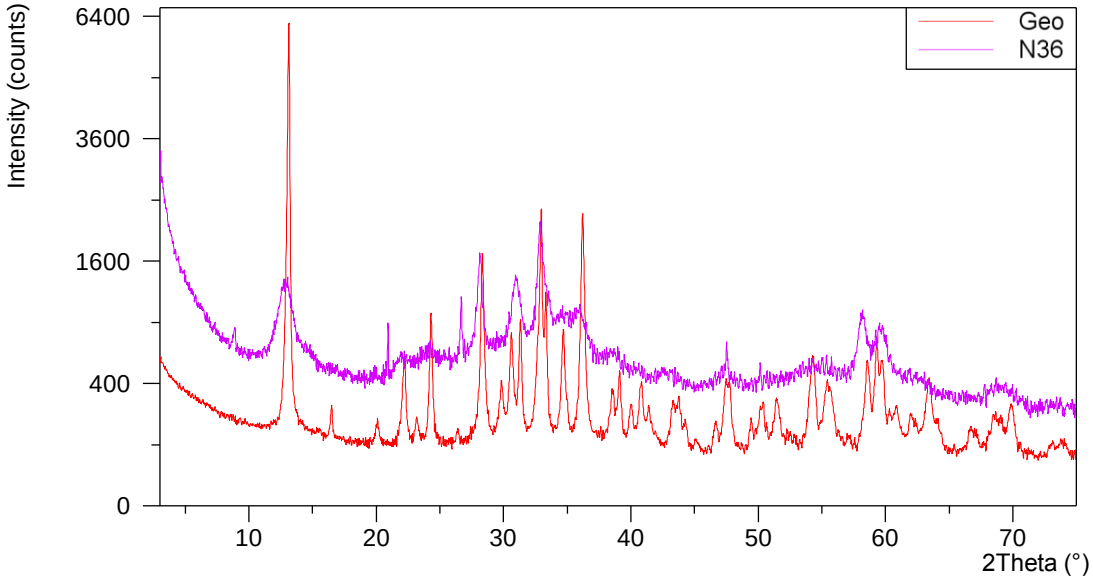

Figure 43. X-ray diffraction patterns of hydrozincite sample (N36) collected at station NS-590 and reference sample (Geo) obtained from supergene Zn deposits, Malfidano Mine, Sardinia-Italy. Pattern of sample N36 is vertically shifted for the sake of clarity.

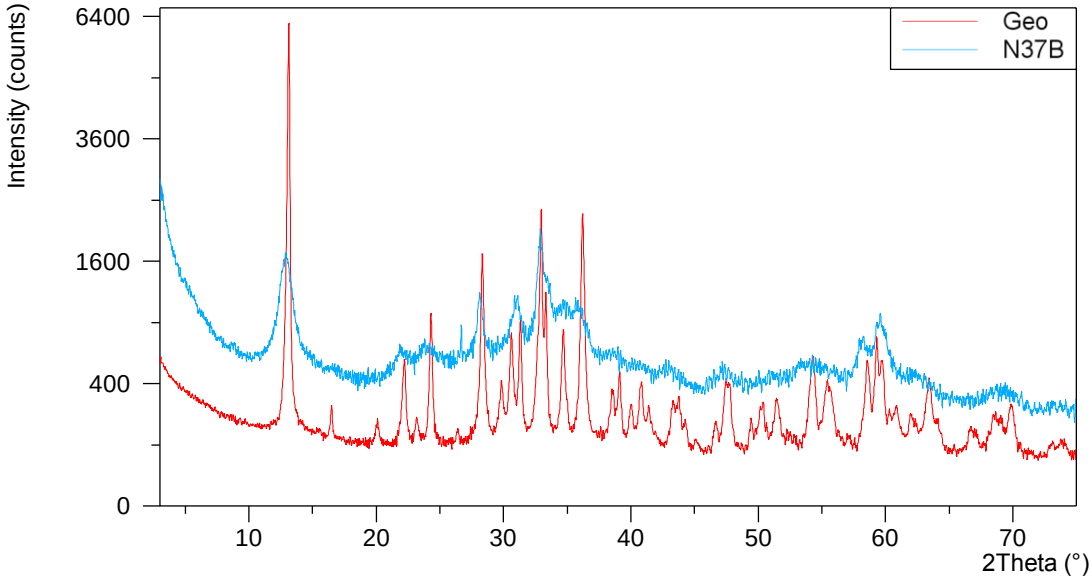

Figure 44. X-ray diffraction patterns of hydrozincite sample (N37B) collected at station NS-420 and reference sample (Geo) obtained from supergene Zn deposits, Malfidano Mine, Sardinia-Italy. Pattern of sample N37B is vertically shifted for the sake of clarity.

Tables 4a and b show the concentrations of the main selected chemical components in some hydrozincite samples collected in the Naracauli stream. The Zn content is in good agreement with the theoretical formula of hydrozincite (Jambor, 1964), notwithstanding possible presence of other Zn-phases not determined by XRD. Contents of Pb, Cd and Ni are the most abundant metals following Zn. This result is in agreement with previous observations showing that the precipitation of hydrozincite removes not only Zn from waters, but also other metals such as Cd, Pb, Ni and Cu (Podda et al., 2000; Zuddas et al., 2005), and it is also consistent with the decrease in metals observed in water along the Naracauli stream (see Paragraph 4.2.3). The concentration of Fe is particularly high in the solid sample N32 due to the presence of amorphous iron-hydroxide at this site (see Fig. 13).

Table 4a. Concentrations of the main selected chemical components in some hydrozincite samples collected in the Naracauli stream.

Sample	Station	Date	Zn	Pb	Cd	Ni	Cu
			mg/kg	mg/kg	mg/kg	mg/kg	mg/kg
N32	NS-170	05/21/2009	465,000	5,500	510	420	420
N37B	NS-420	06/10/2009	490,000	1,600	600	650	120
N39	NS-420	07/15/2009	520,000	860	750	900	60
N41A	NS-420	07/29/2009	510,000	1,100	620	830	80
N42	NS-420	07/29/2009	540,000	870	720	1,000	60
N34	NS-590	05/27/2009	530,000	920	850	930	70
N36	NS-590	06/03/2009	460,000	1,500	790	890	80

Table 4b. Concentrations of the main selected chemical components in some hydrozincite samples collected in the Naracauli stream.

Sample	Fe	Mn	Co	Ca	Mg	SO_4
	mg/kg	mg/kg	mg/kg	mg/kg	mg/kg	mg/kg
N32	50,450	400	50	4,500	590	5,500
N37B	1,650	470	50	6,700	1,080	5,200
N39	130	400	41	5,800	1,050	4,900
N41A	260	310	30	6,000	1,060	4,200
N42	180	360	40	6,700	1,300	5,000
N34	630	650	70	7,300	1,350	5,400
N36	2,560	610	70	7,800	1,510	5,400

REE contents in hydrozincite samples are shown in Appendix D. The highest concentrations are observed in sample N32 (192 mg/kg ΣREE). This is consistent with the presence of amorphous iron-hydroxide and their high capacity to adsorb REE (Quinn et al., 2006). In the other samples total REE content varies between 5 and 28 mg/kg; the most abundant REE are La, Ce and Nd as in the respective water samples (see Appendix B). Figures 45 - 48 show PAAS-normalized concentrations of each REE in water and solid samples collected at the same site. All hydrozincite

samples display similar nearly flat shale-normalized patterns with a negative Ce anomaly, while no Eu anomaly is observed.

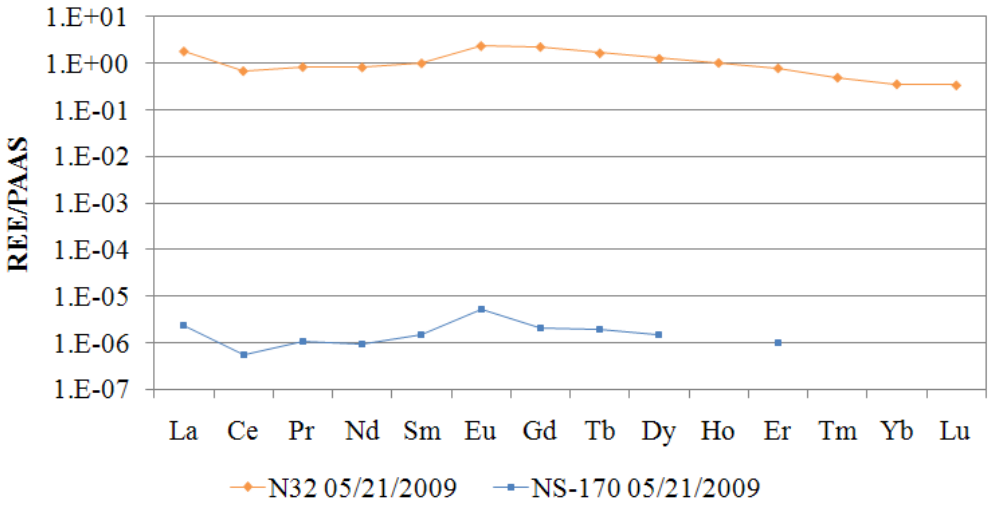

Figure 45. Patterns of REE in hydrozincite sample (N32) and the water sample collected at the same sites (NS-170). Concentrations normalized to the Post-Archean average Australian Shale (PAAS).

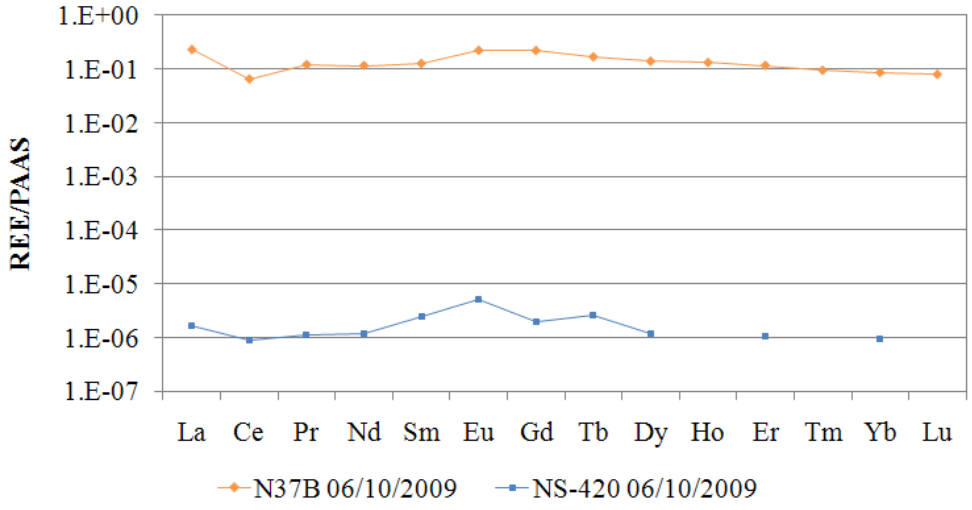

Figure 46. Patterns of REE in hydrozincite sample (N37B) and the water sample collected at the same sites (NS-420). Concentrations normalized to the Post-Archean average Australian Shale (PAAS).

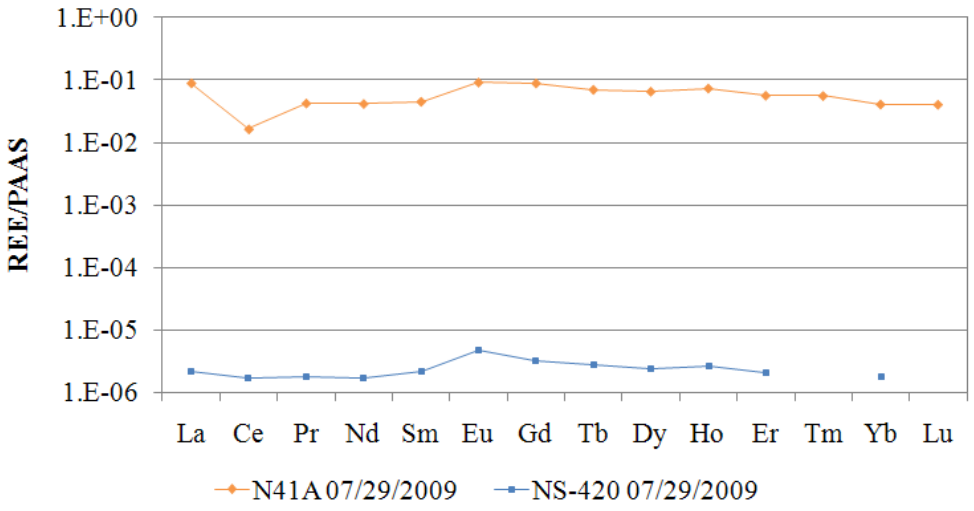

Figure 47. Patterns of REE in hydrozincite sample (N41A) and the water sample collected at the same sites (NS-420). Concentrations normalized to the Post-Archean average Australian Shale (PAAS).

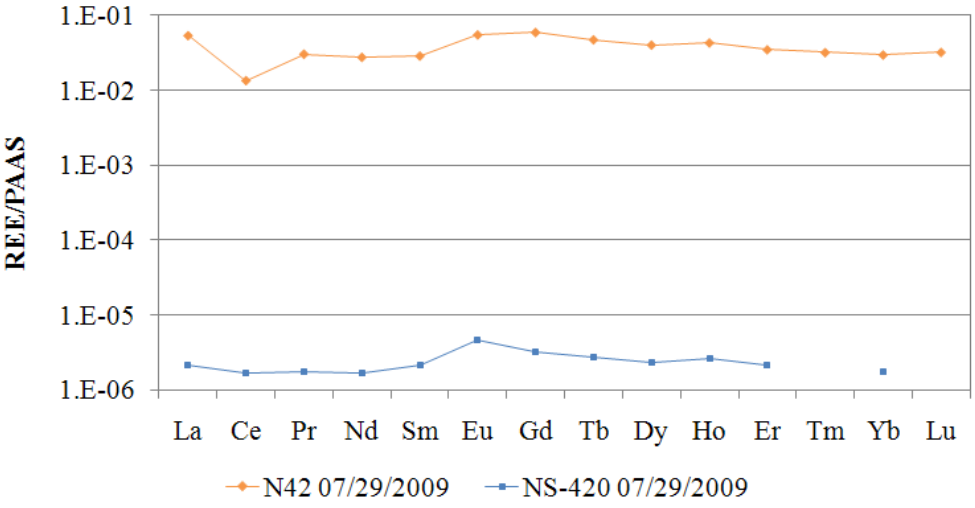

Figure 48. Patterns of REE in hydrozincite sample (N42) and the water sample collected at the same sites (NS-420). Concentrations normalized to the Post-Archean average Australian Shale (PAAS).

4.2.2 Optical microscopy and Scanning electron microscopy analysis: morphological study

Biominerals are composite materials containing an organic matrix and nano- or micro-scale amorphous or crystalline minerals (Gilbert et al., 2005). Figure 49a shows hydrozincite biomineralization observed by Confocal Laser Microscopy. Cyanobacteria can be recognized as a series of attached cells, often fluorescent, that result in filaments tens of micrometers long. The biomineralization consists of globules, external to the bacterial cells, which attach themselves one to another to form sheaths (Podda et al., 2000). Figures 49b and c show an hydrozincite sample collected at the beginning of precipitation, while Figure 49d shows hydrozincite collected several days after precipitation. In the first case, biomineral sheaths form a thin network that can be associated to the initial stage of the development of the biofilm (see Paragraph 1.2 and Fig. 3). In the second case a three-dimensional structure is observed, that can be associated to the mature state of the biofilm (see Paragraph 1.2 and Fig. 3). Larger magnification (Figs. 49e and f) shows that hydrozincite precipitates around organic matter filaments forming globules. In Appendix E other photos of hydrozincite biomineral are shown.

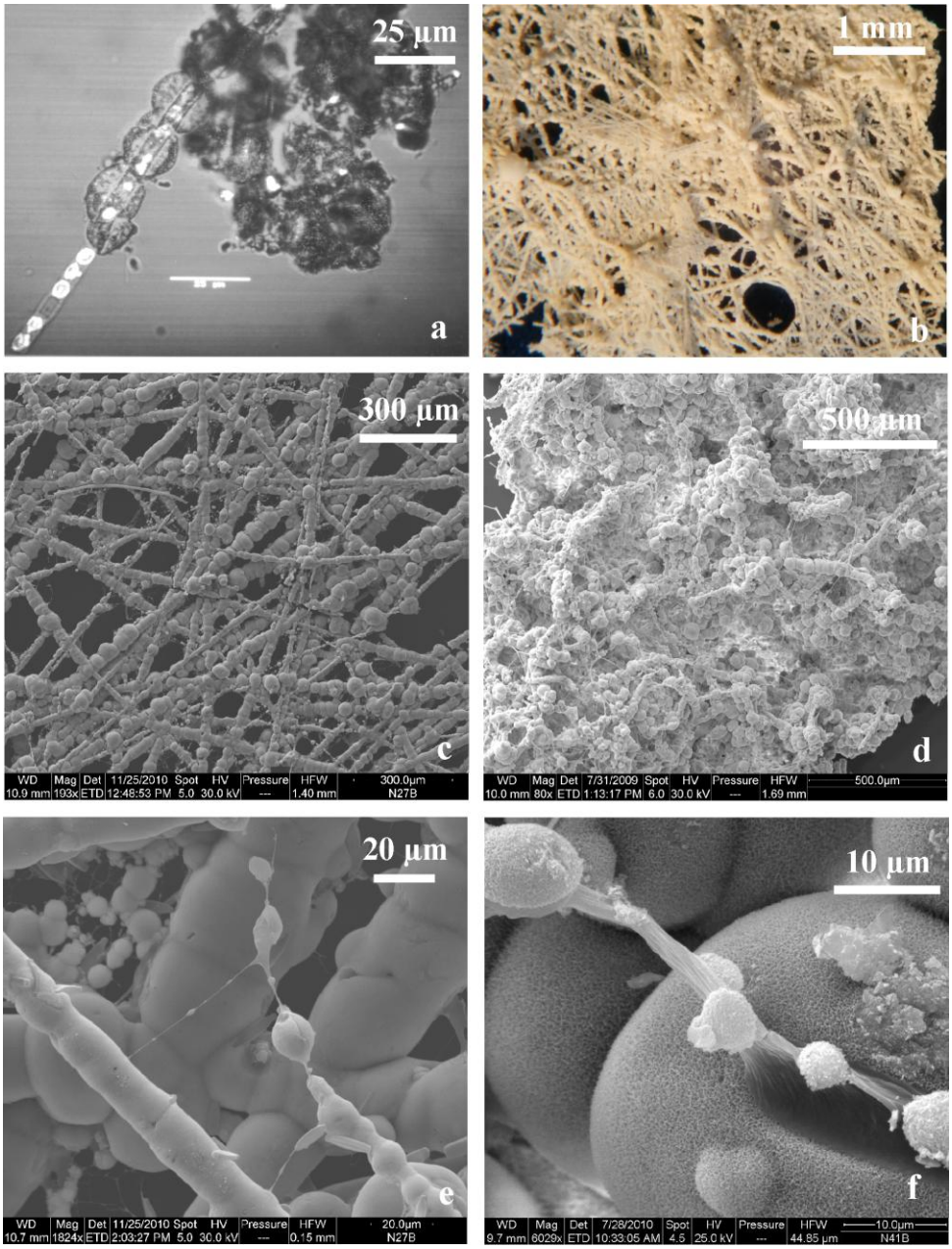

Figure 49. a) Image collected by Confocal Laser Microscopy in the transmission mode. The *Scytonema sp.* is visible as a series of attached cells that result in filaments that are tens of micrometers long, while biomineralization forms globules external to the bacterial cells that attach one to another to form sheaths (by Podda et al. 2000, modified). b and c) Images collected by Optical Microscopy and Scanning Electron Microscopy, respectively. This hydrozincite sample was collected at the beginning of precipitation. Biomineral sheaths form a thin network that can be associated to the initial stage of the development of the biofilm. d) Image collected by Scanning Electron Microscopy. Hydrozincite sheaths form a three-dimensional structure, which can be associated to the mature state of the biofilm. e and f) Images collected by Scanning Electron Microscopy. Hydrozincite precipitates around organic matter filaments forming globules that attach one to another.

To investigate the bacterial control on the hydrozincite shape and to assess if environmental conditions have any influence on biomineralization morphology, a morphological study was carried out on the Naracauli hydrozincite (Medas et al., 2012a and b). The role of bacteria on the hydrozincite shape can be recognized in Figure 50. Figure 50a shows a sheath section, where the biomineral encrusts bacterial filament following its shape. In Figures 50b and c, the presence of a branch on the hydrozincite sheaths is clearly observed. *Scytonema sp*. is characterized by its unique type of branching known as false branching (Fig. 50d). The filament breaks up near a heterocyst and the broken end protrudes out of the sheath as a branch (Rajan, 2001). The filament may break, either due to degeneration of some intercalary cells, or because vegetative cells modify into biconcave, colourless separating discs. Separating discs degenerate so that the filament will be broken. This leads to the formation of two sheathed filaments, each of which grows separately from the other secreting its own mucilage sheath (Whitton et al., 2000). This typical shape is preserved also after the bioprecipitation of hydrozincite around the bacterial filaments, as shown in Figures 50b and c.

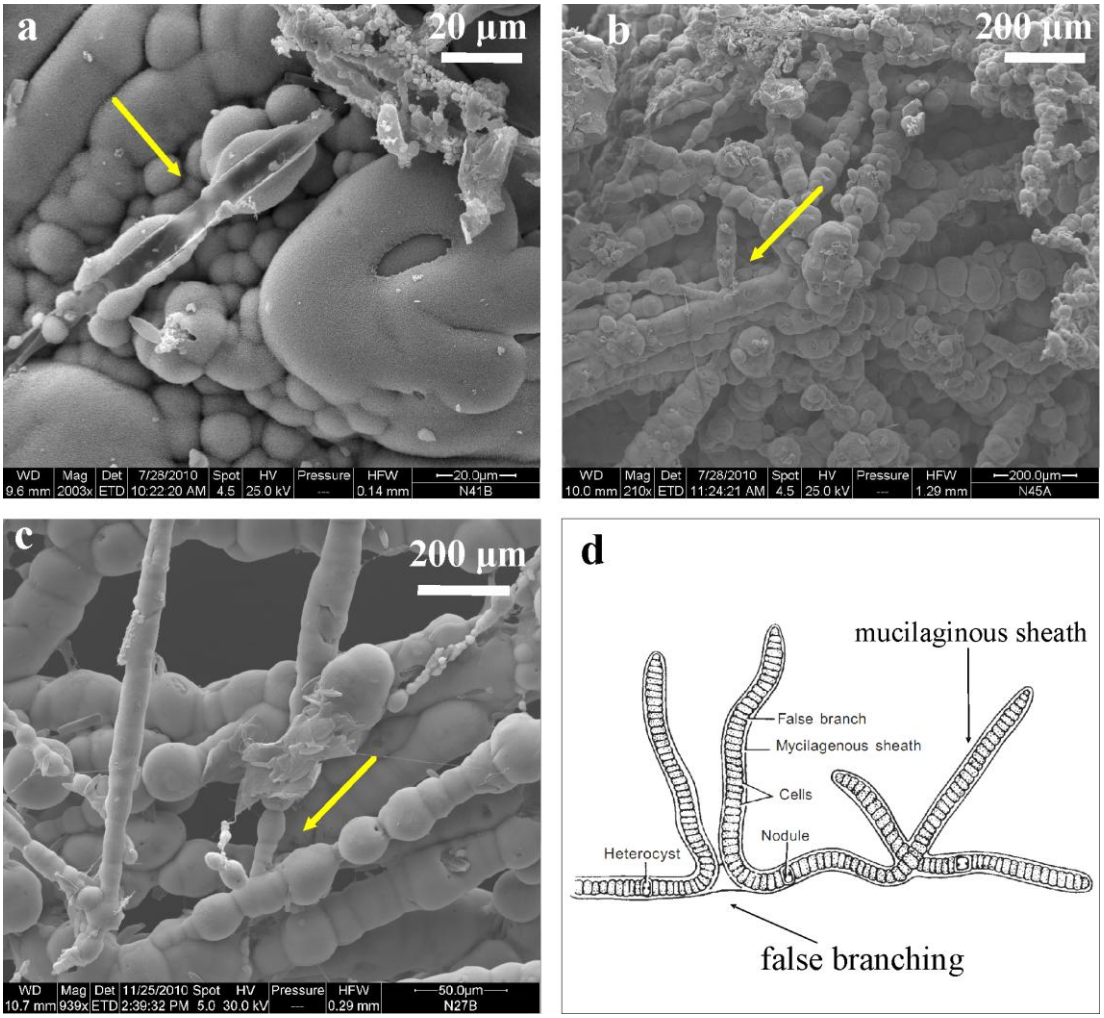

Figure 50. a, b and c) Images collected by Scanning Electron Microscopy. a) A sheath section, that shows as the biomineral encrusts bacterial filament following its shape. b and c) A branch in the hydrozincite sheath is indicated by the arrow. This branch results from false branching of the *Scytonema sp*. d) False branching in *Scytonema sp*. (by Margaret et al., 2007, modified). The filament breaks up near a heterocyst and the broken end protrudes out of the sheath as a branch. Each filament grows separately from the other secreting its own mucilage sheath.

More detailed investigations were carried out on globules and sheaths, measuring diameter distribution in some hydrozincite samples collected in 2009 during different seasonal periods. Hydrozincite samples collected in spring (Fig. 51a) are characterized by globules having a diameter between 20 and 40 µm, with a mean diameter of 30 µm. In contrast, hydrozincite samples collected in late summer (Fig. 51b) are characterized by few short-length sheaths, whose globules show a greater

variability in diameter. About 90% of globules measured range between 30 and 80 µm, with a mean diameter of 50 µm.

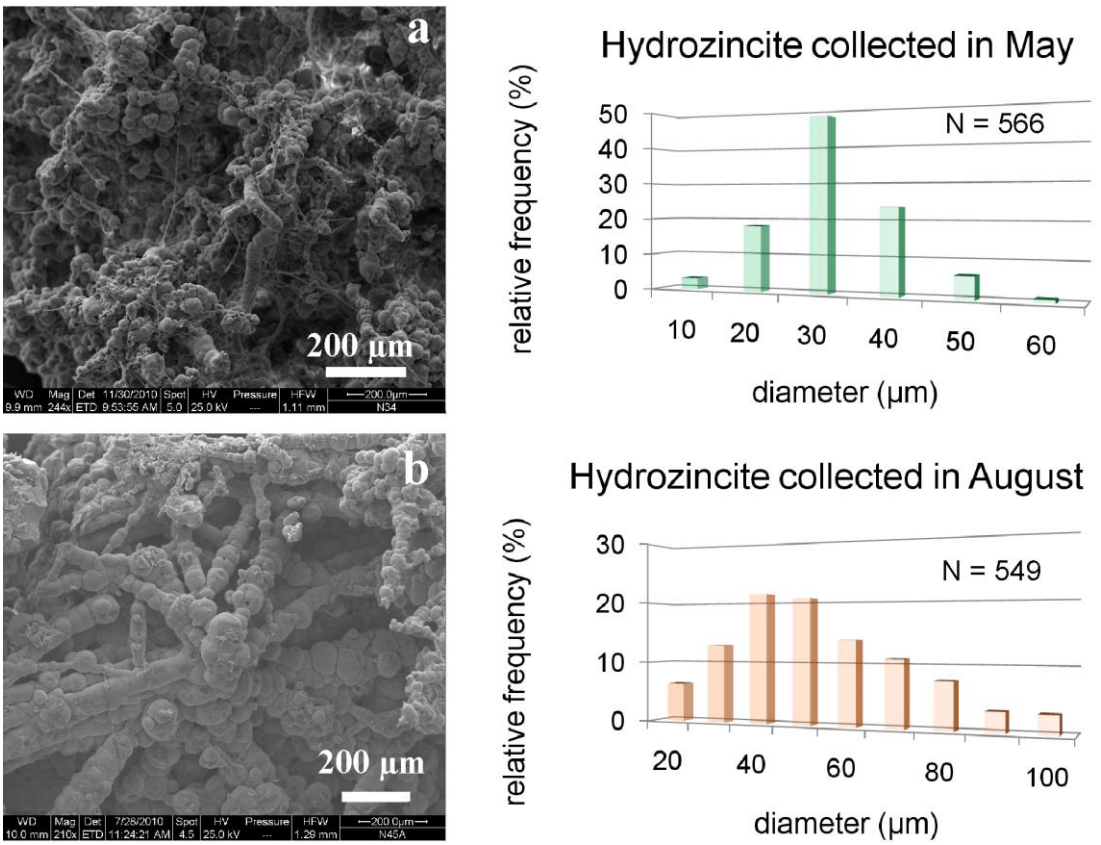

Figure 51. Images collected by Scanning Electron Microscopy. a) Hydrozincite globules and sheaths in samples collected in May. b) Hydrozincite globules and sheaths in samples collected in August. On the right, the frequency histograms of the globule diameters are shown. N indicates number of measurements of hydrozincite samples.

Another control exerted by *Scytonema sp.* on the biomineralization morphology is shown in Figures 52 and 53. Figure 52 shows the features of bacteria biofilm grown under moderate flow condition; it can be observed that sheaths are generally elongated according to the water flow direction. On the other hand, Figure 53 shows hydrozincite precipitated under high flow conditions. In this case, sheaths are very large, and become thinner at the final ends. The flow direction is indicated by an arrow in both Figures.

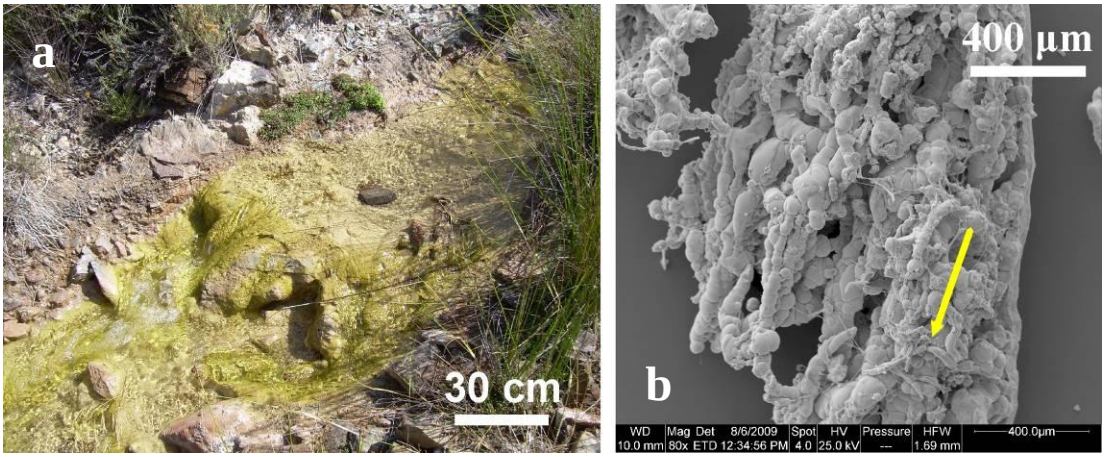

Figure 52. a) Station NS-420 where the hydrozincite sample of Fig. 52b was collected. b) Image collected by Scanning Electron Microscopy. Hydrozincite precipitated under low flow condition. Sheaths are elongated according to the water flow direction (yellow arrow).

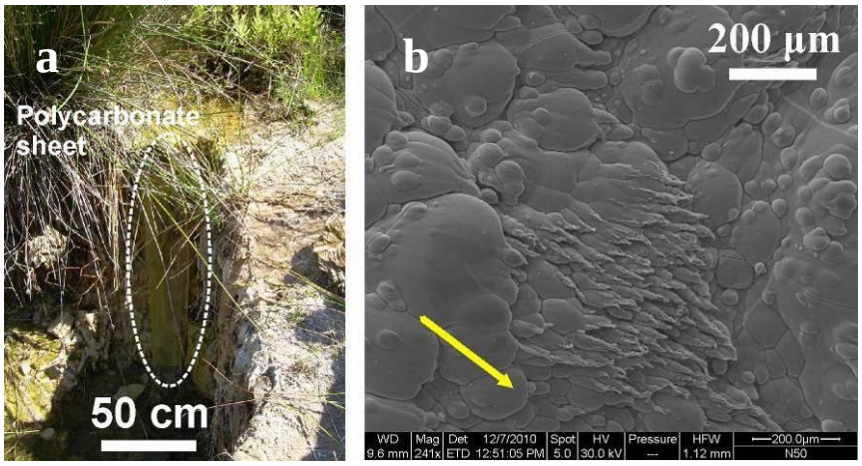

Figure 53. a) Polycarbonate sheet nailed on a small waterfall in the Naracauli stream (station NS-590). b) Image collected by Scanning Electron Microscopy. Hydrozincite collected from the polycarbonate sheet. This hydrozincite was precipitated under high flow conditions. Sheaths are very large, and become thinner at the final ends. The flow direction is indicated by an arrow.

Podda et al. (2000) described hydrozincite biomineralization as an epicellular biomineralization, considering that under natural conditions microorganisms are characterized by electronegative surfaces that can bind Zn^{2+}. Simultaneously, the CO_2 fixation from dissolved HCO_3^- and release of OH^- during photosynthesis lead to the shift of carbonate species equilibrium. This process results in a local

oversaturation with respect to hydrozincite around the bacteria. The following reactions were proposed:

$HCO_3^- + H_2O \leftrightarrow (CH_2O) + OH^- + O_2$ (photosynthesis)
$HCO_3^- + OH^- \leftrightarrow CO_3^{2-} + H_2O$
$2CO_3^{2-} + 5Zn^{2+} + 6H_2O \leftrightarrow Zn_5(CO_3)_2(OH)_6 + 6H^+$

An *in vitro* investigation (De Giudici et al., 2007), using cyanobacteria and water collected at Naracauli, showed different morphological and crystallinity characteristics between natural and *in vitro*-formed hydrozincite. For a significant hydrozincite precipitation to happen *in vitro* the presence of live cyanobacteria was required while cyanobacterial lysate or cyanobacterial exopolymers did not induce an effective hydrozincite biomineralization. These observations suggest a clear control of the *Scytonema sp*. both on hydrozincite precipitation and biomineral morphology in response of different environmental conditions. De Giudici et al. (2009) confirmed that Naracauli hydrozincite is a BCM, and revealed by NMR analysis the presence of peaks from organic biopolymers, most likely exopolysaccharides (EPS). It is in fact known that many cyanobacteria, including *Scytonema sp*., produce mucilaginous external layers (Nicolaus et al., 1999; Li et al., 2001) mainly made up of EPS. EPS has been shown to protect against solar radiation (Garcia-Pichel et al., 1991; Ehling-Schulz et al., 1997), dehydration (Scott et al., 1996), and phagocytosis (Schwarzmann et al., 1971) and is a key component of biofilms, helping in maintaining their structural integrity (Phoenix et al., 2008). EPS filaments are clearly visible in SEM photos of Naracauli hydrozincite (see Figs. 49e and f, 50a and c, and Appendix E).

The composition and quantity of bacterial exopolysaccharides can change depending on natural conditions (Mayer et al., 1999; Li et al., 2001; De Carvalho et al., 2010). Taking into account the potential benefits and detrimental side effects of biominerals, they conspicuously appear to parallel those afforded by EPS (Phoenix et al., 2008). For example, Phoenix et al. (2001) revealed that mineralized bacteria, isolated from

the Krisuvik hot spring (Iceland) have a marked resistance to UV compared to non-mineralized bacteria. Biomineralization is useful to attenuate the harmful wavebands of UV radiation and, simultaneous bacterial photosynthesis is not interrupted. The larger diameter observed for hydrozincite biomineralization collected in late summer can be ascribed to a difference in the production of external mucilage sheath by cyanobacteria colonies in response to stress conditions (Li et al., 2001 and cited references). Another control exerted by *Scytonema sp*. on the biomineralization is revealed by variations of hydrozincite morphology as a function of the water flow. All hydrozincite sheaths precipitated under low flow conditions have more or less a constant diameter, whereas under high flow conditions sheaths become thinner at the final ends. Purevdorj et al. (2002) have shown that hydrodynamics influences structure and behaviour of the biofilms. In fact, biofilms grown under turbulent flow form filamentous streamers. Observed differences in hydrozincite shape can be ascribed to the influence of hydrodynamics on the structure of the biofilm and, consequently, on biomineral shape.

4.2.3 Variations in water geochemistry and Optimum condition of bioprecipitation

As previously said, hydrozincite precipitation occurs usually in late spring or early summer. Precipitation timing however, as well as duration and abundance, may vary remarkably from one year to another. In 2009 a peak in the hydrozincite mineralization process was observed. To investigate variation in water chemical characteristics induced by hydrozincite precipitation, some parameters involved in biomineral precipitation (Zn, alkalinity, pH, hydrozincite SI) have been plotted against distance in the part of the Naracauli stream where biomineralization occurs. Figure 54 shows that Zn concentration decreases continuously from station NS-100 to station NS-590. This behaviour is the result of: i) the precipitation of hydrozincite, and ii) the dilution effect caused by the inflow of seep water (station C, see Fig. 11)

rich in alkalinity and poor in zinc, as compared to waters from the Naracauli stream (see Appendix A). Specifically, alkalinity in the Naracauli stream waters decreases from station NS-100 to station NS-170 (Fig. 55) because of hydrozincite precipitation; between station NS-170 and station NS-330 alkalinity increases because of alkaline seepage water (station C; see Appendix A); further downstream alkalinity decreases because of hydrozincite precipitation. Increase in pH, observed in Figure 56, can be ascribed to the photosynthetic process due to the presence of cyanobacteria that releases OH^- in solution (Zuddas et al., 2005). In general, the highest quantity of bioprecipitation occurs at stations NS-420 and NS-590, accordingly, the highest values of hydrozincite SI are observed at these sites (Fig. 57).

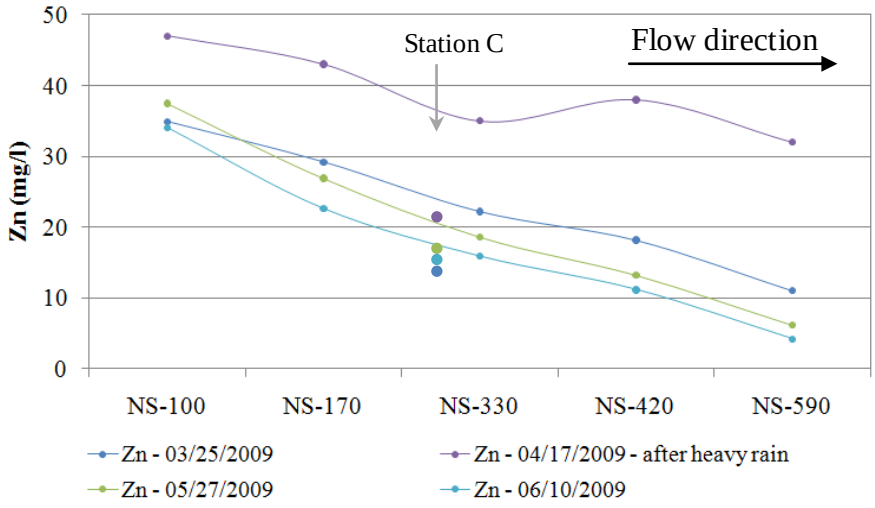

Figure 54. Variation in Zn concentration in waters where hydrozincite precipitates. Zn content at station C is also indicated.

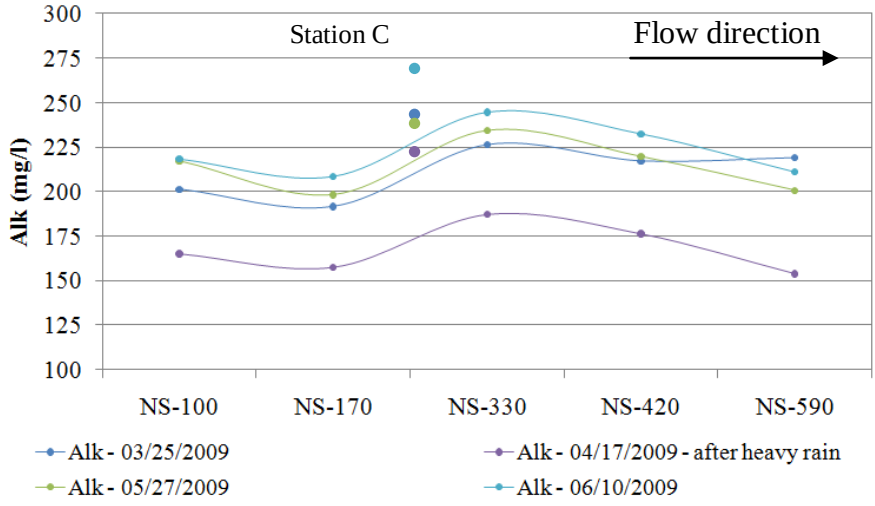

Figure 55. Variation in alkalinity concentration in waters where hydrozincite precipitates. Alkalinity content at station C is also indicated.

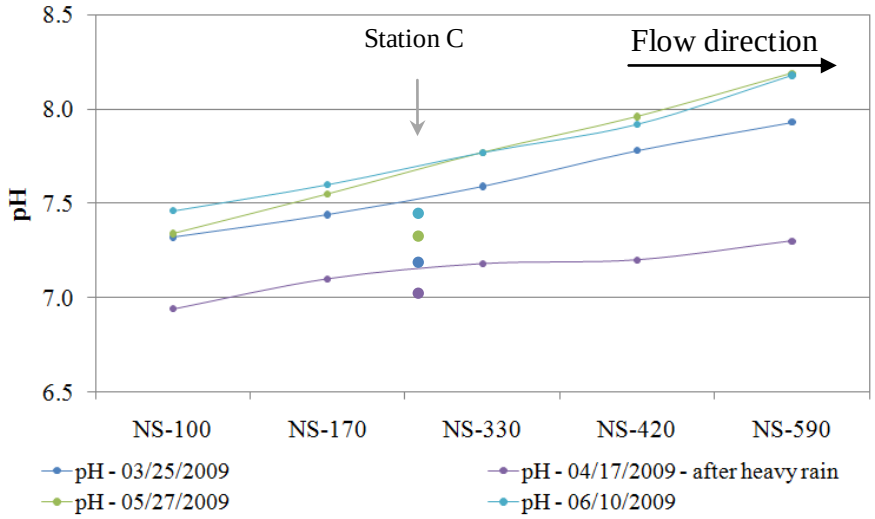

Figure 56. Variation in pH in waters where hydrozincite precipitates. pH values at station C are also indicated.

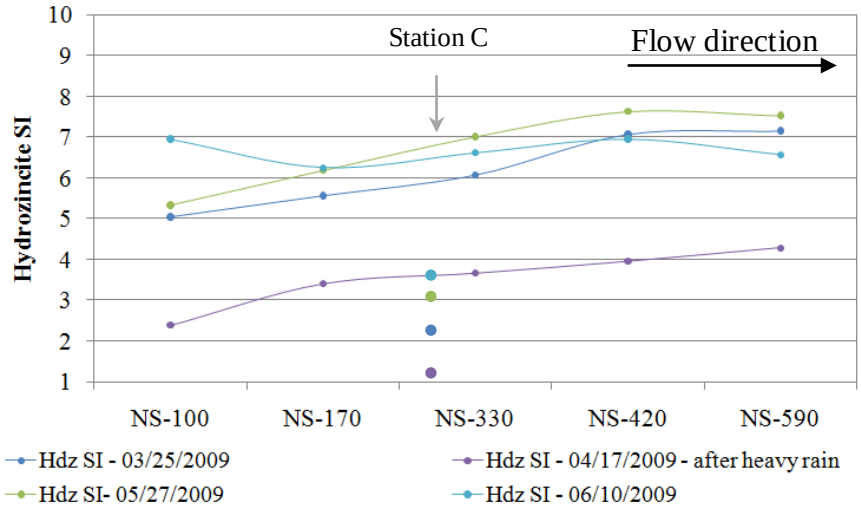

Figure 57. Variations in SI with respect to hydrozincite values in waters where hydrozincite precipitates. Hydrozincite SI at station C are also indicated.

Figure 58 shows variation in Cd, Ni and Pb concentrations in the Naracauli stream waters where hydrozincite precipitation occurs (see Fig. 11). These metals decrease from station NS-100 to station NS-590. The marked decrease in Cd is due to the inflow of seepage water with low Cd (station C) in the Naracauli stream, between station NS-170 and station NS-330.

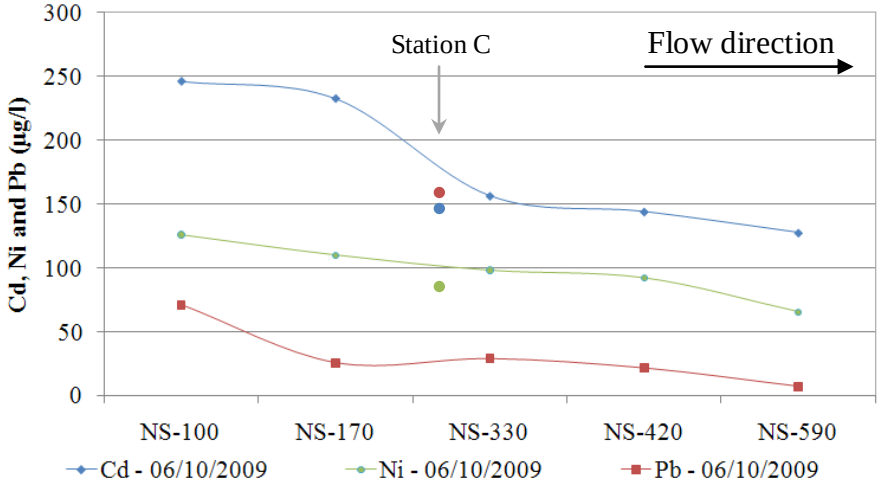

Figure 58. Variation in Cd, Ni and Pb concentrations in waters where hydrozincite precipitates. Cd, Ni and Pb contents at station C are also indicated.

It is useful to recall the significant variations observed in waters collected under periods of contrasting rainfall. Concentrations of Zn increase in rainy periods (October-April), reaching the highest values after heavy rainfalls, because of higher runoff interacting with tailings and mine wastes (see Fig. 54 and also Paragraph 4.1). On the contrary, alkalinity, pH and hydrozincite SI values decrease in rainy periods (Figs. 55 - 57). According to field evidence, heavy rain events stop the biomineralization process. By contrast, light rains do not result in significant changes in Zn concentration, alkalinity, pH and SI, and do not affect the intensity of biomineralization.

Figure 59 shows the relation between Zn^{2+}/CO_3^{2-} molar ratio and the SI with respect to hydrozincite. The Zn^{2+}/CO_3^{2-} values in waters collected from March to November 2009 varied from 1 to 2100. The lowest values, between 1 and 10, were observed in May and June at sites where hydrozincite was more abundant (NS-420 and NS-590) and hydrozincite SI reached the highest values. After heavy rainfall, Zn^{2+}/CO_3^{2-} values in the Naracauli stream waters increased up to 400 in spring and up to 2100 in autumn. Contrastingly, hydrozincite SI values decrease after rain events. This behaviour can be explained taking into account the effects of runoff flowing into the stream: high runoff carries high Zn contents which are leached from the mining-related wastes, and the acidic contribution of rain water causes the decrease in carbonate ions. Moreover, Figure 59 shows inverse relation between pH values and Zn^{2+}/CO_3^{2-} molar ratio, probably reflecting a higher Zn mobility at lower pH. The highest pH, the highest values of hydrozincite SI, and lowest Zn^{2+}/CO_3^{2-} values were observed in waters collected at stations NS-420 and NS-590 in late spring. In particular, hydrozincite SI reached values as high as 8 (Fig. 59). Such a value might be affected by the presence of Zn-rich fine particles in the water samples. However, as mentioned above (see Paragraph 3.1), significant differences in Zn concentration between aliquots filtered through 0.4 μm and 0.01 μm pore-size filters was not observed. Thus, slow kinetic processes due the high number of molecules involved in the elementary reaction of hydrozincite precipitation might be a more realistic explanation for the observed SI values.

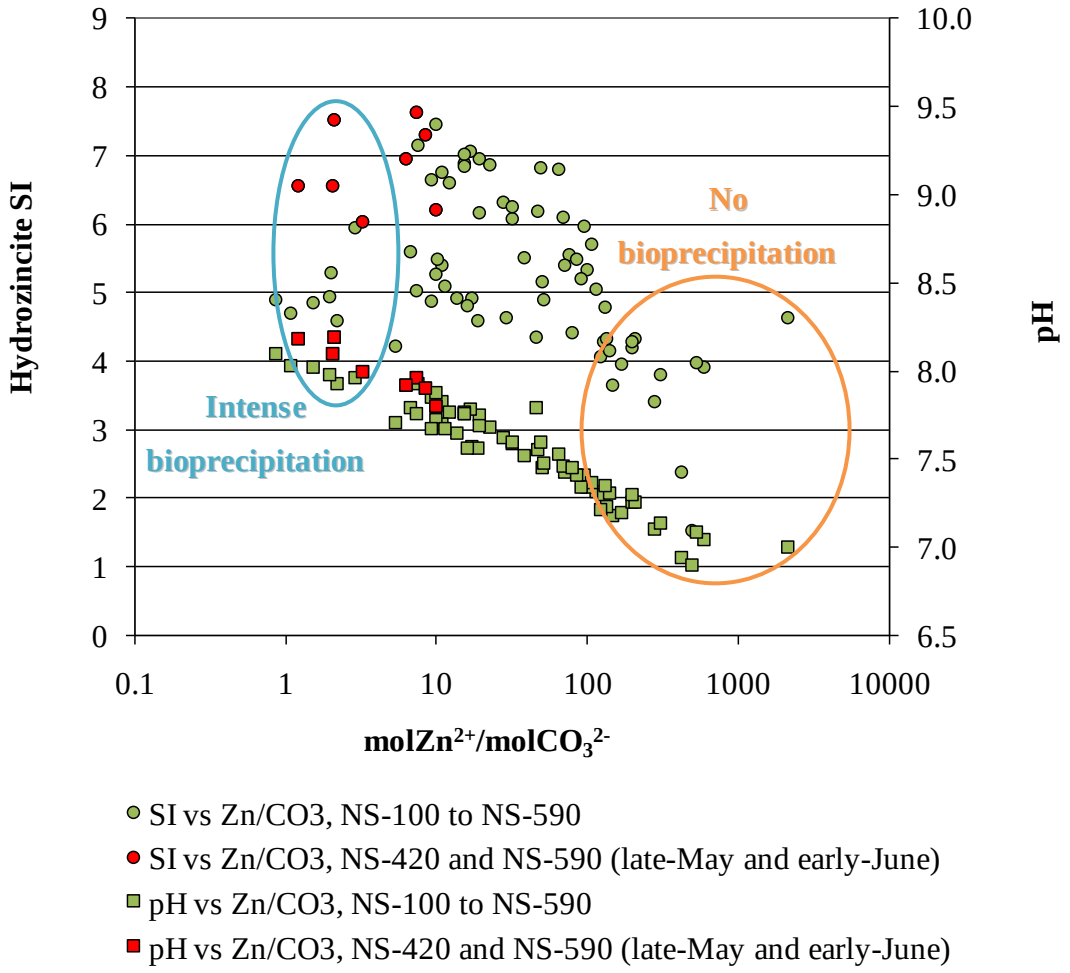

Figure 59. Plot showing hydrozincite SI vs Zn^{2+}/CO_3^{2-} molar ratio, and pH vs Zn^{2+}/CO_3^{2-} molar ratio in samples collected during 2009. Stations NS-420 and NS-590 are the stations of more efficient biomineralization.

4.3 Diel cycles in dissolved metals concentrations in the Naracauli stream

In the past, scientists assumed that a stream water sample collected at any time of the day would provide an accurate assessment of metal concentrations on that day. Many studies, however, show that dissolved concentrations of some trace metals in stream water vary by time of day (Bourg et al., 1996; Brick et al., 1996; Nimick et al., 2003; Nimick et al., 2005; Chapin et al., 2007; Kay et al., 2011). The specific mechanism that causes the variation in diurnal concentration is not known, but the effect likely

results from a combination of geochemical, biological, and physical processes that affect the partitioning of trace elements between the dissolved and solid phases (Lambing et al., 1999). To verify if diel variations occur along the Naracauli stream, a diel sampling was performed at station NS-420. Results of the diel sampling are reported in Appendix F.

Air and water temperature show a well defined diurnal cycle despite small differences between day and night in water temperature, i.e. only 5.2°C. Maximum water temperature is observed between the h 13:00 and h 17:00 (Fig. 60). Water temperature varies less than air temperature because water has higher specific heat. The pH values vary between 7.7 and 8.1 (Fig. 61); the highest values were observed during the sunny hours and the lowest during the night or early morning. Dissolved oxygen (DO) does not show significant diel variations (Fig. 62).

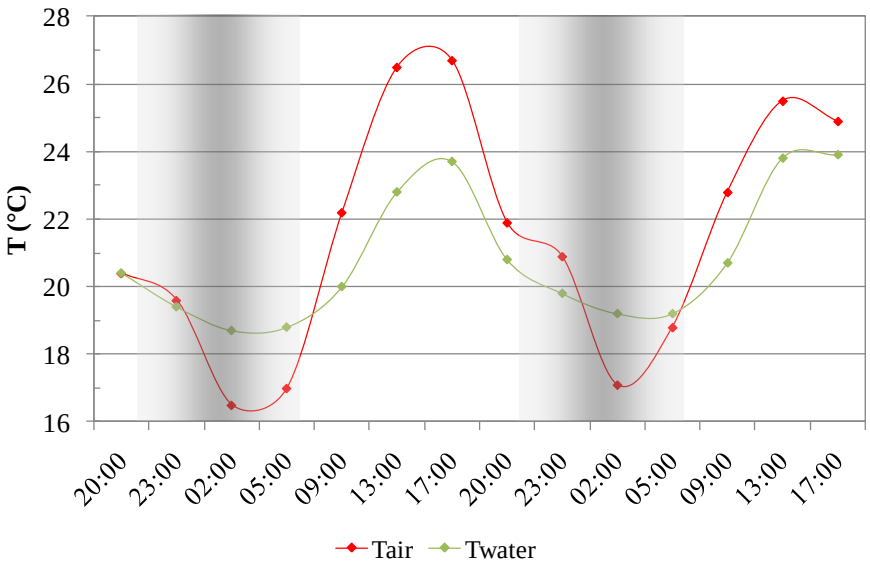

Figure 60. Variations in water and air temperatures during late spring low-flow diel sampling conducted 13 - 15 June 2011, station NS-420 (Naracauli stream). Shaded bars show night hours (sunrise 5:24, sunset 21:22).

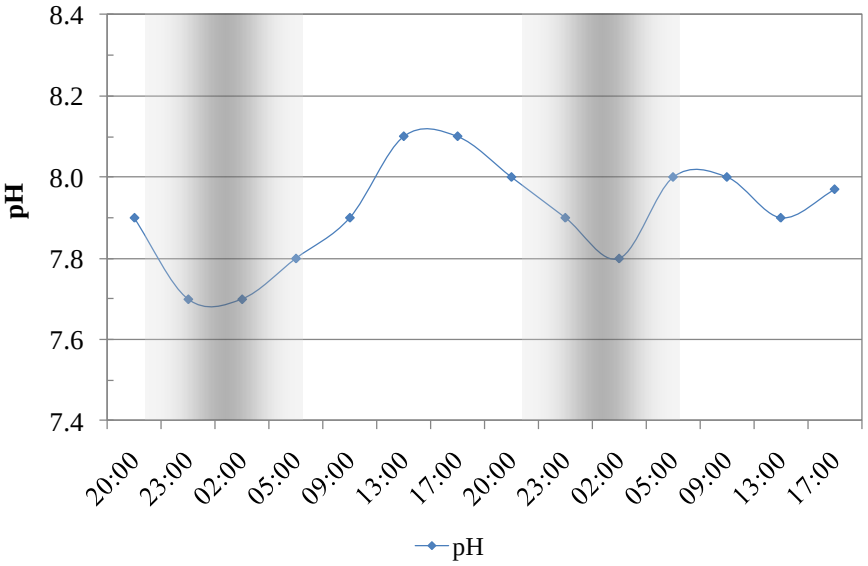

Figure 61. Variation in pH during late spring low-flow diel sampling conducted 13 - 15 June 2011, station NS-420 (Naracauli stream). Shaded bars show night hours (sunrise 5:24, sunset 21:22).

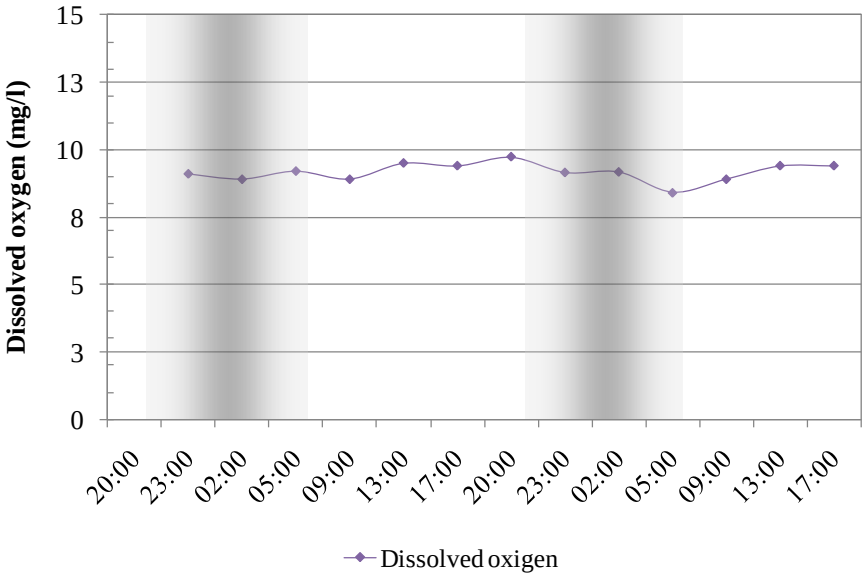

Figure 62. Variations in dissolved oxygen during late spring low-flow diel sampling conducted 13 - 15 June 2011, station NS-420 (Naracauli stream). Shaded bars show night hours (sunrise 5:24, sunset 21:22).

Among minor and trace elements, Zn, Co, Ni and Mn show well defined diurnal cycles (Figs. 63 - 65). Zn concentrations show the more consistent variation: the difference between the minimum (3 mg/l) and maximum (4.7 mg/l) Zn concentrations is 1.7 mg/l (about 35%). The minimum values occur at h 17:00 and maxima between h 02:00 and h 05:00. Zn speciation is dominated by Zn^{2+} and $ZnSO_4^0$ species.

The timing of diel cycles in Co and Ni (Fig. 64) are very similar to that for Zn, but the ranges of Co and Ni concentrations are much smaller than Zn. Co and Ni speciation is dominated by Co^{3+}, Ni^{2+} and $NiSO_4^0$ species.

The diel variation in Mn is 30 µg/l (Fig. 65). The minimum values occur at h 17:00 and maxima between h 05:00 and h 09:00. Mn speciation is dominated by $MnSO_4^0$ and $MnCO_3^0$ species.

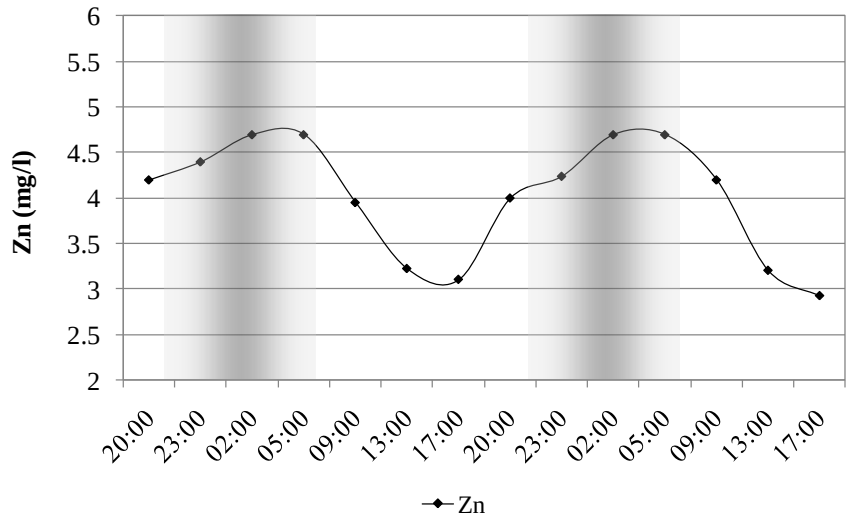

Figure 63. Variations in Zn concentrations during late spring low-flow diel sampling conducted 13 - 15 June 2011, station NS-420 (Naracauli stream). Shaded bars show night hours (sunrise 5:24, sunset 21:22).

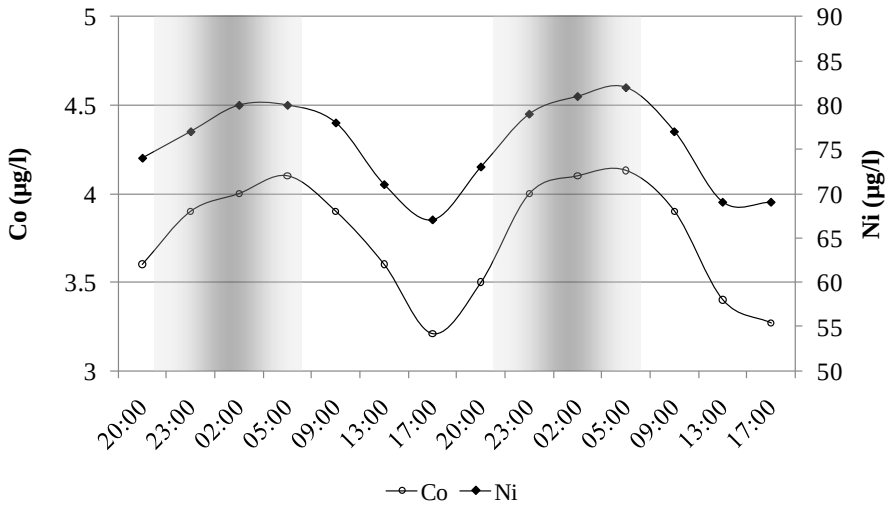

Figure 64. Variations in Co and Ni concentrations during late spring low-flow diel sampling conducted 13 - 15 June 2011, station NS-420 (Naracauli stream). Shaded bars show night hours (sunrise 5:24, sunset 21:22).

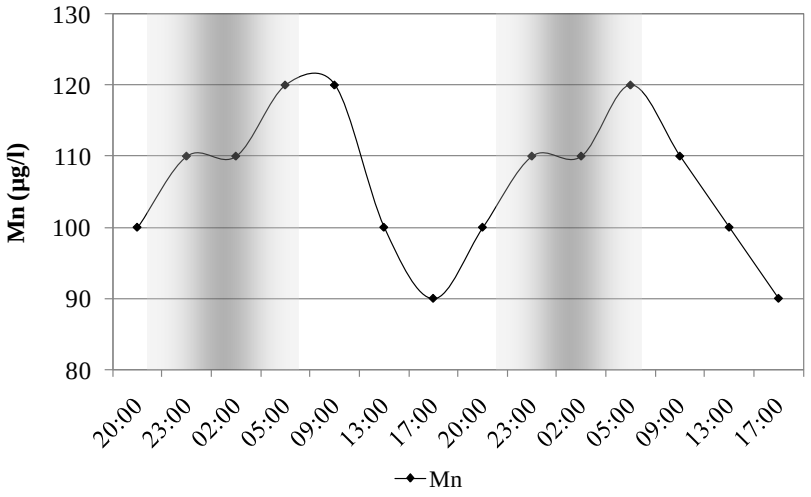

Figure 65. Variations in Mn concentrations during late spring low-flow diel sampling conducted 13 - 15 June 2011, station NS-420 (Naracauli stream). Shaded bars show night hours (sunrise 5:24, sunset 21:22).

The correlation of diel variations in Zn concentrations and selected field parameters (Figs. 66 - 68) was examined to understand the possible causes of diel cycles. Zn

concentration and temperature show a very strong negative correlation (R^2 = 0.95). Diel variations in temperature and dissolved Zn concentration are shown in Figure 66. The timing in which the maximum values of temperature and minimum Zn contents are measured are concurrent, this is in agreement with the strong inverse correlation.

Zn contents and pH values show a poor negative correlation (R^2 = 0.29). Diel variations in pH and dissolved Zn concentration are shown in Figure 67. The minimum pH values generally are reached at about h 23:00. Near sunrise (about h 05:00) pH begins to increase, almost simultaneously as Zn concentrations begin to fall. The highest values of pH are reached between h 13:00 and h 17:00, which correspond with minimum Zn concentrations. Observed pH variations are in agreement with other studies that attribute diel cycle in pH to photosynthetic activity (Wright et al., 1967; Fuller et al., 1989).

Zn concentrations and electrical conductivity show a moderate negative correlation (R^2 = 0.49) but conductivity does not show a well defined diel cycle (Fig. 68).

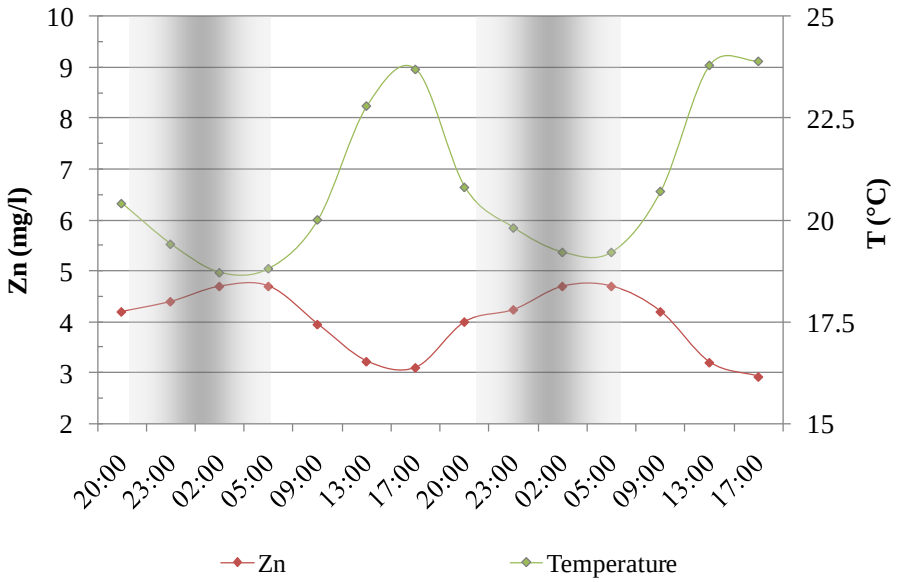

Figure 66. Variations in Zn concentrations and water temperature during late spring low-flow diel sampling conducted 13 - 15 June 2011, station NS-420 (Naracauli stream). Shaded bars show night hours (sunrise 5:24, sunset 21:22).

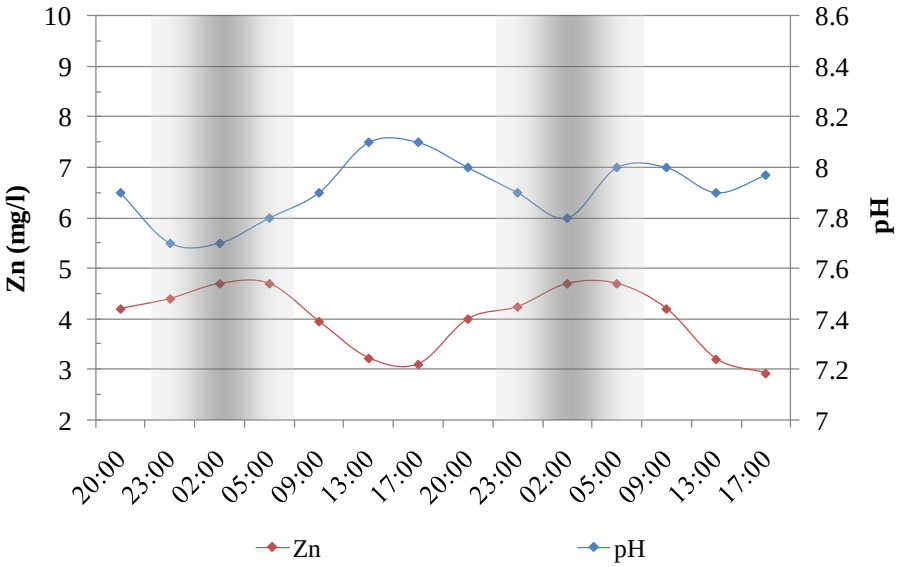

Figure 67. Variations in Zn concentrations and pH during late spring low-flow diel sampling conducted 13 - 15 June 2011, station NS-420 (Naracauli stream). Shaded bars show night hours (sunrise 5:24, sunset 21:22).

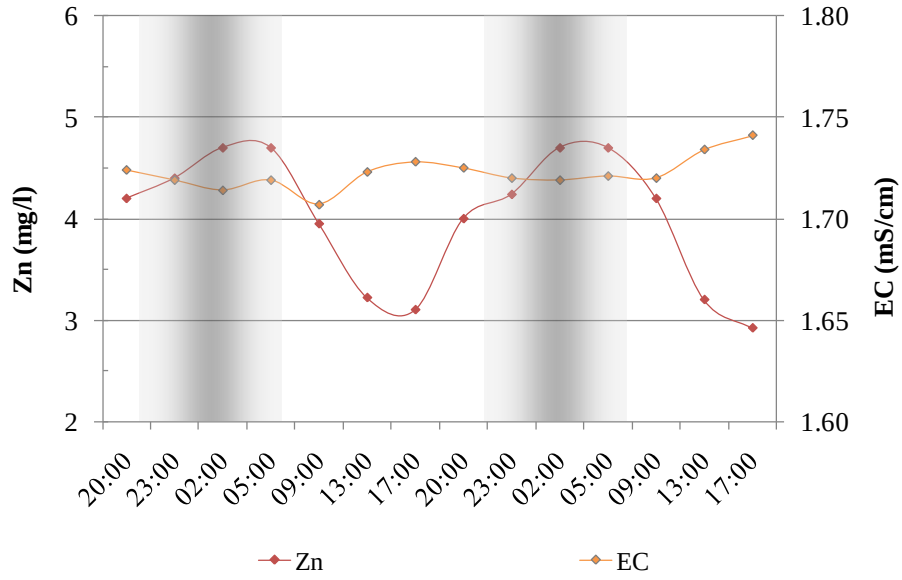

Figure 68. Variations in Zn concentrations and electrical conductivity (EC) during late spring low-flow diel sampling conducted 13 - 15 June 2011, station NS-420 (Naracauli stream). Shaded bars show night hours (sunrise 5:24, sunset 21:22).

Taking into account the obtained results, several processes are probably responsible for diel Zn cycle. Considering the relations among temperature, pH and Zn contents,

temperature and pH would seem to be the parameters that control variations in Zn concentration. Water temperature varies due to change in air temperature and incident solar radiation. The diel pH cycle derives from photosynthesis (predominant during the day) and respiration (predominant during the night) as described by the following equation (Jørgensen et al., 1979; Bourg et al., 2000):

$$6CO_2 + 12H_2O \leftrightarrow C_6H_{12}O_6 + 6O_2 + 6H_2O$$

Diel changes in temperature and pH could result in cyclic precipitation and dissolution of amorphous hydrous oxides, carbonates, or other minerals containing Zn. Figure 69 shows diel variations in hydrozincite SI and Zn^{2+}/CO_3^{2-} molar ratio. The highest values of hydrozincite SI were calculated in waters collected during the daytime; these high hydrozincite SI values correspond to values of Zn^{2+}/CO_3^{2-} molar ratio close to 1. These conditions are in agreement with the optimum conditions for hydrozincite precipitation (see Paragraph 4.2.3), and might explain the decrease in Zn concentration during daytime. Considering that, even if hydrozincite SI varies, the stream remained substantially supersaturated and that variations in pH are not so great, an effective dissolution of hydrozincite likely cannot explain the observed trend. The Zn cycle could be attributed to a more pronounced precipitation of hydrozincite at high pH and high temperature (Preis et al., 2001) during the day, and a lower or absent precipitation during the night, when pH and temperature decrease. Moreover, even if the bulk stream water does not produce cyclic hydrozincite precipitation and dissolution, it may occur on biofilms or cell surfaces, where water chemistry may differ widely from the bulk water (Hartley et al. 1996; Woodruff et al., 1999; Gadd, 2010).

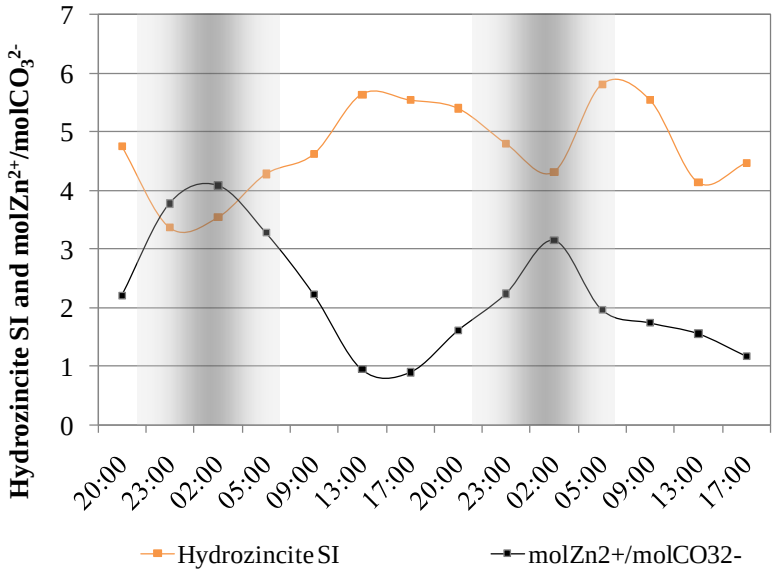

Figure 69. Variations in hydrozincite SI and Zn^{2+}/CO_3^{2-} molar ratio during late spring low-flow diel sampling conducted 13 - 15 June 2011, station NS-420 (Naracauli stream). Shaded bars show night hours (sunrise 5:24, sunset 21:22).

In addition, diel changes in temperature and pH could affect adsorption/desorption reactions and, consequently, Zn concentration in the Naracauli stream. Adsorption/desorption processes can take place at the surface of inorganic substrates such as hydrous metal oxides (Dobson et al., 1997) and carbonates (Comans et al., 1987; Kobayashi et al., 2004; Lafuente et al., 2008), as well as organic substrates such as biofilms (Gray et al., 1995; Hill et al., 2000; Fein et al., 2001; Wilson et al., 2001; Fein, 2006). Many studies show that cation adsorption onto colloids and/or bacterial surfaces and biofilms is an endothermic process (Johnson, 1990; Machesky, 1990; Dianati Tilaki et al., 2004; Gammons et al., 2005) and a pH-dependent process (Smith, 1999; Yee et al., 2001; Borrok et al., 2004). Thus, during the night and early morning, when water temperature and pH are lower, adsorption of Zn would decrease, resulting in higher concentrations in waters. In contrast, during the morning and afternoon, when water temperature and pH increase, adsorption would increase and remove Zn from solution. Adsorption/desorption reactions are a possible explanation for diel cycles, and they are supported by the strong relationship in the

symmetry of plots of Zn concentration, temperature, and pH, and the nearly coincident timing of the maxima and minima (see Figs. 66 and 67).

CHAPTER 5 SUMMARY AND CONCLUSIONS

The results of this study demonstrate the main chemical characteristics of the waters in the Naracauli stream catchment area and their variations under different seasonal conditions. The investigated waters show different salinity and element concentrations depending on the interaction of water with mineralized bodies, mine tailings and wastes, the composition of these materials, and the flow conditions. Waters from tributaries show the lowest concentrations of contaminants. The highest contents in harmful and toxic elements were observed in waters at stations A and B that drain flotation tailings and mine wastes.

Upstream of the Rio Pitzinurri, the mobility of Zn, Pb, Cd, Cu and Ni is controlled by the bioprecipitation of hydrozincite, which leads to natural reduction of metal concentrations in contaminated waters. The optimum conditions for hydrozincite formation occur in spring following a rainy winter, when the hydraulic regime in the stream reaches steady state conditions, i.e. weeks after abundant rainfall. The efficiency of the process is related to specific hydrochemical conditions. In particular, the Zn content, pH, alkalinity, and hydrozincite SI values play a relevant role in the biomineralization efficiency. Heavy rain events occurring in late spring appear to inhibit biomineralization, likely due to the decrease in the SI value resulting from the dilution effect of rain water. Conversely, when the biomineralization process reaches its maximum intensity, the highest values of SI and pH are observed, in agreement with the greater stability of the hydrozincite solid in contact with slightly alkaline waters. Contemporarily, the Zn^{2+}/CO_3^{2-} molar ratio reaches a value close to 1 in stations of more efficient biomineralization, suggesting that this value might correspond to more favourable conditions for activating the hydrozincite precipitation.

The previously demonstrated biological control on Naracauli biomineralization was further constrained in this work, showing that morphological parameters, such as

length and diameter of sheaths, depend on the influence of environmental conditions on bacteria morphology.

Diel cycles in dissolved Zn, Co, Ni and Mn were found to occur at station NS-420. The highest change in concentration was observed for Zn. Increased nocturnal concentrations could result from a combination of geochemical and biological processes. The results may be explained in terms of adsorption-desorption reactions (onto colloids, carbonates, bacterial surfaces and biofilms) and/or different rates of mineral precipitation between morning and night time. Diel metal cycles should be taken into account to evaluate environmental conditions, potential risks and cleanup of contaminated sites.

The innovative approach of this work was to combine geochemical and mineralogical investigations with biological information, specifically on the structure and development of biofilm under different water chemistry and flow conditions. Information on variables that control the biomineralization process is fundamental for the development of bioremediation strategies. This work will lay a solid foundation for designing future bioremediation methodologies for waters influenced by mining activities. In fact, obtained results suggest that the bioprecipitation of hydrozincite could be applied to attenuate metal pollution in mining environments where no problems of water acidification exist. The microbial inoculation together with the alterations and control of hydrochemical parameters may be an attractive approach for *in situ* bioremediation providing that necessary conditions for hydrozincite precipitation are achieved.

Future research should be directed to verify if diel cycles are affected by seasonal conditions, and clarify microbiological seasonal dynamics in the Naracauli stream, specifically the conditions that favour *Scytonema sp*. predominance, together with an appropriate understanding of microbe-metal-related reactions. This information will help to assess the best conditions to develop bioremediation techniques, and allow for optimization of the biomineralization process by controlling the physico-chemical conditions of the contaminated are

REFERENCES

Armstrong R.D., Todd M., Atkinson J.W., Scott K. (1997). Electroseparation of cobalt and nickel from a simulated wastewater. J. Appl. Electrochem., 27(8): 965-969.

Assorgia A., Brotzu P., Morbidelli L., Nicoletti M., Traversa G. (1984). Successione e cronologia (K-Ar) degli eventi vulcanici del complesso calco-alcalino oligo-miocenico dell'Arcuentu (Sardegna centro-occidentale). Period. Mineral., 53: 89-102.

Banfield J.F., Welch S.A., Zhang H., Ebert T.T., Penn RL. (2000). Aggregation-based crystal growth and microstructure development in natural iron oxyhydroxide biomineralization products. Science, 289(5480): 751-754.

Bazylinski D. A., Frankel R. B. (2003). Biologically Controlled Mineralization in Prokaryotes. In Biomineralization. P.M. Dove, S. Weiner and J.J. De Yoreo (Eds.). Mineral. Soc. Amer., Washington, D.C. Rev. Mineral. Geochem., 54: 217-247.

Bhaskar P.V., Bhosle N.B. (2006). Bacterial extracellular polymeric substance (EPS): a carrier of heavy metals in the marine food-chain. Environ. Int., 32(2): 191-198.

Borrok D., Fein J.B., and Kulpa C.F., (2004). Proton and Cd adsorption onto natural bacterial consortia: testing universal adsorption behavior. Geochim. Cosmochim Ac., 68(15): 3231-3238.

Bourg A.C.M., Bertin C. (1996). Diurnal variations in the water chemistry of a river contaminated by heavy metals: natural biological cycling and anthropic influence. Water Air Soil Poll., 86(1-4): 101-116.

Bourg A. C. M., Kedziorek M. A. M., Crouzet C. (2000). Seasonal Cycles of Dissolved Cd, Mn and Zn in River Water Caused by Variations in pH Induced by Biological Activity. Aquat. Geochem., 6(4): 461-471.

Boyd R.S. (2010). Heavy metal pollutants and chemical ecology: exploring new frontiers. J. Chem. Ecol., 36(1): 46-58.

Braissant O., Decho A.W., Dupraz C., Glunk C., Przekop K.M., Visscher P.T. (2007). Exopolymeric substances of sulfate-reducing bacteria: Interactions with

calcium at alkaline pH and implication for formation of carbonate minerals. Geobiology, 5(4): 401-411.

Brick C. M., Moore J. N. (1996). Diel Variation of Trace Metals in the Upper Clark Fork River, Montana. Environ. Sci. Technol., 30(6): 1953-1960.

Bundy M.E., Oreskes N., Hanchar J.M. (1996). Origin of convex-upward REE trend in bog seep and mine effluent twaters in Paradise Basin, San Juan Mountains. Geol. Soc. Am. Abstr. Prog., 28: A-469.

Carmignani L., Barca S., Oggiano G., Pertusati I., Conti P., Eltrudis A., Funedda A., Pasci S. (1996). Carta Geologica della Sardegna 1:200.000. Serv Geol d'Italia.

Cavinato A., Zuffardi P. (1948). Geologia della miniera di Montevecchio. In: Notizie sull'industria del Piombo e dello Zinco in Italia, 1: 427-464. Montevecchio Società Italiana del Piombo e dello Zinco.

Chapin T.P., Nimick D. A., Gammons C. H., Wanty R. B. (2007). Diel Cycling of Zinc in a Stream Impacted by Acid Rock Drainage: Initial Results from a new in situ Zn Analyzer. Environ. Monit. Assess., 133(1-3): 161-167.

Cidu R., Biddau R. (2007). Transport of trace elements at different seasonal conditions: effects on the quality of river water in a Mediterranean area. Appl. Geochem., 22(12): 2777-2794.

Cidu R., Frau R. (2009). Distribution of trace elements in filtered and non filtered aqueous fractions: Insights from rivers and streams of Sardinia (Italy). Appl. Geochem., 24(4): 611-623.

Civilini M., Ceccon L., De Bertoldi M. (2006). Biological Waste water Treatments for Metallurgical Industries. Ann. Microbiol., 56(1): 7-12.

Comans R.N. J., Middelburg J.J. (1987). Sorption of trace metals on calcite: Applicability of the surface precipitation model. Geochim. Cosmochim. Ac., 51(9): 2587-2591.

Concas E., Caroli S. (1994). Le Miniere di Gennamari e Ingurtosu. Pezzini (Ed.), Viareggio.

Cuif J.P., Dauphin Y., Sorauf J.E. (2011). Biominerals and Fossils Through Time. Cambridge University Press (Ed.).

Cutting R.S., Coker V.S, Telling N.D., Kimber R.L., Pearce C.I., Ellis B.L., Lawson R.S., Van Der Laan G., Pattrick R.A.D., Vaughan D.J., Arenholz E., Lloyd J.R. (2010). Optimizing Cr(VI) and Tc(VII) remediation through nanoscale biomineral engineering. Environ. Sci. Technol., 44(7): 2577-2584.

Decho A.W. (2000). Microbial biofilms in intertidal systems: an overview. Cont. Shelf Res., 20(10-11): 1257-1273.

De Carvalho C.C.C.R., Fernandes P. (2010). Production of Metabolites as Bacterial Responses to the Marine Environment. Mar. Drugs, 8(3): 705-727.

De Giudici G., Podda F., Caredda A., Tombolini R., Casu M., Ricci C. (2007). In vitro investigation of hydrozinicte biomineralization. In: Bullen, T.D. and Wang, Y. (Eds.), Water Rock Interaction 12, vol. 2. London: Taylor and Francis: 415-419.

De Giudici G., Podda F., Sanna R., Musu E., Tombolini R., Cannas C., Musinu A., Casu M. (2009). Structural properties of biologically controlled hydrozincite: An HRTEM and NMR spectroscopic study. Am. Mineral., 94(11-12): 1698-1706.

Dianati Tilaki R., Mahmood S. (2004). Study on removal of Cadmium from water by adsorption on GAC, BAC and Biofilter, Pak. J. Biol. Sci., 7(5): 865-869.

Diels L., De Smet M., Hooyberghs L., Corbisier P. (1999). Heavy metals bioremediation of soil. Mol. Biotechnol., 12(2): 149-158.

Dittrich M., Obst M., 2004. Are picoplankton responsible for calcite precipitation in lakes? Ambio, 33(8): 559-564.

Dittrich M., Sibler S. (2010). Calcium carbonate precipitation by cyanobacterial polysaccharides. In Tufas and Speleothems: Unravelling the Microbial and Physical Controls. Pedely H.M. and Rogerson M. (Eds.). Geol. Soc. SP., 336(1): 51-63.

Dobson K.D., Connor P.A., McQuillan A.J. (1997). Monitoring Hydrous Metal Oxide Surface Charge and Adsorption by STIRS. Langmuir, 13(10): 2614-2616.

Dong D., Nelson Y.M., Lion L.W., Shuler M.L., Ghiorse W.M. (2000). Adsorption of Pb and Cd onto metal oxides and organic material in natural surface coatings as determined by selective extractions: new evidence for the importance of Mn and Fe oxides. Wat. Res., 34(2): 427-436.

Dupraz C., Visscher P.T. (2005). Microbial lithification in marine stromatolites and hypersaline mats. Trends Microbiol., 13(9): 429-438.

Dupraz C., Reid R.P., Braissant O., Decho A.W., Norman R.S., Visscher P.T. (2009). Processes of carbonate precipitation in modern microbial mats. Earth-Sci. Rev., 96(3): 141-162.

Ehling-Schulz M., Bilger W., Scherer S. (1997). UV-B-induced synthesis of photoprotective pigments and extracellular polysaccharides in the terrestrial Cyanobacterium Nostoc commune. J. Bacteriol., 179(6): 1940-1945.

Elderfield H., Upstill-Goddard R., Sholkovitz E.R. (1990). The rare earth elements in rivers, estuaries, and coastal seas and their significance to the composition of ocean water. Geochim. Cosmochim. Ac., 54(4): 971-991.

Fein J.B., Martin, A.M., Wightman P.G. (2001). Metal adsorption onto bacterial surfaces: development of a predictive approach. Geochim. Cosmochim. Ac., 65(23): 4267-4273.

Fein J.B. (2006). Thermodynamic modeling of metal adsorption onto bacterial cell walls: current challenges. Adv. Agron., 90: 179-202.

Flemming H.C., Wingender J. (2010). The biofilm matrix. Nat. Rev. Microbiol., 8(9): 623-633.

Fuller C.C., Davis J.A. (1989). Influence of coupling of sorption and photosynthetic processes on trace element cycles in natural waters. Nature, 340: 52-54.

Gadd G.M. (2004). Microbial influence on metal mobility and application for bioremediation. Geoderma, 122(2-4): 109-119.

Gadd G.M. (2010). Metals, minerals and microbes: geomicrobiology and bioremediation. Microbiology, 156(3): 609-643.

Gammons C., Nimick D., Parker S., Cleasby T., Mccleskey R. (2005). Diel behaviour of iron and other heavy metals in a mountain stream with acidic to neutral pH: Fisher Creek, Montana, USA. Geochim. Cosmochim. Ac., 69(10): 2505-2516.

Garcia-Pichel F., Castenholz R.W. (1991). Characterization and biological implications of scytonemin, a cyanobacterial sheath pigment. J. Phycol., 27(3): 395-409.

Ghose, S. (1964). The crystal structure of hydrozincite, $Zn_5(OH)_6(CO_3)_2$. Acta Crystallogr., 17: 1051-1057.

Gilbert P.U.P.A., Abrecht M., Frazer B.H. (2005). The Organic-Mineral Interface in Biominerals. In Molecular Geomicrobiology. Banfield J.F., Nealson K.H., Cervini-Silva J. (Eds.). Mineral. Soc. Amer., Washington D.C. Rev. Mineral. Geochem., 59. 157-185.

González-Muñoz M.T., Rodriguez-Navarro C., Martínez-Ruiz F., J.M. Arias, M.L. Merroun, M. Rodriguez-Gallego (2010). Bacterial biomineralization: new insights from Myxococcus-induced mineral precipitation. Geol. Soc., London, SP, 336: 31-50.

Gosselin D.C., Smith M.R., Lepel E.A., Laul J. (1992). Rare earth elements in chloride-rich groundwater, Palo Duro Basin, Texas, USA. Geochim. Cosmochim. Ac., 56(4): 1495-1505.

Gray B.R., Hill W.R. (1995). Nickel sorption by periphyton exposed to different light intensities, J. N. Am. Benthol. Soc., 14(2): 299-305.

Handley-Sidhu S., Renshaw J.C., Moriyama S., Stolpe B., Mennan C., Bagheriasl S., Yong P., Stamboulis A., Paterson-Beedle M., Sasaki K., Pattrick R.A., Lead J.R., Macaskie L.E. (2011). Uptake of Sr^{2+} and Co^{2+} into biogenic hydroxyapatite: implications for biomineral ion exchange synthesis. Environ. Sci. Technol., 45(16): 6985-90.

Hartley A.M., House W.A., Leadbeater B.S.C., Callow M.E. (1996). The use of microelectrodes to study precipitation of calcite upon algal biofilms, J. Colloid Interface Sci., 183(2): 498-505.

Hazen R.M., Papineau D., Bleeker W., Downs R.T., Ferry J.M., McCoy T.J., Sverjensky D.A., Yang,H. (2008). Mineral evolution. Am. Mineral. 93(11-12): 1693-1720.

Hazen R.M., Ferry J.M. (2010). Mineral evolution: Mineralogy in the fourth dimension. Elements, 6(1): 9-12.

Hill W.R., Bednarek A.T., Larsen I.L. (2000). Cadmium sorption and toxicity in autotrophic biofilms. Can. J. Fish. Aquat. Sci., 57: 530-537.

Hoyle J., Elderfield H., Gledhill A., and Greaves M. (1984) .The behavior of the rare earth elements during mixing of river and sea waters. Geochim. Cosmochim. Ac., 48(1): 143-149.

Iwamoto T., Nasu M. (2001). Current bioremediation practice and perspective. J. Biosci. Bioeng., 92(1): 1-8.

Jambor, J. L. (1964). Studies of basic copper and zinc carbonates. 1. Synthetic zinc carbonates and their relationship to hydrozincite. Can. Mineral., 8: 92-108.

James R.B. (2001). Remediation-By-Reduction Strategies for Chromate-Contaminated Soils. Environ. Geochem. Hlth., 23(3): 175-179.

Jiménez-Lopez C., Rodriguez-Navarro A., Dominguez-Verahttp J.M., Garcia-Ruiz J.M. (2003). Influence of lysozyme on the precipitation of calcium carbonate: A kinetic and morphologic study. Geochim. Cosmochim. Ac., 67(9): 1667-1676.

Jiménez-Lopez C., Jroundi F., Rodríguez-Gallego M., Arias J.M., González-Muñoz M.T. (2007). Biomineralization induced by Myxobacteria, in Communicating Current Research and Educational Topics and Trends. Appl. Microbiol., vol. 1: 143-154.

Johnson B.B. (1990). Effect of pH, Temperature, and Concentration on the Adsorption of Cadmium on Goethite. Environ. Sci. Technol., 24(1): 112-118.

Johnson K.L., Younger P.L. (2005). Manganese removal from minewaters using a novel enhanced bioremediation method. J. Environ. Qual. 34, 987-993.

Jørgensen B.B., Revsbech N.P., Blackburn T.H., Cohen Y. (1979). Diurnal cycle of oxygen and sulfide microgradients and microbial photosynthesis in a cyanobacterial mat sediment. Appl. Environ. Microbiol., 38(1): 46-58.

Karatan E., Watnick P. (2009). Signals, regulatory networks, and materials that build and break bacterial biofilms. Microbiol. Mol. Bio. R., 73(2): 310-347.

Kay R.T., Groschen G.E., Cygan G., Dupré D.H. (2011). Diel cycles in dissolved barium, lead, iron, vanadium, and nitrite in a stream draining a former zinc smelter site near Hegeler, Illinois. Chem. Geol., 283(1-2): 99-108.

Kobayashi H., Satoh K., Sawada K. (2004). Adsorption of divalent heavy metal ions on calcium carbonate (calcite). Bunseki Kagaku, 53(2): 101-107.

Lafuente A.L., González C., Quintana J.R., Vázquez A., Romero A. (2008). Mobility of heavy metals in poorly developed carbonate soils in the Mediterranean region. Geoderma, 145(3-4): 238-244.

Labrenz M., Druschel G.K., Thomsen-Ebert T., Gilbert B., Welch S.A., Kemner K.M., Logan G.A., Summons R.E., De Stasio G., Bond P.L., Lai B., Kelly S.D., Banfield J.F. (2000). Formation of sphalerite (ZnS) deposits in natural biofilms of sulfate-reducing bacteria. Science, 290(5497): 1744-1747.

Lambing J. H., Nimick D.A., Cleasby T.E. (1999). Short-term variation of trace-element concentrations during base flow and rainfall runoff in small basins, August 1999. In Integrated investigations of environmental effects of historical mining in the Basin and Boulder mining districts, Boulder River watershed, Jefferson County, Montana, Nimick D.A., Church S.E., Finger S.E., (Eds.). U.S. Geological Survey Professional Paper 1652-D7: 263-278.

Lattanzi P., Meneghini C., De Giudici G., Podda F. (2010a). Uptake of Pb by hydrozincite, $Zn_5(CO_3)_2(OH)_6$ - implications for remediation. J. Hazard. Mater., 177(1-3): 1138-1144.

Lattanzi P., Maurizio C., Meneghini C., De Giudici G., Podda F. (2010b). Uptake of Cd in hydrozincite, $Zn_5(CO_3)_2(OH)_6$: evidence from X-ray absorption spectroscopy and anomalous X-ray diffraction. Eur. J. Mineral., 22(4): 557-564.

Lattanzi P, Meneghini C, De Giudici G, Medas D, Podda F (2010c). Report of experiment CH-2838. ESRF, Grenoble.

Lee S.G., Lee D.H., Kim Y., Chae B.G., Kim W.Y., Woo N.C. (2003). Rare earth elements indicators of groundwater environment changes in fractured rock system: evidence from fracture-filling calcite. Appl. Geochem., 18(1): 135-143.

Leybourne M.I., Goodfellow W.D., Boyle D.R, Hall, G.M. (2000). Rapid development of negative Ce anomalies in surface waters and contrasting REE patterns in groundwaters associated with Zn-Pb massive sulphide deposits. Appl. Geochem., 15(6): 695-723.

Li P., Harding S.E., Liu Z. (2001). Cyanobacterial exopolysaccharides: their nature and potential biotechnological applications. Biotechnol. Genet. Eng. Rev., 18: 375-404.

Liang C., Bruell C.J., Marley M.C., Sperry K.L. (2004). Persulfate oxidation for in situ remediation of TCE. I. Activated by ferrous ion with and without a persulfate-thiosulfate redox couple. Chemosphere, 55(9) 1213-1223.

Livingston B., Killian C., Wilt F., Cameron A., Landrum M., Ermolaeva O., Sapojnikov V., Maglott D., Buchanan A.M., Ettensohn C.A. (2006). A genome-wide analysis of biomineralization-related proteins in the sea urchin Strongylocentrotus purpuratus. Dev. Boil., 300(1): 335-348.

Lloyd J. R., Lovley D.R. (2001). Microbial detoxification of metals and radionuclides. Curr. Opin. Biotechnol., 12(3): 248-253.

Lloyd J. R., Renshaw J.C. (2005). Bioremediation of radioactive waste: radionuclide-microbe interactions in laboratory and field-scale studies. Curr. Opin. Biotechnol., 16(3): 254-260.

Loi M (1992) Studio degli sterili della miniera di Ingurtosu e loro interazione con le acque del rio Naracauli, Degree thesis University of Cagliari.

Lowenstam H. A., (1981). Minerals formed by organisms. Science 211(4487), 1126-1131.

Lowenstam H. A., Weiner S. (1989). On biomineralization, Oxford University Press, Inc., New York.

Macaskie L.E., Bonthrone K.M., Yong P., Goddard D.T. (2000). Enzymatically mediated bioprecipitation of uranium by Citrobacter sp.: a concerted role for exocellular lipopolysaccharide and associated phosphatase in biomineral formation. Microbiology, 146(2000): 1855-1867.

Machesky M.L. (1990). Influence of temperature on ion adsorption by hydrous metal oxides In Chemical modeling of aqueous systems II, Melchior D.C., and Bassett R.L., (Eds.), Washington D.C., American Chemical Society Symposium Series 416: 283-292.

Mann S. (1983). Mineralization in biological systems. Struct. Bonding 54: 125-174.

Mann S. (2001). Biomineralization: Principles and Concepts. In Bioinorganic Materials Chemistry. Vol. 17. Oxford University Press, Oxford.

Marcello A., Pretti S., Valera P., Agus M., Boni M., Fiori M. (2004). Metallogeny in Sardinia (Italy): from the Cambrian to the Tertiary, 32nd international geological congress, APAT 4, 14-36, Firenze.

Margaret E., Angela G. (2007). Algae. In Practical Manual for Botany, New Age International Pvt. Ltd., Vol. 1: 1-26.

Mayer C., Moritz R., Kirschner C., Borchard W., Maibaum R., Wingender J., Flemming H.C. (1999). The role of intermolecular interactions: studies on model systems for bacterial biofilms. Int. J. Biol. Macromol. 26(1): 3-16.

McLennan S.M., (1989). Rare earth elements in sedimentary rocks. Influence of provenance and sedimentary processes. In Geochemistry and Mineralogy of Rare Earth Elements, Lipin B.R., McKay G.A. (Eds.), Mineral. Soc. Amer., Washington, D.C., Rev. Mineral., 21(1): 169-200.

Medaković D., Popović S. (2012). Unusual Crystal Formation in Organisms-Exceptions that Confirm Biomineralization Rules. In Crystallization and Materials Science of Modern Artificial and Natural Crystals, Borisenko Eò. (Ed.), InTech, 157-184.

Medas D., Cidu R., Lattanzi P., Podda F., De Giudici G. (2012). Natural Biomineralization in the Contaminated Sediment-water System at the Abandoned Mine of Ingurtosu. In Bio-Geo-Interactions in Metal Contaminated Soils, Kothe E. and Varma A. (Eds.), Soil Biology 31, Springer.

Medas D., Cidu R., Lattanzi P., Podda F., Wanty R.B., De Giudici G. (2012?). Hydrozincite seasonal precipitation at Naracauli (Sardinia-Italy): hydrochemical factors and morphological features of the biomineralization process. Appl. Geochem., SI WRI13, DOI: 10.1016/j.apgeochem.2012.02.016.

Medina D.D., Mastai Y. (2011). Biomimetic Polymers for Chiral Resolution and Antifreeze Applications. In On biomimetics, Assoc. Prof. Dr. Lilyana D. Pramatarova (Eds.), InTech, 321-354.

Meldrum F.C., Cölfen H. (2008). Controlling mineral morphologies and structures in biological and synthetic systems. Chem. Rev., 108(11): 4332-4432.

Mezzolani S., Simoncini A. (1993). Paesaggi e architetture delle miniere. Archivio fotografico sardo, Nuoro.

Mohamed Z.A. (2001) Removal of cadmium and manganese by a non-toxic strain of the freshwater cyanobacterium Gloethece magna. Water Res., 35: 4405-4409.

Mullin J.W. (1992). Crystallization. 3rd edn., Butterworth Heinemann, London.

Nair A., Abdalla G., Mohmed I. Premkumar K. (2005). Physicochemical parameters and correlation coefficient of ground waters of north-east Libiya. Pollut. Res., 24(1): 1-6.

Nicolaus B., Panico A., Lama L., Romano I., Manca M.C., De Giulio A., Gambacorta A. (1999). Chemical composition and production of exopolysaccharides from representative members of heterocystous and non-heterocystous cyanobacteria. Phytochemistry 52(4): 639-647.

Nimick D.A., Gammons C.H., Cleasby T.E., Madison J.P., Skaar D., Brick C.M., (2003). Diel cycles in dissolved metal concentrations in streams - Occurrence and possible causes. Water Resour. Res., 39(9): 1247-1264.

Nimick D.A., Cleasby T.E., McCleskey R.B (2005). Seasonality of diel cycles of dissolved trace-metal concentrations in a Rocky Mountain stream. Environ. Geol., 47(5):603-614.

Nordstrom D.K. (1977). Thermochemical redox equilibria of Zoßell's solution. Geochim. Cosmochim. Ac., 41(12): 1835-1841.

Nordstrom D.K., Carlson-Foscz V., Oreskes N. (1995). Rare Earth Element (REE) Fractionation During Acidic Weathering of San Juan Tuff, Colorado. Abstract, Ann. Mtg. Geol. Soc. Am., New Orleans, LA, A-199.

Pala A., Costamagna L.G., Muscas A. (1996). Valutazione delle riserve idriche nei bacini dei Rii Piscinas e Naracauli (Sardegna Meridionale). Boll. Soc. Geol. Ital., 115: 717-735.

Panwichian S., Kantachote D., Wittayaweerasak B., Mallavarapu M. (2011). Removal of heavy metals by exopolymeric substances produced by resistant purple non sulfur bacteria isolated from contaminated shrimp ponds. Electron. J. Biotechn., 14(4): 1-13.

Parkhurst D.L., Appelo C.A.J. (1999). User's guide to PHREEQC (version 2) - A computer program for speciation, batch-reaction, one-dimensional transport, and

inverse geochemical calculations. U.S. Geol. Surv. Water-Resour. Invest. Rep. 99-4259.

Patermaraxis G., Fountoukidis E. (1990). Disinfection of water by electrochemical treatment. Wat. Res., 24(12): 1491-1496.

Pentecost A. (1985). Association of cyanobacteria with tufa deposits: identity, enumeration and nature of the sheath material revealed by histochemistry. Geomicrobiol. J., 4(3): 285-298.

Phoenix V.R., Konhauser K.O., Adams D.G., Bottrell S.H. (2001). Role of biomineralization as an ultraviolet shield: implications for Archean life. Geology 29(9): 823-826.

Phoenix V.R., Konhauser K.O. (2008). Benefits of bacterial biomineralization. Geobiology, 6(3): 303-308.

Podda F., Zuddas P., Minacci A., Pepi M., Baldi F. (2000). Heavy metal coprecipitation with hydrozincite [Zn5 (CO3)2(OH)6] from mine waters caused by photosynthetic microorganisms. Appl. Environ. Microbiol., 66(11): 5092-5098.

Pourret O., Davranche M., Gruau G., Aline Dia, (2008). New insights into cerium anomalies in organic-rich alkaline waters. Chem. Geol., 251(1-4): 120-127.

Preis W.,Gamsjäger H.(2001). (Solid + solute) phase equilibria in aqueous solution. XIII. Thermodynamic properties of hydrozincite and predominance diagrams for (Zn^{2+} + H_2O + CO_2). J. Chem. Thermodyn., 33(7): 803-819.

Progemisa (2001). Le miniere di Montevecchio e Ingurtosu Gennamari. In Progetto Montevecchio Ingurtosu: 176-189.

Purevdorj B., Costerton J.W., Stoodley P. (2002). Influence of Hydrodynamics and Cell Signaling on the Structure and Behavior of *Pseudomonas aeruginosa* Biofilms. Appl. Environ. Microb., 68(9): 4457-4464.

Quinn K. A., Byrne R.H., Schijf J. (2006). Sorption of Yttrium and Rare Earth Elements by Amorphous Ferric Hydroxide: Influence of pH and Ionic Strength. Mar. Chem., 99(1-4): 128-150.

Rajan S.S. (2001). Introduction to algae, 1st edn. Anmol Publications Pvt. Ltd, New Delhi.

Renshaw J.C., Handly-Sidhu S., Macaskie L. (2010). Microbial biominerals: Role in radionuclide remediation. In Goldschmidt Conference Abstracts 2010, Geochim. Cosmochim. Ac. A863.

Riding R.E. (2000). Microbial carbonate: the geological record of calcified algal mats and biofilms. Sedimentology, 47(s1): 179-214.

Salvadori I., Zuffardi P. (1973). Guida per l'escursione a Montevecchio e all'Arcuentu. Itinerari Geologici, Mineralogici e Giacimentologici in Sardegna, 1: 29-46.

Schindler P., Reinert M., Gamsjäger H. (1969). Loslichkeitskonstanten und freieBildungsenthalpien von $ZnCO_3$(s) und $Zn_5(OH)_6(CO_3)_2$ bei 25°C. Helv. Chim. Acta, 52, 2327-2332.

Schwarzmann S., Boring J.R. III (1971). Antiphagocytic effect of slime from a mucoid strain of Pseudomonas aeruginosa. Infect. Immun., 3(6): 762-767.

Scott C., Fletcher R.L., Bremer G.B. (1996). Observations on the mechanisms of attachment of some marine fouling blue-green algae. Biofouling, 10(1-3): 161-176.

Secchi F.A.G., Brotzu P., Callegari E. (1991). The Arburese igneous complex (SW Sardinia). An example of dominant igneous fractionation leading to peraluminous cordierite-bearing leucogranites as residual melts. Chem. Geol., 92(1-3): 213-249.

Sella Q. (1999). Sulle condizioni dell'industria mineraria nell'isola di Sardegna: relazione alla commissione parlamentare d'inchiesta. Manconi F., Nuoro: Illisso.

Sholkovitz E.R., (1992). Chemical evolution of rare earth elements: fractionation between colloidal and solution phases of filtered river water. Earth Planet. Sc. Lett., 114(1): 77-84.

Sholkovitz E.R. (1995). The aquatic chemistry of rare earth elements in rivers and estuaries. Aquat. Geochem., 1(1): 1-34.

Simões M., Simões L.C., Vieira M.J. (2010). A review of current and emergent biofilm control strategies. Food Sci. and Technol., 43(4): 573-583.

Simon F.G., Meggyes T. (2000). Removal of organic and inorganic pollutants from groundwater using permeable reactive barriers. Part 1., Treatment processes for pollutants. Land Contam. Reclam., 8(2): 103-116.

Singh R., Pauland D., Jain R.K. (2006). Biofilms: implications in bioremediation. Trends Microbiol., 14(9): 389-397.

Skinner, H. C. W., 2005. Biominerals. Mineral. Mag. 69: 621-641.

Skinner H.C.W., Jahren A.H. (2007). Biomineralization. In Biogeochemistry, vol. 8, Schlesinger W.H. (Ed.), Treatise on Geochemistry, Oxford, Elsevier-Pergamon, Chapter 4, revised, 2nd edn: 117-184.

Smith K.S. (1999). Metal sorption on mineral surfaces: an overview with examples relating to mineral deposits. In The Environmental Geochemistry of Mineral Deposits, Plumlee G.S., Logsdon M.J. (Eds.), Part A: Processes, Techniques, and Health Issues. Rev. Econ. Geol., Soc. Eco. Geo., 6A: 161-182.

Stara P., Rizzo R., Tanca G.A. (1996). Iglesiente e Arburese. Miniere e Minerali, vol. 2, EMSA (Ed.) Cagliari.

Stolz J.F., (2000). Structure of Microbial Mats and Biofilm. In Microbial Sediments, Riding R.E., Awramik S.M. (Eds.), Springer-Verlag Berlin Heidelberg: 1-8.

Sutherland I.W. (2001a). Biofilm exopolysaccharides: a strong and sticky framework. Microbiology, 147(1): 3-9.

Sutherland I.W. (2001b). The biofilm matrix - an immobilized but dynamic microbial environment. Trends Microbiol., 9(5): 222-227.

Tang J., Johannesson K.H. (2003). Speciation of rare earth elements in natural terrestrial waters: Assessing the role of dissolved organic matter from the modeling approach. Geochim. Cosmochim. Ac., 67(13): 2321-2339.

Thompson J.B., Schultze-Lam S., Beveridge T.J., Des Marais D. (1997). Whiting events: biogenic origin due to the photosynthetic activity of cyanobacterial picoplankton. Limnol. Oceanogr., 42(1): 133-141.

Thompson J.B., Ferris F.G. (1990). Cyanobacterial precipitation of gypsum, calcite, and magnesite from natural alkaline lake water. Geology, 18(10): 995-998.

Tröster I., Schäfer L., Fryda M., Matthée T. (2002). Electrochemical advanced oxidation process using DiaChem® electrodes. Diam. Rela. Mater., 11(3-6): 640-645.

Tsezos M.,Hatzikioseyian A., Remoundaki E. (2004). Mining and Metallurgical Effluents Treatment by Biofilm Reactors: The Contribution of Biological Processes In Proceedings of ASEM workshop on EU/ASIA S&T Cooperation on Clean Technologies, 3-6 November 2004, Hanoi, Vietnam: 435-444.

U.S. Environmental Protection Agency (2001). A Citizen's Guide to Bioremediation. EPA 542-F-01-001, Office of Solid Waste and Emergency Response.

U.S. Geological Survey. Bioremediation: Nature's Way to a Cleaner Environment. (1997). Retrieved July 7, 2004 from http://water.usgs.gov/wid/html/bioremed.html.

Van Cappellen P.V. (2003). Biomineralization and Global Biogeochemical Cycles. In Biomineralization. P.M. Dove, S. Weiner and J.J. De Yoreo (Eds.). Mineral. Soc. Amer., Washington, D.C. Rev. Mineral. Geochem., 54: 57-381.

Vidic R.D., Pohland F.G. (1996). Treatment Walls. Technology Evaluation Report TE-96-01, Groundwater Remediation Technologies Analysis Center, Pittsburgh, PA.

Vidali M., (2001). Bioremediation. An overview. Pure Appl. Chem., 73(7): 1163-1172.

Weiner S., Dove P.M. (2003). An Overview of Biomineralization and the Problem of the Vital Effect. In Biomineralization. P.M. Dove, S. Weiner and J.J. De Yoreo (Eds.). Mineral. Soc. Amer., Washington, D.C. Rev. Mineral. Geochem., 54: 1-31.

White C., S.C. Wilkinson, Gadd G.M. (1995). The Role of Microorganisms in Biosorption of Toxic Metals and Radionuclides. Int. Biodeter. Biodegr., 35(1-3): 17-40.

White C., Gadd G.M. (1998). Accumulation and effects of cadmium on sulphate-reducing bacterial biofilms. Microbiology, 144(5): 1407-1415.

White C., Gadd G.M. (2000). Copper accumulation by sulfate-reducing bacterial biofilms. FEMS Microbiol. Lett. 183(2): 313-318.

Whitton B.A., Potts M. (2000). Introduction to the Cyanobacteria. In The ecology of cyanobacteria, their diversity in time and space, Whitton B.A., Potts M. (Eds.), Kluwer Academic Publishers, Netherlands: 1-11.

Wilson A.R., Lion L.W., Nelson Y.M., Shuler M.L., Ghiorse W.C. (2001). The effects of pH and surface composition on Pb adsorption to neutral freshwater biofilms. Environ. Sci. Technol., 35(1): 3182-3189.

Woodruff S., House W.A., Callow M.E., Leadbeater B.S.C. (1999). The effects of a developing biofilm on chemical changes across the sediment-water interface in a freshwater environment. Internation. Rev. Hydrobiol., 84: 509-532.

Wright J.C., Mills I.K. (1967). Productivity studies on the Madison River, Yellowstone National Park, Limnol. Oceanogr., 12(4): 568-577.

Yee N., Fein J. (2001). Cd Adsorption Onto Bacterial Surfaces: A Universal Adsorption Edge? Geochem. Cosmochim. Ac., 65(13): 2037-2042.

Yoreo J.J., Vekilov P.G. (2003). Principles of Crystal Nucleation and Growth. In Biomineralization. P.M. Dove, S. Weiner and J.J. De Yoreo (Eds.). Mineral. Soc. Amer., Washington, D.C. Rev. Mineral. Geochem., 54: 57-93.

Zhang X.Q., Bishop P.L., Kupferle M.J. (1998). Measurement of polysaccharides and proteins in biofilm extracellular polymers. Wat. Sci. Technol. 37(4-5): 345-348.

Zivanovic S., Li J., Davidson P.M., Kit K. (2007). Physical, Mechanical, and Antibacterial Properties of Chitosan/PEO Blend Films. Biomacromolecules, 8(5): 1505-1510.

Zuddas P., Podda F. (2005). Variations in physico-chemical properties of water associated with bioprecipitation of hydrozincite [$Zn_5(CO_3)_2(OH)_6$] in the waters of Rio Naracauli, Sardinia (Italy). Appl. Geochem., 20(3): 507-517.

APPENDIX A1

ANALYTICAL RESULTS OF THE NARACAULI STREAM WATERS SAMPLED FROM 2009 TO 2011: PHYSICO-CHEMICAL PARAMETERS AND CHEMICAL COMPONENTS.

Sample no.	**Date**	**Type**	**T** °C	**pH**	**E_h** V	**EC** mS/cm	**TDS** g/l	**Ca** mg/l	**Mg** mg/l	**Na** mg/l	**K** mg/l	**Zn** mg/l	**HCO_3** mg/l	**Cl** mg/l	**SO_4** mg/l	**NO_3** mg/l	**Br** mg/l	**F** mg/l	**SiO_2** mg/l
NS-100	03/18/2009	*st*	15	7.4	0.47	1.59	1	154	64	57	6.6	38	216	107	500	3.8	n.d.	0.4	9.2
NS-100	03/25/2009	*st*	16	7.3	0.49	1.61	1	153	61	58	6.2	35	201	109	476	n.d.	n.d.	n.d.	8.6
NS-100	04/17/2009	*st*	17	6.9	0.60	1.31	1.1	165	61	62	6.2	47	165	109	593	n.d.	n.d.	n.d.	9.5
NS-100	05/07/2009	*st*	18	7.2	0.54	1.53	1.1	166	66	64	6	37	201	114	584	n.d.	n.d.	n.d.	10
NS-100	05/21/2009	*st*	19	7.2	0.52	1.41	1.1	154	63	62	5.9	34	212	109	551	n.d.	n.d.	n.d.	10
NS-100	05/27/2009	*st*	18	7.3	0.53	1.38	1.1	160	65	62	5.8	38	217	106	536	n.d.	n.d.	n.d.	10
NS-100	06/03/2009	*st*	19	7.4	0.53	1.33	1	143	58	56	6.6	41	201	104	527	n.d.	n.d.	n.d.	11
NS-100	06/10/2009	*st*	18	7.5	0.45	1.4	1	149	61	57	6.4	34	218	104	512	n.d.	n.d.	n.d.	7.7
NS-100	06/17/2009	*st*	19	7.3	0.47	n.d.	1.1	157	65	62	6.2	35	218	106	512	n.d.	n.d.	n.d.	11
NS-100	06/25/2009	*st*	19	7.4	0.46	1.36	1.1	153	62	62	6.4	33	189	104	536	n.d.	n.d.	n.d.	11
NS-100	07/08/2009	*st*	20	7.1	0.42	1.19	0.9	120	46	58	6.5	44	134	99	437	n.d.	n.d.	n.d.	11
NS-100	07/15/2009	*st*	20	7.3	0.46	1.12	0.8	116	44	60	6.6	36	124	94	407	n.d.	n.d.	n.d.	12
NS-100	07/29/2009	*st*	20	7.4	0.45	1.12	0.8	103	36	50	5.5	31	134	89	383	n.d.	n.d.	n.d.	12
NS-100	10/19/2009	*st*	17	6.9	0.47	0.77	0.6	70	23	50	7	32	102	76	237	3.9	n.d.	0.3	12
NS-100	11/11/2009	*st*	10	7	0.49	1.18	0.9	96	29	54	8	119	77	68	471	8.12	n.d.	0.3	11
NS-100	11/28/2009	*st*	16	7.1	0.48	1.11	0.8	104	34	56	7.2	56	101	87	398	5.8	0.2	0.3	11
NS-100	03/17/2010	*st*	18	7.3	0.44	1.42	1	152	64	57	7.1	31	209	88	495	2.3	n.d.	n.d.	8.9
NS-100	04/21/2010	*st*	18	7.4	0.46	1.46	1	152	68	61	7.5	27	222	91	500	1.3	n.d.	0.3	8.7
NS-100	06/30/2010	*st*	19	7.5	0.47	1.42	1	143	51	58	10	57	134	90	540	2.9	n.d.	0.3	13
NS-100	10/29/2010	*st*	17	7.2	0.48	1.27	1	121	43	56	10	58	97	91	510	8.8	n.d.	0.3	12
NS-100	12/01/2010	*st*	17	7.2	0.61	1.42	1.1	133	51	53	8	86	139	78	560	8.9	n.d.	0.3	11
NS-100	01/26/2011	*st*	17	7.3	0.51	1.44	1	164	64	55	5.3	37	217	90	502	n.d.	n.d.	n.d.	10

st = stream; n.d. = not determined

Sample no.	**Date**	**Type**	**Al** µg/l	**B** µg/l	**Be** µg/l	**Li** µg/l	**Rb** µg/l	**Sr** µg/l	**Ba** µg/l	**Fe** µg/l	**Mn** µg/l	**Cd** µg/l	**Cr** µg/l	**Co** µg/l	**Ni** µg/l	**Cu** µg/l	**Pb** µg/l	**Mo** µg/l	**Ga** µg/l	**Tl** µg/l	**Bi** µg/l	**U** µg/l	**Ag** µg/l	**Sb** µg/l
NS-100	03/18/2009	*st*	2.3	33	< 0.4	39	13	280	22	265	1160	345	< 0.5	21	130	5.1	76	1.2	< 0.1	0.4	< 2	0.39	< 0.2	2.5
NS-100	03/25/2009	*st*	< 1	35	< 0.4	50	13	270	22	< 20	1240	318	< 0.5	23	150	5	59	1.3	< 0.1	0.4	< 2	0.65	< 0.2	2.6
NS-100	04/17/2009	*st*	146	42	< 0.4	35	12	260	22	< 10	920	395	58	27	127	20	47	7.6	< 0.1	0.4	< 0.2	0.58	< 0.2	2.3
NS-100	05/07/2009	*st*	< 9	37	< 0.3	34	13	280	22	< 41	1040	277	< 1	23	130	4.0	38	1.4	< 0.1	0.4	< 0.1	0.63	< 0.1	2.1
NS-100	05/21/2009	*st*	< 9	39	< 0.3	40	13	320	22	< 40	1130	243	< 1	22	129	4.2	40	1.4	0.1	0.4	< 0.1	0.57	< 0.1	2.2
NS-100	05/27/2009	*st*	< 9	45	< 0.3	40	13	320	22	< 40	1040	242	< 1	21	124	5.2	54	1.3	0.1	0.4	< 0.1	0.56	< 0.1	2.3
NS-100	06/03/2009	*st*	< 9	37	< 0.3	33	12	300	23	< 20	1000	311	< 1	18	113	4.7	81	1.4	< 0.1	0.4	< 0.1	0.44	< 0.1	2.2
NS-100	06/10/2009	*st*	< 9	36	< 0.3	34	13	300	21	91	1200	246	< 1	25	126	4.2	71	1.3	0.1	0.4	< 0.1	0.51	< 0.1	2.2
NS-100	06/17/2009	*st*	< 9	37	< 0.3	37	13	310	22	< 50	1210	246	< 1	23	122	4.1	70	1.3	0.1	0.4	< 0.1	0.45	< 0.1	2.2
NS-100	06/25/2009	*st*	< 13	51	< 0.2	36	14	306	26	< 50	1120	281	< 1	26	121	3.7	70	1.2	0.1	0.3	< 26	0.31	< 0.1	2.2
NS-100	07/08/2009	*st*	< 13	52	< 0.2	27	11	250	27	< 50	666	365	< 1	16	83	5.9	122	0.7	0.1	0.3	< 26	0.2	< 0.1	1.9
NS-100	07/15/2009	*st*	< 13	72	< 0.2	32	9.0	220	23	< 50	607	350	< 1	15	75	5.4	116	0.6	0.1	0.3	< 26	< 0.2	< 0.1	1.8
NS-100	07/29/2009	*st*	< 13	74	< 0.2	33	9.5	220	22	< 30	620	289	< 1	21	70	3.9	99	0.6	0.8	0.2	< 26	0.13	< 0.1	1.8
NS-100	10/19/2009	*st*	< 8	44	< 0.2	13	6.3	150	25	< 34	113	456	< 0.5	3.4	52	5.5	150	< 0.4	< 0.1	0.2	< 0.8	< 0.1	< 0.1	1.5
NS-100	11/11/2009	*st*	18	37	< 0.2	14	6.5	170	30	< 40	81	1215	< 0.5	6.8	80	20	278	< 0.4	< 0.1	0.3	< 0.8	< 0.1	< 0.1	1.3
NS-100	11/28/2009	*st*	8	51	< 0.2	18	6.7	190	30	< 34	283	674	< 0.5	7.5	62	5.7	137	< 0.4	< 0.1	0.2	< 0.8	< 0.1	< 0.1	1.5
NS-100	03/17/2010	*st*	< 1	35	< 0.1	42	14	260	23	< 30	1460	290	< 0.5	26	132	5	55	1.7	0.1	0.4	< 0.2	0.6	< 0.03	2.0
NS-100	04/21/2010	*st*	< 1	37	< 0.1	47	13	270	24	< 30	1470	266	< 0.5	24	122	3.6	53	1.6	0.1	0.4	< 0.2	0.4	< 0.03	2.2
NS-100	06/30/2010	*st*	< 11	50	< 0.1	23	8.3	270	31	< 19	471	609	< 0.6	13	79	5	74	0.5	< 0.1	0.3	< 0.09	< 0.1	< 0.2	1.4
NS-100	10/29/2010	*st*	< 1	48	< 1	20	7.0	260	32	< 25	5.1	645	< 0.3	1.6	69	3.8	134	< 1	< 0.1	< 0.4	< 1	< 0.4	< 0.5	1.3
NS-100	12/01/2010	*st*	< 10	63	< 0.5	29	10	300	28	117	840	870	< 1.5	19	114	10	144	0.8	< 0.1	0.4	< 0.5	0.21	< 0.1	1.5
NS-100	01/26/2011	*st*	< 5	38	< 0.1	38	14	250	24	< 30	1400	320	< 1	29	120	4	26	1.7	< 0.2	0.4	< 0.12	0.66	< 0.03	1.9

st = stream

Sample no.	**Date**	**Type**	**T** °C	**pH**	**E_h** V	**EC** mS/cm	**TDS** g/l	**Ca** mg/l	**Mg** mg/l	**Na** mg/l	**K** mg/l	**Zn** mg/l	**HCO_3** mg/l	**Cl** mg/l	**SO_4** mg/l	**NO_3** mg/l	**Br** mg/l	**F** mg/l	**SiO_2** mg/l
NS-100	02/11/2011	*st*	17	7.3	0.52	1.86	1	156	61	54	5.1	34	212	90	510	2.1	0.2	0.2	9.2
NS-170	03/18/2009	*st*	17	7.5	0.47	1.58	1	146	60	57	6.1	36	214	104	497	n.d.	n.d	n.d	8.6
NS-170	03/25/2009	*st*	16	7.4	0.48	1.59	1	150	63	57	6.2	29	192	109	483	n.d	n.d	n.d	9.1
NS-170	04/17/2009	*st*	17	7.1	0.57	1.36	1.1	162	62	64	5.9	43	157	106	617	n.d	n.d	n.d	9.8
NS-170	05/07/2009	*st*	18	7.4	0.52	1.55	1.2	166	68	66	6.1	30	195	118	602	n.d	n.d	n.d	11
NS-170	05/21/2009	*st*	21	7.5	0.51	1.4	1.1	164	68	65	6.2	24	201	109	545	n.d	n.d	n.d	10
NS-170	05/27/2009	*st*	19	7.6	0.50	1.37	1.1	166	69	66	6.2	27	198	104	530	n.d	n.d	n.d	10
NS-170	06/03/2009	*st*	21	7.6	0.49	1.32	1	143	58	56	6.8	31	184	106	506	n.d	n.d	n.d	10
NS-170	06/10/2009	*st*	21	7.6	0.43	1.37	1	149	61	57	6.5	23	209	106	500	n.d	n.d	n.d	9.8
NS-170	06/17/2009	*st*	22	7.5	0.45	0	1	150	64	61	6	22	198	104	503	n.d	n.d	n.d	10
NS-170	06/25/2009	*st*	20	7.5	0.45	1.35	1	150	60	62	6.3	20	165	104	515	n.d	n.d	n.d	11
NS-170	07/08/2009	*st*	21	7.3	0.42	1.17	0.9	122	46	59	6.9	35	123	99	440	n.d	n.d	n.d	11
NS-170	07/15/2009	*st*	22	7.3	0.45	1.1	0.8	115	43	60	6.4	28	119	94	404	n.d.	n.d	n.d	11
NS-170	07/29/2009	*st*	23	7.5	0.43	1.1	0.7	104	36	51	5.4	20	107	89	367	n.d.	n.d	n.d	11
NS-170	10/19/2009	*st*	17	7.3	0.49	0.75	0.6	72	25	53	6.9	28	89	84	239	3.2	n.d	0.4	11
NS-170	04/21/2010	*st*	20	7.5	0.45	1.45	1	156	65	61	8	18	208	92	500	1.4	n.d	0.4	9.7
NS-170	06/30/2010	*st*	25	7.5	0.46	1.39	1	143	51	59	10	38	101	98	535	2.8	n.d	0.3	12
NS-170	10/29/2010	*st*	15	7.3	0.48	1.3	0.9	120	42	55	10	50	119	88	500	8	n.d	0.3	12
NS-330	03/18/2009	*st*	18	7.7	0.48	1.88	1.3	211	79	62	6.7	23	250	101	695	n.d	n.d	0.3	9.4
NS-330	03/25/2009	*st*	16	7.6	0.48	1.92	1.3	213	80	63	7.4	22	226	104	674	n.d	n.d	n.d	8.3
NS-330	04/17/2009	*st*	18	7.2	0.62	1.45	1.3	202	72	67	6.4	35	187	104	696	n.d	n.d	n.d	10
NS-330	05/07/2009	*st*	18	7.6	0.51	1.73	1.3	206	77	65	6.5	23	233	109	671	n.d	n.d	n.d	8.9

st = stream; n.d. = not determined

Sample no.	**Date**	**Type**	**Al** µg/l	**B** µg/l	**Be** µg/l	**Li** µg/l	**Rb** µg/l	**Sr** µg/l	**Ba** µg/l	**Fe** µg/l	**Mn** µg/l	**Cd** µg/l	**Cr** µg/l	**Co** µg/l	**Ni** µg/l	**Cu** µg/l	**Pb** µg/l	**Mo** µg/l	**Ga** µg/l	**Tl** µg/l	**Bi** µg/l	**U** µg/l	**Ag** µg/l	**Sb** µg/l
NS-100	02/11/2011	*st*	5.7	34	< 0.1	30	14	240	24	< 20	1300	260	< 1	29	110	4	20	1.71	< 0.2	0.4	< 0.1	0.7	< 0.03	1.9
NS-170	03/18/2009	*st*	1.9	24	< 0.4	27	13	260	23	30	1160	342	< 0.5	19	127	4.6	51	1.3	< 0.1	0.3	< 2	0.4	< 0.2	2.4
NS-170	03/25/2009	*st*	< 1	26	< 0.4	28	13	270	22	< 20	1230	307	< 0.5	20	124	2.9	28	1.3	< 0.1	0.4	< 2	0.3	< 0.2	2.3
NS-170	04/17/2009	*st*	169	42	< 0.4	34	13	270	22	322	890	390	59	24	110	22	80	8.9	< 0.1	0.4	< 2	0.4	< 0.2	2.3
NS-170	05/07/2009	*st*	< 9	34	< 0.3	36	14	360	23	< 40	1070	258	< 1	22	122	2.6	25	1.4	0.03	0.4	< 0.1	0.3	< 0.07	2.0
NS-170	05/21/2009	*st*	< 9	48	< 0.3	39	14	360	22	< 40	1180	230	< 1	20	114	2.8	21	1.4	0.03	0.4	< 0.1	0.2	< 0.07	2.0
NS-170	05/27/2009	*st*	< 9	50	< 0.3	41	14	360	22	< 40	1120	229	< 1	20	112	< 2	25	1.4	0.04	0.4	< 0.1	0.3	< 0.07	2.0
NS-170	06/03/2009	*st*	< 9	42	< 0.3	34	13	340	23	< 20	1080	296	< 1	20	106	2.5	41	1.3	0.03	0.4	< 0.1	0.2	< 0.07	2.0
NS-170	06/10/2009	*st*	< 9	38	< 0.3	37	13	330	20	< 20	1270	233	< 1	19	110	2.7	26	1.3	0.04	0.4	< 0.1	0.2	< 0.07	1.9
NS-170	06/17/2009	*st*	< 9	42	< 0.3	41	13	350	21	< 50	1260	224	< 1	21	108	< 2	23	1.3	0.04	0.4	< 1	0.1	< 0.07	1.8
NS-170	06/25/2009	*st*	< 13	49	< 0.2	35	15	290	26	< 50	1020	260	< 1	23	105	1.6	15	1.2	< 0.03	0.3	< 26	< 0.2	< 0.08	1.6
NS-170	07/08/2009	*st*	< 13	52	< 0.2	29	11	250	28	< 50	583	350	< 1	15	78	2.5	39	0.7	0.9	0.3	< 26	< 0.2	< 0.08	1.5
NS-170	07/15/2009	*st*	< 13	63	< 0.2	26	9.7	210	23	< 50	540	342	< 1	15	71	2.6	44	0.6	0.04	0.3	< 26	< 0.2	< 0.08	1.4
NS-170	07/29/2009	*st*	< 13	76	< 0.2	35	9.9	220	21	< 30	563	264	< 1	18	63	1.5	16	0.6	0.7	0.2	< 26	< 0.2	< 0.08	1.2
NS-170	10/19/2009	*st*	< 8	62	< 0.2	19	5.7	150	25	< 34	106	398	< 0.5	3.8	45	3.5	82	< 0.4	< 0.1	0.3	< 0.8	< 0.1	< 0.1	1.3
NS-170	04/21/2010	*st*	< 1	37	< 0.1	46	13	260	23	< 30	1410	247	< 0.5	22	114	1.7	15	1.6	0.04	0.4	< 0.2	0.1	< 0.03	1.7
NS-170	06/30/2010	*st*	< 11	53	< 0.1	23	8.8	270	31	25	439	584	< 0.6	12	82	< 3	15	0.5	< 0.1	0.3	< 0.1	< 0.1	< 0.2	0.8
NS-170	10/29/2010	*st*	< 1	49	< 1	21	7.0	260	32	< 25	8.8	637	< 0.3	1.7	69	2.2	47	< 1	< 0.1	< 0.4	< 1	< 0.4	< 0.5	0.9
NS-330	03/18/2009	*st*	<1	26	< 0.4	32	14	330	19	< 20	750	223	< 0.5	14	131	3.6	32	1.1	< 0.1	0.4	< 2	0.6	< 0.2	2.0
NS-330	03/25/2009	*st*	3.5	24	< 0.4	32	14	320	19	< 20	757	204	< 0.5	13	122	4.4	31	1.1	< 0.1	0.3	< 2	0.6	< 0.2	2.0
NS-330	04/17/2009	*st*	< 2	38	< 0.4	36	12	290	20	21	660	307	< 0.5	16	112	5.1	59	1.14	< 0.1	0.3	< 0.2	0.6	< 0.2	1.9
NS-330	05/07/2009	*st*	< 9	36	< 0.3	39	14	410	21	< 40	627	199	< 1	13	105	2.3	29	1.11	0.02	0.4	< 0.1	0.6	< 0.1	1.9

st = stream

Sample no.	**Date**	**Type**	**T** °C	**pH**	**E_h** V	**EC** mS/cm	**TDS** g/l	**Ca** mg/l	**Mg** mg/l	**Na** mg/l	**K** mg/l	**Zn** mg/l	**HCO_3** mg/l	**Cl** mg/l	**SO_4** mg/l	**NO_3** mg/l	**Br** mg/l	**F** mg/l	**SiO_2** mg/l
NS-330	05/21/2009	*st*	20	7.7	0.49	1.7	1.3	232	83	67	6.7	17	216	109	713	n.d.	n.d.	n.d.	8.8
NS-330	05/27/2009	*st*	19	7.8	0.49	1.71	1.4	252	91	72	6.5	19	234	106	728	n.d.	n.d.	n.d.	8.6
NS-330	06/03/2009	*st*	21	7.8	0.47	1.71	1.4	230	82	67	7.2	19	227	106	800	n.d.	n.d.	n.d.	11
NS-330	06/10/2009	*st*	20	7.8	0.42	1.81	1.5	249	87	67	7.2	16	245	104	823	n.d.	n.d.	n.d.	10
NS-330	06/17/2009	*st*	20	7.6	0.45	n.d.	1.5	242	82	60	7.2	15	253	109	835	n.d.	n.d.	n.d.	10
NS-330	06/25/2009	*st*	20	7.7	0.45	1.85	1.5	232	86	61	7	12	232	106	862	n.d.	n.d.	n.d.	9.6
NS-330	07/08/2009	*st*	21	7.9	0.42	1.72	1.4	228	75	63	7.1	16	224	104	792	n.d.	n.d.	n.d.	10
NS-330	07/15/2009	*st*	22	7.6	0.44	1.69	1.4	252	85	71	6.8	14	214	97	748	n.d.	n.d.	n.d.	10
NS-330	07/29/2009	*st*	21	7.7	0.40	1.71	1.4	242	79	66	6.2	9.9	248	96	751	n.d.	n.d.	n.d.	9
NS-330	08/19/2009	*st*	21	7.5	0.46	1.52	1.2	208	74	66	8.1	16	194	93	642	2.24	0.4	0.3	7.7
NS-330	04/21/2010	*st*	18	7.6	0.45	1.98	1.6	280	97	72	7.9	13	265	97	896	0.5	n.d.	0.4	7.8
NS-330	06/30/2010	*st*	22	7.9	0.47	1.92	1.5	271	88	67	10	12	281	97	800	0.2	n.d.	0.5	10
NS-330	01/26/2011	*st*	16	7.7	0.52	1.73	1.3	215	77	61	5.6	20	229	89	700	2	0.2	0.3	9.9
NS-330	02/02/2011	*st*	16	7.3	0.52	1.48	1.1	180	64	59	6	37	183	93	600	3.3	0.4	0.3	9.7
NS-330	02/02/2011	*st*	16	7.5	0.52	1.53	1.1	190	66	60	6	37	178	96	581	3.3	0.3	0.3	9.8
NS-330	02/11/2011	*st*	17	7.8	0.51	2.19	1.2	210	75	60	6	22	222	94	640	1.3	0.3	0.3	9.7
NS-420	03/18/2009	*st*	18	7.8	0.49	1.86	1.2	208	79	69	7.3	19	220	102	638	n.d.	n.d.	n.d.	8.8
NS-420	03/25/2009	*st*	17	7.8	0.46	1.91	1.3	223	83	64	7.5	18	217	101	659	n.d.	n.d.	n.d.	7.2
NS-420	04/17/2009	*st*	18	7.2	0.62	1.08	1.3	199	72	68	6	38	176	104	678	n.d.	n.d.	n.d.	9.8
NS-420	05/07/2009	*st*	19	7.8	0.52	1.72	1.4	223	82	69	6	18	230	109	763	n.d.	n.d.	n.d.	9.8
NS-420	05/21/2009	*st*	21	7.8	0.55	1.68	1.3	230	83	68	6.2	12	209	106	737	n.d.	n.d.	n.d.	9.2
NS-420	05/27/2009	*st*	20	8	0.47	1.7	1.4	253	91	73	6	13	220	106	737	n.d.	n.d.	n.d.	9.1

st = stream; n.d. = not determined

Sample no.	**Date**	**Type**	**Al** µg/l	**B** µg/l	**Be** µg/l	**Li** µg/l	**Rb** µg/l	**Sr** µg/l	**Ba** µg/l	**Fe** µg/l	**Mn** µg/l	**Cd** µg/l	**Cr** µg/l	**Co** µg/l	**Ni** µg/l	**Cu** µg/l	**Pb** µg/l	**Mo** µg/l	**Ga** µg/l	**Tl** µg/l	**Bi** µg/l	**U** µg/l	**Ag** µg/l	**Sb** µg/l
NS-330	05/21/2009	*st*	< 9	37	< 0.3	41	15	450	21	< 40	580	163	< 1	11	100	< 2	22	1.1	0.02	0.4	< 0.1	0.5	< 0.07	1.9
NS-330	05/27/2009	*st*	< 9	40	< 0.3	45	15	450	20	< 40	374	155	< 1	10	99	2.4	31	1.1	0.03	0.4	< 0.1	0.7	< 0.07	1.9
NS-330	06/03/2009	*st*	< 9	43	< 0.3	40	15	450	22	< 20	583	192	< 1	9.9	96	2.4	34	1.1	< 0.02	0.4	< 0.1	0.6	< 0.07	1.9
NS-330	06/10/2009	*st*	< 9	35	< 0.3	41	15	440	20	< 20	560	156	< 1	9.4	98	2.5	29	1.1	0.02	0.4	< 0.1	0.8	< 0.07	1.9
NS-330	06/17/2009	*st*	< 9	36	< 0.3	42	15	460	20	< 50	451	137	< 1	8.0	99	< 2	27	1.1	0.02	0.4	< 0.1	0.8	< 0.07	1.9
NS-330	06/25/2009	*st*	< 13	44	< 0.2	39	20	410	23	< 50	285	134	< 1	7.4	102	2.1	13	1.1	< 0.03	0.4	< 26	0.7	< 0.08	1.8
NS-330	07/08/2009	*st*	< 13	44	< 0.2	41	18	370	24	< 50	235	162	< 1	6.0	94	3	3.0	1.0	< 0.03	0.4	< 26	0.6	< 0.08	1.8
NS-330	07/15/2009	*st*	< 13	51	< 0.2	38	16	330	20	< 50	213	152	< 1	5.7	91	2.5	22	0.9	0.72	0.4	< 26	0.5	< 0.08	1.7
NS-330	07/29/2009	*st*	< 13	66	< 0.2	58	16	350	18	< 30	173	102	< 1	4.8	86	2.4	18	0.9	0.57	0.4	< 26	0.6	< 0.1	1.6
NS-330	08/19/2009	*st*	< 8	50	< 0.2	36	13	360	20	< 40	220	152	< 0.5	5.0	88	< 3	18	0.9	< 0.1	0.4	< 0.8	0.5	< 0.1	1.6
NS-330	04/21/2010	*st*	1.1	36	< 0.1	54	15	370	21	< 20	423	144	< 0.5	10	100	3.2	23	1.2	0.027	0.4	< 0.2	1.1	< 0.03	1.9
NS-330	06/30/2010	*st*	< 11	44	< 0.1	39	15	340	19	< 19	242	117	< 0.6	6.1	85	3.6	23	1.1	< 0.07	0.5	< 0.1	1.2	< 0.2	1.6
NS-330	01/26/2011	*st*	< 5	38	< 0.1	40	14	290	23	< 30	770	210	< 1	17	100	3	24	1.3	1	0.4	< 0.1	0.7	< 0.03	1.7
NS-330	02/02/2011	*st*	< 16	39	0.6	33	12	250	27	< 15	580	360	< 1.3	16	113	6	49	1.2	< 0.12	0.4	< 1	0.5	< 0.2	1.5
NS-330	02/02/2011	*st*	< 16	41	< 0.6	33	12	250	24	< 15	570	360	< 1.3	16	107	5	44	1.1	< 0.12	0.4	< 1	0.5	< 0.2	1.5
NS-330	02/11/2011	*st*	< 5	36	< 0.1	35	14	330	23	41	750	200	< 1	18	122	3	26	1.4	< 0.2	0.4	< 0.1	0.7	< 0.03	1.7
NS-420	03/18/2009	*st*	< 1	27	< 0.4	33	13	320	19	< 20	720	220	< 0.5	13	108	2.2	18	1.0	< 0.12	0.4	< 2	0.4	< 0.2	1.8
NS-420	03/25/2009	*st*	5.1	26	< 0.4	33	14	330	20	< 20	752	202	< 0.5	12	127	3.3	19	1.1	< 0.12	0.4	< 2	0.5	< 0.2	1.9
NS-420	04/17/2009	*st*	< 2	43	< 0.4	36	12	280	21	16	670	372	< 0.5	18	112	2.3	37	1.0	< 0.1	0.3	< 0.	0.4	< 0.2	1.8
NS-420	05/07/2009	*st*	< 9	32	< 0.3	39	14	410	22	< 40	558	189	< 1	13	101	< 2	17	1.1	< 0.02	0.4	< 0.1	0.3	< 0.07	1.8
NS-420	05/21/2009	*st*	< 9	38	< 0.3	43	15	450	21	< 40	533	153	< 1	9.9	92	< 2	12	1.2	< 0.02	0.4	< 0.1	0.3	< 0.07	1.7
NS-420	05/27/2009	*st*	< 9	45	< 0.3	43	15	450	20	< 40	514	145	< 1	9.3	91	< 2	17	1.1	0.02	0.4	< 0.1	0.4	< 0.07	1.7

st = stream

Sample no.	**Date**	**Type**	**T** °C	**pH**	**E_h** V	**EC** mS/cm	**TDS** g/l	**Ca** mg/l	**Mg** mg/l	**Na** mg/l	**K** mg/l	**Zn** mg/l	**HCO_3** mg/l	**Cl** mg/l	**SO_4** mg/l	**NO_3** mg/l	**Br** mg/l	**F** mg/l	**SiO_2** mg/l
NS-420	06/03/2009	*st*	22	7.9	0.45	1.69	1.4	236	84	67	7.7	14	221	104	734	n.d.	n.d.	n.d.	9.5
NS-420	06/10/2009	*st*	21	7.9	0.41	1.81	1.5	254	88	80	7.6	11	232	104	796	n.d.	n.d.	n.d.	9.4
NS-420	06/17/2009	*st*	21	7.8	0.44	n.d.	1.5	261	90	67	7	9.5	238	106	859	n.d.	n.d.	n.d.	9.8
NS-420	06/25/2009	*st*	20	7.8	0.45	1.84	1.5	267	90	66	6.7	8.2	220	106	850	n.d.	n.d.	n.d.	9.5
NS-420	07/08/2009	*st*	21	7.7	0.42	1.72	1.5	267	90	66	7.2	12	212	101	799	n.d.	n.d.	n.d.	10
NS-420	07/15/2009	*st*	22	7.7	0.45	1.68	1.4	248	85	71	6.9	10	212	101	725	n.d.	n.d.	n.d.	9.9
NS-420	07/29/2009	*st*	21	7.8	0.42	1.71	1.3	231	81	69	6.1	6.31	226	96	739	n.d.	n.d.	n.d.	9.1
NS-420	08/19/2009	*st*	22	7.7	0.45	1.5	1.2	209	71	66	8.3	11	192	96	599	6.2	n.d.	0.5	7.6
NS-420	10/19/2009	*st*	17	7.7	0.48	1.41	1.2	197	69	65	8.4	10	196	94	658	1.2	n.d.	0.4	7.3
NS-420	11/28/2009	*st*	17	7.6	0.47	1.74	1.4	240	80	66	8.1	13	225	93	752	1.3	n.d.	0.4	8.1
NS-420	11/11/2009	*st*	16	7	0.47	1.43	1.1	157	53	63	7.6	69	115	79	590	5.7	n.d.	0.4	8.6
NS-420	03/17/2010	*st*	17	7.6	0.45	1.72	1.3	226	83	65	7.6	15	224	89	660	1	n.d.	0.4	7.3
NS-420	04/21/2010	*st*	19	7.8	0.44	1.98	1.6	280	95	72	8	9.8	251	96	895	0.4	n.d.	0.4	8.2
NS-420	06/30/2010	*st*	22	8.1	0.47	1.92	1.5	271	88	67	10	5.8	278	97	800	0.3	n.d.	0.5	9.9
NS-420	10/29/2010	*st*	16	7.8	0.48	1.88	1.4	244	86	69	10	11	245	100	740	1.2	n.d.	0.4	11
NS-420	12/01/2010	*st*	17	7.5	0.61	1.55	1.1	160	60	56	9	65	129	82	640	5.4	n.d.	0.4	10
NS-420	01/26/2011	*st*	16	7.8	0.52	1.73	1.2	215	74	59	6	19	212	100	656	0.9	0.3	0.2	9.9
NS-590	03/18/2009	*st*	19	7.9	0.49	1.85	1.3	210	80	69	6.3	12	217	109	653	1.2	1.3	0.3	8.6
NS-590	03/25/2009	*st*	16	7.9	0.45	1.9	1.3	224	84	70	6.7	11	219	104	650	n.d.	n.d.	n.d.	7.5
NS-590	04/17/2009	*st*	18	7.3	0.47	1.4	1.2	189	69	68	6	32	154	106	668	n.d.	n.d.	n.d.	10
NS-590	05/07/2009	*st*	21	7.8	0.51	1.7	1.3	219	81	69	6.3	14	216	112	722	n.d.	n.d.	n.d.	9.3
NS-590	05/21/2009	*st*	23	8	0.51	1.67	1.4	234	85	70	6.3	6	189	109	752	n.d.	n.d.	n.d.	8.9

st = stream; n.d. = not determined

Sample no.	**Date**	**Type**	**Al** µg/l	**B** µg/l	**Be** µg/l	**Li** µg/l	**Rb** µg/l	**Sr** µg/l	**Ba** µg/l	**Fe** µg/l	**Mn** µg/l	**Cd** µg/l	**Cr** µg/l	**Co** µg/l	**Ni** µg/l	**Cu** µg/l	**Pb** µg/l	**Mo** µg/l	**Ga** µg/l	**Tl** µg/l	**Bi** µg/l	**U** µg/l	**Ag** µg/l	**Sb** µg/l
NS-420	06/03/2009	*st*	< 9	37	< 0.3	39	14	440	22	< 20	522	176	< 1	9.0	89	< 2	19	1.2	< 0.02	0.4	< 0.1	0.4	< 0.07	1.7
NS-420	06/10/2009	*st*	< 9	36	< 0.3	41	15	440	21	21	495	144	< 1	8.4	92	< 2	21	1.1	0.02	0.4	< 0.1	0.6	< 0.07	1.8
NS-420	06/17/2009	*st*	< 9	35	< 0.3	40	15	460	20	< 50	409	130	< 1	7.0	90	< 2	11	1.1	< 0.02	0.4	< 0.1	0.5	< 0.07	1.8
NS-420	06/25/2009	*st*	< 13	45	< 0.2	40	20	410	23	< 50	271	127	< 1	6.4	94	9.6	6.4	1.1	< 0.03	0.4	< 26	0.5	< 0.08	1.7
NS-420	07/08/2009	*st*	< 13	44	< 0.2	40	18	370	23	< 50	206	154	< 1	5.2	84	1.7	8.9	0.9	< 0.03	0.4	< 26	0.4	< 0.08	1.6
NS-420	07/15/2009	*st*	< 13	51	< 0.2	37	16	330	20	< 50	190	148	< 1	5.2	81	1.7	10	0.9	0.7	0.4	< 26	0.3	< 0.08	1.5
NS-420	07/29/2009	*st*	16.1	56	< 0.2	47	16	350	19	< 30	141	99	< 1	4.0	77	1.8	8.5	0.9	0.6	0.4	< 26	0.4	<0.11	1.5
NS-420	08/19/2009	*st*	< 8	50	< 0.2	37	14	360	20	< 40	93	149	< 0.5	4.4	82	< 3	7.8	0.9	< 0.1	0.4	< 0.8	0.3	< 0.1	1.4
NS-420	10/19/2009	*st*	< 8	53	< 0.2	44	11	300	21	< 34	326	213	< 0.5	5.8	88	< 3	18	0.8	< 0.1	0.4	< 0.8	0.4	< 0.1	1.4
NS-420	11/11/2009	*st*	< 8	43	< 0.2	25	9	300	28	< 40	240	700	< 0.5	7.7	96	6.5	82	0.5	< 0.1	0.3	< 0.8	0.3	< 0.1	1.2
NS-420	11/28/2009	*st*	< 8	43	< 0.2	41	14	410	20	7.6	430	183	< 0.5	7.1	90	< 3	16	0.9	< 0.1	0.4	< 0.8	0.5	< 0.1	1.5
NS-420	03/17/2010	*st*	4.4	34	< 0.1	50	14	300	21	< 40	580	187	< 0.5	12	99	2.3	17	1.2	0.03	0.4	< 0.2	0.4	0.04	1.7
NS-420	04/21/2010	*st*	< 1	38	< 0.1	54	15	370	22	< 40	345	140	< 0.5	7.5	88	1.9	11	1.2	0.02	0.4	< 0.2	0.8	< 0.03	1.7
NS-420	06/30/2010	*st*	< 11	37	< 0.1	38	15	370	19	< 19	165	108	< 0.6	4.1	71	< 3	7.3	1.1	< 0.05	0.5	< 0.1	0.7	< 0.2	1.4
NS-420	10/29/2010	*st*	< 1	43	< 1	42	14	340	20	< 25	390	119	< 0.3	8.7	95	3.7	15	< 1.4	< 0.1	< 0.4	< 1	0.5	< 0.5	1.3
NS-420	12/01/2010	*st*	< 10	42	< 0.1	31	11	260	25	< 30	640	700	< 1	16	110	5.9	67	0.8	< 0.2	0.4	< 0.1	0.2	< 0.03	1.3
NS-420	01/26/2011	*st*	< 1	38	< 0.1	40	14	290	23	< 30	720	210	< 1	17	90	2	19	1.3	< 0.2	0.4	< 0.1	0.4	< 0.03	1.5
NS-590	03/18/2009	*st*	2.0	29	< 0.4	35	14	320	19	< 20	700	210	< 0.5	12	110	1.6	7.6	1.0	<0 .1	0.4	< 2	0.2	< 0.2	1.6
NS-590	03/25/2009	*st*	3.3	26	< 0.4	34	14	330	19	< 20	750	192	0.6	12	94	2.2	6.3	1.1	< 0.1	0.4	< 2	0.3	< 0.2	1.9
NS-590	04/17/2009	*st*	< 2	43	< 0.4	43	12	290	20	< 10	550	367	< 0.5	17	101	1.4	25	1.0	< 0.1	0.3	< 0.2	0.2	< 0.2	1.5
NS-590	05/07/2009	*st*	< 9	34	< 0.3	40	13	400	22	< 40	542	204	< 1	11	89	< 2	13	1.1	< 0.02	0.4	< 0.1	0.2	< 0.07	1.6
NS-590	05/21/2009	*st*	< 9	37	< 0.3	42	14	430	21	< 40	469	153	< 1	7.6	73	< 2	8.9	1.1	< 0.02	0.4	< 0.1	0.2	< 0.07	1.5

st = stream

Sample no.	**Date**	**Type**	**T** °C	**pH**	**E_h** V	**EC** mS/cm	**TDS** g/l	**Ca** mg/l	**Mg** mg/l	**Na** mg/l	**K** mg/l	**Zn** mg/l	**HCO_3** mg/l	**Cl** mg/l	**SO_4** mg/l	**NO_3** mg/l	**Br** mg/l	**F** mg/l	**SiO_2** mg/l
NS-590	05/27/2009	*st*	21	8.2	0.44	1.69	1.4	249	90	73	6.4	6.1	201	106	758	n.d.	n.d.	n.d.	9.1
NS-590	06/03/2009	*st*	25	8.1	0.45	1.66	1.4	239	85	68	7.8	5.4	198	101	760	n.d.	n.d.	n.d.	9.2
NS-590	06/10/2009	*st*	24	8.2	0.39	1.79	1.4	254	90	68	7.5	4.2	211	104	787	n.d.	n.d.	n.d.	8.8
NS-590	06/17/2009	*st*	24	8	0.42	n.d.	1.5	253	89	66	7.3	2.9	228	109	874	n.d.	n.d.	n.d.	9.3
NS-590	06/25/2009	*st*	20	8	0.45	1.83	1.5	255	88	66	6.4	3.1	209	106	832	n.d.	n.d.	n.d.	9.4
NS-590	07/08/2009	*st*	24	7.9	0.42	1.72	1.4	238	80	66	6.1	3.9	200	101	793	n.d.	n.d.	n.d.	9.4
NS-590	07/15/2009	*st*	24	8	0.43	1.67	1.3	246	82	69	6.5	3.8	202	99	728	n.d.	n.d.	n.d.	9.5
NS-590	07/29/2009	*st*	22	8.1	0.41	1.72	1.3	246	82	71	6	2.3	220	96	713	n.d.	n.d.	n.d.	8.3
NS-590	08/19/2009	*st*	24	8	0.44	1.49	1.2	212	72	67	7.6	4.2	186	94	605	1.9	0.3	0.5	6.4
NS-590	10/19/2009	*st*	16	8	0.41	1.38	1.2	208	71	65	11	5.4	206	90	633	1.5	n.d.	0.5	7.7
NS-590	11/28/2009	*st*	16	7.7	0.47	1.68	1.3	231	76	65	8	5.9	216	90	696	1.3	0.3	0.6	6.2
NS-590	03/17/2010	*st*	19	7.7	0.47	1.72	1.3	226	84	66	7.1	9.7	202	88	728	1.1	n.d.	0.3	7.6
NS-590	04/21/2010	*st*	19	8	0.43	1.97	1.6	280	94	71	7.4	3.3	222	94	896	0.4	n.d.	0.4	8.4
NS-590	10/29/2010	*st*	14	8	0.48	1.81	1.3	232	83	68	10	3.6	240	102	725	1.3	n.d.	0.4	9.9
NS-590	06/30/2010	*st*	22	8.4	0.49	1.9	1.5	274	89	68	10	1.6	253	96	800	n.d.	n.d.	0.5	9.5
NS-590	12/01/2010	*st*	17	7.6	0.58	1.48	1.1	158	58	56	9	60	131	84	590	5.9	n.d.	0.3	9.9
NS-590	01/26/2011	*st*	15	7.9	0.52	1.68	1.2	202	72	61	5.7	13	198	79	668	1	0.2	0.3	9.7
NS-590	02/02/2011	*st*	15	7.4	0.52	1.43	1.1	170	60	58	5.4	38	152	90	580	3.2	0.2	0.4	9.8
NS-590	02/02/2011	*st*	16	7.4	0.53	1.4	1.1	168	59	58	5.3	37	151	90	570	3.1	0.3	0.3	9.9
NS-630	03/18/2009	*st*	14	7.4	0.50	1.04	0.6	89	36	59	4.3	7.2	135	91	270	n.d.	n.d.	n.d.	14
NS-1200	03/18/2009	*st*	14	7.7	0.51	1.04	0.6	91	36	62	4.2	7.3	126	91	278	n.d.	n.d.	n.d.	14
NS-1200	04/17/2009	*st*	16	7.2	0.48	0.85	0.6	74	29	58	4	12	99	89	241	n.d.	n.d.	n.d.	15

st = stream; n.d. = not determined

Sample no.	**Date**	**Type**	**Al** µg/l	**B** µg/l	**Be** µg/l	**Li** µg/l	**Rb** µg/l	**Sr** µg/l	**Ba** µg/l	**Fe** µg/l	**Mn** µg/l	**Cd** µg/l	**Cr** µg/l	**Co** µg/l	**Ni** µg/l	**Cu** µg/l	**Pb** µg/l	**Mo** µg/l	**Ga** µg/l	**Tl** µg/l	**Bi** µg/l	**U** µg/l	**Ag** µg/l	**Sb** µg/l
NS-590	05/27/2009	*st*	< 9	45	< 0.3	43	14	450	20	< 40	449	139	< 1	7.2	71	< 2	12	1.1	0.02	0.4	< 0.1	1.4	< 0.07	1.4
NS-590	06/03/2009	*st*	< 9	38	< 0.3	38	14	440	22	< 20	498	160	< 1	6.9	66	< 2	11	1.1	< 0.02	0.4	< 0.1	0.2	< 0.07	1.4
NS-590	06/10/2009	*st*	< 9	33	< 0.3	37	14	430	20	< 20	446	127	< 1	6.2	65	< 2	6.9	1.1	< 0.02	0.4	< 0.1	0.4	<0 .07	1.5
NS-590	06/17/2009	*st*	< 9	35	< 0.3	39	15	470	21	< 50	367	118	< 1	5.1	62	< 2	6.5	1.1	< 0.02	0.4	< 0.1	0.4	< 0.07	1.6
NS-590	06/25/2009	*st*	< 13	49	< 0.2	42	19	410	23	< 50	258	125	< 1	5.1	71	1.7	4.2	1.1	< 0.03	0.4	< 26	0.4	< 0.08	1.5
NS-590	07/08/2009	*st*	< 13	46	< 0.2	39	17	370	23	< 50	180	150	< 1	3.9	62	1.6	5.5	0.9	0.7	0.4	< 26	0.2	< 0.08	1.3
NS-590	07/15/2009	*st*	< 13	61	< 0.2	42	16	340	20	< 50	160	136	< 1	3.6	59	1.4	6.0	0.9	0.6	0.4	< 26	< 0.2	< 0.08	1.2
NS-590	07/29/2009	*st*	< 13	59	< 0.2	51	16	350	19	< 30	118	92	< 1	2.9	53	1.3	7.7	0.9	0.6	0.4	< 26	0.3	< 0.1	1.3
NS-590	08/19/2009	*st*	< 8	50	< 0.2	37	13	360	20	< 40	92	140	< 0.5	3.2	58	< 3	7.7	0.9	< 0.1	0.4	< 0.8	0.1	< 0.1	1.2
NS-590	10/19/2009	*st*	< 8	54	< 0.2	46	12	300	21	< 34	287	173	< 0.5	5.1	72	< 3	6.4	0.8	< 0.1	0.4	< 0.8	0.2	< 0.1	1.3
NS-590	11/28/2009	*st*	< 8	44	< 0.2	40	13	390	19	8	352	163	< 0.5	5.4	70	< 3	6.7	0.9	< 0.1	0.3	< 0.8	0.2	< 0.1	1.2
NS-590	03/17/2010	*st*	1.1	36	< 0.1	53	13	310	21	< 20	534	184	< 0.5	9.7	92	1.8	11	1.2	0.02	0.4	< 0.2	0.2	0.04	1.5
NS-590	04/21/2010	*st*	< 1	35	< 0.1	57	15	370	21	< 20	302	119	< 0.5	5.6	65	1.3	3.5	1.2	0.01	0.4	< 0.2	0.5	< 0.03	1.5
NS-590	10/29/2010	*st*	1.2	44	< 0.1	44	13	370	20	< 25	300	109	< 0.3	5.8	55	1.1	12	1.1	< 0.1	< 0.4	< 1	< 0.4	< 0.5	1.1
NS-590	06/30/2010	*st*	< 11	38	< 0.1	38	15	380	19	< 19	112	83	< 0.6	2.5	47	< 3	6.3	1.2	< 0.05	0.5	< 0.1	0.6	< 0.2	1.3
NS-590	12/01/2010	*st*	< 10	64	< 0.5	35	10	320	25	< 25	430	690	< 1.5	13	99	2.7	32	0.7	< 0.1	0.3	< 0.5	< 0.1	< 0.1	1.0
NS-590	01/26/2011	*st*	< 5	38	< 0.1	40	14	330	25	< 30	500	210	< 1	12	90	2	20	1.3	< 0.2	0.4	< 0.1	0.2	< 0.03	1.3
NS-590	02/02/2011	*st*	< 16	41	< 0.6	32	10	220	24	< 15	470	420	< 1	13	90	3	31	1.0	< 0.1	0.3	< 1.2	0.2	< 0.2	1.1
NS-590	02/02/2011	*st*	< 16	42	< 0.6	32	11	220	24	< 15	470	430	< 1	13	90	3	27	0.9	< 0.1	0.3	< 1.2	0.2	< 0.2	1.1
NS-630	03/18/2009	*st*	7.6	33	< 0.4	19	5.0	180	20	43	220	98	< 0.8	3.8	43	2.2	8.7	0.7	< 0.1	0.1	< 1	0.2	<0.1	1.0
NS-1200	03/18/2009	*st*	5.6	34	< 0.4	19	5	190	20	22	173	103	< 0.8	3.1	34	3.4	15	0.7	< 0.1	0.1	< 1	0.2	< 0.1	1.1
NS-1200	04/17/2009	*st*	49	49	< 0.4	21	4	150	19	250	152	131	< 0.5	3.8	44	4.6	28	0.8	< 0.1	< 0.1	< 0.2	0.2	< 0.2	1.0

st = stream

Sample no.	**Date**	**Type**	**T** °C	**pH**	**E_h** V	**EC** mS/cm	**TDS** g/l	**Ca** mg/l	**Mg** mg/l	**Na** mg/l	**K** mg/l	**Zn** mg/l	**HCO_3** mg/l	**Cl** mg/l	**SO_4** mg/l	**NO_3** mg/l	**Br** mg/l	**F** mg/l	**SiO_2** mg/l
NS-1200	05/07/2009	*st*	18	7.9	0.50	1.02	0.7	101	40	63	4.3	11	140	99	323	n.d.	n.d.	n.d.	16
NS-1200	10/19/2009	*st*	17	7.4	0.45	1.07	0.8	123	45	76	5.6	6.8	166	114	339	2.3	n.d.	0.3	12
NS-1200	04/21/2010	*st*	16	7.8	0.45	1.02	0.6	93	34	58	5.2	5.6	141	91	275	4	n.d.	0.3	17
NS-1200	06/30/2010	*st*	22	8	0.45	1.52	1.1	174	60	64	6.8	9.8	193	107	550	0.8	n.d.	0.4	14
NS-1200	10/29/2010	*st*	15	7.6	0.49	1.16	0.7	103	39	70	5.3	6.1	176	122	290	1.7	n.d.	0.4	16
NS-1200	01/26/2011	*st*	11	7.8	0.55	0.97	0.6	86	35	55	3.7	7	119	87	260	5.7	0.4	0.3	15
NS-1600	03/18/2009	*st*	15	7.8	0.48	0.97	0.6	73	32	65	3.9	5.9	147	91	237	n.d.	n.d.	n.d.	17
NS-1600	10/29/2010	*st*	17	7.9	0.48	1.02	0.6	84	34	65	4.9	3.8	187	107	223	0.8	n.d.	0.6	20
NS-1600	12/01/2010	*st*	16	8	0.56	0.76	0.4	53	22	52	4.8	9	93	87	162	6.6	n.d.	0.4	16
NS-1600	01/26/2011	*st*	12	7.9	0.59	0.88	0.5	76	30	52	3.6	6	126	75	213	3.4	0.2	0.3	17
NS-2250	03/18/2009	*st*	16	7.7	0.44	1.02	0.6	76	33	66	3.9	8.4	133	97	259	n.d.	n.d.	n.d.	15
NS-2270	03/18/2009	*st*	16	7.8	0.42	1.04	0.6	76	35	67	3.8	9.6	121	99	263	n.d.	n.d.	n.d.	14
NS-2270	07/23/2010	*st*	24	7.9	0.49	1.19	0.8	108	46	67	5	6.7	190	94	335	0.3	n.d.	0.7	17
NS-2270	08/05/2010	*st*	25	7.7	0.52	1.19	0.8	113	49	71	5	7.5	188	96	350	0.6	n.d.	0.6	16
NS-2470	07/23/2010	*st*	24	7.8	0.48	1.19	0.8	107	46	80	5	7.6	180	98	340	n.d.	n.d.	n.d.	15
NS-2470	10/29/2010	*st*	17	7.6	0.48	1.23	0.8	113	46	71	6.5	9	171	109	350	0.7	n.d.	0.6	16
NS-2640	07/15/2009	*st*	23	7.7	0.43	1.16	0.8	119	52	74	4.7	11	159	101	380	n.d.	n.d.	n.d.	15
NS-2640	07/29/2009	*st*	23	7.7	0.41	1.15	0.8	113	50	71	4	8.8	160	98	386	n.d.	n.d.	n.d.	16
NS-2640	06/30/2010	*st*	25	7.9	0.45	1.14	0.7	97	41	65	5.2	8.2	179	106	308	0.4	n.d.	0.6	15
NS-2640	07/23/2010	*st*	24	7.9	0.49	1.18	0.8	107	45	67	5.4	6.4	175	100	340	0.6	n.d.	0.6	15
NS-2640	08/05/2010	*st*	25	7.8	0.51	1.22	0.8	112	50	72	5.2	6.5	180	100	350	1.5	n.d.	0.6	14
NS-2640	01/26/2011	*st*	10	7.8	0.54	0.95	0.6	83	35	63	3.6	11	123	102	250	3.2	0.4	0.4	14

st = stream; n.d. = not determined

Sample no.	**Date**	**Type**	**Al** µg/l	**B** µg/l	**Be** µg/l	**Li** µg/l	**Rb** µg/l	**Sr** µg/l	**Ba** µg/l	**Fe** µg/l	**Mn** µg/l	**Cd** µg/l	**Cr** µg/l	**Co** µg/l	**Ni** µg/l	**Cu** µg/l	**Pb** µg/l	**Mo** µg/l	**Ga** µg/l	**Tl** µg/l	**Bi** µg/l	**U** µg/l	**Ag** µg/l	**Sb** µg/l
NS-1200	05/07/2009	*st*	< 9	41	< 0 .3	23	5	240	23	<40	135	121	< 1	2.9	34	< 2	29	0.7	< 0.02	0.1	< 0.1	0.3	< 0.07	1.2
NS-1200	10/19/2009	*st*	9.6	52	< 0.2	30	4	220	29	< 34	12	130	< 0.5	1.2	24	3.8	61	1.0	< 0.1	0.1	< 0.8	0.6	< 0.1	1.7
NS-1200	04/21/2010	*st*	< 1	37	< 0.1	30	4.5	210	21	< 30	55	76	< 0.5	1.0	24	2.2	14	0.8	< 0.01	0.1	< 0.2	0.4	< 0.03	1.0
NS-1200	06/30/2010	*st*	< 11	41	< 0.1	28	6.7	310	34	< 19	31	162	< 0.6	0.9	33	< 3	25	0.9	< 0.05	< 0.23	< 0.1	0.9	< 0.2	1.6
NS-1200	10/29/2010	*st*	1.7	41	< 1	22	4.1	215	28	< 25	19	84	20.3	0.6	18	2.7	34	< 1	< 0.1	< 0.4	< 1	0.6	< 0.5	1.6
NS-1200	01/26/2011	*st*	10.5	37	< 0.1	20	4.7	220	22	54	130	87	<1	2.8	33	3	24	0.9	< 0.2	0.1	< 0.1	0.3	< 0.03	0.9
NS-1600	03/18/2009	*st*	2.0	36	< 0.4	22	5.0	180	27	< 20	170	74	< 0.8	2.6	28	1.6	8.3	0.8	< 0.1	0.2	<1	0.6	< 0.1	1.4
NS-1600	10/29/2010	*st*	1.7	43	< 1	29	5.1	210	38	650	55	49	< 0.3	0.6	13	1.2	3.6	1.4	< 0.1	< 0.4	< 1	1.2	< 0.5	1.5
NS-1600	12/01/2010	*st*	< 10	60	< 0.5	16	3.6	148	24	49	58	95	< 1.5	1.4	18	3.5	20	0.7	< 0.1	< 0.2	< 0.5	0.3	< 0.1	1.1
NS-1600	01/26/2011	*st*	< 5	38	< 0.1	23	4.8	220	28	39	96	66	< 1	1.8	26	2	21	0.9	< 0.2	0.1	< 0.1	0.6	< 0.03	1.2
NS-2250	03/18/2009	*st*	1.8	35	< 0.4	21	4.7	180	27	< 20	99	113	< 0.8	1.8	27	3.2	24	0.8	< 0.1	0.1	< 1	0.5	< 0.1	1.6
NS-2270	03/18/2009	*st*	2.2	37	< 0.4	22	4.7	190	26	45	101	120	< 0.8	1.7	27	2.9	26	0.8	< 0.1	0.1	< 1	0.5	< 0.1	1.6
NS-2270	07/23/2010	*st*	< 5	52	< 0.9	38	5.0	270	38	< 10	56	106	< 1	1.1	19	2.6	29	1.4	0.01	< 0.9	< 0.05	0.7	0.05	2.0
NS-2270	08/05/2010	*st*	< 7	46	< 1	33	5.7	290	39	< 10	50	104	0.37	1.0	20	3.6	35	1.4	< 0.1	< 0.4	< 1	1.0	< 0.5	2.0
NS-2470	07/23/2010	*st*	< 5	53	< 0.9	38	4.9	260	36	< 10	62	116	< 1	1.5	20	2.9	27	1.4	0.02	< 0.9	< 0.05	0.8	< 0.05	2.1
NS-2470	10/29/2010	*st*	< 10	47	< 1	32	5.2	270	35	< 25	40	111	< 0.3	1.1	20	3.7	34	< 1	< 0.1	< 0.4	< 1	0.8	< 0.5	1.7
NS-2640	07/15/2009	*st*	< 13	64	< 0.2	34	6.5	280	34	< 50	75	143	< 1	1.8	23	4.6	52	1.1	1.3	0.2	< 26	0.4	< 0.08	2.1
NS-2640	07/29/2009	*st*	< 13	66	< 0.2	41	6.4	290	33	< 30	57	124	< 1	1.7	21	4.6	50	1.2	1.1	0.2	< 26	0.4	< 0.1	2.1
NS-2640	06/30/2010	*st*	< 11	42	< 0.1	28	5.2	240	33	< 19	55	117	0.07	1.4	21	3.0	26	1.3	< 0.05	< 0.23	< 0.1	0.7	< 0.2	1.8
NS-2640	07/23/2010	*st*	< 5	54	< 0.9	37	4.9	270	36	13	69	112	< 1	1.4	19	2.9	23	1.4	0.02	< 0.9	< 0.05	0.6	< 0.05	2.1
NS-2640	08/05/2010	*st*	7	47	< 1	30	5.4	290	37	< 10	63	102	< 0.3	1.4	20	3.0	22	1.5	< 0.1	< 0.4	< 1	0.7	< 0.5	1.9
NS-2640	01/26/2011	*st*	< 5	41	< 0.1	22	4.3	240	29	< 40	51	110	< 1	1.4	26	4	40	0.8	< 0.2	0.1	< 0.1	0.5	< 0.03	1.3

st = stream

Sample no.	**Date**	**Type**	**T** °C	**pH**	**E_h** V	**EC** mS/cm	**TDS** g/l	**Ca** mg/l	**Mg** mg/l	**Na** mg/l	**K** mg/l	**Zn** mg/l	**HCO_3** mg/l	**Cl** mg/l	**SO_4** mg/l	**NO_3** mg/l	**Br** mg/l	**F** mg/l	**SiO_2** mg/l
NS-2640	02/02/2011	*st*	12	7.4	0.52	0.72	0.5	51	24	57	3	11	94	93	165	3.2	0.4	0.4	14
NS-2640	02/02/2011	*st*	12	7.4	0.54	0.74	0.5	51	24	59	3.2	10	92	94	166	3.3	0.4	0.4	14
NS-2640	02/11/2011	*st*	12	7.9	0.52	0.89	0.6	75	32	61	3.3	10	120	95	228	3	0.3	0.4	14
NS-2940	03/18/2009	*st*	15	7.6	0.48	1.05	0.6	77	34	69	4.3	10	136	106	275	n.d.	n.d.	n.d.	14
NS-2940	07/08/2009	*st*	25	7.7	0.44	1.15	0.8	105	47	68	4.6	11	163	106	381	n.d.	n.d.	n.d.	15
NS-2940	07/15/2009	*st*	24	7.8	0.43	1.17	0.8	118	52	75	4.6	9.7	156	104	396	n.d.	n.d.	n.d.	14
NS-2940	07/29/2009	*st*	23	7.8	0.41	1.17	0.8	117	52	76	4.1	7.5	146	103	372	n.d.	n.d.	n.d.	14
NS-2940	10/19/2009	*st*	16	7.6	0.45	1.08	0.8	121	51	76	5.3	8.5	171	111	374	0.4	n.d.	0.7	13
NS-2940	11/28/2009	*st*	15	7.5	0.45	1.1	0.7	96	41	73	6	11	148	115	300	1.14	0.4	0.6	13
NS-2940	03/17/2010	*st*	16	7.8	0.47	0.98	0.6	84	37	65	4	9.1	129	95	250	2.4	n.d.	0.5	15
NS-2940	04/21/2010	*st*	20	7.7	0.43	1.08	0.7	94	38	63	5.4	8.2	154	98	288	1.1	n.d.	0.6	14
NS-2940	06/30/2010	*st*	25	7.9	0.47	1.15	0.7	98	41	66	5.3	8.1	175	102	314	0.3	n.d.	0.6	15
NS-2940	07/23/2010	*st*	24	8	0.48	1.19	0.8	106	45	68	5.3	6.1	170	101	340	0.1	n.d.	0.6	14
NS-2940	10/29/2010	*st*	17	7.9	0.49	1.23	0.8	112	48	72	6	8.7	175	109	350	0.9	n.d.	0.5	15
NS-2940	12/01/2010	*st*	16	7.8	0.56	0.82	0.5	56	25	53	4.8	14	92	90	191	5.2	n.d.	0.5	14
NS-3500	03/18/2009	*st*	16	7.8	0.42	1.09	0.6	76	36	75	4.2	9.1	128	112	267	1.8	n.d.	0.3	13
NS-3650	03/18/2009	*st*	15	8.1	0.41	0.77	0.4	48	24	57	3.8	2.3	95	89	150	n.d.	n.d.	n.d.	13
NS-4410	03/18/2009	*st*	16	7.8	0.45	0.79	0.5	48	25	61	3.7	3.3	120	91	161	n.d.	n.d.	n.d.	13
NS-4630	03/18/2009	*st*	15	7.8	0.52	0.77	0.4	47	24	59	3.6	2.7	108	91	144	n.d.	n.d.	n.d.	13
NS-5300	03/18/2009	*st*	16	7.8	0.51	0.77	0.4	49	24	60	3.6	2.8	107	91	149	n.d.	n.d.	n.d.	13

st = stream; n.d. = not determined

Sample no.	**Date**	**Type**	**Al** µg/l	**B** µg/l	**Be** µg/l	**Li** µg/l	**Rb** µg/l	**Sr** µg/l	**Ba** µg/l	**Fe** µg/l	**Mn** µg/l	**Cd** µg/l	**Cr** µg/l	**Co** µg/l	**Ni** µg/l	**Cu** µg/l	**Pb** µg/l	**Mo** µg/l	**Ga** µg/l	**Tl** µg/l	**Bi** µg/l	**U** µg/l	**Ag** µg/l	**Sb** µg/l
NS-2640	02/02/2011	*st*	21	45	< 0.6	15	3.1	140	24	64	48	100	< 1	1.4	21	4	34	0.5	< 0.1	< 0.2	< 1	0.2	< 0.18	1.0
NS-2640	02/02/2011	*st*	20	46	< 0.6	16	3.1	120	23	46	47	100	< 1	1.4	21	4	36	0.6	< 0.1	< 0.2	< 1	0.2	< 0.18	1.0
NS-2640	02/11/2011	*st*	8.8	39	< 0.1	18	4.2	180	27	< 15	63	105	< 1	1.6	27	4	33	0.8	< 0.2	0.1	< 0.1	0.4	< 0.03	1.0
NS-2940	03/18/2009	*st*	1.3	37	< 0.4	21	4.7	200	26	< 20	93	130	< 0.8	1.8	28	2.8	20	0.7	< 0.1	0.1	< 1	0.5	< 0.1	1.6
NS-2940	07/08/2009	*st*	< 13	51	< 0.2	31	7.0	286	40	< 50	95	147	< 1	2.1	23	3.9	47	1.2	1.2	0.2	< 26	0.5	< 0.1	2.2
NS-2940	07/15/2009	*st*	< 13	69	< 0.2	37	6.5	2809	34	< 50	123	127	< 1	2.8	23	3.4	35	1.2	1.2	0.2	< 26	0.3	< 0.1	2.0
NS-2940	07/29/2009	*st*	< 13	71	< 0.2	43	6.4	290	32	< 30	109	106	< 1	2.8	21	3.0	22	1.2	1.1	0.2	< 26	0.3	< 0.1	1.9
NS-2940	10/19/2009	*st*	< 8	47	< 0.2	40	4.7	270	33	< 34	95	119	< 0.5	2.2	22	4.1	30	1.3	< 0.1	0.2	< 0.8	0.6	< 0.1	1.9
NS-2940	11/28/2009	*st*	11	42	< 0.2	25	4.8	260	30	82	52	145	< 0.5	1.3	22	5	50	1.2	< 0.1	0.1	< 0.8	0.5	< 0.1	1.8
NS-2940	07/23/2010	*st*	< 5	55	< 0.9	36	5.0	270	37	< 10	116	102	< 1	2.4	19	< 2.5	15	1.5	0.02	< 0.9	< 0.05	0.7	< 0.05	2.1
NS-2940	03/17/2010	*st*	2.7	40	< 0.1	34	4.6	220	28	< 20	77	116	< 0.5	1.7	26	3.5	24	0.9	0.01	0.1	< 0.2	0.5	< 0.03	1.6
NS-2940	04/21/2010	*st*	3.0	43	< 0.1	40	5.0	250	32	< 20	56	111	< 0.5	1.6	24	3.2	17	1.1	0.01	0.1	< 0.2	0.6	< 0.03	1.9
NS-2940	06/30/2010	*st*	< 11	43	< 0.1	28	5.3	240	34	75	83	111	0.07	2.0	21	6.1	25	1.3	< 0.05	< 0.2	< 0.1	0.6	< 0.2	1.8
NS-2940	10/29/2010	*st*	3.6	46	< 1	32	5.1	270	33	< 25	80	103	< 0.3	1.8	21	2.9	20	< 1.4	< 0.1	< 0.4	< 1	1.1	< 0.5	1.7
NS-2940	12/01/2010	*st*	< 10	70	< 0.5	17	3.6	170	27	56	48	136	< 1.5	1.4	21	6.4	51	0.7	< 0.1	< 0.2	< 0.5	0.2	< 0.1	1.3
NS-3500	03/18/2009	*st*	1.9	38	< 0.4	20	4.5	190	27	< 20	99	124	< 0.8	2.0	26	2.8	24	0.8	< 0.1	0.1	< 1	0.4	< 0.1	1.5
NS-3650	03/18/2009	*st*	13	31	< 0.4	12	2.9	130	19	640	457	29	< 0.8	2.0	14	2.1	35	< 0.5	< 0.1	< 0.1	< 1	0.3	< 0.1	0.8
NS-4410	03/18/2009	*st*	5.6	43	< 0.4	20	3.0	170	22	234	445	35	< 0.8	1.6	13	1.9	14	< 0.5	< 0.1	< 0.1	< 1	0.3	< 0.1	0.9
NS-4630	03/18/2009	*st*	11	40	< 0.4	17	2.7	160	22	390	410	30	< 0.8	1.6	12	1.9	24	< 0.5	< 0.1	< 0.1	< 1	0.3	< 0.1	0.9
NS-5300	03/18/2009	*st*	7.5	37	< 0.4	16	2.7	150	23	217	299	30	< 0.8	1.1	12	2.3	14	< 0.5	< 0.1	< 0.1	< 1	0.3	< 0.1	0.9

st = stream

APPENDIX A2

ANALYTICAL RESULTS OF THE TRIBUTARY STREAM WATERS SAMPLED FROM 2009 TO 2011: PHYSICO-CHEMICAL PARAMETERS AND CHEMICAL COMPONENTS.

Sample no.	**Date**	**Type**	**T** °C	**pH**	**E_h** V	**EC** mS/cm	**TDS** g/l	**Ca** mg/l	**Mg** mg/l	**Na** mg/l	**K** mg/l	**Zn** mg/l	**HCO_3** mg/l	**Cl** mg/l	**SO_4** mg/l	**NO_3** mg/l	**Br** mg/l	**F** mg/l	**SiO_2** mg/l
Rio Pitzinurri	03/18/2009	*st*	13	8.2	0.44	0.52	0.3	25	12	59	3.3	0.3	96	79	38	n.d.	n.d.	n.d.	21
Rio Pitzinurri	10/19/2009	*st*	17	7.3	0.46	0.69	0.4	44	20	82	3.9	2.7	143	136	71	1.4	n.d.	0.8	22
Rio Pitzinurri	04/21/2010	*st*	15	8.3	0.47	0.55	0.3	28	13	57	3.2	0.3	102	91	37	6.3	n.d.	0.3	24
Rio Pitzinurri	06/30/2010	*st*	20	7.3	0.45	1.50	1.1	168	59	67	6.7	19	210	104	529	0.8	n.d.	n.d.	16
Rio Pitzinurri	10/29/2010	*st*	13	7.9	0.45	0.70	0.4	37	17	71	3.6	2.1	132	124	56	2.0	n.d.	0.3	23
Rio Sa Roa	03/18/2009	*st*	17	7.5	0.44	1.60	0.9	73	50	123	5.0	26	74	275	281	1.3	n.d.	0.4	8.7
Rio Sa Roa	04/17/2009	*st*	18	7.0	0.45	1.04	0.7	49	35	107	4.5	20	68	191	215	n.d.	n.d.	n.d.	11
Rio Sa Roa	02/02/2011	*st*	11	7.7	0.53	0.85	0.5	38	28	93	3.4	12	74	155	160	0.6	0.5	0.1	11
Rio Sa Roa	02/02/2011	*st*	12	7.3	0.54	0.91	0.5	38	28	93	3.5	0.4	14	158	160	0.9	0.4	0.2	11
Rio Bau	03/18/2009	*st*	15	8.3	0.40	0.68	0.4	40	23	57	3.5	0.6	86	86	122	5.7	0.2	0.2	13
Rio Sciopadroxiu	03/18/2009	*st*	14	8.1	0.43	0.50	0.3	41	8	45	1.8	0.4	134	73	17	n.d.	n.d.	n.d.	16

st = stream; n.d. = not determined

Sample no.	**Date**	**Type**	**Al** µg/l	**B** µg/l	**Be** µg/l	**Li** µg/l	**Rb** µg/l	**Sr** µg/l	**Ba** µg/l	**Fe** µg/l	**Mn** µg/l	**Cd** µg/l	**Cr** µg/l	**Co** µg/l	**Ni** µg/l	**Cu** µg/l	**Pb** µg/l	**Mo** µg/l	**Ga** µg/l	**Tl** µg/l	**Bi** µg/l	**U** µg/l	**Ag** µg/l	**Sb** µg/l
Rio Pitzinurri	03/18/2009	*st*	13	41	< 0.4	13	1.4	97	16	85	26	4.2	< 0.8	0.1	1.6	1.3	3	0.7	< 0.1	< 0.1	< 1	0.2	< 0.1	0.3
Rio Pitzinurri	10/19/2009	*st*	< 8	46	< 0.2	14	2.2	160	41	< 34	41	22	< 0.5	0.6	7.8	3.8	2.9	0.8	< 0.1	< 0.1	< 0.8	0.2	0.01	1.8
Rio Pitzinurri	04/21/2010	*st*	1.5	35	< 0.1	15	1.5	120	14	<	47	2.4	< 0.5	0.4	3	0.9	2.1	0.8	< 0.01	< 0.1	< 0.2	0.3	< 0.03	0.2
Rio Pitzinurri	06/30/2010	*st*	< 11	41	< 0.1	27	6.3	300	31	< 19	18	228	< 0.6	0.6	39	5.3	90	0.7	< 0.05	< 0.2	< 0.1	0.7	< 0.2	1.8
Rio Pitzinurri	10/29/2010	*st*	2.9	41	< 1	12	1.7	140	27	25	15	15	< 0.3	0.3	4.4	3.3	4.9	< 1.4	< 0.1	< 0.4	0.2	< 0.4	< 0.5	1
Rio Sa Roa	03/18/2009	*st*	< 1	55	< 0.4	18	2.7	280	25	< 20	48	305	< 0.8	1.1	26	3.4	21	< 0.5	< 0.1	< 0.1	< 1	< 0.1	< 0.1	1.3
Rio Sa Roa	04/17/2009	*st*	4.6	66	< 0.4	14	2.2	190	25	11	31	204	< 0.5	1.0	16	5.7	22	< 0.8	< 0.1	< 0.1	< 0.2	< 0.1	< 0.2	1.3
Rio Sa Roa	02/02/2011	*st*	< 16	61	< 0.6	10	1.4	140	22	36	20	117	< 1.3	0.6	12	5	29	< 0.3	< 0.1	< 0.2	< 1	< 0.1	< 0.2	0.6
Rio Sa Roa	02/02/2011	*st*	< 16	62	< 0.6	10	1.4	160	22	44	18	117	< 1.3	0.6	12	5	19	< 0.3	< 0.1	< 0.2	< 1	< 0.1	< 0.2	0.6
Rio Bau	03/18/2009	*st*	11	37	< 0.4	15	2.5	130	18	427	550	4.7	< 0.8	1.7	9.4	1.9	22	< 0.5	< 0.1	< 0.1	< 1	0.3	< 0.1	0.6
Rio Sciopadroxiu	03/18/2009	*st*	9.2	32	< 0.4	2	0.6	170	10	169	9.5	2.7	< 0.8	0.1	0.6	< 0.3	3.5	< 0.5	< 0.1	< 0.1	< 1	0.1	< 0.1	< 0.3

st = stream

APPENDIX A3

ANALYTICAL RESULTS OF THE TAILINGS DRAINAGES AND MINE GALLERY WATERS SAMPLED FROM 2009 TO 2011: PHYSICO-CHEMICAL PARAMETERS AND CHEMICAL COMPONENTS.

Sample no.	**Date**	**Type**	**T** °C	**pH**	**E_h** V	**EC** mS/cm	**TDS** g/l	**Ca** mg/l	**Mg** mg/l	**Na** mg/l	**K** mg/l	**Zn** mg/l	**HCO_3** mg/l	**Cl** mg/l	**SO_4** mg/l	**NO_3** mg/l	**Br** mg/l	**F** mg/l	**SiO_2** mg/l
A	03/18/2009	*td*	19	6.9	0.47	2.66	2.3	148	42	55	6.3	600	21	99	1347	10	n.d.	0.3	11
A	03/25/2009	*td*	12	6.6	0.55	2.76	2.4	153	42	55	7.5	630	23	101	1365	n.d.	n.d.	n.d.	12
A	04/17/2009	*td*	18	6.5	0.66	1.94	2.6	158	40	55	6.1	640	34	87	1568	n.d.	n.d.	n.d.	13
A	05/07/2009	*td*	22	6.5	0.54	2.46	2.6	160	42	56	6.7	690	22	94	1503	n.d.	n.d.	n.d.	14
A	11/11/2009	*td*	14	6.6	0.45	2.68	2.8	209	48	59	9.0	704	21	71	1700	14.3	n.d.	0.4	8.6
A	12/01/2010	*td*	16	6.7	0.50	2.29	2.7	161	38	51	9.0	710	31	71	1672	n.d.	n.d.	0.3	13
A	02/02/2011	*td*	13	6.6	0.59	2.28	2.4	141	32	50	6.1	699	39	70	1360	n.d.	n.d.	n.d.	12
A	02/02/2011	*td*	14	6.9	0.65	2.13	2.3	140	32	47	5.9	634	44	70	1368	n.d.	n.d.	n.d.	13
A	02/11/2011	*td*	10	6.8	0.53	3.28	2.8	170	42	52	6.5	760	26	79	1690	12	n.d.	0.3	14
B	03/25/2009	*td*	16	6.6	0.51	2.60	2.2	107	67	70	5.6	530	17	157	1263	n.d.	n.d.	n.d.	12
B	04/17/2009	*td*	21	6.4	0.66	1.51	1.5	76	49	73	4.2	300	28	138	796	n.d.	n.d.	n.d.	17
B	05/07/2009	*td*	25	6.5	0.52	2.10	1.9	95	62	75	5.0	463	20	155	1051	n.d.	n.d.	n.d.	12
B	05/21/2009	*td*	24	6.2	0.58	2.19	2.1	111	71	84	5.7	514	13	172	1171	n.d.	n.d.	n.d.	13
B	05/27/2009	*td*	21	6.4	0.53	2.22	2.2	117	75	83	5.1	533	13	165	1213	n.d.	n.d.	n.d.	13
B	12/01/2010	*td*	18	7.0	0.61	2.35	2.3	104	71	55	8.0	540	45	77	1400	9.8	n.d.	0.3	13
B	02/02/2011	*td*	13	6.6	0.54	1.43	1.3	61	40	61	3.6	280	27	106	680	4.3	0.5	0.2	6.5
B	02/02/2011	*td*	15	7.0	0.52	1.45	1.2	65	41	64	3.4	280	35	106	664	4.3	0.3	0.2	6.5
B	02/11/2011	*td*	14	7.0	0.52	1.82	1.7	87	53	66	4.2	390	20	116	920	4.2	0.3	0.2	13
C	03/25/2009	*td*	12	7.2	0.52	1.94	1.3	221	80	63	6.6	15	244	106	662	n.d.	n.d.	n.d.	7.5
C	04/17/2009	*td*	20	7.0	0.56	1.57	1.3	224	77	66	6.3	22	220	101	707	n.d.	n.d.	n.d.	9.1
C	05/07/2009	*td*	18	7.3	0.53	1.79	1.5	237	85	69	6.6	20	247	109	811	n.d.	n.d.	n.d.	9.6
C	05/21/2009	*td*	20	7.4	0.49	1.73	1.4	236	86	68	6.2	19	248	104	760	n.d.	n.d.	n.d.	8.9

td = tailng drainages; n.d. = not determined

Sample no.	**Date**	**Type**	**Al** µg/l	**B** µg/l	**Be** µg/l	**Li** µg/l	**Rb** µg/l	**Sr** µg/l	**Ba** µg/l	**Fe** µg/l	**Mn** µg/l	**Cd** µg/l	**Cr** µg/l	**Co** µg/l	**Ni** µg/l	**Cu** µg/l	**Pb** µg/l	**Mo** µg/l	**Ga** µg/l	**Tl** µg/l	**Bi** µg/l	**U** µg/l	**Ag** µg/l	**Sb** µg/l
A	03/18/2009	*td*	2.5	25	< 0.4	19	5.7	320	21	< 20	144	5700	< 0.5	9.3	320	19	875	< 0.7	< 0.1	0.3	< 2	< 0.1	0.3	< 0.3
A	03/25/2009	*td*	< 1	25	< 0.4	19	5.9	330	21	< 20	154	5980	< 0.5	9.6	273	15	611	< 0.7	< 0.1	0.3	< 2	< 0.1	0.3	< 0.3
A	04/17/2009	*td*	< 2	43	< 0.4	15	5.8	270	16	< 10	1100	5500	< 0.5	41	287	29	507	< 0.8	< 0.1	0.3	< 0.2	< 0.1	0.3	0.3
A	05/07/2009	*td*	< 9	32	< 0.3	14	7.1	310	21	< 40	101	6130	< 1	8.9	279	12	970	< 0.1	0.2	0.3	< 0.1	< 0.1	0.3	0.3
A	11/11/2009	*td*	15.8	36	0.23	17	8.1	310	25	< 40	675	7170	< 1	40	360	112	1010	< 0.4	0.2	0.4	< 0.8	< 0.1	0.4	0.7
A	12/01/2010	*td*	< 10	58	< 0.5	20	7.3	320	21	< 25	1110	6500	< 1	70	360	68	600	< 0.8	0.2	0.4	< 0.5	< 0.1	0.3	0.4
A	02/02/2011	*td*	< 16	31	< 0.6	14	6.3	220	18	< 20	980	5300	< 1	49	333	87	490	< 0.3	0.2	0.4	< 1.2	< 0.1	0.2	0.3
A	02/02/2011	*td*	< 16	34	< 0.6	15	6.3	210	19	< 21	1000	5500	< 1	50	344	83	566	< 0.3	0.2	0.4	< 1.2	< 0.1	0.2	0.3
A	02/11/2011	*td*	< 5	32	< 0.1	15	6.6	260	18	< 20	820	5800	< 1	33	350	79	700	< 0.1	< 0.2	0.4	< 0.1	0.02	0.2	< 0.3
B	03/25/2009	*td*	1.5	36	< 0.4	63	2.1	310	16	< 20	2960	5040	< 0.5	51	128	8	87	< 0.7	0.1	< 0.1	< 2	< 0.1	0.2	0.5
B	04/17/2009	*td*	< 2	54	< 0.4	29	2.3	190	14	25	1570	3000	< 0.5	46	100	4	35	< 0.8	0.1	< 0.1	< 0.2	< 0.1	< 0.2	0.4
B	05/07/2009	*td*	< 9	43	< 0.3	38	2.6	239	17	< 40	1990	3900	< 1	41	102	5	88	< 0.1	0.1	< 0.1	< 0.1	< 0.1	0.2	0.4
B	05/21/2009	*td*	< 9	54	< 0.3	50	3.0	280	16	< 40	2350	4570	< 1	43	112	5	134	0.07	0.2	< 0.1	< 0.1	< 0.1	0.2	0.2
B	05/27/2009	*td*	< 9	60	< 0.3	53	2.7	290	15	< 40	2320	4660	< 1	44	119	5	154	< 0.1	0.2	< 0.1	< 0.1	< 0.1	0.2	0.4
B	12/01/2010	*td*	< 10	69	< 0.5	39	2.5	320	17	< 25	2310	5060	< 1	77	146	11	94	< 0.6	0.2	< 0.2	< 0.5	< 0.1	0.2	0.4
B	02/02/2011	*td*	< 16	44	< 0.6	23	1.7	150	13	< 20	980	2300	< 1	32	72	5.8	43	< 0.3	< 0.1	< 0.2	< 1	< 0.1	< 0.2	0.3
B	02/02/2011	*td*	< 16	43	< 0.6	23	1.7	140	12	< 20	973	2300	< 1	32	66	6.6	45	< 0.3	< 0.1	< 0.2	< 1.	< 0.1	< 0.2	0.3
B	02/11/2011	*td*	< 5	41	< 0.1	31	1.9	190	14	< 20	1200	3200	< 1	29	95	7.1	64	< 0.1	< 0.2	0.1	< 0.1	< 0.02	0.1	< 0.3
C	03/25/2009	*td*	3.8	23	< 0.4	24	12	330	21	< 20	4.5	166	< 0.5	1.2	78	7.6	185	0.7	< 0.1	0.3	< 2	0.9	< 0.2	2.0
C	04/17/2009	*td*	< 2	44	< 0.4	36	10	310	25	< 10	6	188	9.4	0.9	94	8.8	210	1.7	< 0.1	0.3	< 0.2	0.7	< 0.2	1.9
C	05/07/2009	*td*	< 9	31	< 0.3	38	12	430	25	< 40	5.4	163	< 1	0.6	78	6.5	206	0.7	0.02	0.3	< 0.1	0.9	< 0.1	2.1
C	05/21/2009	*td*	< 9	32	< 0.3	37	12	450	24	< 40	6.0	148	< 1	0.6	77	5.7	191	0.8	0.02	0.3	< 0.1	1.0	< 0.1	2.2

td = tailng drainages

Sample no.	**Date**	**Type**	**T** °C	**pH**	**E_h** V	**EC** mS/cm	**TDS** g/l	**Ca** mg/l	**Mg** mg/l	**Na** mg/l	**K** mg/l	**Zn** mg/l	**HCO_3** mg/l	**Cl** mg/l	**SO_4** mg/l	**NO_3** mg/l	**Br** mg/l	**F** mg/l	**SiO_2** mg/l
C	05/27/2009	*td*	19	7.3	0.5	1.73	1.4	250	89	69	6.5	19	243	106	758	n.d.	n.d.	n.d.	9.0
C	06/03/2009	*td*	20	7.4	0.46	1.79	1.4	251	87	64	7.6	18	254	104	778	n.d.	n.d.	n.d.	8.6
C	06/10/2009	*td*	20	7.4	0.43	1.88	1.4	255	88	64	7.5	18	269	106	769	n.d.	n.d.	n.d.	8.7
C	06/17/2009	*td*	20	7.6	0.45	n.d.	1.5	251	85	61	6.9	19	266	109	844	n.d.	n.d.	n.d.	9.5
C	06/25/2009	*td*	20	7.4	0.44	1.86	1.5	256	86	62	6.2	19	256	106	829	n.d.	n.d.	n.d.	9.8
C	07/08/2009	*td*	21	7.2	0.42	1.83	1.5	259	87	65	6.9	18	263	106	837	n.d.	n.d.	n.d.	9.4
C	07/15/2009	*td*	21	7.2	0.45	1.83	1.5	278	95	74	6.5	15	258	106	793	n.d.	n.d.	n.d.	9.5
C	07/29/2009	*td*	21	7.5	0.41	1.78	1.4	231	77	66	5.8	13	249	101	757	n.d.	n.d.	n.d.	8.9
C	10/19/2009	*td*	20	7.0	0.48	1.63	1.3	232	83	70	8.9	13	271	100	661	0.4	n.d.	0.5	8.0
C	11/28/2009	*td*	20	7.0	0.42	1.74	1.3	232	78	72	7.1	16	257	100	712	0.4	0.2	0.3	7.7
C	03/17/2010	*td*	17	7.3	0.31	1.89	1.4	258	89	68	7.3	14	277	93	780	nd	n.d.	0.4	8.0
C	04/21/2010	*td*	20	7.5	0.44	2.03	1.6	295	98	73	7.9	13	282	95	899	nd	n.d.	0.3	5.9
C	06/30/2010	*td*	20	7.6	0.47	1.94	1.5	268	88	69	9.0	15	285	99	780	nd	n.d.	0.4	10
C	10/29/2010	*td*	20	7.4	0.19	1.83	1.4	230	80	70	9.0	12	275	109	700	0.2	n.d.	0.37	9.9
C	12/01/2010	*td*	20	7.3	0.53	1.62	1.1	188	66	62	10.0	15	209	93	590	1.4	n.d.	0.4	8.7
Ledoux Gallery	03/18/2009	*g*	19	7.9	0.46	0.86	0.5	60	31	64	3.4	2.2	201	79	152	n.d.	n.d.	n.d.	27
Ledoux Gallery	04/17/2009	*g*	18	6.3	0.48	0.81	0.5	57	34	56	3.3	11	131	87	210	n.d.	n.d.	n.d.	22
Ledoux Gallery	05/07/2009	*g*	19	8.0	0.48	0.83	0.5	63	33	58	3.2	4.2	201	87	173	n.d.	n.d.	n.d.	26
Ledoux Gallery	10/19/2009	*g*	20	8.0	0.48	0.69	0.5	60	28	63	3.2	0.8	218	79	111	1.2	n.d.	0.8	32
Ledoux Gallery	04/21/2010	*g*	20	8.0	0.44	0.83	0.5	63	31	61	3.7	1.7	202	84	138	1.0	n.d.	0.9	26
Ledoux Gallery	06/30/2010	*g*	20	8.1	0.46	0.81	0.5	57	28	60	3.7	0.9	211	84	118	1.0	n.d.	1	29
Ledoux Gallery	07/23/2010	*g*	20	8.0	0.49	0.80	0.5	56	27	58	3.8	0.8	204	84	112	2.8	n.d.	0.7	28
Ledoux Gallery	10/29/2010	*g*	20	7.9		0.77	0.5	56	26	60	3.8	0.7	204	86	104	1.4	n.d.	0.84	29

td = tailng drainages; g = mine gallery; n.d. = not determined

Sample no.	**Date**	**Type**	**Al** µg/l	**B** µg/l	**Be** µg/l	**Li** µg/l	**Rb** µg/l	**Sr** µg/l	**Ba** µg/l	**Fe** µg/l	**Mn** µg/l	**Cd** µg/l	**Cr** µg/l	**Co** µg/l	**Ni** µg/l	**Cu** µg/l	**Pb** µg/l	**Mo** µg/l	**Ga** µg/l	**Tl** µg/l	**Bi** µg/l	**U** µg/l	**Ag** µg/l	**Sb** µg/l
C	05/27/2009	*td*	< 9	39	< 0.3	40	13	460	23	< 40	4.2	146	< 1	0.6	74	5.3	191	0.8	0.02	0.3	< 0.1	1.0	< 0.1	2.1
C	06/03/2009	*td*	< 9	34	< 0.3	37	12	470	23	< 20	4.6	152	< 1	0.6	75	5.4	203	0.8	0.02	0.3	< 0.1	1.0	< 0.1	2.2
C	06/10/2009	*td*	< 9	33	< 0.3	38	12	440	22	< 20	4.6	148	< 1	0.6	77	5.5	173	0.7	0.02	0.3	< 0.1	1.1	< 0.1	2.1
C	06/17/2009	*td*	< 9	39	< 0.3	43	13	500	24	< 50	5.6	151	< 1	0.7	84	5.3	183	0.8	0.03	0.4	< 0.1	1.2	< 0.1	2.2
C	06/25/2009	*td*	< 13	46	< 0.2	37	17	420	28	< 50	6.6	157	< 1	0.8	94	5.8	189	0.9	< 0.03	0.4	< 26	1.2	< 0.1	2.4
C	07/08/2009	*td*	14	43	< 0.2	40	17	400	28	< 50	13	147	< 1	1.2	88	9.3	242	0.9	0.9	0.4	< 26	1.2	0.15	2.7
C	07/15/2009	*td*	< 13	52	< 0.2	40	15	370	24	< 50	9.1	139	< 1	1.1	89	6.7	208	0.8	0.9	0.4	< 26	0.9	< 0.1	2.4
C	07/29/2009	*td*	< 13	58	< 0.2	49	15	370	23	< 30	7.6	121	< 1	0.9	83	5.6	243	0.8	0.8	0.4	< 26	0.9	< 0.1	2.3
C	10/19/2009	*td*	< 8	47	< 0.2	46	12	340	22	164	18	156	< 0.5	1.1	79	7.8	146	0.7	< 0.1	0.4	< 0.8	1.1	< 0.1	2.3
C	11/28/2009	*td*	< 8	42	< 0.2	37	12	400	21	225	10	150	< 0.5	0.8	70	7.4	112	0.7	< 0.1	0.3	< 0.8	1.0	< 0.1	2.2
C	03/17/2010	*td*	6.1	36	< 0.1	43	12	340	24	<	8.2	133	< 0.5	0.8	86	5.9	131	1.1	0.05	0.4	< 0.2	1.3	0.08	2.3
C	04/21/2010	*td*	1.8	36	< 0.1	49	13	370	24	<	6.0	136	< 0.5	0.7	86	5.0	67	1.0	0.02	0.4	< 0.2	1.5	< 0.03	2.1
C	06/30/2010	*td*	< 11	41	< 0.1	36	13	360	21	45	19	120	< 0.6	1.3	80	5.4	38	1.0	< 0.1	0.4	< 0.1	1.5	< 0.2	1.9
C	10/29/2010	*td*	3.4	39	< 1	38	12	320	21	1211	131	61	< 0.3	5.4	76	3.2	58	< 1	0.15	< 0.4	< 1	< 0.4	< 0.5	1.6
C	12/01/2010	*td*	< 10	63	< 0.5	34	12	330	52	< 25	110	48	< 1.5	5.3	120	< 2	160	1.8	< 0.1	0.4	< 0.5	1.2	< 0.1	3.1
Ledoux Gallery	03/18/2009	*g*	6.8	39	< 0.4	47	7.1	160	43	142	444	18	< 0.8	5.3	32	2.5	27	1.6	< 0.1	0.3	<1	0.5	< 0.1	2.3
Ledoux Gallery	04/17/2009	*g*	28	42	< 0.4	45	7.4	150	32	159	1240	87	<0 .5	20	67	4.0	42	0.8	< 0.1	0.4	< 0.2	0.6	< 0.2	2.1
Ledoux Gallery	05/07/2009	*g*	< 9	40	< 0.3	39	7.5	220	40	< 40	662	23	< 1	8.6	41	< 2	3	1.3	< 0.02	0.4	< 0.1	1.3	< 0.1	2.6
Ledoux Gallery	10/19/2009	*g*	< 8	40	< 0.2	43	6.1	170	50	< 34	204	5.1	< 0.5	2.1	16	< 3	2	1.8	< 0.1	0.3	< 0.8	1.8	< 0.1	1.9
Ledoux Gallery	04/21/2010	*g*	2.5	40	< 0.1	57	7.4	200	47	< 20	288	8.6	< 0.5	3.3	24	1.4	1	1.7	0.02	0.3	< 0.2	1.6	< 0.03	2.3
Ledoux Gallery	06/30/2010	*g*	< 11	35	< 0.1	33	6.6	170	47	21	200	5.2	< 0.6	2.5	17	< 3	1	1.8	< 0.05	0.3	< 0.1	1.7	< 0.2	1.9
Ledoux Gallery	07/23/2010	*g*	5.0	38	< 0.9	37	5.7	170	48	< 10	183	5.1	< 1	2.1	15	< 2	1	1.8	0.01	< 0.9	< 0.05	1.9	< 0.05	1.9
Ledoux Gallery	10/29/2010	*g*	3.8	43	< 1	38	6.3	170	47	90	139	4.2	< 0.3	1.5	11	1.5	4	1.9	< 0.1	< 0.4	< 1	1.6	< 0.5	1.7

td = tailng drainages; g = mine gallery

APPENDIX B1

ANALYTICAL RESULTS OF THE NARACAULI STREAM WATERS SAMPLED FROM 2009 TO 2011: Y AND RARE EARTH ELEMENTS

Sample no	Date	Type	Y ng/l	La ng/l	Ce ng/l	Pr ng/l	Nd ng/l	Sm ng/l	Eu ng/l	Gd ng/l	Tb ng/l	Dy ng/l	Ho ng/l	Er ng/l	Tm ng/l	Yb ng/l	Lu ng/l	Th ng/l	[1]∑ REE µg/l	[2](La/Lu)$_N$	[3]Ce*	[4]Eu*
NS-100	03/18/2009	*st*	590	740	367	81	290	58	26	90	12	58	11	24	2.2	11	1.7	< 22	1.77	4.9	0.16	0.81
NS-100	03/25/2009	*st*	380	404	60	32	120	20	10	34	4.5	22	5.2	14	1.6	7.9	1.4	< 22	0.74	3.3	0.05	0.85
NS-100	04/17/2009	*st*	770	943	341	92	341	59	26	110	13	62	13	32	3.7	19	2.5	< 22	2.06	4.3	0.12	0.70
NS-100	05/07/2009	*st*	360	410	132	40	145	28	11	44	6.1	26	5.7	14	1.5	7	1.4	< 14	0.87	3.3	0.11	0.67
NS-100	05/21/2009	*st*	259	268	68	20	73	15	11	22	3.3	15	4.2	9	1.1	4	< 1	< 14	0.51		0.09	1.40
NS-100	05/27/2009	*st*	252	260	57	21	71	15	8	22	2.6	13	3.8	8	1.1	5	1.3	< 14	0.49	2.3	0.08	1.00
NS-100	06/03/2009	*st*	236	276	72	24	80	17	10	25	3.5	17	4	9	1.2	5.6	< 1	< 14	0.54		0.09	1.10
NS-100	06/10/2009	*st*	290	340	154	33	123	25	13	42	5.1	23	5.4	12	1	5.6	< 1	< 14	0.78		0.15	0.89
NS-100	06/17/2009	*st*	223	313	216	38	134	32	14	40	5.1	23	4.2	9.2	1.1	5	1	< 14	0.84	3.5	0.22	0.90
NS-100	06/25/2009	*st*	136	117	< 25	11	37	8	6	12	2.1	7.4	< 2	5	< 1	3	< 1	< 14	0.21			1.38
NS-100	07/08/2009	*st*	188	201	61	21	75	14	7.4	22	3.6	14	3.8	11	1.1	6	1	< 14	0.44	2.3	0.10	0.95
NS-100	07/15/2009	*st*	186	228	136	30	110	23	6	26	3.5	18	4.2	8	1	9.7	1	< 14	0.60	2.6	0.18	0.57
NS-100	07/29/2009	*st*	119	114	52	14	53	< 10	5	14	1.7	9	2.4	5.4	< 1	4.2	< 1	< 14	0.28		0.14	
NS-100	10/19/2009	*st*	76	90	< 40	13	37	8	3	6	< 1.2	6	1.4	3	< 1	< 3	< 1	< 20	0.17			1.02
NS-100	11/11/2009	*st*	1720	4000	1560	550	1750	272	124	350	39	195	30	71	7.5	35	4	< 20	8.99	11	0.12	0.93
NS-100	11/28/2009	*st*	104	214	46	21	70	12	5	12	2	11	1.8	4	< 1	3	< 1	< 20	0.40		0.07	0.98
NS-100	03/17/2010	*st*	389	590	439	69	218	33	21	51	7	34	6	14	1	6	1	< 12	1.49	6.7	0.24	1.15
NS-100	04/21/2010	*st*	120	137	19	11	40	8	2.6	10	1.1	4.5	1.9	3.5	0.5	< 2	< 0.5	< 12	0.24		0.05	0.67
NS-100	06/30/2010	*st*	60	90	46	9	27	< 8	<5	<6	<5	<5	< 5	< 5	< 4	< 6	< 5	< 36	0.17		0.17	
NS-100	10/29/2010	*st*	100	93	20	8	29	< 4	4	9	< 1	6	1.9	< 3	< 1	2.8	< 1	< 44	0.17		0.08	
NS-100	12/01/2010	*st*	1580	3100	1180	290	1130	180	77	304	34	167	29	75	6	37	6	< 60	6.62	5.9	0.13	0.73
NS-100	01/26/2011	*st*	375	341	75	28	100	18	9	31	4	22	6	13	1.4	7	1.1	< 24	0.66	3.5	0.08	0.84

st = stream; [1] = La to Lu; [2]$(La/Lu)_{water}/(La/Lu)_{PAAS}$; [3] = $(Ce_{water}/Ce_{PAAS})/[(La_{water}/La_{PAAS})+(Pr_{water}/Pr_{PAAS})]$; [4] = $(Eu_{water}/Eu_{PAAS})/[(Sm_{water}/Sm_{PAAS})+(Gd_{water}/Gd_{PAAS})]$

Sample no	Date	Type	Y ng/l	La ng/l	Ce ng/l	Pr ng/l	Nd ng/l	Sm ng/l	Eu ng/l	Gd ng/l	Tb ng/l	Dy ng/l	Ho ng/l	Er ng/l	Tm ng/l	Yb ng/l	Lu ng/l	Th ng/l	[1]∑ REE µg/l	[2](La/Lu)$_N$	[3]Ce*	[4]Eu*
NS-100	02/11/2011	*st*	420	440	130	40	150	27	13	48	6	27	6	16	1.7	7	1.2	< 24	0.91	4.2	0.10	0.79
NS-170	03/18/2009	*st*	360	404	123	38	129	19	9.7	37.1	5.4	24	4.9	12	1.4	7.4	1.2	< 22	0.82	3.8	0.10	0.79
NS-170	03/25/2009	*st*	149	124	31	11	36	6	5.2	11	1.8	7.7	2	4.8	< 1	3	< 1	< 22	0.24		0.09	1.40
NS-170	04/17/2009	*st*	760	940	580	117	430	90	37	137	17	77	15	33	3.6	17	2.5	< 22	2.50	4.3	0.19	0.75
NS-170	05/07/2009	*st*	146	226	81	18	55	12	6.5	18	2.5	11	2.7	5	< 1	1.9	< 1	< 14	0.44		0.13	1.00
NS-170	05/21/2009	*st*	95	91	44	9.3	32	8	5.5	9.7	1.5	6.8	< 2	2.8	< 1	< 2	< 1	< 14	0.21		0.16	1.45
NS-170	05/27/2009	*st*	99	89	27	68	27	7	5.1	6	1.5	5.7	< 2	3.3	< 1	2.3	< 1	< 14	0.24		0.03	1.85
NS-170	06/03/2009	*st*	111	113	49	10	37	9	6.2	12	2.1	6.9	2	4	< 1	2.2	< 1	< 14	0.25		0.15	1.37
NS-170	06/10/2009	*st*	69	67	34	5.9	23	6	5.2	7	1.6	4.2	< 2	3	< 1	< 2	< 1	< 14	0.16		0.18	1.86
NS-170	06/17/2009	*st*	48	41	< 25	< 5	15	< 5	4.9	5.2	< 1	3.7	< 2	< 2	< 1	< 2	< 1	< 14	0.07			
NS-170	06/25/2009	*st*	24	23	< 25	< 5	< 10	< 5	4.2	< 3	< 1	< 3	< 2	< 2	< 1	< 2	< 1	< 14	0.03			
NS-170	07/08/2009	*st*	47	45	35	6	23	5	6.4	7	1.2	4.5	< 2	2	< 1	< 2	< 1	< 14	0.14		0.24	2.47
NS-170	07/15/2009	*st*	57	< 70	42	< 13	31	< 10	4.4	< 8	1.2	8	< 2	4	< 1	< 3	< 1	< 14	0.09			
NS-170	07/29/2009	*st*	24	< 70	28	< 13	< 23	< 10	3	< 8	< 1	< 6	< 2	< 4	< 1	< 3	< 1	< 14	0.03			
NS-170	10/19/2009	*st*	36	56	< 40	6	19	5	< 3	< 4	< 1	2.6	<1	< 3	<1	< 3	< 1	< 20	0.09			
NS-170	04/21/2010	*st*	24	18	5	< 2	5.7	1	1.1	< 2	0.3	< 2	0.4	< 1	< 0.3	< 1	< 0.5	< 12	0.03			
NS-170	06/30/2010	*st*	26	85	108	13	36	< 8	< 5	< 6	< 5	< 5	< 5	< 5	<4	< 6	< 5	< 36	0.24		0.37	
NS-170	10/29/2010	*st*	42	31	16	3.2	12	< 4	4	3.7	< 1	< 3	< 1	< 2	< 1	< 2	< 1	< 44	0.07		0.17	
NS-330	03/18/2009	*st*	180	166	53	18	63	12	7	18	3	13	< 4	5.7	< 1	4.5	< 1	< 22	0.36		0.10	1.08
NS-330	03/25/2009	*st*	153	140	44	14	44	15	6.1	12.7	2.2	9	< 4	7	< 1	3.6	< 1	< 22	0.30		0.11	1.04
NS-330	04/17/2009	*st*	470	514	183	54	200	33	13	56	7.5	36	8	19	2.5	11	1.6	< 22	1.14	3.6	0.12	0.66
NS-330	05/07/2009	*st*	133	131	49	14	47	9.2	6	15	2.2	9.2	1.9	6	< 1	3	< 1	< 14	0.29		0.12	1.14

st = stream; [1] = La to Lu; [2]$(La/Lu)_{water}/(La/Lu)_{PAAS}$; [3] = $(Ce_{water}/Ce_{PAAS})/[(La_{water}/La_{PAAS})+(Pr_{water}/Pr_{PAAS})]$; [4] = $(Eu_{water}/Eu_{PAAS})/[(Sm_{water}/Sm_{PAAS})+(Gd_{water}/Gd_{PAAS})]$

Sample no	Date	Type	Y ng/l	La ng/l	Ce ng/l	Pr ng/l	Nd ng/l	Sm ng/l	Eu ng/l	Gd ng/l	Tb ng/l	Dy ng/l	Ho ng/l	Er ng/l	Tm ng/l	Yb ng/l	Lu ng/l	Th ng/l	[1]∑ REE µg/l	[2](La/Lu)$_N$	[3]Ce*	[4]Eu*
NS-330	05/21/2009	*st*	71	57	< 25	6	19	< 5	4.5	8	1.4	5.2	< 2	2.1	< 1	< 2	< 1	< 14	0.10			
NS-330	05/27/2009	*st*	135	140	52	15	56	12	6.5	16	2.6	11	2.1	5	< 1	4.5	< 1	< 14	0.32		0.12	1.08
NS-330	06/03/2009	*st*	96	89	41	11	37	8	6	12	2.2	7.6	< 2	3	< 1	3.2	< 1	< 14	0.22		0.14	1.38
NS-330	06/10/2009	*st*	113	120	69	15	59	9	6	15	2.3	9.3	2.3	4.7	< 1	3.2	< 1	< 14	0.31		0.18	1.15
NS-330	06/17/2009	*st*	95	86	29	9	33	9	6	9	2.2	7	< 2	4	< 1	2	< 1	< 14	0.20		0.11	1.56
NS-330	06/25/2009	*st*	49	44	< 25	< 5	12	< 5	4.1	4.3	1.1	< 3	< 2	2	< 1	< 2	< 1	< 14	0.07			
NS-330	07/08/2009	*st*	101	87	51	12	44	7.5	5.4	12	2.2	8.8	2	5.4	< 1	3.1	< 1	< 14	0.24		0.18	1.27
NS-330	07/15/2009	*st*	87	78	46	< 13	36	10	4.1	8.7	1.5	8.1	< 2	4.9	< 1	3	< 1	< 14	0.20			1.03
NS-330	07/29/2009	*st*	94	67	45	< 13	38	< 10	4.5	< 8	1.8	9	< 2	4.8	< 1	3.2	< 1	< 14	0.17			
NS-330	08/19/2009	*st*	41	< 44	< 40	4	9	4	< 3	< 4	< 1	5	1	< 3	< 1	< 3	< 1	< 20	0.02			
NS-330	04/21/2010	*st*	56	69	13	7.1	19	< 4	1.9	4	0.9	3	1	1.5	< 0.3	< 2	< 0.5	<12	0.12		0.06	
NS-330	06/30/2010	*st*	62	66	70	10	33	<10	< 5	< 8	< 5	< 5	< 5	< 5	< 4	< 6	< 5	< 36	0.18		0.31	
NS-330	01/26/2011	*st*	136	117	28	8	34	7	4	12	1.5	7	1.8	6	< 1	< 10	< 1	< 24	0.23		0.09	0.97
NS-330	02/02/2011	*st*	460	550	175	56	220	38	17	58	8	38	8	18	2	11	2	< 24	1.20	3.1	0.11	0.82
NS-330	02/02/2011	*st*	420	520	176	58	200	37	17	56	8	35	7	16	2.3	10	1.8	< 24	1.14	3.3	0.11	0.84
NS-330	02/11/2011	*st*	220	220	115	26	95	16	11	30	3.6	18	3.5	8	< 1	5	< 1	< 24	0.55		0.17	1.09
NS-420	03/18/2009	*st*	60	44	< 40	< 13	< 34	< 6	3.8	< 5	1.2	3.1	< 4	< 3	< 1	< 3	< 1	< 22	0.05			
NS-420	03/25/2009	*st*	67	94	72	8.8	26	< 6	4.2	7	< 1	4	< 4	3	< 1	< 3	< 1	< 22	0.22		0.26	
NS-420	04/17/2009	*st*	192	141	63	< 13	48	7	5.9	10.9	2.1	9.3	< 4	4.9	< 1	4	< 1	< 22	0.30			1.52
NS-420	05/07/2009	*st*	60	53	22	5.2	16.5	< 5	3.5	5	1	4	< 2	2	< 1	< 2	< 1	< 14	0.11		0.14	
NS-420	05/21/2009	*st*	28	< 17	< 25	< 5	7	< 5	< 3	< 4	< 1	< 3	< 2	< 2	< 1	< 2	< 1	< 14	0.01			
NS-420	05/27/2009	*st*	44	52	38	5.8	21	5	5.5	6.1	1.5	3.9	< 2	< 2	< 1	< 2	< 1	< 14	0.14		0.24	2.30

st = stream; [1] = La to Lu; [2]$(La/Lu)_{water}/(La/Lu)_{PAAS}$; [3] = $(Ce_{water}/Ce_{PAAS})/[(La_{water}/La_{PAAS})+(Pr_{water}/Pr_{PAAS})]$; [4] = $(Eu_{water}/Eu_{PAAS})/[(Sm_{water}/Sm_{PAAS})+(Gd_{water}/Gd_{PAAS})]$

Sample no	Date	Type	Y ng/l	La ng/l	Ce ng/l	Pr ng/l	Nd ng/l	Sm ng/l	Eu ng/l	Gd ng/l	Tb ng/l	Dy ng/l	Ho ng/l	Er ng/l	Tm ng/l	Yb ng/l	Lu ng/l	Th ng/l	[1]∑ REE µg/l	[2](La/Lu)$_N$	[3]Ce*	[4]Eu*
NS-420	06/03/2009	*st*	50	48	32	< 5	23	5	5	7	1.2	3	< 2	< 2	< 1	< 2	< 1	< 14	0.12			1.93
NS-420	06/10/2009	*st*	55	62	71	9.7	40	14	5.7	9.1	2	5.6	< 2	3	< 1	2.6	< 1	< 14	0.22		0.33	1.18
NS-420	06/17/2009	*st*	27	24	< 25	< 5	< 10	< 5	3.3	3.4	1	< 3	< 2	< 2	< 1	< 2	< 1	< 14	0.03			
NS-420	06/25/2009	*st*	21	< 22	< 25	< 5	10	< 5	< 3	< 3	< 1	< 3	< 2	< 2	< 1	< 2	< 1	< 14	0.01			
NS-420	07/08/2009	*st*	33	33	< 25	< 5	15	5	4.2	3.4	< 1	3	< 2	< 2	< 1	< 2	< 1	< 14	0.06			2.39
NS-420	07/15/2009	*st*	39	< 70	39	< 13	< 24	< 10	< 3	< 8	1	4	< 2	< 4	< 1	< 3	< 1	< 14	0.04			
NS-420	07/29/2009	*st*	68	81	135	16	58	12	5	15	2.1	11	2.6	6	< 1	4.9	< 1	< 14	0.35		0.44	0.86
NS-420	08/19/2009	*st*	10	< 44	< 40	< 3	8	< 5	< 3	< 2	<1	< 2	< 1	< 3	< 1	< 3	< 1	< 20	0.01			
NS-420	10/19/2009	*st*	22	< 44	< 40	< 3	<8	< 5	< 3	2.2	< 1	< 3	< 1	< 3	< 1	< 3	< 1	< 20	0.002			
NS-420	11/11/2009	*st*	310	740	360	76	220	32	14	46	5.1	24	4.8	13	1.2	7	< 1	< 20	1.54		0.16	0.83
NS-420	11/28/2009	*st*	25	< 44	< 40	4	12	3	<3	3	< 1	< 2	<1	< 3	< 1	< 3	< 1	< 20	0.02			
NS-420	03/17/2010	*st*	46	56	60	8	21	4	1	6	0.5	5	1	1	0.4	< 1	< 0.5	<12	0.16		0.32	0.46
NS-420	04/21/2010	*st*	21	12	<4	< 2	<5	4	1	<2	<0.3	< 2	< 0.3	< 1	< 0.3	< 1	< 0.5	<12	0.02			
NS-420	06/30/2010	*st*	15	27	36	< 9	12	< 8	< 5	<6	< 5	< 5	< 5	< 5	<4	< 6	< 5	<36	0.08			
NS-420	10/29/2010	*st*	33	19	< 16	2	10	< 4	2.5	3.3	< 1	< 3	< 1	< 2	< 1	< 2	< 1	< 44	0.04			
NS-420	12/01/2010	*st*	610	1230	690	110	390	68	27	100	12	53	10	23	2.5	13	1.6	< 60	2.73	8.7	0.19	0.74
NS-420	01/26/2011	*st*	76	74	32	7	24	7	3	8	1.5	5	1.7	3	< 1	< 3	< 1	< 24	0.17		0.15	0.93
NS-590	03/18/2009	*st*	22	26	23	< 13	< 34	< 6	3.7	< 5	< 1	< 3	< 4	< 2	< 1	< 3	< 1	< 22	0.05			
NS-590	03/25/2009	*st*	18	29	32	< 13	< 34	< 6	3.8	< 5	< 3	< 1	< 4	< 2	< 1	< 3	< 1	< 22	0.06			
NS-590	04/17/2009	*st*	78	77	41	< 13	< 34	8	4.2	7	1.5	5.4	< 4	2	< 1	< 3	< 1	< 22	0.15			1.32
NS-590	05/07/2009	*st*	25	26	< 25	< 5	12	< 5	3	< 4	< 1	2	< 2	< 2	< 1	< 2	< 1	< 14	0.04			
NS-590	05/21/2009	*st*	24	24	< 25	< 5	10	< 5	3.7	< 4	< 1	3.2	< 2	< 2	< 1	< 2	< 1	< 14	0.04			

st = stream; [1] = La to Lu; [2]$(La/Lu)_{water}/(La/Lu)_{PAAS}$; [3] = $(Ce_{water}/Ce_{PAAS})/[(La_{water}/La_{PAAS})+(Pr_{water}/Pr_{PAAS})]$; [4] = $(Eu_{water}/Eu_{PAAS})/[(Sm_{water}/Sm_{PAAS})+(Gd_{water}/Gd_{PAAS})]$

Sample no	Date	Type	Y ng/l	La ng/l	Ce ng/l	Pr ng/l	Nd ng/l	Sm ng/l	Eu ng/l	Gd ng/l	Tb ng/l	Dy ng/l	Ho ng/l	Er ng/l	Tm ng/l	Yb ng/l	Lu ng/l	Th ng/l	[1]∑ REE µg/l	[2](La/Lu)$_N$	[3]Ce*	[4]Eu*
NS-590	05/27/2009	*st*	19	28	< 25	< 5	16	< 15	4.2	4.2	< 1	< 2	< 2	< 2	< 1	< 2	< 1	< 14	0.05			
NS-590	06/03/2009	*st*	23	40	33	< 5	17	< 5	5	< 4	1.2	< 2	< 2	< 2	< 1	< 2	< 1	< 14	0.10			
NS-590	06/10/2009	*st*	13	< 22	< 25	< 5	< 10	< 4	4.1	< 3	< 1	< 2	< 2	< 2	< 1	< 2	< 1	< 14	0.004			
NS-590	06/17/2009	*st*	15	28	25	< 5	12	< 5	4	3	< 1	< 3	< 2	< 2	< 1	< 2	< 1	< 14	0.07			
NS-590	06/25/2009	*st*	12	< 22	< 25	< 5	< 10	< 5	3.1	< 3	< 1	< 2	< 2	< 2	< 1	< 2	< 1	< 14	0.003			
NS-590	07/08/2009	*st*	14	< 22	< 25	< 5	< 10	< 5	4	< 3	< 1	< 2	< 2	< 2	< 1	< 2	< 1	< 14	0.004			
NS-590	07/15/2009	*st*	22	< 70	31	< 13	< 24	< 10	< 3	< 8	< 1	< 6	< 2	< 4	< 1	< 3	< 1	< 14	0.03			
NS-590	07/29/2009	*st*	35	< 70	57	< 13	30	< 10	3	9.1	1	< 6	< 2	< 4	< 1	< 3	< 1	< 14	0.10			
NS-590	08/19/2009	*st*	9	< 44	< 40	< 3	8	< 5	< 3	< 2	< 1	< 2	< 1	< 3	< 1	<3	< 1	< 20	0.01			
NS-590	10/19/2009	*st*	8	< 44	< 40	< 3	<8	< 5	< 3	< 2	< 1	< 2	< 1	< 3	< 1	< 3	< 1	< 20	-			
NS-590	11/28/2009	*st*	10	< 44	< 40	< 3	<8	3	< 3	< 2	<1	< 2	< 1	< 3	< 1	< 3	< 1	< 20	0.003			
NS-590	03/17/2010	*st*	16	26	16	1.8	7	< 4	1	2	< 0.3	< 2	< 0.3	< 1	< 0.3	< 1	< 0.5	<12	0.05		0.23	
NS-590	04/21/2010	*st*	5	6	4	< 2	< 5	1.9	< 1	< 2	< 0.3	< 2	0.3	< 1	< 0.3	< 1	< 0.5	<12	0.01			
NS-590	06/30/2010	*st*	14	42	60	< 9	19	< 8	< 5	< 6	< 5	< 5	< 5	< 5	< 4	< 6	< 5	<36	0.12			
NS-590	10/29/2010	*st*	25	12	< 16	2	9	< 4	2	2	< 1	3	< 1	2	< 1	2	< 1	< 44	0.03			
NS-590	12/01/2010	*st*	130	195	< 260	18	60	9	6	17	2	8	1	5	< 1	< 3	< 1	< 60	0.32			1.05
NS-590	01/26/2011	*st*	36	62	29	5	20	< 10	4	5	< 1	3	< 1	2	< 1	< 3	< 1	< 24	0.13		0.17	
NS-590	02/02/2011	*st*	143	200	69	15	62	13	6	12	2.5	9	2.2	5	< 1	3	< 1	< 24	0.40		0.13	1.13
NS-590	02/02/2011	*st*	128	159	63	16	55	7	8	16	2.6	9	2	6	< 1	< 10	< 1	< 24	0.34		0.13	1.58
NS-630	03/18/2009	*st*	44	34	45	< 13	< 34	< 6	4.4	7.2	1.2	4.3	< 4	3	< 1	3	< 1	< 22	0.10			
NS-1200	03/18/2009	*st*	64	40	30	< 13	< 34	< 6	3.3	7	1.1	5.6	< 4	3	< 1	3	< 1	< 22	0.09			
NS-1200	04/17/2009	*st*	198	2190	268	33	128	31	11	35	5.3	28	5.9	14	2.3	11	2	24	2.76	12	0.06	0.78

st = stream; [1] = La to Lu; [2]$(La/Lu)_{water}/(La/Lu)_{PAAS}$; [3] = $(Ce_{water}/Ce_{PAAS})/[(La_{water}/La_{PAAS})+(Pr_{water}/Pr_{PAAS})]$; [4] = $(Eu_{water}/Eu_{PAAS})/[(Sm_{water}/Sm_{PAAS})+(Gd_{water}/Gd_{PAAS})]$

Sample no	Date	Type	Y ng/l	La ng/l	Ce ng/l	Pr ng/l	Nd ng/l	Sm ng/l	Eu ng/l	Gd ng/l	Tb ng/l	Dy ng/l	Ho ng/l	Er ng/l	Tm ng/l	Yb ng/l	Lu ng/l	Th ng/l	[1]∑ REE µg/l	[2](La/Lu)$_N$	[3]Ce*	[4]Eu*
NS-1200	05/07/2009	*st*	75	73	42	11	33	7	4	12	1.3	5	< 2	4.4	< 1	3.8	< 1	< 14	0.20		0.17	0.97
NS-1200	10/19/2009	*st*	45	64	< 40	8	26	5	< 3	6	< 1	3	< 1	< 3	< 1	<3	< 1	< 20	0.11			
NS-1200	04/21/2010	*st*	38	34	17	5	17	3	1	3	0.8	2	1.03	1.8	< 0.3	2	< 0.5	<1 2	0.09		0.15	0.78
NS-1200	06/30/2010	*st*	59	66	36	< 9	18	< 8	< 5	< 6	< 5	5	< 5	< 5	< 4	< 6	< 5	< 36	0.13			
NS-1200	10/29/2010	*st*	69	47	28	7	24	5	3	8	1.1	6	1.4	3.2	< 1	4	< 1	< 44	0.14		0.17	1.06
NS-1200	01/26/2011	*st*	65	243	73	10	40	10	4	9	1.5	7	2.4	5	< 1	4	1	< 24	0.41	2.8	0.12	0.99
NS-1600	03/18/2009	*st*	84	47	23	< 13	< 34	3.5	5.3	7.9	1.2	4.9	< 4	4.2	< 1	3	< 1	< 22	0.10			2.11
NS-1600	10/29/2010	*st*	57	30	33	5	20	5	5	6	1.3	4	1.1	3	< 1	2.5	< 1	< 44	0.12		0.31	2.12
NS-1600	12/01/2010	*st*	100	117	< 260	21	83	17	8	18	3	15	3	8	< 1	7	1	< 60	0.30	1.3		1.07
NS-1600	01/26/2011	*st*	86	128	58	13	47	12	5	14	1.7	8	2	5	< 1	3	< 1	< 24	0.30		0.15	0.90
NS-2250	03/18/2009	*st*	127	110	36	14	51	9.8	6.9	14	2	10	< 4	5	1	3.6	< 1	< 22	0.26		0.10	1.34
NS-2270	03/18/2009	*st*	128	120	39	15	53	11	7.1	13	1.9	11	< 4	6	< 1	3.4	< 1	< 22	0.28		0.10	1.41
NS-2270	07/23/2010	*st*	59	56	31	9	30	8	3	7	< 2	5	<1	2	< 2	< 2	< 2	< 40	0.15		0.16	0.94
NS-2270	08/05/2010	*st*	187	116	57	14	57	11	7	17	2.4	13	2.7	7	< 1	4	< 1	< 44	0.31		0.15	1.15
NS-2470	07/23/2010	*st*	53	38	16	4	16	< 5	< 3	3	< 2	3	<1	2	< 2	< 2	< 2	< 40	0.08		0.14	
NS-2470	10/29/2010	*st*	121	93	48	12	47	9	5	12	2.1	10	2.5	7	< 1	5	1	< 44	0.25	1.1	0.16	1.10
NS-2640	07/15/2009	*st*	128	155	91	17	64	11	9	15	2.1	11	2.5	4.1	< 1	3.2	< 1	< 14	0.38		0.19	1.60
NS-2640	07/29/2009	*st*	175	537	530	76	240	20	10	33	4.1	18	4.2	11	1.4	8	1.2	< 14	1.49	5.1	0.29	0.87
NS-2640	06/30/2010	*st*	74	67	34	< 9	31	< 8	< 5	7	< 5	6	< 5	< 5	< 4	< 6	< 5	< 40	0.15			
NS-2640	07/23/2010	*st*	43	49	16	6	23	4	< 3	4	< 2	3	< 1	< 2	< 2	< 2	< 2	< 40	0.11		0.10	
NS-2640	08/05/2010	*st*	103	65	48	8	29	5	4	10	2	6	1.9	5	< 1	< 3	< 1	< 44	0.18		0.23	1.22
NS-2640	01/26/2011	*st*	121	139	70	17	68	12	7	17	2.5	11	2.7	6	1	5	< 1	< 24	0.36		0.16	1.12

st = stream; [1] = La to Lu; [2]$(La/Lu)_{water}/(La/Lu)_{PAAS}$; [3] = $(Ce_{water}/Ce_{PAAS})/[(La_{water}/La_{PAAS})+(Pr_{water}/Pr_{PAAS})]$; [4] = $(Eu_{water}/Eu_{PAAS})/[(Sm_{water}/Sm_{PAAS})+(Gd_{water}/Gd_{PAAS})]$

Sample no	Date	Type	Y ng/l	La ng/l	Ce ng/l	Pr ng/l	Nd ng/l	Sm ng/l	Eu ng/l	Gd ng/l	Tb ng/l	Dy ng/l	Ho ng/l	Er ng/l	Tm ng/l	Yb ng/l	Lu ng/l	Th ng/l	[1]∑ REE µg/l	[2](La/Lu)$_N$	[3]Ce*	[4]Eu*
NS-2640	02/02/2011	*st*	140	178	190	30	107	24	8	27	4	18	4	12	1.2	9	1.6	< 24	0.61	1.3	0.30	0.73
NS-2640	02/02/2011	*st*	136	174	170	28	106	27	10	28	4	18	4	10	1.3	8	1.5	< 24	0.59	1.3	0.28	0.85
NS-2640	02/11/2011	*st*	110	130	62	21	64	14	8	19	2	11	2.8	7	< 1	4	< 1	< 24	0.34		0.13	1.12
NS-2940	03/18/2009	*st*	102	73	< 40	< 13	< 34	4.6	4.1	6.2	1.1	5	< 4	4.4	< 1	3.9	< 1	< 22	0.10			1.76
NS-2940	07/08/2009	*st*	110	120	42	13.2	52	9	8.3	12	1.8	9	2	4.2	< 1	2.6	< 1	< 14	0.28		0.11	1.82
NS-2940	07/15/2009	*st*	94	95	58	< 13	42	10	6.2	12	1.6	7	< 2	5.1	< 1	< 3	< 1	< 14	0.24			1.31
NS-2940	07/29/2009	*st*	63	< 70	23	< 13	< 24	< 10	4.6	< 6	1.12	< 6	< 2	< 4	< 1	< 3	< 1	< 14	0.03			
NS-2940	10/19/2009	*st*	54	61	< 40	8	25	< 5	< 3	4	< 1	3.2	< 1	< 3	< 1	< 3	< 1	< 20	0.10			
NS-2940	11/28/2009	*st*	79	151	135	23	78	13	6	12	2	9	1.3	4	< 1	< 3	< 1	< 20	0.43		0.26	1.13
NS-2940	03/17/2010	*st*	67	88	49	12	42	6	3	7	1.4	5	0.9	1.7	< 0.3	1.9	< 0.5	<12	0.22		0.17	1.08
NS-2940	04/21/2010	*st*	47	44	9	3.4	12	2.1	< 1	< 3	0.5	2	0.8	< 2	0.4	1.6	< 0.5	<12	0.08		0.08	
NS-2940	06/30/2010	*st*	62	79	54	10	29	5	< 3	5	< 2	6	< 1	2	< 2	< 2	< 2	< 40	0.19		0.21	
NS-2940	07/23/2010	*st*	29	21	15	3	6	< 3	<3	< 3	< 2	< 5	<1	< 2	< 2	< 2	< 2	< 40	0.05		0.21	
NS-2940	10/29/2010	*st*	166	330	340	44	164	35	15	34	5	24	4.6	13	1	9	1.5	< 60	1.02	2.5	0.31	1.02
NS-3500	03/18/2009	*st*	95	85	37	10	35	7	6	8	1.1	7.4	1.5	4	< 1	< 3	< 1	< 22	0.20		0.14	1.87
NS-3650	03/18/2009	*st*	265	238	359	52	203	44	18	59	7.4	37	6.4	15	1.55	11	1.5	< 22	1.05	1.8	0.37	0.81
NS-4410	03/18/2009	*st*	115	80	101	17	71	14	6.8	18	2.7	11	< 4	6.4	< 1	4.7	< 1	< 22	0.33		0.32	1.00
NS-4630	03/18/2009	*st*	158	131	182	28	104	25	10	29	4.3	17	4	10	1.2	6	1.3	< 22	0.55	1.1	0.35	0.86
NS-5300	03/18/2009	*st*	95	80	100	15	65	15	8	16	2.2	11	< 4	5.6	< 1	4.5	< 1	< 22	0.32		0.33	1.21

st = stream; [1] = La to Lu; [2]$(La/Lu)_{water}/(La/Lu)_{PAAS}$; [3] = $(Ce_{water}/Ce_{PAAS})/[(La_{water}/La_{PAAS})+(Pr_{water}/Pr_{PAAS})]$; [4] = $(Eu_{water}/Eu_{PAAS})/[(Sm_{water}/Sm_{PAAS})+(Gd_{water}/Gd_{PAAS})]$

APPENDIX B2

ANALYTICAL RESULTS OF THE TRIBUTARY STREAM WATERS SAMPLED FROM 2009 TO 2011: Y AND RARE EARTH ELEMENTS

Sample no	**Date**	**Type**	**Y** ng/l	**La** ng/l	**Ce** ng/l	**Pr** ng/l	**Nd** ng/l	**Sm** ng/l	**Eu** ng/l	**Gd** ng/l	**Tb** ng/l	**Dy** ng/l	**Ho** ng/l	**Er** ng/l	**Tm** ng/l	**Yb** ng/l	**Lu** ng/l	**Th** ng/l	**[1]∑ REE** µg/l	**[2](La/Lu)$_N$**	**[3]Ce***	**[4]Eu***
Rio Pitzinurri	03/18/2009	*st*	50	46	73	< 13	39	11	3.2	9	1.5	7.3	< 4	4.8	< 1	3.9	< 1	< 22	0.20			0.8
Rio Pitzinurri	10/19/2009	*st*	23	< 44	< 40	4.3	12	3	< 3	4	< 1	2.7	< 1	< 3	< 1	< 3	< 1	< 20	0.03			
Rio Pitzinurri	04/21/2010	*st*	19	18	23	4	13	4	1	2	0.7	2	0.8	2	0.51	2	< 0.5	< 12	0.07		0.31	0.8
Rio Pitzinurri	06/30/2010	*st*	126	281	270	37	130	10	5	13	< 5	8	< 5	6	<4	< 6	< 5	< 36	0.76		0.29	1.0
Rio Pitzinurri	10/29/2010	*st*	41	29	23	5.5	22	< 4	4	4	< 1	4	1	3	< 1	3	< 1	< 44	0.10		0.21	
Rio Sa Roa	03/18/2009	*st*	106	151	46	< 13	38	4.3	6.3	9.9	1.4	5.9	< 4	3.8	< 1	< 3	< 1	< 22	0.27			2.0
Rio Sa Roa	04/17/2009	*st*	109	154	74	19.1	70	13	8	16	2.1	10	< 4	5	< 1	4	< 1	< 22	0.38		0.15	1.3
Rio Sa Roa	02/02/2011	*st*	157	290	172	34	140	31	11	32	5	19	4	10	< 1	8	1.2	< 24	0.76	2.7	0.19	0.8
Rio Sa Roa	02/02/2011	*st*	150	250	170	33	130	35	12	34	5	20	4	9	1.5	8	1.5	< 24	0.71	1.9	0.21	0.8
Rio Sa Roa	02/11/2011	*st*	101	160	70	17	68	10	7	16	2	12	2.6	5	< 1	4	< 1	< 24	0.37		0.14	1.2
Rio Bau	03/18/2009	*st*	184	142	208	31.4	119	29	9.8	39	5.3	23	4.4	12	1.4	8	1	< 22	0.63	1.6	0.36	0.7
Rio Sciopadroxiu	03/18/2009	*st*	38	< 27	< 40	< 13	< 34	8.2	3	< 5	1	5.6	< 4	3.1	< 1	< 3	< 1	< 22	0.02			

st = stream; [1] = La to Lu; [2]$(La/Lu)_{water}/(La/Lu)_{PAAS}$; [3] = $(Ce_{water}/Ce_{PAAS})/[(La_{water}/La_{PAAS})+(Pr_{water}/Pr_{PAAS})]$; [4] = $(Eu_{water}/Eu_{PAAS})/[(Sm_{water}/Sm_{PAAS})+(Gd_{water}/Gd_{PAAS})]$

APPENDIX B3

ANALYTICAL RESULTS OF THE TAILING DRAINAGES AND MINE GALLERY WATERS SAMPLED FROM 2009 TO 2011: Y AND RARE EARTH ELEMENTS.

Sample no	**Data**	**Type**	**Y** ng/l	**La** ng/l	**Ce** ng/l	**Pr** ng/l	**Nd** ng/l	**Sm** ng/l	**Eu** ng/l	**Gd** ng/l	**Tb** ng/l	**Dy** ng/l	**Ho** ng/l	**Er** ng/l	**Tm** ng/l	**Yb** ng/l	**Lu** ng/l	**Th** ng/l	**[1]∑ REE** µg/l	**[2](La/Lu)$_N$**	**[3]Ce***	**[4]Eu***
A	03/18/2009	*td*	11100	29100	7700	3160	10800	1670	551	2368	255	1090	200	450	49	239	38	< 22	58	8.7	0.09	0.6
A	03/25/2009	*td*	11400	29900	8300	3000	10200	1520	508	2320	247	1060	192	455	46	228	34	< 22	58	10.0	0.09	0.6
A	04/17/2009	*td*	24400	35200	15100	4380	16100	2660	1020	4470	511	2260	430	1040	109	550	79	< 22	84	5.1	0.13	0.7
A	05/07/2009	*td*	11800	35000	9600	3860	13300	1900	720	3210	330	1360	230	570	59	290	44	< 14	70	9.0	0.09	0.6
A	11/11/2009	*td*	14200	33100	15300	4800	15400	2480	1100	3300	332	1600	250	600	66	280	32	< 20	79	11.7	0.14	0.9
A	12/01/2010	*td*	22000	46000	18000	4700	17700	2900	1120	4800	560	2300	400	800	100	490	77	< 60	100	6.8	0.13	0.7
A	02/02/2011	*td*	17000	32000	13000	4000	15000	2200	830	3700	400	1800	340	800	80	400	60	< 24	75	6.0	0.13	0.6
A	02/02/2011	*td*	18000	35000	14000	4400	17000	2500	1000	4400	500	2100	400	900	90	450	70	< 24	83	5.7	0.12	0.7
A	02/11/2011	*td*	19000	37000	15000	4600	18000	2800	1000	4700	500	2100	400	900	100	420	70	< 24	88	6.0	0.13	0.6
B	03/25/2009	*td*	6900	14500	8200	1255	4520	680	228	1230	127	560	104	236	21	107	17	< 22	32	9.7	0.20	0.5
B	04/17/2009	*td*	2970	6470	4030	574	2000	300	118	546	60	234	45	106	10	46	6.6	< 22	15	11.1	0.22	0.6
B	05/07/2009	*td*	5600	12800	7870	1170	3900	550	190	1030	110	460	91	190	20	76	12	< 14	28	12.1	0.21	0.5
B	05/21/2009	*td*	7470	18100	11800	1768	6120	930	334	1660	168	680	139	290	28	133	20	< 14	42	10.3	0.22	0.6
B	05/27/2009	*td*	6800	16900	10400	1570	5420	820	293	1490	154	610	123	270	27	123	18	< 14	38	10.8	0.21	0.6
B	12/01/2010	*td*	9900	27000	21000	2360	8750	1320	490	2270	220	940	160	410	33	150	28	< 60	65	10.9	0.27	0.6
B	02/02/2011	*td*	2600	5500	3500	550	1900	300	120	500	60	250	48	115	11	56	9	< 24	13	6.9	0.21	0.7
B	02/02/2011	*td*	2500	5700	3600	540	200	310	120	540	60	250	50	110	12	55	8	< 24	12	8.1	0.21	0.6
B	02/11/2011	*td*	3700	8600	5100	820	3000	460	160	800	80	330	69	160	15	67	11	< 24	20	8.9	0.20	0.6
C	03/25/2009	*td*	273	310	61	26	98	20	10	24	3.8	18	4.5	11.5	1.5	8.3	1.2	< 22	1	2.9	0.07	1.1
C	04/17/2009	*td*	220	289	110	33	128	23	12	35	4.3	19	< 4	8	1.2	7.2	< 1	< 22	1		0.12	1.0
C	05/07/2009	*td*	220	265	91	29	100	24	12	35	4.7	21	3.9	9.3	1.5	6.6	1.1	< 14	1	2.7	0.11	0.9

td = tailing drainages; [1] = La to Lu; [2]$(La/Lu)_{water}/(La/Lu)_{PAAS}$; [3] = $(Ce_{water}/Ce_{PAAS})/[(La_{water}/La_{PAAS})+(Pr_{water}/Pr_{PAAS})]$; [4] = $(Eu_{water}/Eu_{PAAS})/[(Sm_{water}/Sm_{PAAS})+(Gd_{water}/Gd_{PAAS})]$

Sample no	**Data**	**Type**	**Y** ng/l	**La** ng/l	**Ce** ng/l	**Pr** ng/l	**Nd** ng/l	**Sm** ng/l	**Eu** ng/l	**Gd** ng/l	**Tb** ng/l	**Dy** ng/l	**Ho** ng/l	**Er** ng/l	**Tm** ng/l	**Yb** ng/l	**Lu** ng/l	**Th** ng/l	**[1]∑ REE** µg/l	**[2](La/Lu)$_N$**	**[3]Ce***	**[4]Eu***
C	05/21/2009	*td*	218	237	73	29	96	19	9	30	3.4	17	3.5	10	1	5.5	1.1	< 14	0.5	2.4	0.10	0.8
C	05/27/2009	*td*	190	220	47	23	83	19	11	25	3.8	13.7	3.7	8	< 1	5	< 1	< 14	0.5		0.07	1.2
C	06/03/2009	*td*	201	225	49	23	87	22	12	25	4	17.3	4	8	1.4	7	1.2	< 14	0.5	2.1	0.07	1.2
C	06/10/2009	*td*	183	211	43	23	80	10	12	27	4	17	3.4	8.4	1.1	5.5	< 1	< 14	0.4		0.07	1.5
C	06/17/2009	*td*	188	221	59	23	81	18	9.9	26	4.4	16	3.9	8	1.3	6.7	< 1	< 14	0.5		0.09	1.0
C	06/25/2009	*td*	179	150	31	15	57	12	9	17	2.5	11	3.1	6	< 1	4	< 1	< 14	0.3		0.07	1.4
C	07/08/2009	*td*	320	407	345	63	250	57	24	65	9	38	7	19	2	12	2	< 14	1.3	2.3	0.24	0.9
C	07/15/2009	*td*	220	232	78	26	103	23	9.7	26	4.2	20	4.1	10	1.5	8	1.1	< 14	0.5	2.4	0.11	0.9
C	07/29/2009	*td*	199	248	160	34	131	30	12	35	4.1	22	4.2	8	< 1	6.4	1	< 14	0.7	2.8	0.19	0.8
C	10/19/2009	*td*	157	135	116	23	77	12	8	21	3.4	16	2.7	5.3	< 1	3.2	< 1	< 20	0.4		0.24	1.1
C	11/28/2009	*td*	90	120	40	14	44	11	5	11	1.8	6	1.3	4	< 1	3	< 1	< 20	0.3		0.11	1.1
C	03/17/2010	*td*	170	230	332	46	134	30	15	31	5	16	3	7	1	6	1	< 12	0.9	2.6	0.37	1.2
C	04/21/2010	*td*	72	55	12	4.3	15	2	1.5	2.6	0.9	4	0.9	2	0.3	1.8	< 0.5	< 12	0.1		0.08	1.5
C	06/30/2010	*td*	69	64	51	< 9	25	< 8	< 5	< 6	< 5	< 5	< 5	< 5	< 4	< 6	< 5	< 36	0.1			
C	10/29/2010	*td*	84	79	74	11	48	10	5	11	1.6	7	1.9	4	< 1	1.6	< 1	< 44	0.3		0.28	1.1
C	12/01/2010	*td*	76	63	< 260	6	21	< 9	5	7	1.3	7	1.2	4	< 1	3	< 1	< 60	0.1			
Ledoux Gallery	03/18/2009	*g*	233	209	154	38	144	33	15	35	5.7	27	4.7	10	1.1	6	< 1	< 22	0.7		0.20	1.0
Ledoux Gallery	04/17/2009	*g*	800	494	488	81	321	84	28	103	14	73	14	29	3.7	23	3.2	< 22	1.8	1.7	0.28	0.7
Ledoux Gallery	05/07/2009	*g*	211	71	42	8.1	31	6.6	6.8	8.3	1.3	9	< 2	4	< 1	3	< 1	< 14	0.2		0.19	2.1
Ledoux Gallery	10/19/2009	*g*	104	< 44	46	7.1	< 23	5	< 3	7	1.2	7	1.3	3.5	< 1	< 3	< 1	< 20	0.1			
Ledoux Gallery	04/21/2010	*g*	116	34	32	6.1	20	2.5	2	6	0.9	4.8	1.6	3.7	0.3	3	< 0.5	< 12	0.1		0.25	1.1
Ledoux Gallery	06/30/2010	*g*	142	112	64	< 9	26	< 8	< 4	8	< 5	9	< 5	6	< 4	< 6	< 5	< 36	0.2			
Ledoux Gallery	07/23/2010	*g*	113	31	29	4	18	5	3	< 10	< 2	7	2	3	< 2	2	< 2	< 40	0.1		0.29	
Ledoux Gallery	10/29/2010	*g*	175	61	62	12	53	14	8	15	2.5	13	2.7	7	1.2	6	1.1	< 44	0.3	0.6	0.26	1.3

td = tailing drainages; [1] = La to Lu; [2]$(La/Lu)_{water}/(La/Lu)_{PAAS}$; [3] = $(Ce_{water}/Ce_{PAAS})/[(La_{water}/La_{PAAS})+(Pr_{water}/Pr_{PAAS})]$; [4] = $(Eu_{water}/Eu_{PAAS})/[(Sm_{water}/Sm_{PAAS})+(Gd_{water}/Gd_{PAAS})]$

APPENDIX C

XRD PATTERNS OF THE NARACAULI HYDROZINCITE SAMPLES

(Patterns of the Naracauli hydrozincite samples are vertically shifted for the sake of clarity).

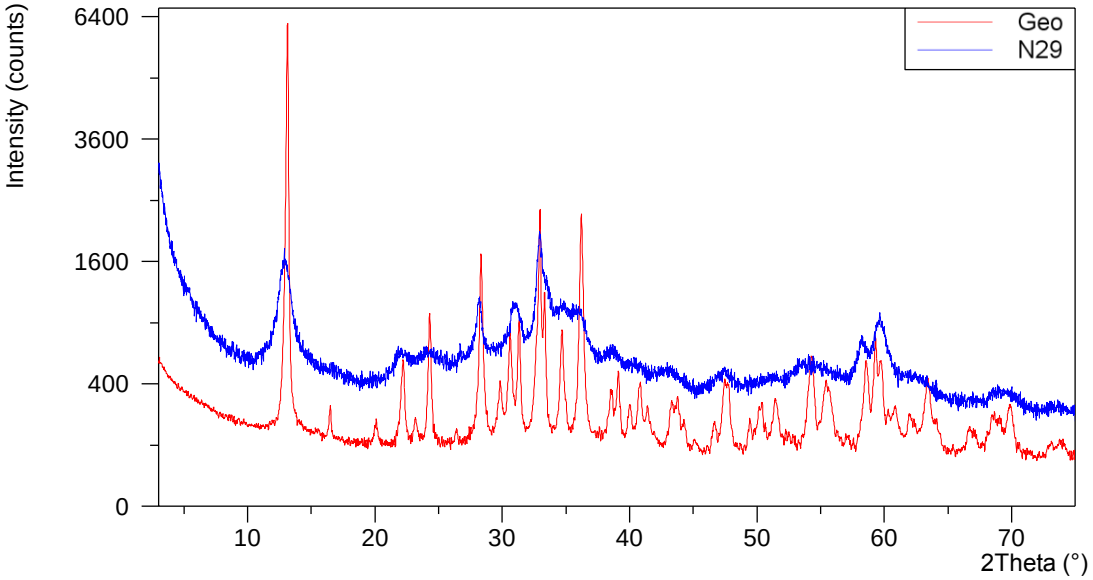
Intensity (counts)
6400
3600
1600
400
0
10
20
30
40
50
60
70
2Theta (°)
Geo
N29

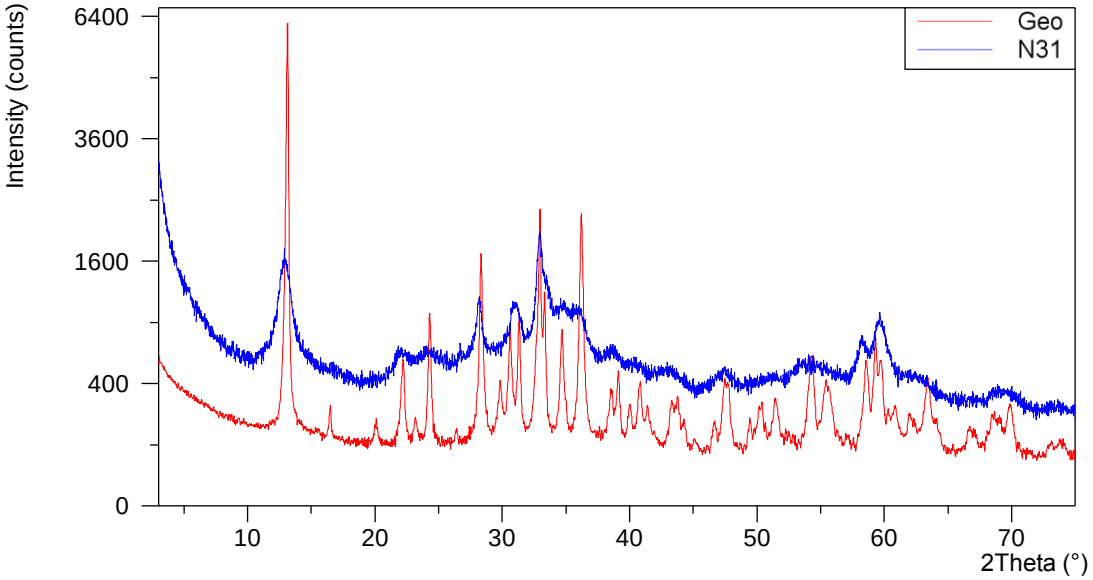
Intensity (counts)
6400
3600
1600
400
0
10
20
30
40
50
60
70
2Theta (°)
Geo
N31

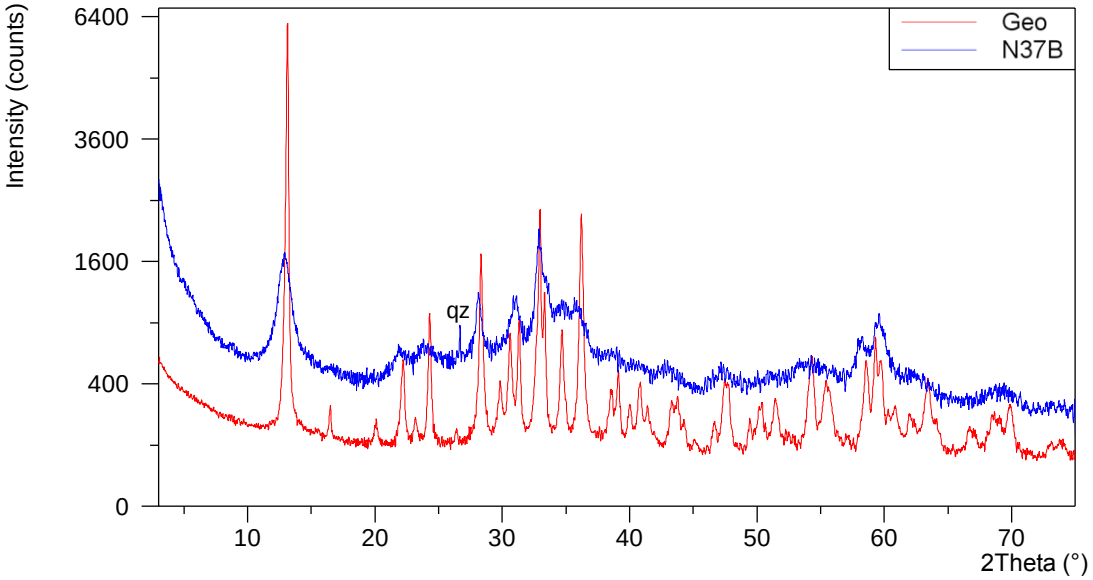
Intensity (counts)
6400
3600
1600
400
0
10
20
30
40
50
60
70
2Theta (°)
Geo
N37B
qz

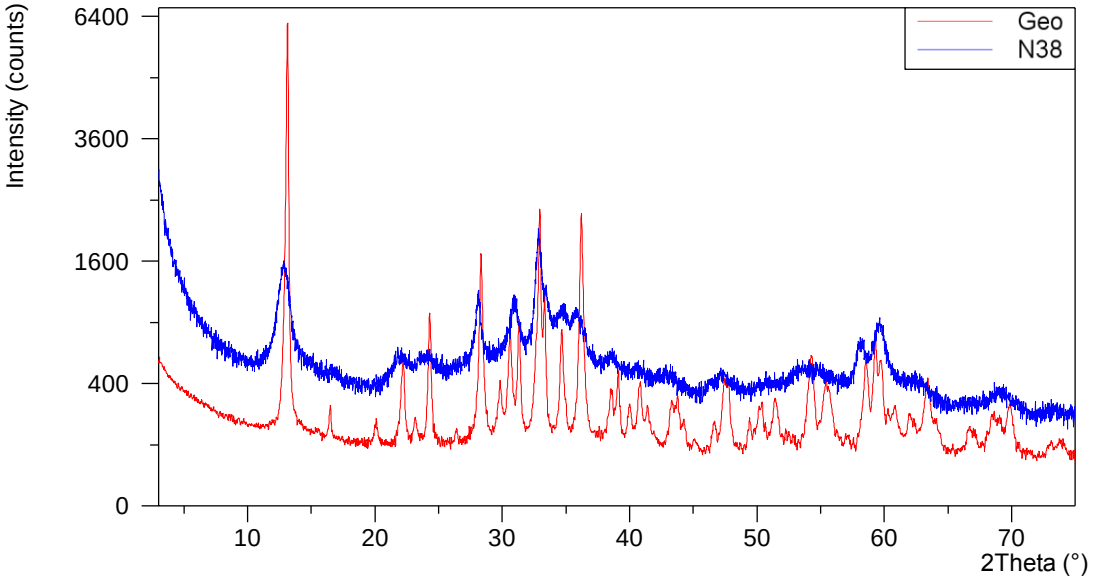
Intensity (counts)
6400
3600
1600
400
0
10
20
30
40
50
60
70
2Theta (°)
Geo
N38

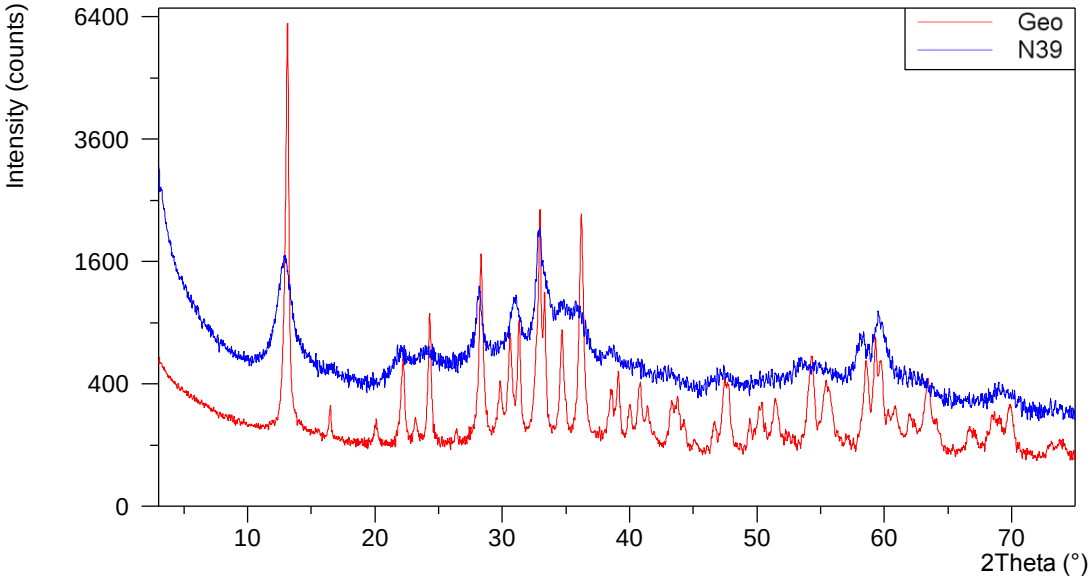
Intensity (counts)
6400
3600
1600
400
0
10
20
30
40
50
60
70
2Theta (°)
Geo
N39

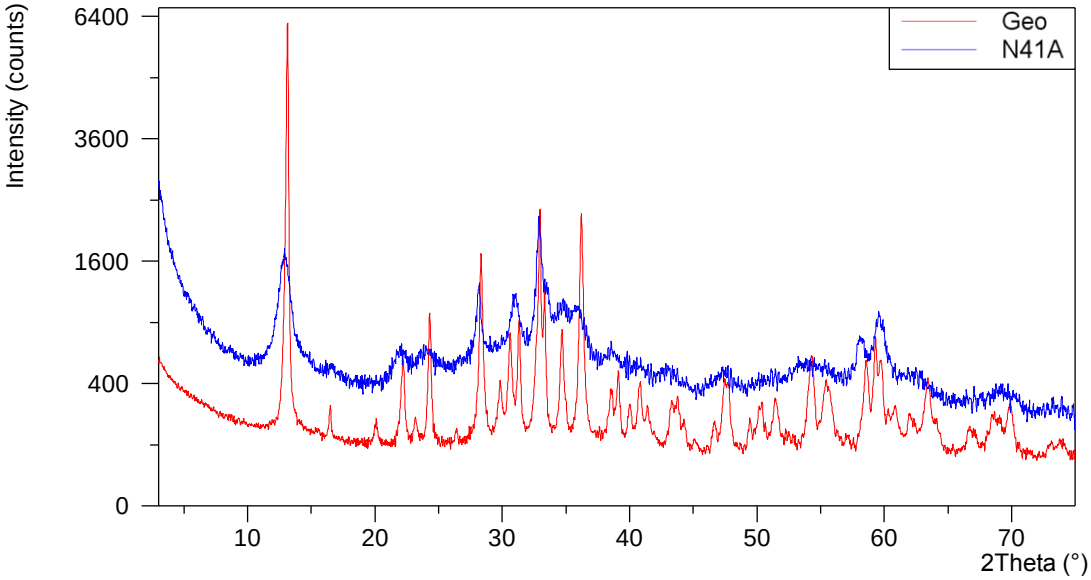
Intensity (counts)
6400
3600
1600
400
0
10
20
30
40
50
60
70
2Theta (°)
Geo
N41A

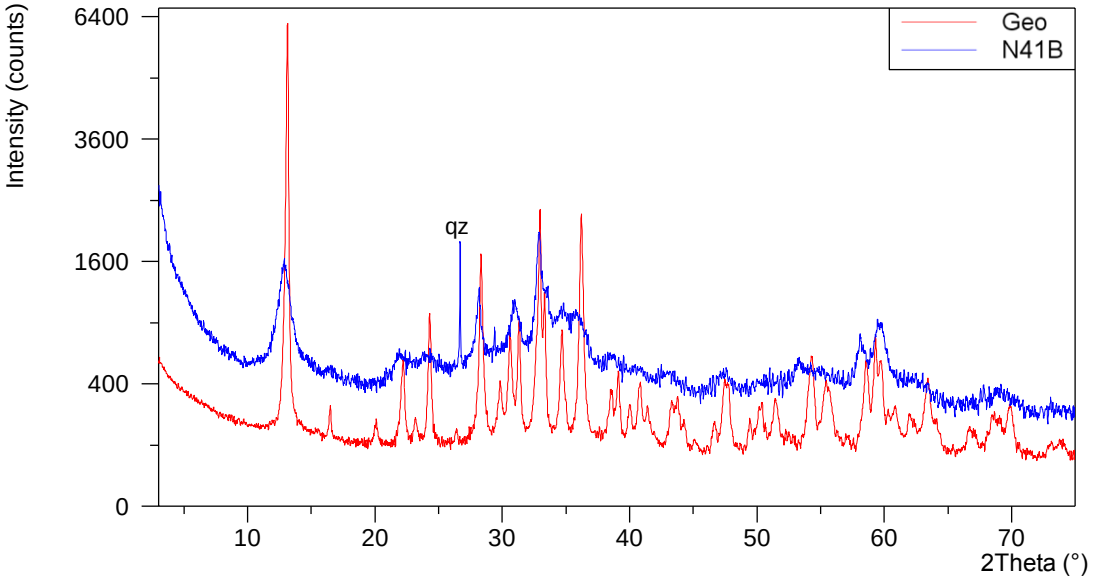
Intensity (counts)
6400
3600
1600
400
0
10
20
30
40
50
60
70
2Theta (°)
qz
Geo
N41B

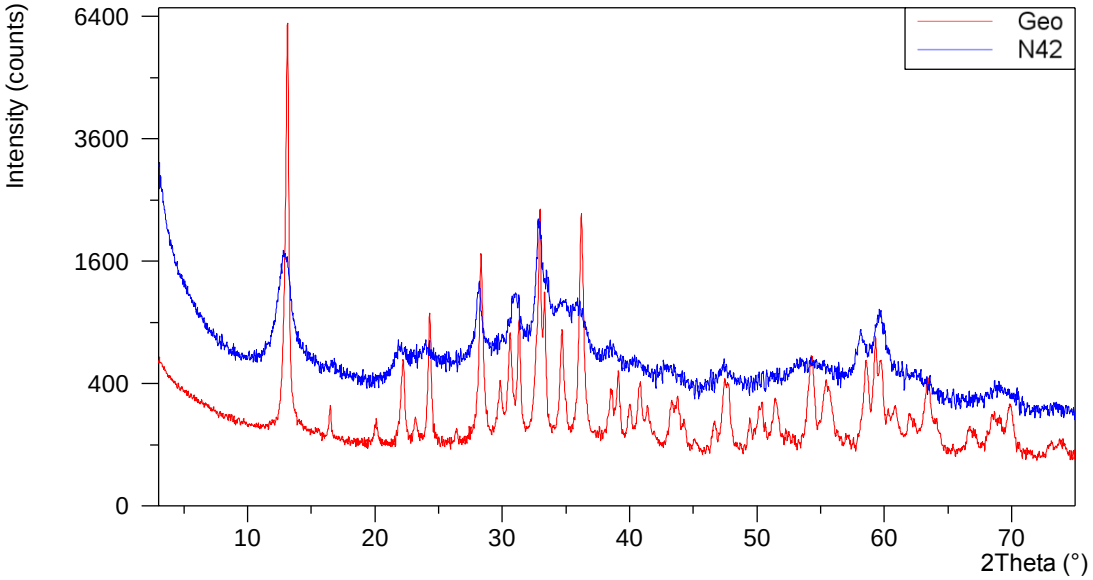
Intensity (counts)
6400
3600
1600
400
0
10
20
30
40
50
60
70
2Theta (°)
Geo
N42

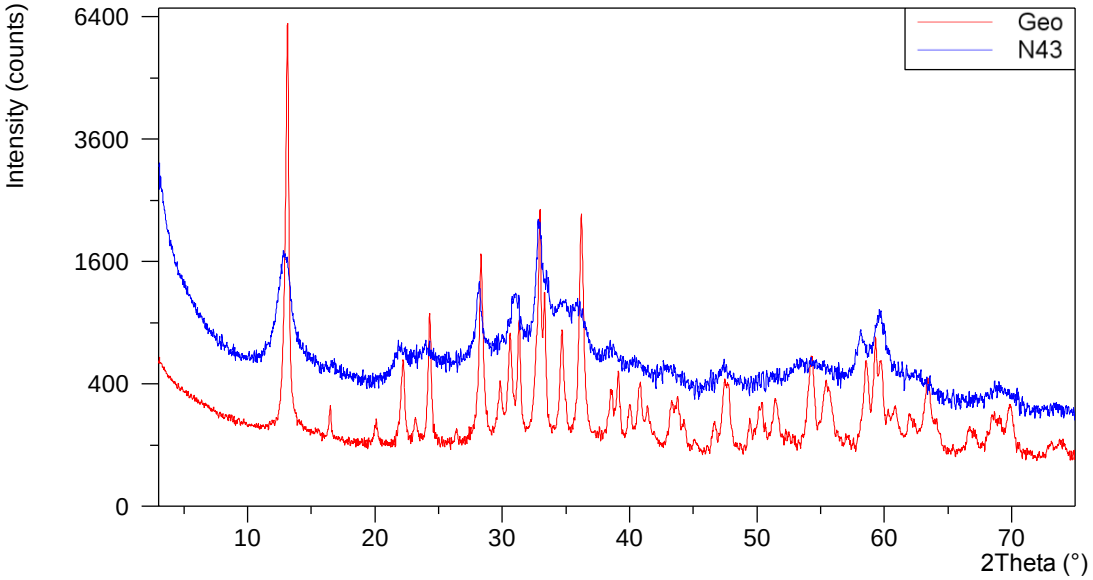
Intensity (counts)
6400
3600
1600
400
0
10
20
30
40
50
60
70
2Theta (°)
Geo
N43

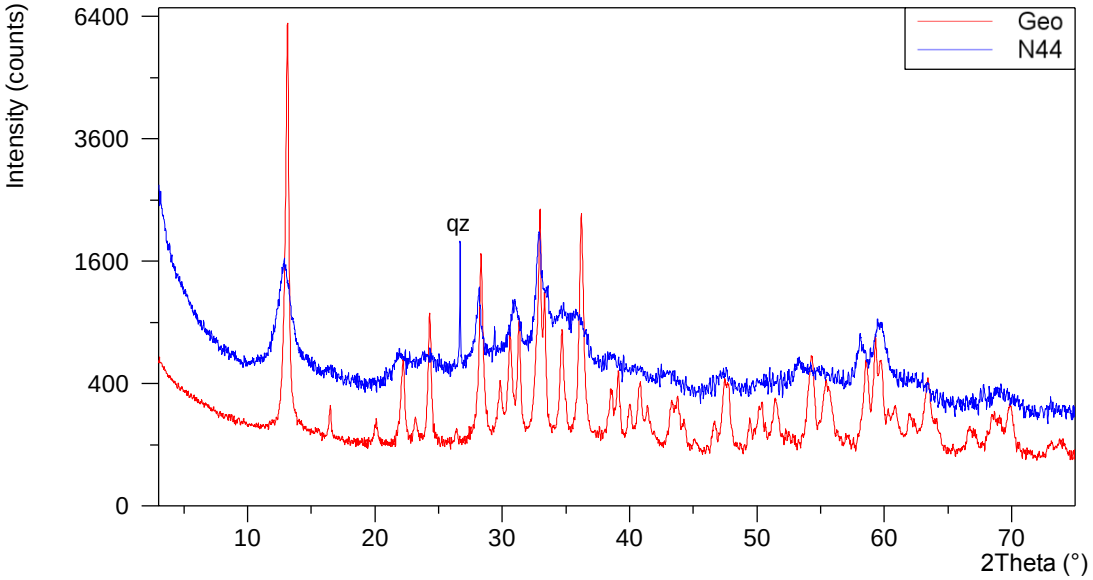
Intensity (counts)
6400
3600
1600
400
0
qz
10
20
30
40
50
60
70
2Theta (°)
Geo
N44

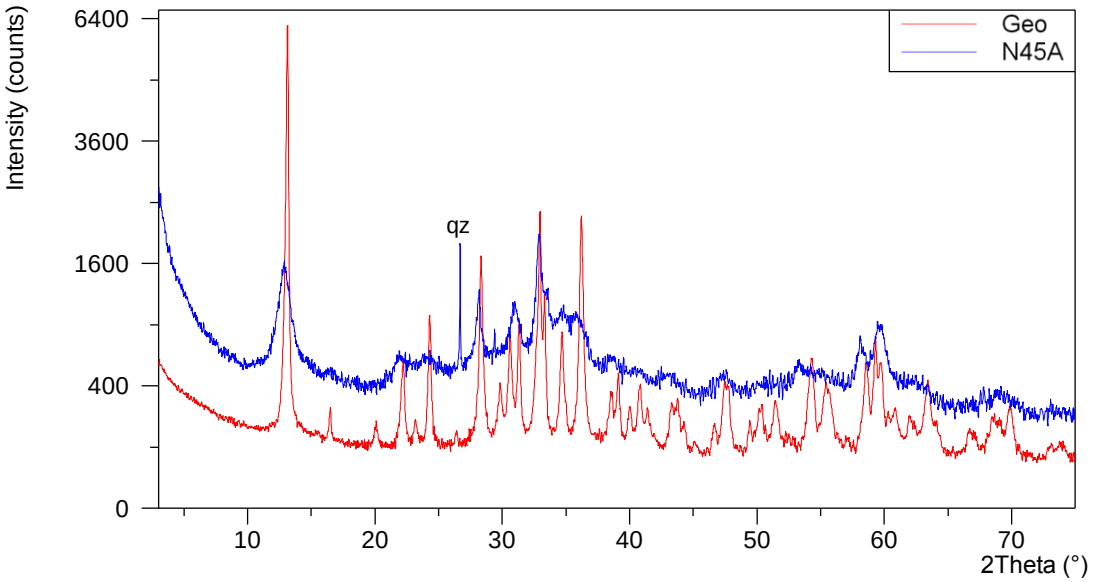
Intensity (counts)
6400
3600
1600
400
0
10
20
30
40
50
60
70
2Theta (°)
qz
Geo
N45A

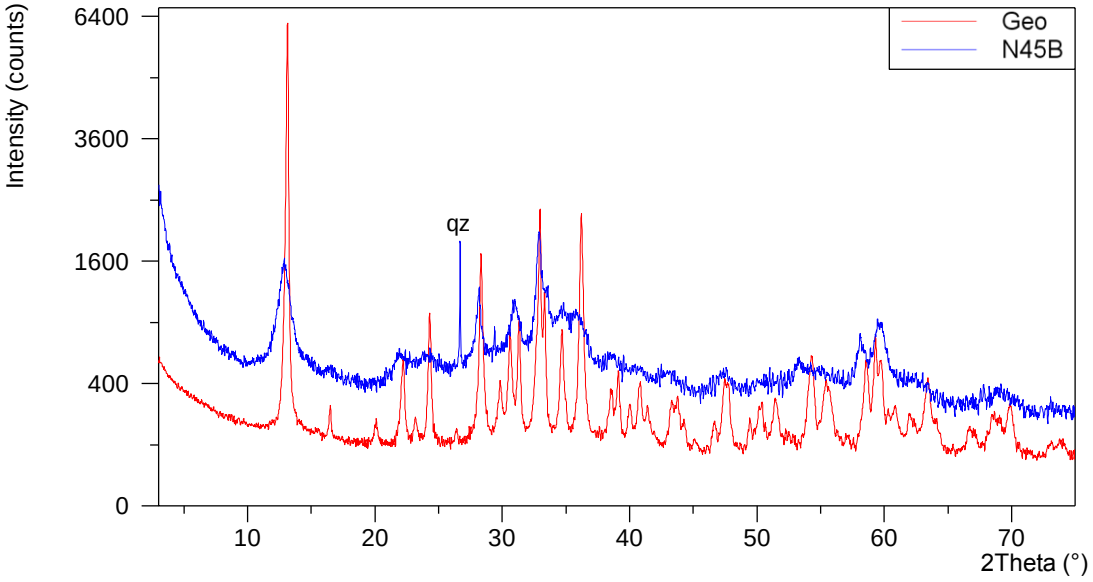
Intensity (counts)
6400
3600
1600
400
0
10
20
30
40
50
60
70
2Theta (°)
qz
Geo
N45B

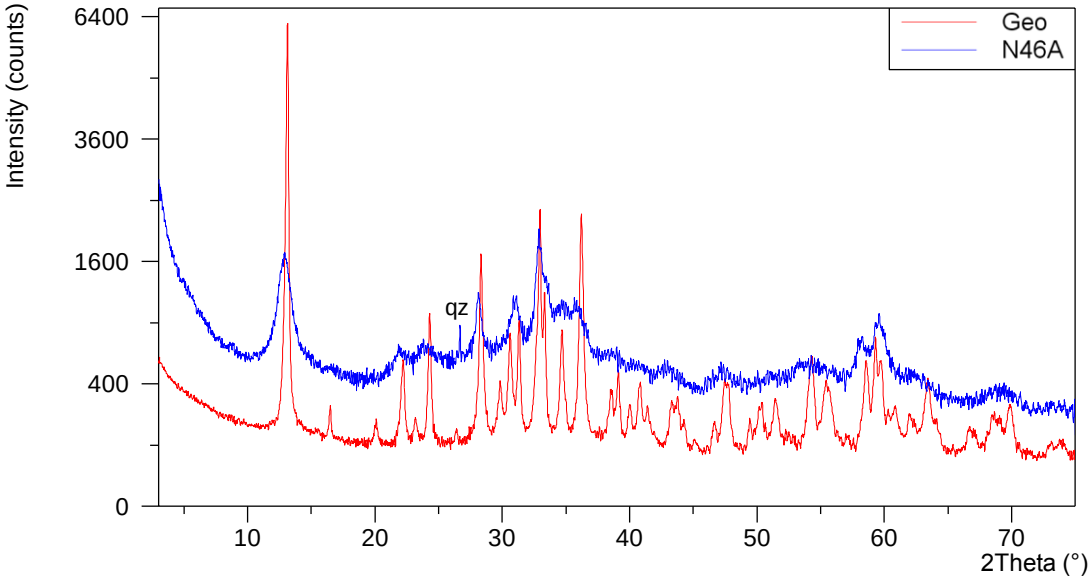
Intensity (counts)
6400
3600
1600
400
0
10
20
30
40
50
60
70
2Theta (°)
qz
Geo
N46A

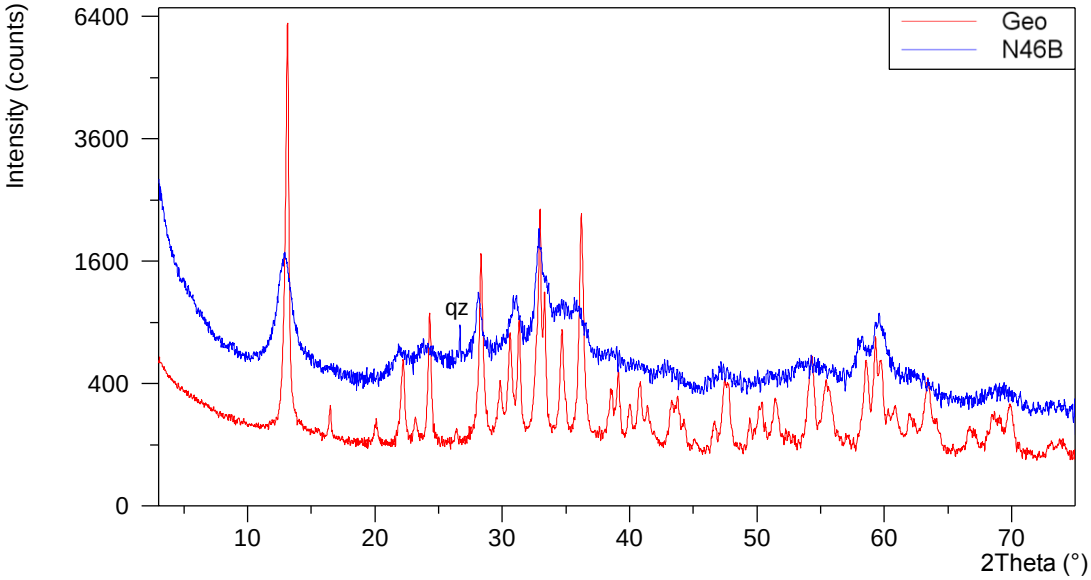
Intensity (counts)
6400
3600
1600
400
0
10
20
30
40
50
60
70
2Theta (°)
qz
Geo
N46B

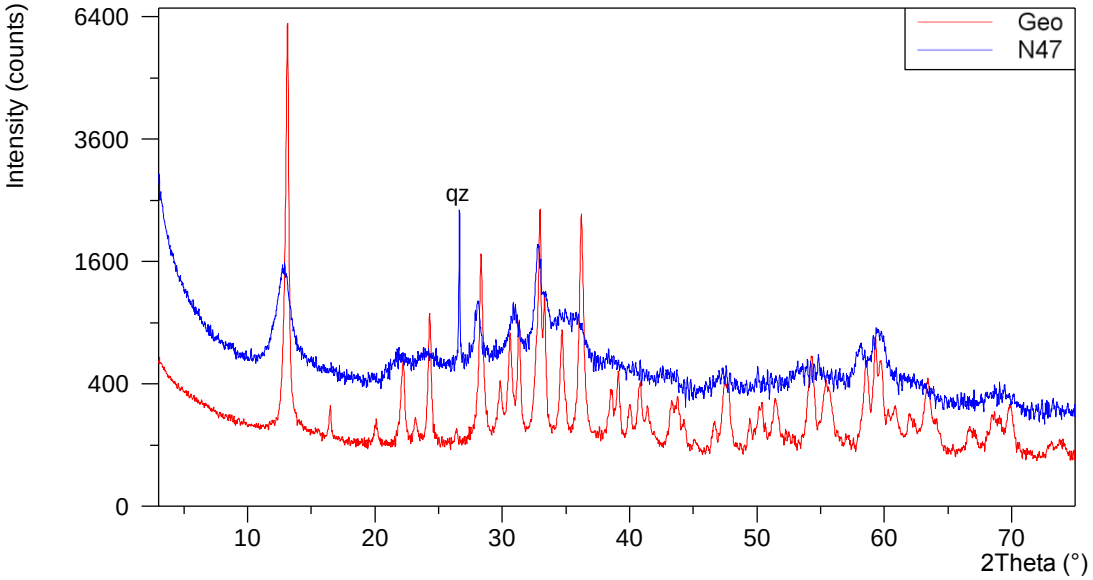
Intensity (counts)
6400
3600
1600
400
0
10
20
30
40
50
60
70
2Theta (°)
qz
Geo
N47

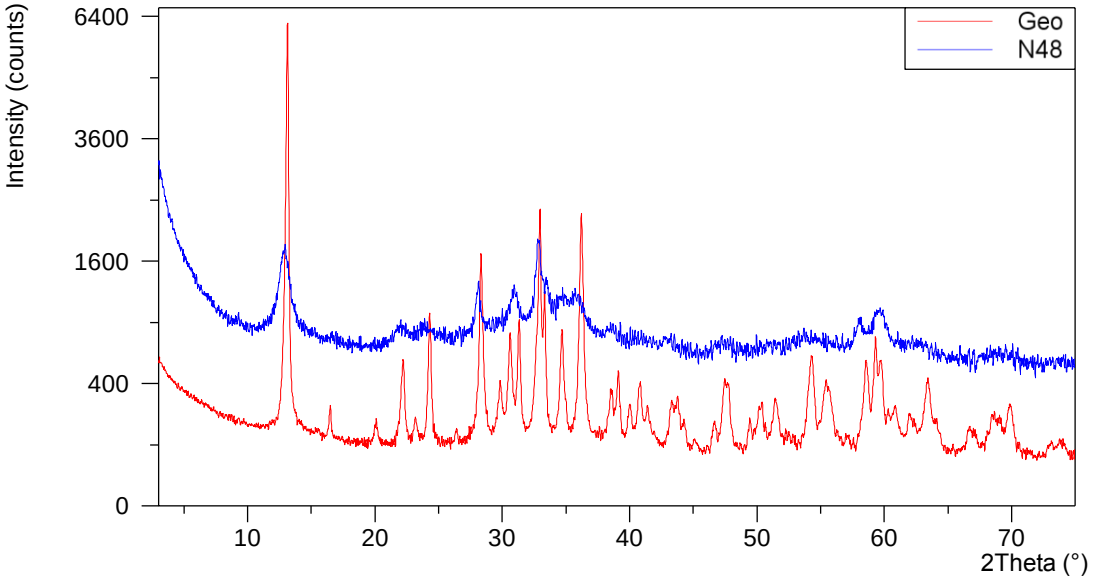
Intensity (counts)
6400
3600
1600
400
0
10
20
30
40
50
60
70
2Theta (°)
Geo
N48

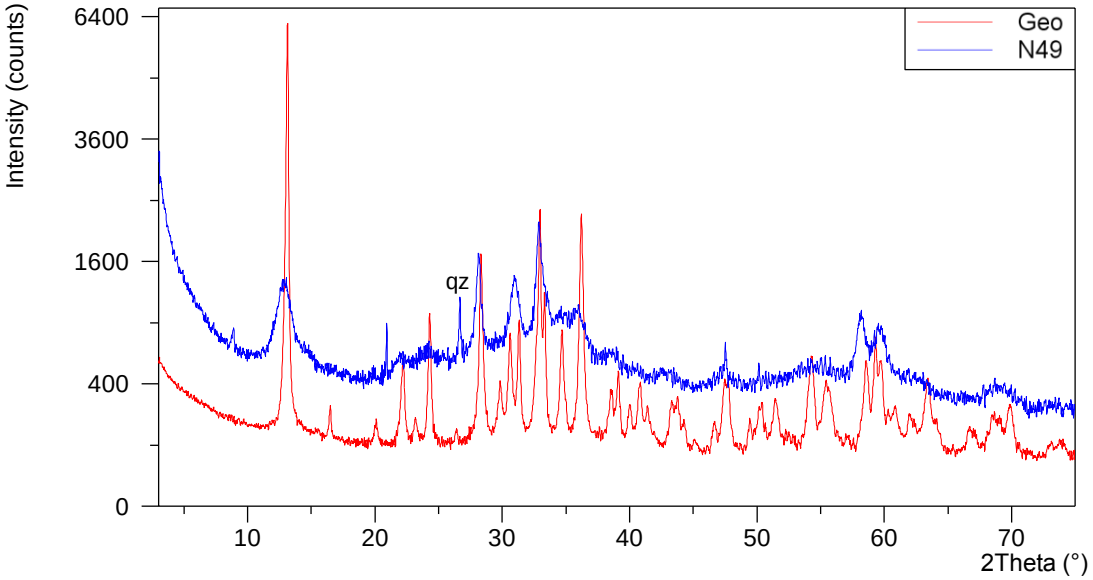
Intensity (counts)
6400
3600
1600
400
0
10
20
30
40
50
60
70
2Theta (°)
qz
Geo
N49

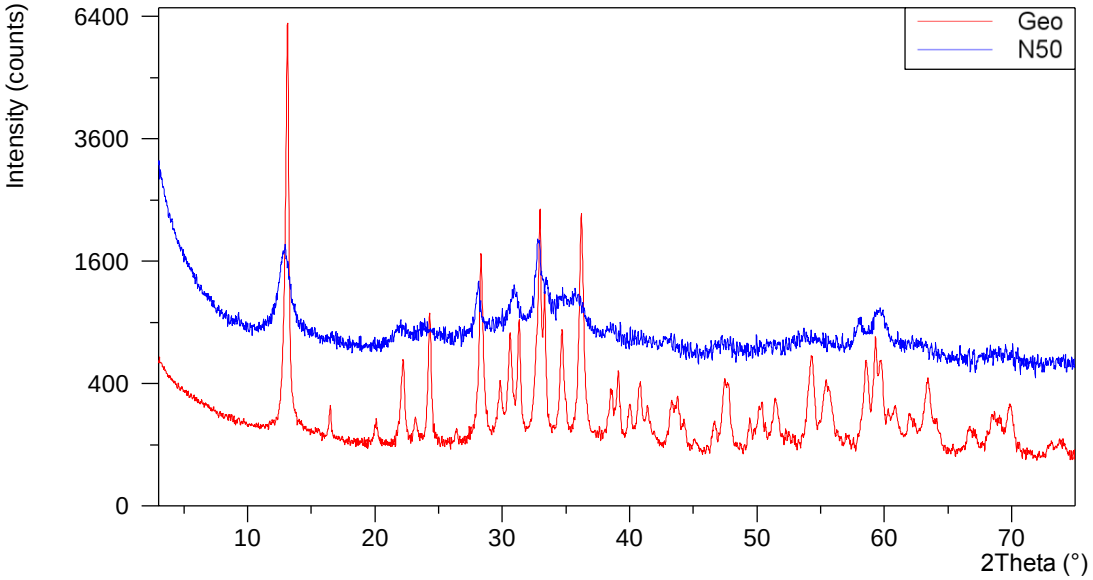
Intensity (counts)
6400
3600
1600
400
0
10
20
30
40
50
60
70
2Theta (°)
Geo
N50

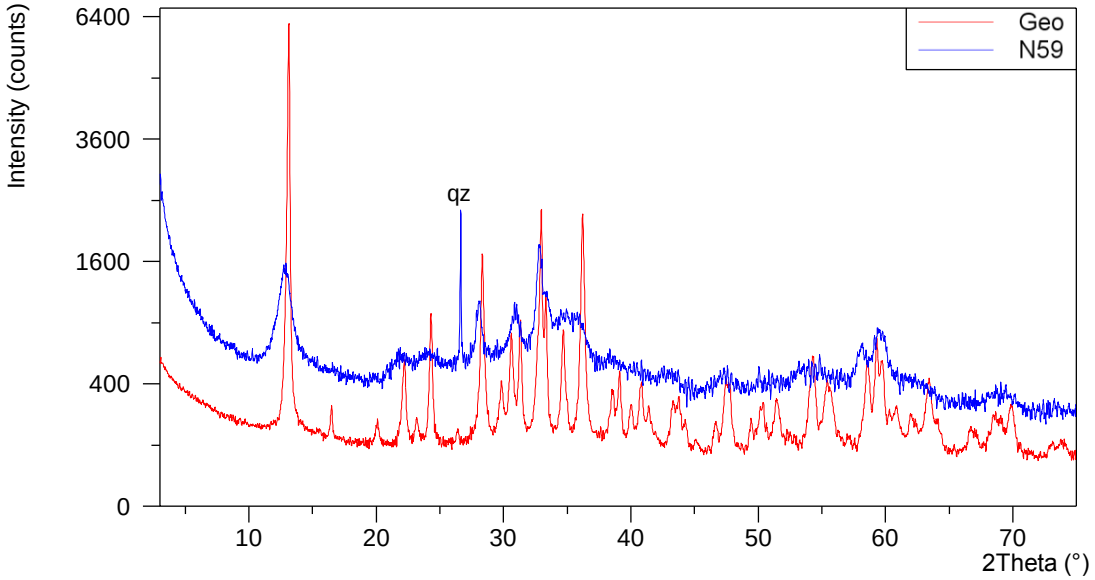
Intensity (counts)
6400
3600
1600
400
0
10
20
30
40
50
60
70
2Theta (°)
qz
Geo
N59

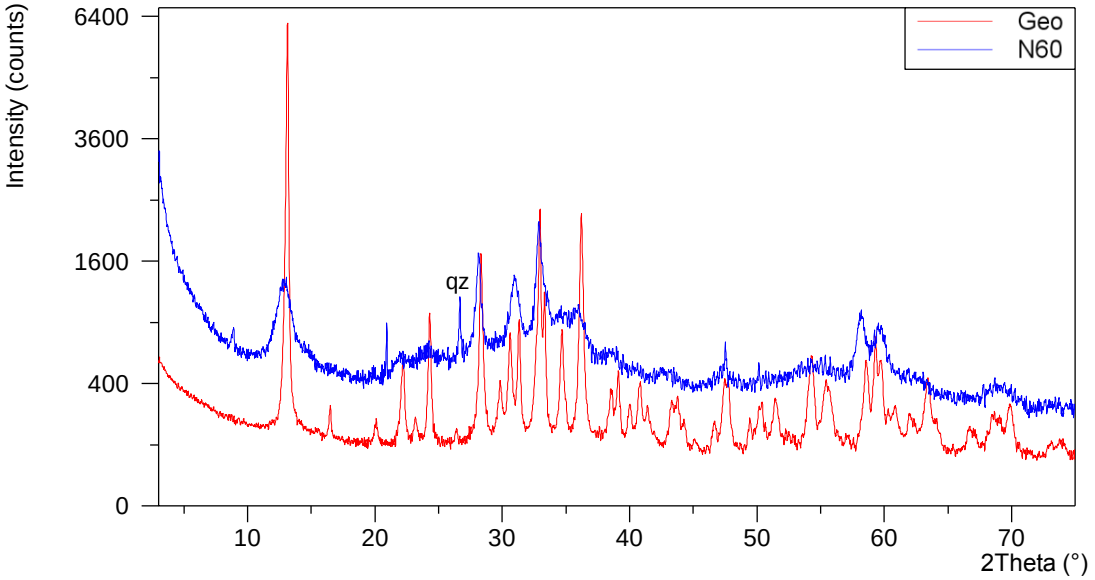
Intensity (counts)
6400
3600
1600
400
0
10
20
30
40
50
60
70
2Theta (°)
qz
Geo
N60

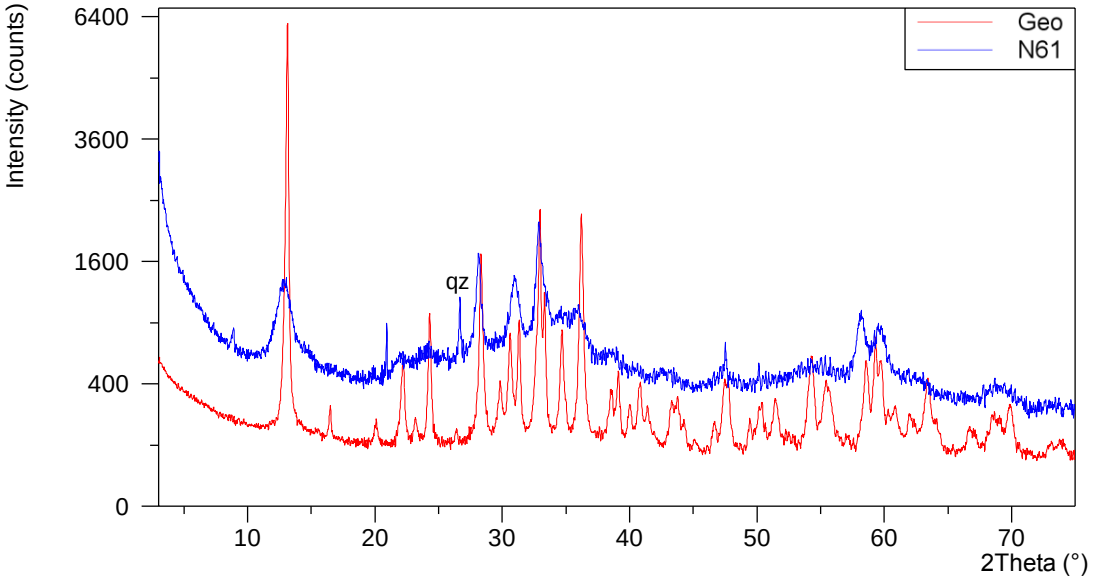
Intensity (counts)
6400
3600
1600
400
0
10
20
30
40
50
60
70
2Theta (°)
qz
Geo
N61

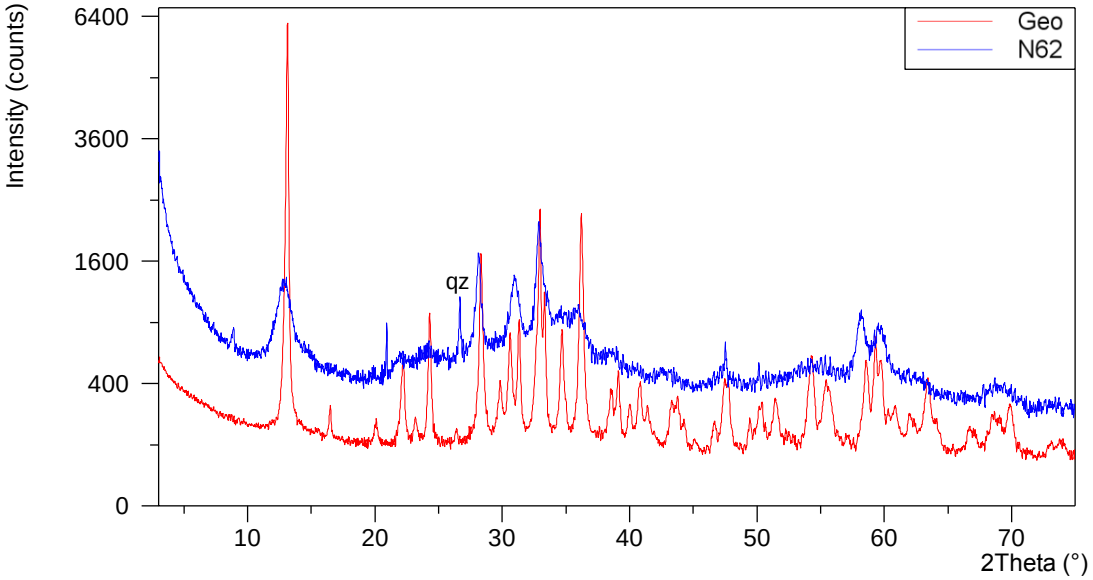
Intensity (counts)
6400
3600
1600
400
0
10
20
30
40
50
60
70
2Theta (°)
qz
Geo
N62

APPENDIX D

ANALYTICAL RESULTS OF THE NARACAULI HYDROZINCITE SAMPLES COLLECTED IN 2009: Y AND RARE EARTH ELEMENTS.

Sample	Station	Date	Y	La	Ce	Pr	Nd	Sm	Eu	Gd	Tb	Dy
			mg/kg	mg/kg	mg/kg	mg/kg	mg/kg	mg/kg	mg/kg	mg/kg	mg/kg	mg/kg
N32	NS170	21/05/2009	60	71	55	7.5	28	5.7	2.6	11	1.3	6.0
N37B	NS420	10/06/2009	8.2	8.8	5.1	1.1	3.9	0.7	0.2	1.0	0.1	0.7
N39	NS420	15/07/2009	3.1	1.9	0.7	0.2	0.8	0.1	0.05	0.2	0.04	0.2
N41A	NS420	29/07/2009	4.6	3.4	1.3	0.4	1.4	0.3	0.1	0.4	0.05	0.3
42	NS420	29/07/2009	2.9	2.1	1.1	0.3	0.9	0.2	0.06	0.3	0.04	0.2
N34	NS590	27/05/2009	3.4	3.7	2.0	0.4	1.5	0.3	0.1	0.4	0.06	0.3
N36	NS590	03/06/2009	5.2	8.4	8.8	1.4	5.2	1.0	0.3	1.2	0.1	0.7

Sample	Station	Date	Ho	Er	Tm	Yb	Lu	Th	[1]∑ REE	[2](La/Lu)$_N$	[3]Ce*	[4]Eu*
			mg/kg	mg/kg	mg/kg	mg/kg	mg/kg	mg/kg	mg/kg			
N32	NS170	21/05/2009	1.0	2.3	0.2	1.0	0.1	< 0.40	192	5.4	0.26	0.72
N37B	NS420	10/06/2009	0.1	0.3	0.04	0.2	0.03	0.5	22	2.9	0.18	0.64
N39	NS420	15/07/2009	0.04	0.1	0.01	0.08	0.01	< 0.40	5	1.9	0.12	0.71
N41A	NS420	29/07/2009	0.07	0.2	0.02	0.1	0.02	< 0.40	8	2.2	0.13	0.68
42	NS420	29/07/2009	0.04	0.1	0.01	0.08	0.01	< 0.40	5	1.7	0.16	0.62
N34	NS590	27/05/2009	0.06	0.1	0.02	0.08	0.01	0.8	9	3.2	0.18	0.64
N36	NS590	03/06/2009	0.1	0.3	0.04	0.3	0.03	1.3	28	3.3	0.30	0.53

[1] = La to Lu; [2]$(La/Lu)_{water}/(La/Lu)_{PAAS}$; [3] = $(Ce_{water}/Ce_{PAAS})/[(La_{water}/La_{PAAS})+(Pr_{water}/Pr_{PAAS})]$; [4] = $(Eu_{water}/Eu_{PAAS})/[(Sm_{water}/Sm_{PAAS})+(Gd_{water}/Gd_{PAAS})]$

APPENDIX E

SEM IMAGES OF THE NARACAULI HYDROZINCITE SAMPLES

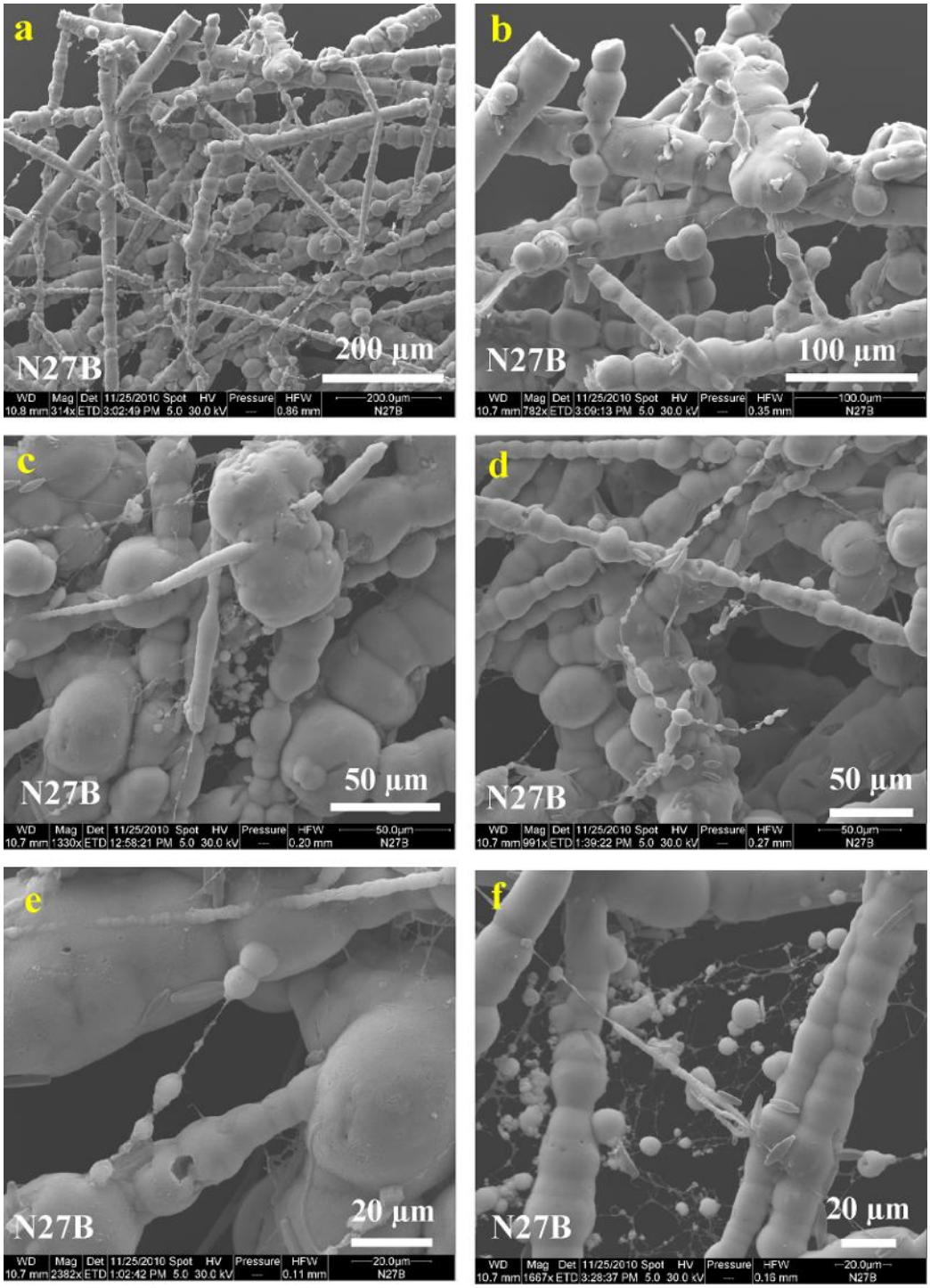

Figure E.1. Hydrozincite sample (N27B) collected at the beginning of precipitation. a) The thin network formed by the biomineral. b, c, d, e and f) Magnifications of the same sample that show as the biomineral precipitates around the organic filaments forming globules.

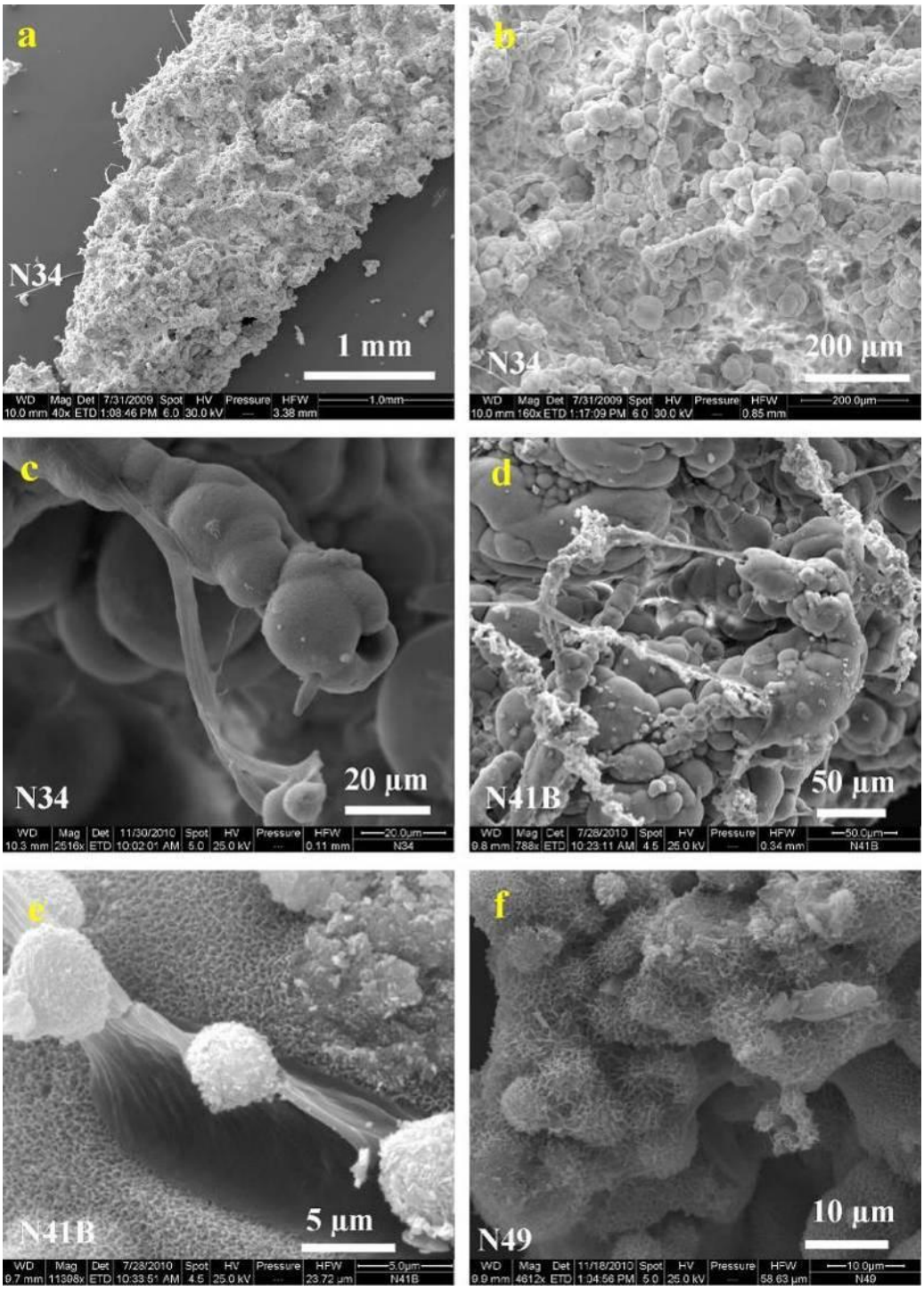

Figure E.2. a and b) Hydrozincite sample (N34) collected after several days of bioprecipitation. The biomineral sheaths form a three-dimensional structure. c) Magnification of the sample N34. d and e) Hydrozincite collected by a polycarbonate sheet. The organic matter is well visible. f) The sponge like surface of hydrozincite, made up of sub-micrometric mesocrystals (platelets).

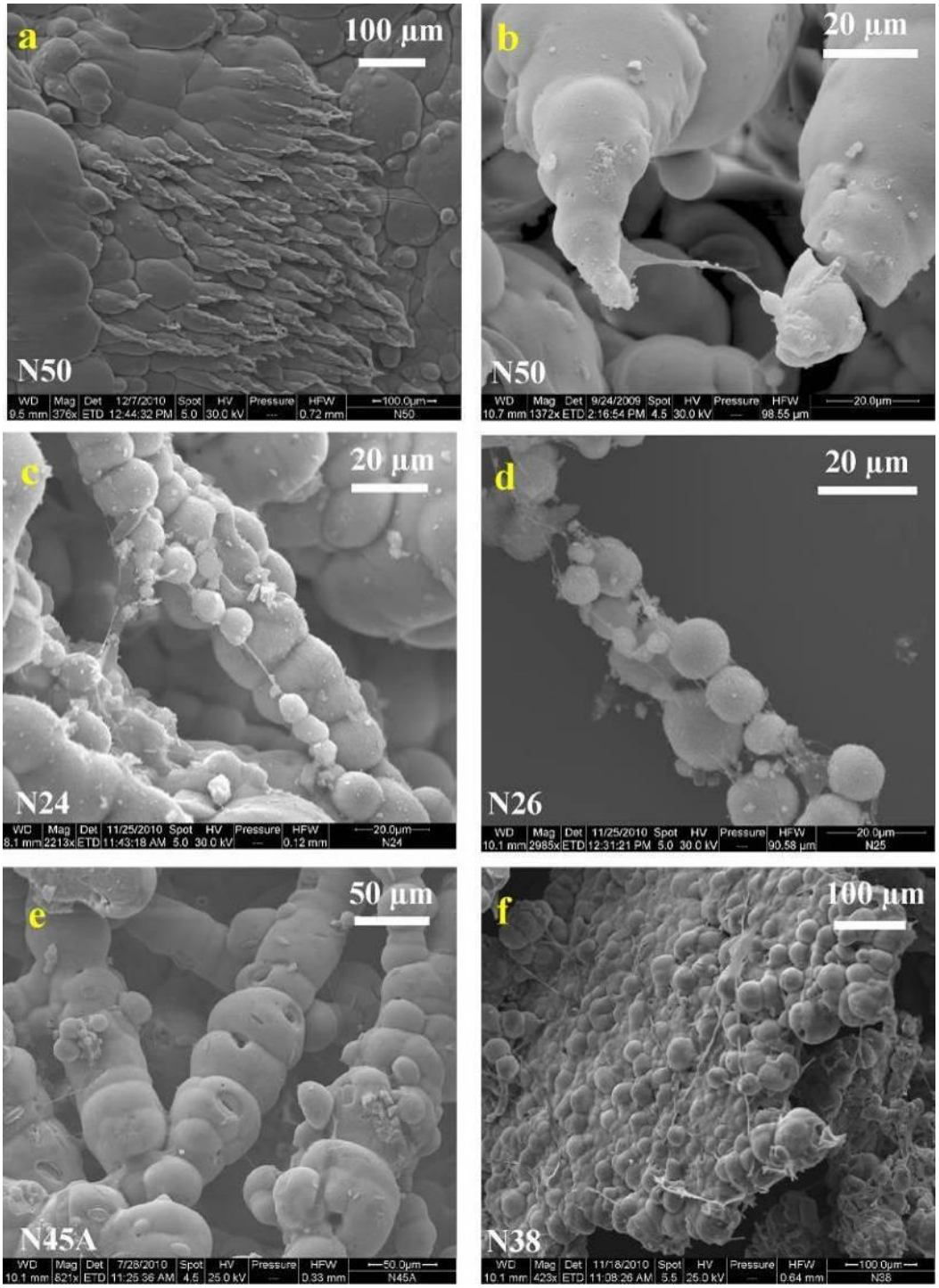

Figure E.3. a and b) Hydrozincite precipitated under high flow conditions. Biomineral sheaths become thinner at the final ends, which indicate the flow direction. c and d) Hydrozincite globules around the organic filaments. e) Hydrozincite precipitated in summer (August), characterized by large globules. f) Hydrozincite collected by a polycarbonate sheet.

APPENDIX F

ANALYTICAL RESULTS OF THE SHORT-TERM CHEMICAL VARIATIONS AT STATION NS-420: PHYSICO-CHEMICAL PARAMETERS AND CHEMICAL COMPONENTS

Sample No	**Date**	**Time**	**T_{water}** °C	**T_{air}** °C	**pH**	**EC** mS/cm	**TDS** g/l	**O_2** mg/l	**Ca** mg/l	**Mg** mg/l	**Na** mg/l	**K** mg/l	**Zn** mg/l	**HCO_3** mg/l	**Cl** mg/l	**SO_4** mg/l	**SiO_2** mg/l
NS-420	06/13/2011	20:00	20.4	20.4	7.9	1.72	1.45	n.d.	274	84	71.6	6.8	4.2	254	91	772	8.5
NS-420	06/13/2011	23:00	19.4	19.6	7.7	1.72	1.44	9.1	248	75	66	7.0	4.4	254	91	802	8.4
NS-420	06/14/2011	02:00	18.7	16.5	7.7	1.71	1.45	8.9	259	78.8	67.6	7.1	4.7	258	91	799	8.3
NS-420	06/14/2011	05:00	18.8	17	7.8	1.72	1.42	9.2	251	76.4	66.4	6.7	4.7	252	91	781	7.8
NS-420	06/14/2011	09:00	20	22.2	7.9	1.71	1.41	8.9	248	76	66.5	6.9	4.0	240	91	784	7.8
NS-420	06/14/2011	13:00	22.8	26.5	8.1	1.72	1.40	9.5	248	74.8	66	6.9	3.2	260	91	760	7.6
NS-420	06/14/2011	17:00	23.7	26.7	8.1	1.73	1.38	9.4	234	75.4	63.6	6.8	3.1	258	91	757	7.9
NS-420	06/14/2011	20:00	20.8	21.9	8	1.73	1.48	9.7	283	91.7	74.4	6.7	4.0	260	97	787	9.1
NS-420	06/14/2011	23:00	19.8	20.9	7.9	1.72	1.45	9.1	267	86	71.7	6.7	4.2	257	91	775	9
NS-420	06/15/2011	02:00	19.2	17.1	7.8	1.72	1.41	9.2	255	82.8	68.3	6.6	4.7	262	97	757	9.2
NS-420	06/15/2011	05:00	19.2	18.8	8	1.72	1.38	8.4	249	79.2	66.8	6.7	4.7	260	97	733	7.8
NS-420	06/15/2011	09:00	20.7	22.8	8	1.72	1.37	8.9	244	79.2	65.6	6.8	4.2	254	97	739	7.4
NS-420	06/15/2011	13:00	23.8	25.5	7.9	1.73	1.35	9.4	241	76.8	64.2	6.7	3.2	252	97	724	7.2
NS-420	06/15/2011	17:00	23.9	24.9	7.97	1.74	1.35	9.4	241	77.2	66.6	7.1	2.9	257	97	724	7.6

n.d. = not determined

Sample no	Date	Time	Al µg/l	B µg/l	Be µg/l	Li µg/l	Rb µg/l	Sr µg/l	Ba µg/l	Fe µg/l	Mn µg/l	Cd µg/l	Cr µg/l	Co µg/l	Ni µg/l	Cu µg/l	Pb µg/l	Mo µg/l	Ga µg/l	Tl µg/l	Bi µg/l	U µg/l	Ag µg/l	Sb µg/l
NS-420	06/13/2011	20:00	< 5	31	< 0.1	36	15.6	380	19	< 30	100	105	< 0.7	3.6	74	< 2	1.7	1.3	< 0.03	0.4	< 0.08	0.6	< 0.03	1.1
NS-420	06/13/2011	23:00	< 5	30	< 0.1	36	15.3	370	18	< 30	110	102	< 0.7	3.9	77	< 2	1.7	1.2	< 0.03	0.4	< 0.08	0.5	< 0.03	1.1
NS-420	06/14/2011	02:00	< 5	30	< 0.1	37	15.4	380	19	< 30	110	108	< 0.7	4	80	< 2	2.0	1.2	< 0.03	0.4	< 0.08	0.5	< 0.03	1.1
NS-420	06/14/2011	05:00	< 5	30	< 0.1	37	15.5	379	19	< 30	120	108	< 0.7	4.1	80	< 2	1.9	1.3	< 0.03	0.4	< 0.08	0.5	< 0.03	1.1
NS-420	06/14/2011	09:00	< 5	30	< 0.1	36	15.4	380	19	< 30	120	108	< 0.7	3.9	78	< 2	2.4	1.2	< 0.03	0.4	< 0.08	0.5	< 0.03	1.1
NS-420	06/14/2011	13:00	< 5	30	< 0.1	36	15.3	380	19	< 30	100	98	< 0.7	3.6	71	< 2	1.9	1.2	< 0.03	0.4	< 0.08	0.6	< 0.03	1.1
NS-420	06/14/2011	17:00	< 5	32	< 0.1	37	15.7	380	19	< 30	90	95	< 0.7	3.2	67	< 2	2.3	1.3	< 0.03	0.4	< 0.08	0.6	< 0.03	1.1
NS-420	06/14/2011	20:00	< 5	30	< 0.1	36	15.5	380	18	< 30	100	101	< 0.7	3.5	73	< 2	1.5	1.3	< 0.03	0.4	< 0.08	0.6	< 0.03	1.1
NS-420	06/14/2011	23:00	< 5	30	< 0.1	35	15.5	380	20	< 30	110	100	< 0.7	4	79	< 2	1.8	1.2	< 0.03	0.4	< 0.08	0.5	< 0.03	1.1
NS-420	06/15/2011	02:00	< 5	31	< 0.1	37	15.5	380	19	< 30	110	100	< 0.7	4.1	81	< 2	2.0	1.2	< 0.03	0.4	< 0.08	0.5	< 0.03	2.0
NS-420	06/15/2011	05:00	< 5	31	< 0.1	37	15.5	380	18	< 30	120	100	< 0.7	4.1	82	< 2	1.8	1.2	< 0.03	0.4	< 0.08	0.5	< 0.03	1.1
NS-420	06/15/2011	09:00	< 5	31	< 0.1	37	15.6	380	19	< 30	110	101	< 0.7	3.9	77	< 2	2.2	1.2	< 0.03	0.4	< 0.08	0.6	< 0.03	1.1
NS-420	06/15/2011	13:00	< 5	32	< 0.1	37	15.7	380	19	< 30	100	93	< 0.7	3.4	69	< 2	1.9	1.2	< 0.03	0.4	< 0.08	0.6	< 0.03	1.1
NS-420	06/15/2011	17:00	< 5	35	< 0.1	38	16.2	390	19	< 30	90	95	< 0.7	3.3	69	< 2	1.9	1.2	< 0.03	0.4	< 0.08	0.6	< 0.03	1.1